

**UTILISATION OF GREEN CHEMICAL  
TECHNOLOGIES FOR THE VALORISATION OF  
THAI AGRICULTURAL WASTE**

**CHANETTEE SIKHOM**

DOCTOR OF PHILOSOPHY

UNIVERSITY OF YORK  
CHEMISTRY

March 2018



## Abstract

Biorefinery concepts are important for countries with economies closely linked with agriculture, such as Thailand. The use of agricultural waste streams or residues for the production of fuels, chemicals and materials is vital for the move towards a sustainable circular economy. Two such wastes (rice straw and prawn head waste), were selected for valorisation through the use of supercritical carbon dioxide (scCO<sub>2</sub>) extraction and microwave-assisted pyrolysis (MAP).

scCO<sub>2</sub> extraction was investigated as a suitable technology for lipid recovery from rice straw. Yields obtained from scCO<sub>2</sub> extraction of rice straw were comparable to hexane Soxhlet, with yields of 0.7% by dry weight at 65 °C and 400 bar. Extracts consists of a valuable mixture of compounds including free fatty acids (FFA) and fatty alcohols, sterols and wax esters. This method also serves as a pre-treatment step to provide enhanced interactions between microwaves and the resulting extracted biomass. Wax removal by scCO<sub>2</sub> has an influence on the dielectric property of the rice straw, leading to a constant high heating rate and higher final temperatures. The decomposition of rice straw occurred in MAP at around 120 °C, approximately 200 °C earlier than in the conventional heating. The influence of moisture content, particle size and also inorganic content was investigated. It was found the K<sub>3</sub>PO<sub>4</sub> present in the straw (also present in fertilisers) had a profound effect on MAP resulting in rapid heating and biomass gasification. Such gases may be used as synthesis gas for the production of fuels and chemicals.

scCO<sub>2</sub> extraction was effectively utilised for the recovery of hydrophobic compounds from prawn residue (*Litopenaeus vannamei*). The optimisation of lipid extraction from cephalothorax (heads) by scCO<sub>2</sub> demonstrated yields of 1.14% at 400 bar and 40 °C for 2 hours (40 g min<sup>-1</sup>). Extraction efficiency strongly correlated density, with the highest yield being obtained at the highest density of CO<sub>2</sub>, 0.96 g/cm<sup>3</sup>. The FFA profile of the scCO<sub>2</sub> extract differed to that of the hexane Soxhlet in abundance, 20789.8 ± 257.3 µg/g of dry biomass compared to 2819.4 ± 87.8 µg/g of dry plant by scCO<sub>2</sub> (40°C and 400 bar for 2 hours). Water content of the biomass adversely affects the efficiency of scCO<sub>2</sub> extraction. Autolysis of the waste for 6 hours at 50 °C under nitrogen prior to scCO<sub>2</sub> extraction was found to significantly improve the yield of PUFA. *L.vannamei* waste can potentially serve as new source of ω-3 and ω-6 PUFA.





# Table of Contents

<b>Abstract</b> .....	<b>3</b>
<b>Table of Contents</b> .....	<b>5</b>
<b>List of Tables</b> .....	<b>11</b>
<b>List of Figures</b> .....	<b>14</b>
<b>Acknowledgements</b> .....	<b>22</b>
<b>Declaration</b> .....	<b>23</b>
<b>1 Introduction</b> .....	<b>25</b>
<b>1.1 Scope of the project</b> .....	<b>25</b>
1.1.1 Extraction of lipids from the waste biomass .....	25
1.1.2 Optimisation of supercritical extraction.....	25
1.1.3 Combination of supercritical carbon dioxide and microwave technologies. ....	25
1.1.4 Study of autocatalysis on gasification of rice straw during microwave pyrolysis...	26
1.1.5 Production of n-3 and n-6 PUFA via endogenous enzymes of prawn-waste .....	26
<b>1.2 Towards sustainable development</b> .....	<b>26</b>
<b>1.3 Green chemistry</b> .....	<b>27</b>
<b>1.4 Feedstock</b> .....	<b>30</b>
1.4.1 Rice straw .....	30
1.4.2 Prawn by-products.....	33
<b>1.5 Bio-refinery Concept</b> .....	<b>37</b>
<b>1.6 Green chemistry and Biorefinery as sustainable partnership</b> .....	<b>38</b>
1.6.1 Extraction.....	39
1.6.2 Biochemical process.....	44
1.6.3 Thermochemical processes .....	45
<b>1.7 Introduction to the work within this thesis</b> .....	<b>52</b>
<b>2 ScCO<sub>2</sub> extraction as a first step in a holistic rice straw biorefinery</b> .....	<b>54</b>

<b>2.1</b>	<b>Introduction</b> .....	<b>54</b>
<b>2.2</b>	<b>Characterisation of main group of compounds in rice straw waxes</b> .....	<b>55</b>
2.2.1	Free fatty acids in rice straw .....	56
2.2.2	<i>n</i> -Alkane in rice straw .....	64
2.2.3	Fatty alcohols in rice straw.....	66
2.2.4	Fatty aldehydes in rice straw.....	67
2.2.5	Sterols in rice straw .....	69
2.2.6	Steroid ketone .....	73
2.2.7	Wax esters.....	77
<b>2.3</b>	<b>Supercritical carbon dioxide (scCO<sub>2</sub>) extraction of rice straw</b> .....	<b>79</b>
2.3.1	Extraction yields .....	80
2.3.2	Effect of temperature and pressure on scCO <sub>2</sub> extraction efficiency .....	81
2.3.3	Identification and quantification of group of key compounds in scCO <sub>2</sub> -rice straw extracts.....	82
2.3.4	Time optimization study .....	95
2.3.5	Differential scanning calorimetry (DSC).....	97
2.3.6	Scanning electron microscopic (SEM).....	98
2.3.7	Application to biorefineries.....	99
<b>2.4</b>	<b>A comparison of the microwave assisted pyrolysis of rice straw and supercritical extracted rice straw</b> .....	<b>99</b>
2.4.1	Temperature and Pressure profiles .....	100
2.4.2	Heating and pressure change rates .....	103
2.4.3	Comparison of Conventional and Microwave heating. ....	107
2.4.4	Products distribution .....	109
2.4.5	Product analysis.....	110
<b>2.5</b>	<b>Conclusion and Future work</b> .....	<b>114</b>
<b>3</b>	<b><i>The influence of potassium ions in microwave-assisted pyrolysis of rice straw</i></b> .....	<b>116</b>
<b>3.1</b>	<b>Introduction</b> .....	<b>116</b>
<b>3.2</b>	<b>The study on effect of moisture content in microwave-assisted pyrolysis</b> .....	<b>117</b>

3.2.1	Temperature and pressure profiles .....	118
3.2.2	Heating and pressure change rates .....	120
3.2.3	Thermogravimetric analysis (TGA).....	124
<b>3.3</b>	<b>The influence of silicate ions in microwave pyrolysis of rice straw.....</b>	<b>129</b>
3.3.1	Temperature and pressure profiles .....	130
3.3.2	Heating and pressure change rates .....	131
3.3.3	Thermogravimetric analysis (TGA).....	132
3.3.4	Elemental surface analysis of untreated and water-washed rice straw .....	134
<b>3.4</b>	<b>The study on the effect of potassium ions by potassium salt impregnation.....</b>	<b>139</b>
3.4.1	Temperature and pressure profile after salt impregnations.....	141
3.4.2	The comparison of pressure change rates of impregnated rice straw. ....	142
3.4.3	Influence of acid-base properties and concentration of potassium in thermal behaviour of impregnated rice straw .....	145
3.4.4	Thermal analysis .....	150
<b>3.5</b>	<b>Conclusion and Future work.....</b>	<b>152</b>
<b>4</b>	<b><i>Prawn waste residues as a source of valuable lipophilic compounds.....</i></b>	<b>156</b>
<b>4.1</b>	<b>Introduction .....</b>	<b>156</b>
<b>4.2</b>	<b>Solvent extraction of Pacific white shrimp waste residues.....</b>	<b>157</b>
4.2.1	Fatty acids in Pacific white shrimp by-product as extracted by hexane Soxhlet. .	159
4.2.2	Fatty alcohol in <i>L.vannamei</i> waste by-product.....	166
4.2.3	Monoglycerides .....	166
4.2.4	Diglycerides.....	171
4.2.5	1-O-Alkylglycerol ether lipids.....	174
4.2.6	Sterols.....	178
<b>4.3</b>	<b>Supercritical extraction of lipid from Pacific white shrimp by-product.....</b>	<b>180</b>
<b>1.1</b>	<b>Composition of extracted lipids.....</b>	<b>183</b>
<b>4.4</b>	<b>Comparison of supercritical carbon dioxide extracts and hexane Soxhlet of <i>Litopenaeus vannamei</i> by-product .....</b>	<b>185</b>

4.4.1	Comparison of fatty acids between hexane extract and scCO <sub>2</sub> extracts from <i>L. vannamei</i> by-product. ....	188
<b>4.5</b>	<b>Effect of extraction time .....</b>	<b>190</b>
<b>4.6</b>	<b>Conclusion.....</b>	<b>192</b>
<b>5</b>	<b><i>The influence of inherent prawn enzyme on extraction of PUFA by scCO<sub>2</sub>.....</i></b>	<b>194</b>
<b>5.1</b>	<b>Introduction .....</b>	<b>194</b>
<b>5.2</b>	<b>The influence of moisture content on scCO<sub>2</sub> extraction efficiency. ....</b>	<b>194</b>
5.2.1	Comparison of extraction kinetics and lipid recoveries with different drying methods.....	195
5.2.2	Quantification and comparison of lipid profiles.....	198
<b>5.3</b>	<b>The effect of autolysis time on the enzymatic process at room temperature .....</b>	<b>203</b>
5.3.1	Extraction yields .....	204
5.3.2	Quantification of lipophilic compounds after autolysis at room temperature at different duration.....	206
5.3.3	Proposed enzymatic process during autolysis of prawn by-product.....	215
<b>5.4</b>	<b>Effect of temperature and different atmospheres on autolysis of prawn waste...218</b>	
5.4.1	Extraction yields .....	219
5.4.2	Quantification of lipophilic compounds.....	221
<b>5.5</b>	<b>Conclusion and Future work .....</b>	<b>231</b>
<b>6</b>	<b><i>Materials and method .....</i></b>	<b>234</b>
<b>6.1</b>	<b>Chemicals.....</b>	<b>234</b>
6.1.1	Solvents.....	234
6.1.2	Gases.....	234
6.1.3	Standards .....	234
<b>6.2</b>	<b>Waste biomass.....</b>	<b>235</b>
6.2.1	Rice straw .....	235
6.2.2	Prawn by-product .....	235
6.2.3	Moisture content of biomasses.....	235

<b>6.3</b>	<b>Typical Soxhlet extraction .....</b>	<b>236</b>
<b>6.4</b>	<b>Lab-scale supercritical fluid extraction of rice straw and prawn by-product. ....</b>	<b>236</b>
<b>6.5</b>	<b>Lab-scale supercritical extraction of rice straw and prawn by-product (kinetics). ....</b>	<b>237</b>
<b>6.6</b>	<b>Drying process of prawn-by-products .....</b>	<b>238</b>
6.6.1	Vacuum-microwave drying.....	238
6.6.2	Freeze-drying .....	238
6.6.3	Vacuum-oven drying .....	239
<b>6.7</b>	<b>Analysis of the extracts .....</b>	<b>239</b>
6.7.1	Derivatisation of prior to gas chromatography analysis .....	239
6.7.2	High temperature- gas chromatography (HT-GC) method for analysis of rice straw wax and prawn waste lipid extract.....	239
6.7.3	HT-GC-MS (High temperature-gas chromatography mass spectrometry) procedure for analysis of extracts from rice straw and prawn by-product. ....	240
6.7.4	Differential scanning calorimetry (DSC) analysis .....	241
<b>6.8</b>	<b>Microwave-assisted pyrolysis of rice straw .....</b>	<b>241</b>
6.8.1	Biomass preparation .....	241
6.8.2	Pre-treatment of rice straw with water .....	242
6.8.3	Potassium salt impregnation .....	242
6.8.4	Small scale single microwave-assisted pyrolysis of rice straw. ....	243
<b>6.9</b>	<b>Analysis of products from microwave-assisted pyrolysis of rice straw. ....</b>	<b>243</b>
6.9.1	Inductively Coupled Plasma (ICP).....	243
6.9.2	Scanning electron microscopy (SEM) and Scanning electron microscope coupled with Energy-dispersive X-ray spectroscopy (SEM/EDX).....	243
6.9.3	SEM analysis .....	244
6.9.4	Elemental analysis.....	244
6.9.5	Characterisation of gas fraction.....	244
6.9.6	Characterisation of liquid fraction .....	244
6.9.7	Simultaneous thermal analysis .....	245
<b>6.10</b>	<b>Autolysis of prawn by-product .....</b>	<b>245</b>

6.10.1	Autolysis at room temperature .....	245
6.10.2	Autolysis at different atmospheres and denaturation of the prawn enzyme...245	
<b>7</b>	<b><i>Conclusion and Future work</i> .....</b>	<b>248</b>
<b>7.1</b>	<b>Chapter 2 ScCO<sub>2</sub> extraction as a first step in a holistic rice straw biorefinery.....</b>	<b>248</b>
<b>7.2</b>	<b>Chapter 3 The influence of K<sup>+</sup> in microwave-assisted pyrolysis of rice straw .....</b>	<b>249</b>
<b>7.3</b>	<b>Chapter 4 Prawn waste residues as a source of valuable lipophilic compounds ...</b>	<b>250</b>
<b>7.4</b>	<b>Chapter 5 The influence of moisture content on scCO<sub>2</sub> extraction efficiency.....</b>	<b>251</b>
	<b><i>Abbreviation</i> .....</b>	<b>254</b>
	<b><i>References</i>.....</b>	<b>255</b>

# List of Tables

Table 1-1 Principles of Green chemistry applied in this thesis. ....	29
Table 1-2 Compounds identified in rice straw wax.....	33
Table 1-3 Groups of lipophilic molecules detected in prawn waste lipid. ....	36
Table 1-4 Critical pressure and temperatures of various compounds. <sup>59</sup> .....	42
Table 1-5 tan $\delta$ values of some solvent at 25°C.....	48
Table 2-1 List of free fatty acid present in rice straw wax extracted using hexane, molecular weight and their abundance in $\mu\text{g/g}$ of dry plant. ....	62
Table 2-2 List of identified n-alkanes with their molecular weights and abundances in $\mu\text{g/g}$ of plant .....	65
Table 2-3 List of free fatty alcohols in rice straw wax extracted with hexane and the abundance in $\mu\text{g/g}$ dry biomass.....	67
Table 2-4 List of fatty aldehydes identified in rice straw extract and the abundance in $\mu\text{g/g}$ dry plant .....	68
Table 2-5 Characteristic fragments of campesterol and $\beta$ -sitosterol OTMS. ....	73
Table 2-6 Extraction yields obtained at different pressures and temperatures for rice straw. .	80
Table 2-7 Type and quantity of saturated and unsaturated fatty acids in rice straw waxes obtained from different conditions using $\text{scCO}_2$ extraction for 4 hours. ....	84
Table 2-8 Types and quantity of main hydrocarbons in rice straw waxes obtained from different conditions using $\text{scCO}_2$ extraction for 4 hours.....	87
Table 2-9 Types and quantities of long chain fatty alcohols in rice straw waxes obtained from different conditions using $\text{scCO}_2$ extraction for 4 hours. ....	89
Table 2-10 Types and quantities of long chain fatty aldehydes in rice straw waxes obtained from different conditions using $\text{scCO}_2$ extraction for 4 hours. ....	89
Table 2-11 Types and quantities of long chain fatty aldehydes in rice straw waxes obtained from different conditions using $\text{scCO}_2$ extraction for 4 hours. ....	91

Table 2-12 Types and quantities of steroid ketones in rice straw waxes obtained from different conditions using scCO <sub>2</sub> extraction for 4 hours.....	93
Table 2-13 Types and quantities of wax esters in rice straw waxes obtained from different conditions using scCO <sub>2</sub> extraction for 4 hours.....	94
Table 2-14 Heating rates and maximum temperatures during microwave pyrolysis.....	103
Table 2-15 Pressure change rates and temperature at maximum pressure change rates during microwave pyrolysis.....	106
Table 2-16 Characteristics of untreated and scCO <sub>2</sub> extracted rice straw pre and post microwave pyrolysis.....	113
Table 3-1 The rates of heating and pressure change of untreated, dried and remoistened rice straw during MW pyrolysis.....	123
Table 3-2 ICP results of untreated and water treated rice straws in µg/g of biomass. ....	136
Table 3-3 The maximal temperature change rate and its corresponding temperature of each rice straw .....	142
Table 3-4 ICP results of impregnated rice straw in K-salt and Na-salt solution with high and low concentration. ....	149
Table 4-1 Abundance (in µg/g dry biomass) of free fatty acids in <i>L. vannamei</i> by-product extract using hexane Soxhlet for 2 hours.....	164
Table 4-2 Abundance (in µg/g dry biomass) of 1-hexacosanol in <i>L. vannamei</i> by-product from hexane extract in 2 hours.....	166
Table 4-3 Abundance (in µg/g dry biomass) of monoglycerides in <i>L. vannamei</i> waste from hexane extract. ....	170
Table 4-4 Abundance (in µg/g dry biomass) of diglycerides in <i>L. vannamei</i> by-product.....	173
Table 4-5 Abundance (in µg/g dry biomass) of ethers of glycerol in <i>L. vannamei</i> by-product .	177
Table 4-6 Characteristic fragmentations of Δ <sup>5</sup> -sterols .....	179
Table 4-7 Abundance (in µg/g dry biomass) of ethers of sterols in <i>L. vannamei</i> . ....	180



Table 4-8 Experimental conditions, densities and yields for extractions of <i>L. vannamei</i> by-product .....	181
Table 4-9 Typical abundances (in µg/g dry biomass) of lipid as extracted by hexane Soxhlet in 2 hours and supercritical carbon dioxide in 2 hours of <i>L.vannamei</i> by-product .....	186
Table 5-1 Comparison of lipid composition (in µg/g dry biomass) after different drying methods prior to scCO <sub>2</sub> at 40°C, 400 bar of the fractions collected in 2 hours. ....	201
Table 5-2 Abundances (in µg/g dry biomass) of lipophilic components as extracted by scCO <sub>2</sub> in 2 hours of prawn by-product after autolysis of 3, 6 and 24 hours. ....	206
Table 5-3 Composition of lipids extracted from cephalothorax and hepatopancreas of Pacific white shrimp ( <i>Litopenaeus vannamei</i> ) using Bligh and Dyer method. <sup>72</sup> .....	215
Table 5-4 Abundances (in µg/g dry biomass) of lipid as extracted by supercritical carbon dioxide in 2 hours of prawn by-product after autolysis in different conditions in 24 hours .....	222

# List of Figures

Figure 1-1 Image of open field burning in Loei Province, Thailand. ....	31
Figure 1-2 Structure of Cellulose, Hemicellulose and Lignin. ....	32
Figure 1-3 The Prawn wasted bio-refinery. ....	35
Figure 1-4 Structure of Chitin (left) and Chitosan (Right). ....	35
Figure 1-5 Biorefinery treatment of biomass. ....	39
Figure 1-6 Diagram of Soxhlet apparatus. ....	40
Figure 1-7 Phase diagram for carbon dioxide. <sup>60</sup> ....	41
Figure 1-8 Electromagnetic spectrum. ....	47
Figure 1-9 Conventional pyrolysis process. ....	48
Figure 1-10 Microwave-assisted pyrolysis process. ....	49
Figure 2-1 Gas chromatogram of derivatised rice straw wax obtained from Soxhlet extraction using hexane. ....	56
Figure 2-2 EI Mass spectra of TMS ester of A) hexadecanoic acid(C <sub>16:0</sub> ) and B) octadecanoic acid (C <sub>18:0</sub> ) ....	57
Figure 2-3 EI Mass spectra of TMS esters of A) oleic acid (C <sub>18:1</sub> ) B) linoelic acid (C <sub>18:2</sub> ). ....	58
Figure 2-4 McLafferty rearrangement occurs through a six membered transition state, resulting in $\gamma$ H-transfer and $\beta$ -cleavage, the formation of ions of $m/z$ 132 and 117 was observed. <sup>115</sup> ....	59
Figure 2-5 Formation of EI fragments $m/z$ 145 and 129 for TMS ester of fatty acids. <sup>115,118</sup> ....	60
Figure 2-6 Formation pathway of [M-131] <sup>+</sup> of TMS of azelaic acid. <sup>120</sup> ....	61
Figure 2-7 EI mass spectra of silylated azelaic acid from rice straw. ....	61
Figure 2-8 Typical free fatty acid distribution of rice straw. ....	63
Figure 2-9 EI mass spectra of Tritriacontane (C <sub>33</sub> ) ....	64
Figure 2-10 EI mass spectra of trimethylsilyl ether of 1-Triacontanol (C <sub>30</sub> ) ....	66
Figure 2-11 EI mass spectra of 1- triacontanal (C <sub>30</sub> ) ....	68

Figure 2-12 Structure of sterols present within rice straw wax.....	69
Figure 2-13 The EI Mass spectrum of trimethylsilyl ether of campesterol.....	70
Figure 2-14 The EI Mass spectrum of trimethylsilyl ether of $\beta$ -sitosterol.....	70
Figure 2-15 Formation of the characteristic fragment $m/z$ $[M-90]^+$ .....	71
Figure 2-16 Fragmentation of a $\Delta^5$ -steryl TMS ether to the characteristic $m/z$ 129 ( $[C_{1},C_{3}+TMSO]^+$ ). <sup>135,136,139</sup> .....	71
Figure 2-17 Fragmentation $\Delta^5$ -steryl TMS ether to the characteristic $m/z$ $[M-129]^+$ ( $[M-C_{1},C_{3}-$ TMSO] $)^+$ ions. <sup>138</sup> .....	72
Figure 2-18 Fragmentations of a $\Delta^5$ -steryl TMS ether to the characteristic $m/z$ 255 ( $[M-SC-$ TMSOH] $)^+$ ) by loss of the side chain. <sup>140-142</sup> .....	72
Figure 2-19 Structure of A) stigmast-4-en-3-one and B) (5 $\alpha$ )-stigmastane-3,6-dione.....	73
Figure 2-20 Label of carbon atom in the structure of Stigmast-4-en-3-one.....	74
Figure 2-21 Mechanism of formation of fragment $m/z$ 124 in steroid ketones. <sup>144</sup> .....	74
Figure 2-22 Overall formation of $m/z$ 288 $[M-124]^+$ via hydrogen migration. <sup>143</sup> .....	75
Figure 2-23 Fragmentation of $m/z$ 370 via the loss of ketene from ring A. ....	76
Figure 2-24 EI mass spectra of Stigmast-4-en-3-one.....	76
Figure 2-25 EI mass spectra of (5 $\alpha$ )-Stigmastane-3,6-dione.....	77
Figure 2-26 EI mass spectra of ester of hexadecanoic acid ( $C_{16}$ ) and hexacosanol( $C_{26}$ ): $C_{42}$ ( $C_{16:26}$ ). .....	78
Figure 2-27 Two-level factorial design experiments. ....	79
Figure 2-28 The contour plot of wax yield under different condition of $scCO_2$ extraction as designated according to the two-level factorial design. ....	81
Figure 2-29 Comparison on concentration of free fatty acids in rice straw waxes extracted using $scCO_2$ and hexane Soxhlet for 4 hours. ....	85
Figure 2-30 Comparison on concentration of free fatty acids in rice straw waxes extracted using $scCO_2$ and hexane Soxhlet for 4 hours. ....	87

Figure 2-31 Comparison on concentration of free fatty alcohols in rice straw waxes extracted using scCO <sub>2</sub> and hexane Soxhlet for 4 hours. ....	88
Figure 2-32 Comparison on concentration of fatty aldehydes in rice straw waxes extracted using scCO <sub>2</sub> and hexane Soxhlet for 4 hours. ....	90
Figure 2-33 Comparison on concentration of fatty aldehydes in rice straw waxes extracted using scCO <sub>2</sub> and hexane Soxhlet for 4 hours. ....	92
Figure 2-34 Comparison on concentration of steroid ketones in rice straw waxes extracted using scCO <sub>2</sub> and hexane Soxhlet for 4 hours. ....	93
Figure 2-35 Comparison on concentration of wax esters in rice straw waxes extracted using scCO <sub>2</sub> and hexane Soxhlet for 4 hours. ....	95
Figure 2-36 Variation in total accumulated crude extract against extraction times by scCO <sub>2</sub> extraction at 65 °C and 400 bar. ....	96
Figure 2-37 DSC plot showing the melting profiles for different waxes (A) hexane soxhlet (B) scCO <sub>2</sub> at 65 °C and 400 bar for 4 hours (C) Commercial candelilla wax (D) Commercial beeswax .....	97
Figure 2-38 SEM micrograms of rice straw (a) before scCO <sub>2</sub> extraction (b) after scCO <sub>2</sub> extraction at 65 °C, 400 bar for 4 hours .....	98
Figure 2-39 Particle size distribution of untreated and scCO <sub>2</sub> treated rice straw after milling.	100
Figure 2-40 Temperature profiles of microwave pyrolysis of untreated and B) scCO <sub>2</sub> treated rice straw with different particle sizes. ....	101
Figure 2-41 Pressure profiles of microwave-assisted pyrolysis of untreated and scCO <sub>2</sub> treated rice straw with different particle sizes. ....	102
Figure 2-42 The comparison and the evolution of heating rates and pressure change rates of untreated and scCO <sub>2</sub> treated rice straw according to particle sizes A) >2000 μm, B) 500-2000 μm, C) 300-500 μm, D) 180-500 μm, E) 125-180 μm and F) <125 μm. ....	105
Figure 2-43 TG and DTG curves of the raw materials A) Untreated B) scCO <sub>2</sub> Treated rice straw .....	108
Figure 2-44 TG and DTG curves of solid chars from A) Untreated B) scCO <sub>2</sub> Treated rice straw	109

Figure 2-45 Pyrolytic Product distribution of untreated (U) and scCO <sub>2</sub> treated (T) rice straw.	110
Figure 2-46 FT-IR gas product from microwave pyrolysis of scCO <sub>2</sub> treated (above) and untreated rice straw (below).	111
Figure 2-47 HT-GC-MS chromatograms of bio oil of liquid fractions of A) Rice straw and B) Extracted rice straw.	112
Figure 3-1 Interaction of water in cellulose.	118
Figure 3-2 Comparison of temperature and pressure profiles of untreated, oven-dried and rehydrated rice straws in MAP	119
Figure 3-3 Comparison of rate of heating of untreated rice straw, dried rice straw and rehydrated rice straw in microwave pyrolysis.	121
Figure 3-4 Pressure change rates (A) and total pressure evolution (B) of untreated, oven-dried and rehydrated rice straw in microwave pyrolysis.	122
Figure 3-5 TGA of raw materials before microwave-assisted pyrolysis.	124
Figure 3-6 TGA of solid products after microwave-assisted pyrolysis.	125
Figure 3-7 Profiles of the changes in the dielectric loss ( $\epsilon''$ ) and dielectric constant ( $\epsilon'$ ) of water with changes in temperature.	126
Figure 3-8 Hydrogen bonding of hydroxyl groups and water between cellulose units A) Single hydrogen bonded water B) Double bonded and C) Multi-layer hydrogen bonding between water molecules and cellulose. <sup>182</sup>	128
Figure 3-9 Pre-treatment of rice straw with water	129
Figure 3-10 Temperature and pressure profile of untreated and water treated rice straw.	130
Figure 3-11 Heating rates of untreated and water treated rice straw during microwave pyrolysis.	131
Figure 3-12 Pressure change rate (A) and Pressure evolution (B) of untreated and water treated rice straw during microwave pyrolysis.	132
<b>Figure 3-13</b> Thermogravimetric analysis (TG) of Raw materials (A) and Chars (B).	133
Figure 3-14 XPS of untreated rice straw.	135

Figure 3-15 XPS of water treated rice straw .....	135
Figure 3-16 SEM of A) untreated rice straw and B) water treated rice straw.....	137
Figure 3-17 Elemental mapping analysis using SEM/EDS mapping of Si and K of A) untreated rice straw and B) water washed rice straw.....	137
Figure 3-18 Chemical bonding of potassium and calcium ions. ....	138
Figure 3-19 Temperature and Pressure profiles of the impregnation study of potassium compounds with 20 mg of K <sup>+</sup> per 1 g of washed rice straw.....	141
Figure 3-20 Pressure change rates of untreated, water treated and impregnated rice straw during MAP.....	144
Figure 3-21 Influence of pK <sub>b</sub> of potassium salts in the gasification of during the microwave pyrolysis rice straw. ....	146
Figure 3-22 Self-association cellulose due to the presence of H-bonding. <sup>184</sup> .....	147
Figure 3-23 A propose structure of the complex of deprotonated cellulose, after impregnated in potassium salt solution. <sup>190</sup> .....	148
Figure 3-24 Zoomed in DTG of the raw materials cellulose decomposition region. ....	151
Figure 3-25 DTG of Chars at cellulose decomposition region. ....	152
Figure 4-1 Gas chromatogram of <i>Litopenaeus vannamei</i> from hexane extract A) Without Derivatisation B) with trimethylsilyl derivatization. ....	158
Figure 4-2 EI mass spectra of A) hexadecanoic acid (C <sub>16:0</sub> ) trimethylsilyl ester B) octadecanoic acid (C <sub>18:0</sub> ) trimethylsilyl ester.....	159
Figure 4-3 The mass spectrum of linoleic acid trimethylsilyl ester (C <sub>18:2(n-6)</sub> ) A) EI mass spectra B) FI mass spectra .....	160
Figure 4-4 The mass spectrum of linoleic acid trimethylsilyl ester (C <sub>18:1(n-9)</sub> ) A) EI mass spectra B) FI mass spectra .....	161
Figure 4-5 Characteristic fragmentation of ω ion and α ion for A) n-6 terminal (ω6) in ARA (C <sub>20:4(n-6)</sub> ) B) and C) n-3 terminal (ω3) in EPA (C <sub>20:5(n-3)</sub> ) and DHA (C <sub>20:6(n-3)</sub> ) respectively .....	161
Figure 4-6 EI mass spectra of trimethylsilyl ester of PUFAs A) ARA B) EPA C) DHA.....	162

Figure 4-7 Typical free fatty acid distribution of <i>L. vannamei</i> cepharothorax by hexane Soxhlet extraction in 2 hours. ....	163
<b>Figure 4-8</b> Mass spectra of 1-hexacosanol trimethylsilyl ether (C16 fatty alcohol) from <i>L. vannamei</i> by-product .....	166
Figure 4-9 Characteristic fragments of monoglycerides trimethylsilyl ethers.....	167
Figure 4-10 EI mass spectra of A) Hexadecanoic acid, 2,3 bis-(OTMS) propyl ester ( $\alpha$ -glyceryl palmitate) B) Hexadecanoic acid, 1,3 bis-(OTMS) propyl ester ( $\beta$ -glyceryl palmitate) .....	168
Figure 4-11 Percentage of composition of monoglycerides in <i>L. vannamei</i> from Soxhlet extraction with hexane.....	169
Figure 4-12 EI mass spectra of trimethylsilyl ethers of A) 1,2 Dipalmitin and B) 1,3 Dipalmitin .....	171
Figure 4-13 EI mass spectra potential fragments from trimethylsilyl ethers of 1,2 Dipalmitin and 1,3 Dipalmitin.....	172
Figure 4-14 EI mass spectra potential fragment of m/z 371 from trimethylsilyl ethers of 1,2 Dipalmitin and 1,3 Dipalmitin .....	172
Figure 4-15 EI mass spectra potential fragments of m/z 145 and 129 from trimethylsilyl ethers of 1,2 Dipalmitin and 1,3 Dipalmitin .....	173
Figure 4-16 Structure of Chimyl alcohol (1-O-Hexadecylglycerol) and Batyl alcohol (1-O-Octadecylglycerol).....	174
Figure 4-17 EI mass spectra of A) 1-O-hexadecyl-2,3-di-O-TMS-glycerol B) 1-O-octadecyl-2,3-di-O-TMS glycerol.....	175
Figure 4-18 Scheme of fragmentation of 1-O-hexadecyl-2,3-di-O-TMS-glycerol 1-O-hexadecylglycerol (chimyl alcohol) .....	176
Figure 4-19 EI mass spectra of A) Cholesteryl trimethylsilyl ether B) Campesterol trimethylsilyl ether C) Stigmasteryl trimethylsilyl ether D) $\beta$ -sitosteryl trimethylsilyl ether.....	178
Figure 4-20 Fragmentation scheme of Cholesteryl trimethylsilyl ether. ....	179
Figure 4-21 Experimental design for optimization of supercritical CO <sub>2</sub> extraction .....	181

Figure 4-22 Percentage crude yields of Pacific white shrimp lipid from scCO <sub>2</sub> extraction .....	182
Figure 4-23 A) A depiction of yield of lipid extractives as a function of temperature and pressure. B) A depiction of density of carbon dioxide as a function of temperature and pressure.....	182
Figure 4-24 Breakdown of main groups on Pacific white shrimp by-product extract from scCO <sub>2</sub> extraction .....	183
Figure 4-25 Percentage composition of lipids compounds for <i>L. vannamei</i> as extracted in five different conditions by supercritical carbon dioxide for 2 hours and hexane Soxhlet extraction for 2 hours .....	184
Figure 4-26 Effect of time on percentage yield of lipid extracts at 40°C, 400 bar.....	191
Figure 5-1 Accumulated yields of different drying methods.....	196
Figure 5-2 The influence of different drying methods on the quantities of ARA, EPA and DHA from scCO <sub>2</sub> extraction at 40°C and 400 bar in 2 hours. (Note: Vacuum-microwave drying (VMD), Freeze-drying (FD) and Vacuum-oven drying (VOD)) .....	199
Figure 5-3 Yield of lipid from the mixture of cephalothorax and hepatopancreas of Pacific white shrimp affected by autolysis at 0, 3, 6 and 24 hours. ....	205
Figure 5-4 Abundance of fatty alcohol, ethers of glycerol, monoglycerides, diglycerides and sterols after autolysis of 3, 6 and 24 hours at room temperature (scCO <sub>2</sub> extraction at 40°C, 400 bar for 2 hours).....	209
Figure 5-5 Concentrations of saturated fatty acids (SFAs), monounsaturated fatty acids (MUFAs) and polyunsaturated fatty acids(PUFAs) after autolysis of 3, 6 and 24 hours at room temperature. (scCO <sub>2</sub> extraction at 40°C, 400 bar for 2 hours) .....	210
Figure 5-6 The increase trend of ARA, EPA and DHA after autolysis of 3,6 and 24 hours via scCO <sub>2</sub> extraction at 40°C, 400 bar for 2 hours.....	212
Figure 5-7 Comparison in abundance of ARA, EPA and DHA between scCO <sub>2</sub> extraction in 2 hours at 40°C, 400 bar, with 3, 6 and 24 hours autolysis and hexane soxhlet extraction of fresh prawn waste in 2 hours.....	213
Figure 5-8 Increasing linear trend of cholesterol after autolysis 3, 6 and 24 hours. ....	214
Figure 5-9 Proposed enzymatic process during autolysis of prawn-by products.....	217



Figure 5-10 Yields of crude lipid by scCO <sub>2</sub> in 2h after different condition of autolysis for 24h.	220
Figure 5-11 Concentrations of A) Diglycerides B) Monoglycerides C) Sterols and D) Fatty acids with different pre-treatment conditions prior to scCO <sub>2</sub> extraction at 40°C, 400 bar for 2 hours. .....	226
Figure 5-12 Comparison of SFA, MUFA and PUFA from different conditions prior to scCO <sub>2</sub> extraction at 40°C, 400 bar for 2 hours. ....	227
Figure 5-13 Comparison of abundance in ARA, EPA and DHA from different conditions prior to scCO <sub>2</sub> extraction at 40°C, 400 bar for 2 hours. ....	229
Figure 5-14 Chromatogram of transesterified sample catalysed by L.vannamei by-product. .	230
Figure 6-1 Set-up for drying process. (1) Microwave reactor, (2) sample vessel, (3) system control and monitoring console, (4) and (5) round bottom flasks for collection water, (6) vacuum pump. .....	238
Figure 6-2 Calculation of response factor for silylated cholesterol. ....	240
Figure 6-3 Particle size distribution of untreated and scCO <sub>2</sub> treated rice straw after sieving.	242

# Acknowledgements

Firstly, I would like to thank Dr Andrew Hunt and Professor James Clark for accepting me to undertake this PhD at York. I am grateful to all my supervisors Dr Andrew Hunt, Dr Thomas Farmer, Dr Vitaliy Budarin and Professor James Clark for their encouragement, support and for providing me the chance of attending and presenting at several international conferences.

For financial assistance I would like to thank the Thai Government, the Oil Refinery Contract Contribution Fund and the Ministry of Energy, Thailand. I would also like to thank all the members of the Royal Thai Embassies in London who have helped during my studies in the UK.

I would like to thank several people for their technical support during this project. Paul Elliott for his assistance in the lab. Dr Meg Stark for her assistance with SEM. I would also like to thank Tom Attard for his day to day help around the lab and also for generating an endless source of gossip.

I would like to particularly thank Dr Andrew Hunt for all his help, guidance, inspiration and understanding. A big thanks must also be given to all the people who have helped in proof reading my thesis, including Andy, Tom, Vitaliy and Tom. I would like to thank my housemates Suang who have helped with formatting the thesis and Aum for all Line call support. Thanks Pear for all the laughter and P'Pex for the SEM/EDX. Huge thanks to all members of the group past and present that have helped with work and also having some great times within the green chemistry centre.

I have had a great time in York, thank to all the wonderful people I have met – including friends from Khao San Rd. Thank you all for the amazing memories.

Finally to my family, thank you Mum and Dad for their love and support throughout my studies in York and also in Strasbourg. Thanks for believing in me and always being there for me.

# Declaration

I declare that this thesis is a presentation of original work and I am the sole author. This work has not previously been presented for an award at this, or any other, University. All sources are acknowledged as References. Some of the results of this thesis were obtained in collaboration with other workers, who are fully acknowledged in the text.

Chanettee Sikhom

March 2018

# **Chapter 1**

## **Introduction**

# 1 Introduction

## 1.1 Scope of the project

The project focuses on the use of two different types of waste biomass as feedstocks of sustainable production of high-valued chemicals using Green chemistry technologies. The selected bio-wastes were rice straw and *Litopenaeus vannamei* or Pacific white shrimp by product. The project's main areas of study include:

### 1.1.1 Extraction of lipids from the waste biomass

The lipid composition of rice straw and prawn by-products were extracted using conventional organic solvent and supercritical carbon dioxide. The lipophilic extractives were identified and characterised with potential applications proposed. A comparison between the products obtained from the conventional organic solvent-extraction and supercritical-extraction were also carried to assess the efficiency of the process.

### 1.1.2 Optimisation of supercritical extraction

A two-level factorial design was used to optimise the extraction process. The experimental design can influence the extraction efficiency, including the temperature and pressure applied on the process. Different lipophilic components were able to be selectively extracted by adjusting the condition. High value-added compounds were obtained with the supercritical extraction from rice straw and prawn by-products.

### 1.1.3 Combination of supercritical carbon dioxide and microwave technologies.

The supercritical-extracted residue was valorised in the next step by microwave-assisted pyrolysis in order to evaluate the suitability of this extraction method to be used as pre-treatment step in the rice straw bio-refinery. Comparison of heating and pressure change rates were made in order to understand the thermal behaviour of the biomass towards microwave irradiation. The product distribution of both raw materials was also performed.

#### **1.1.4 Study of autocatalysis on gasification of rice straw during microwave pyrolysis**

To be able to understand the specific thermal behaviour of rice straw, a series of hypotheses was made, and experimental procedure was systematically planned to validate each hypothesis. The decomposition of rice straw occurred at much lower temperature compared to the conventional heating, which was due to the dielectric properties of the biomass.

#### **1.1.5 Production of n-3 and n-6 PUFA via endogenous enzymes of prawn-waste**

Prawn waste contains valuable lipophilic compounds such as polyunsaturated fatty acids especially arachidonic acid (ARA), eicosapentaenoic acid (EPA) and docosahexaenoic acid (DHA) which are present in high concentration. The enzymatic hydrolysis occurred naturally in the biomass resulting in higher extraction lipid yield and more ARA, EPA and DHA were obtained in significantly higher concentration. This could be a promising method of production of n-3 and n-6 polyunsaturated fatty acids which are high valued chemicals.

### **1.2 Towards sustainable development**

Nowadays global attention is drawn to the concept of sustainable development, which has become an important concept since the World Conservation Strategy in 1980. This term strongly concerns the future well-being for the world population and importantly addresses environmental as well as socio-economic points of views.<sup>1</sup> This action of gathering both environmental and socio-economic issues was expressed in the Brundtland Report in 1987 (United Nations Commission on Environment and Development); the definition of sustainable development is as:

*“meeting the need of the present without compromising the ability of future generations to meet their needs”.*<sup>2-4</sup>

The world's industrial economies are predominantly dependent on petroleum resources for both chemical products and energy.<sup>5</sup> Moreover, developing and less developed countries are recently new targets for industrialisation, as a result, the natural reserves within these areas are being consumed at a rapid rate and therefore stress is being placed on the environment.<sup>6</sup> As industrialisation takes place higher living standards will be demanded by billions of people. There are 78 million births per year and 95% of this statistic occurs in less developed countries.

Therefore, the availability of natural resources is only set to decrease.<sup>7</sup> The continued use of the world's resources at the present rate is apparently resulting in global warming, which causes serious environmental and political issue.<sup>8</sup> Due to the depletion of crude oil with this increasing rate of world population and demand, sustainable development by all sectors including policymakers, industries and public is essential.<sup>6</sup> With new regulations, industries are forced to change processes from oil-based to bio-based, as the bio-based products can potentially replace the existing petroleum-based products using an environmental friendly technologies.<sup>5</sup> Using renewable bio-resources or carbon neutral products is environmental advantageous. Currently, chemical products obtained from agriculture feedstocks have been recognised and are becoming increasingly important.<sup>9</sup>

### 1.3 Green chemistry

Over the last two decades, chemists all over the world have been developed new chemistries that are more benign to human health and the environment by using their innovation to create new synthetic methods, reaction conditions, analytical tools, catalysts and processes under the new concept of Green Chemistry. Consequently, the term of Green Chemistry was launched by EPA as:

*“To promote innovative chemical technologies that reduce or eliminate the use or generation of hazardous substances in the design, manufacture and use of chemical products.”<sup>10,11</sup>*

According to Paul Anastas, Green chemistry is “the use of chemistry techniques and methodologies that reduce or eliminate the use or generation of feedstocks, products, by-products, reagents, etc., that are hazardous to human health or the environment.”<sup>11</sup> It is also considered as “a fundamental and important tool in accomplishing pollution prevention”.<sup>6,8,12,13</sup> Green chemistry emphasises on the process of chemical production with less or no environmental issue. In 1997, Paul Anastas and John Warner set up the 12 fundamental principles of Green chemistry, which are as follows.<sup>12</sup>

### **1. Prevention**

It is better to prevent waste than to treat or clean up waste after it is formed.

### **2. Atom economy**

Synthetic methods should be designed to maximise the incorporation of all materials used in the process into the final product.

### **3. Less hazardous chemical synthesis**

Wherever practicable, synthetic methodologies should be designed to use and generate substances that possess little or no toxicity to human health and the environment.

### **4. Designing safer chemicals**

Chemical products should be designed to preserve efficacy of function whilst reducing toxicity.

### **5. Safer solvents and auxiliaries**

The use of auxiliary substances (e.g.: solvents, separation agents etc.) should be made unnecessary wherever possible and, innocuous when used.

### **6. Design for energy efficiency**

Energy requirements should be recognised for their environmental and economic impacts and should be minimised. Synthetic methods should be conducted at ambient temperature and pressure.

### **7. Use of renewable feedstock**

A raw material of feedstock should be renewable rather than depleting wherever technically and economically practicable.

### **8. Reduce derivatives**

Unnecessary derivatisation (blocking group, protection/deprotection and temporary modification of physical/chemical processes) should be avoided whenever possible.

### **9. Catalysis**

Catalytic reagents (as selective as possible) are superior to stoichiometric reagents.

### **10. Design for degradation**

Chemical products should be designed so that at the end of their function they do not persist in the environment and break down into innocuous degradation products.



### 11. Real-time analysis for pollution prevention

Analytical methodologies need to be further developed to allow for real-time, in process monitoring and control prior to the formation of hazardous substances.

### 12. Inherently safer chemistry for accident prevention

Substances and the form of a substance used in a chemical process should be chosen so as to minimize the potential for chemical accidents, including releases, explosions and fires.

By examining the principles of Green chemistry, the work carried out in this thesis is particularly relevant to several principles as listed in **Table 1-1**. In order to reduce the reliance of chemical from fossil fuel, the use of renewable bio-resources will be a potential alternative. The use of starting materials derived from renewable feedstock would be environmentally beneficial, as the production process is often closer to be carbon neutral.

**Table 1-1** Principles of Green chemistry applied in this thesis.

Principles	Descriptions
1	The overall aim of this project is to valorise the use of waste biomass as well as minimise the generation of waste.
5	The use of organic solvents was minimised in the extraction process by using scCO <sub>2</sub> (Chapter 2 and 4) and in microwave-assisted pyrolysis of rice straw (Chapter 2 and 3) as well as in endogenous enzymatic hydrolysis (Chapter 4 and 5) with solvent-free process.
6	Microwave (Chapter 2 and 3) and supercritical fluid technologies (Chapter 2, 3 and 5) were selected as alternatives to those conventional methods which are considered as time consuming and energy intensive.
7	Thai agricultural and aqua-cultural wastes were selected to use in this project for the reason of sustainability.
9	Endogenous protease found in prawn waste was utilised to increase the total recovery of polyunsaturated fatty acids within the prawn waste prior to extraction (Chapter 4 and 5).
12	All the selected techniques, including microwave and supercritical fluid, used in this project are equipped with safety systems to avoid chemical accidents and explosions.

## 1.4 Feedstock

The term of “feedstock” refers to the raw materials used in the process. An important stage of an integrated biorefinery system is the feedstock as it needs to be renewable, consistent and can be supplied regularly. Renewable raw materials are ideally provided from four different sectors: i) agricultural (crop and residues) ii) forestry iii) industries (process residues and leftovers) and households (municipal solid and wastewaters) iv) aquaculture (algae and seaweeds).<sup>14</sup>

In this project, two different sources of waste biomass were selected. The first feedstock is from agriculture, which is rice straw, one of the most abundant agricultural wastes in Asia, especially in Thailand. The second raw material is from aqua-cultural sector, a growing industrial activity, which is prawn by-products.

### 1.4.1 Rice straw

Rice is the world’s second largest cereal crop after wheat (Encyclopedia Britannica).<sup>15</sup> It is a semi-aquatic plant, which is harvested annually. There are a variety of approximately 22 species of the genus *Oryza*. Among all *Oryza sativa* is the widely grown and consumed in the world. It is consumed approximately by 3.5 billion people worldwide. Rice production and consumption are accounted among the highest for Asian people and the rate of consumption has been increasing since 1970.<sup>16</sup> Rice is currently grown in over a hundred countries, with the production of more than 715 million tonnes of rice annually or 480 million tonnes of milled rice.

Rice cultivation is also an important source of income and employment for about 200 million households in the developing world. Therefore, rice straw appears to be one of the most outstanding agricultural residues available nowadays especially in South and South-East Asia including Thailand where rice is widely grown.<sup>17</sup> The production of rice straw is accounted for as the largest amount of crop residues with 330 million metric tonnes generated annually.<sup>15</sup> Thailand is one of the world’s largest rice producer and exporter produced around 31.5 metric tonnes of rice, exporting around 8.9 metric tonnes, contributing about 30% of the global trade. This resulted in approximately 38 million tonnes of rice straw in 2010.<sup>18</sup> Due to the high cost of management and transport, in order to prepare for next cropping, rice straw is usually either subjected to open field burning, which resulted in emission of greenhouse gas emission such

a CO<sub>2</sub>, CO, CH<sub>4</sub>, and N<sub>2</sub>O.<sup>18-22</sup> This habit causes serious problems in terms of environment and human health.<sup>23</sup> **Figure 1-1** illustrates the result of field burning in Thailand.

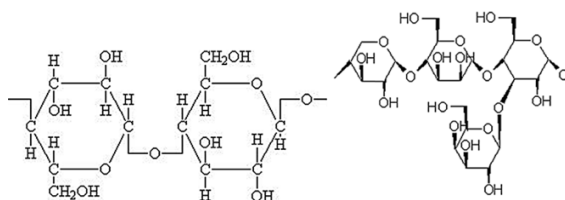


**Figure 1-1** Image of open field burning in Loei Province, Thailand.

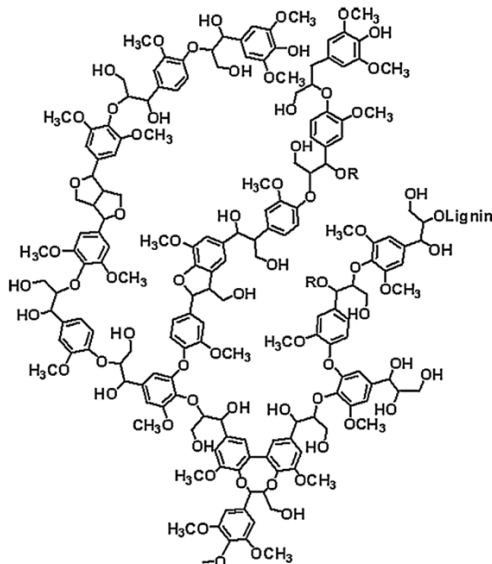
As rice straw is a lignocellulosic biomass, which consists of three main components, cellulose, hemicellulose and lignin (see **Figure 1-2** for chemical structures). Rice straw also contains high concentration of minerals including Na, K, Ca, Mg, Al, Fe, Mn, P and Si.<sup>15,24-27</sup>

To the best of author's knowledge, there is only one study on the extraction of rice straw using different organic solvents including toluene-ethanol, chloroform, dichloromethane, petroleum ether and hexane using Soxhlet apparatus.<sup>28</sup> The group of compounds identified is listed in **Table 1-2**.

A



B



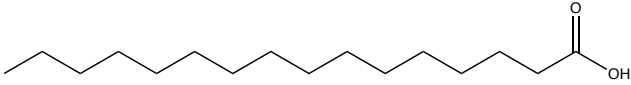
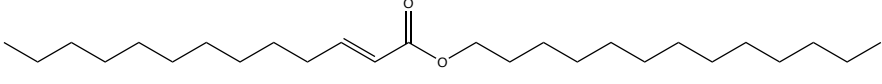
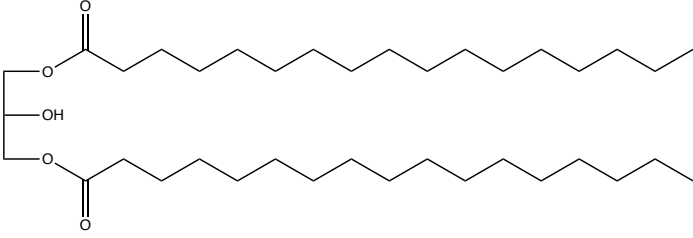
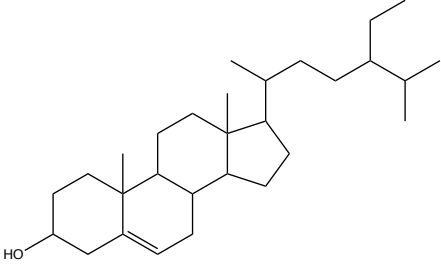
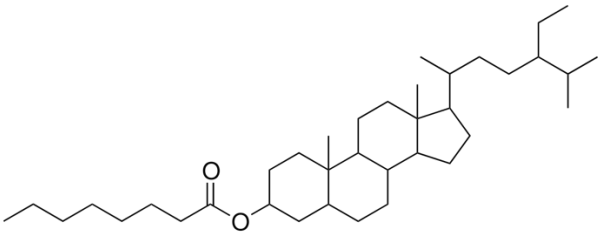
C

**Figure 1-2** Structure of Cellulose, Hemicellulose and Lignin.

(Reproduced from The international Journal of Biological Macromolecules, 85, Sadeek A. Sadeek, Nabel A. Negm, Hassan H.H. Hefni, Mostafa M. Abdel Wahab, Metal adsorption by agricultural biosorbents: Adsorption isotherm, kinetic and biosorbents chemical structures, 400-409, Copyright 2015, with permission from Elsevier 2018.<sup>29</sup>

There were some attentive studies to use rice straw as renewable feedstock to produce fuel and chemicals. Pyrolysis of rice straw can be potentially used as liquid fuel, using fixed bed reactor.<sup>30</sup> Various studies reported the use of rice straw as raw material for ethanol production.<sup>26</sup> There are limited amount of studies based on the use of rice straw as natural wax resources and integration of Green chemistry into the process. Rice straw bio-refinery can be an opportunity in new growing industry in Asia, where it is widely available, especially in Thailand.

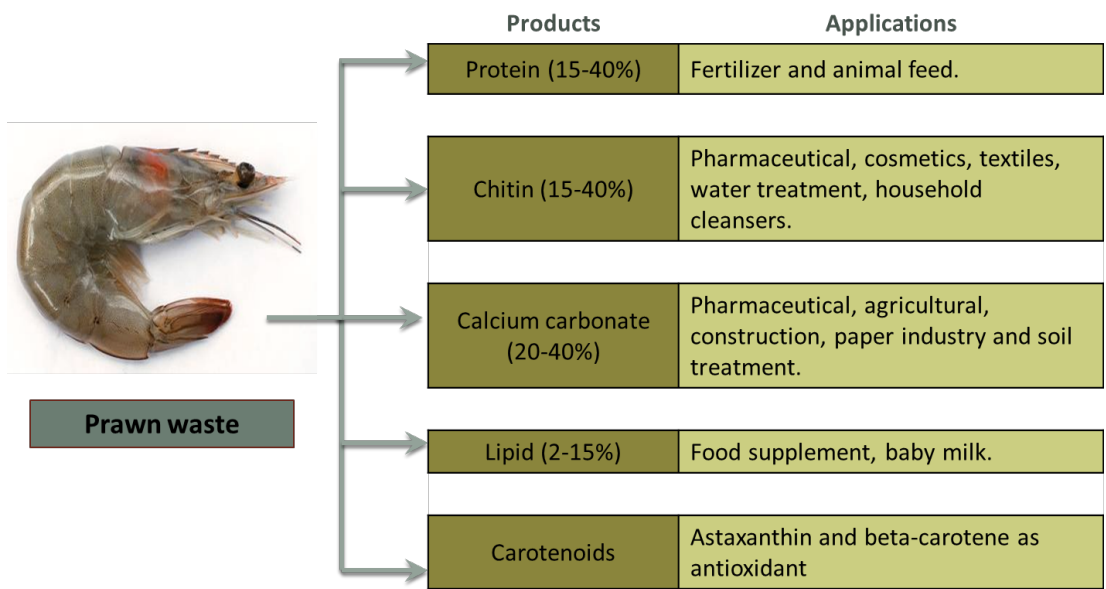
**Table 1-2** Compounds identified in rice straw wax

Compounds	Structures
Fatty acids	
Wax esters	
Diglycerides	
Sterols	
Sterol esters	

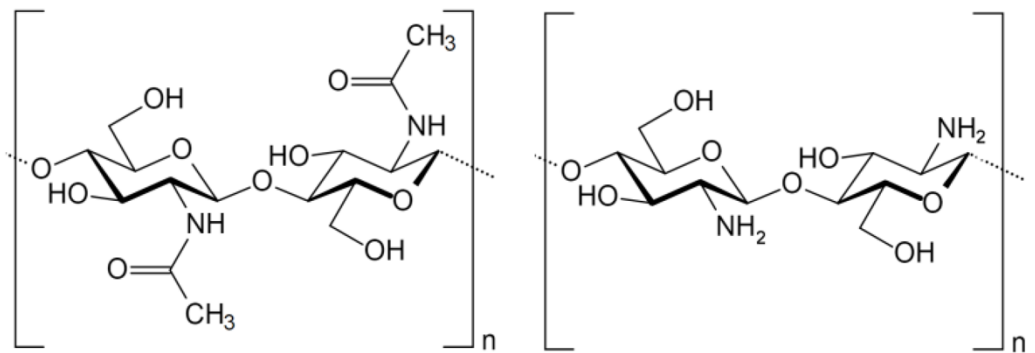
### 1.4.2 Prawn by-products

Aquaculture is the solution 60 million tonnes global production in 2010. Pacific white shrimp (*Litopenaneous vannamei*) is one of the most produced prawn specie in the world.<sup>31</sup> Most shrimps are deshelled then prepared as frozen or canned meat for export. During this process, approximately 40% of the shrimp mass, including cephalothorax (shrimp heads) and shells are removed as by-products, which account for 200,000-300,000 tonnes of shrimp waste a year. This waste is either used to produce low value products, such as animal feeds or disposed of as industrial waste.<sup>32-34</sup>

Prawn waste can be a source of various chemicals, for use in a number of industries (See **Figure 1-3**). Some groups of compounds identified previously was listed in **Table 1-3**. This waste has been used for the production of chitin and chitosan.<sup>35</sup> Chitin and chitosan are of commercial interest due to their high degree of nitrogen compared with cellulose (See structure s of chitin and chitosan in **Figure 1-4**) . Moreover, they possess excellent in terms of physical and chemical properties such as biocompatibility, biodegradability, non-toxicity and absorption ability.<sup>35</sup> Chitin is a naturally abundant amino polysaccharide, the most abundant after cellulose. Chitin is used in various applications such as in pharmaceutical due to its acceleration of wound healing,<sup>36</sup> and in chemistry and industry in enzyme immobilisation.<sup>37</sup> The main commercial sources of chitin are crab and prawn. The industrial process of chitin production involves acid treatment to dissolve calcium carbonate, followed by alkaline treatment to remove protein. Further steps are needed in order to remove pigments and other minerals.<sup>38</sup> Chitosan, one of the most important chitin derivatives in terms of applications, is obtained by partial deacetylation in alkaline solution, usually using sodium hydroxide.<sup>39</sup> Furthermore, it has been reported that valuable products such as astaxanthin,<sup>40-42</sup> as well as lipid especially n-3 and n-6 fatty acids eicosapentaenoic acid (EPA) and docohexaenoic acid (DHA).<sup>33,34,43</sup> EPA and DHA are essential polyunsaturated fatty acids providing significant health benefits for brain function/development and cardiovascular conditions. However, sources of EPA and DHA are now limited for small fatty fish caught in coastal waters for human consumption. Also, it is necessary to direct towards more sustainable sources of these PUFA due to depleting global fish stocks including aquaculture with plant-base feeds to meet the increasing demand. Waste products from shrimp farming are a rich source of proteins, fats, polysaccharides (chitin), metabolites and inorganic minerals.<sup>40,44,45</sup>

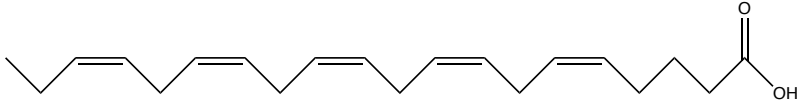
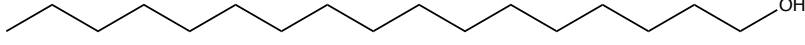
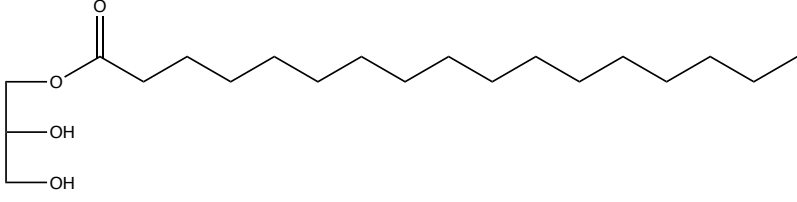
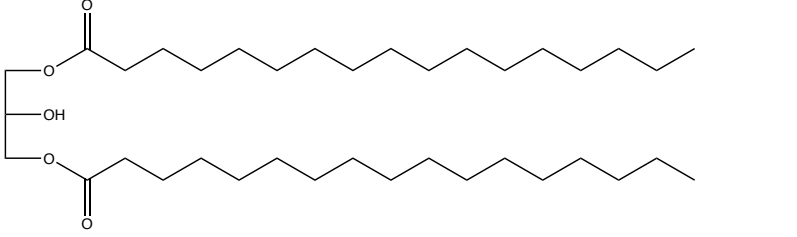
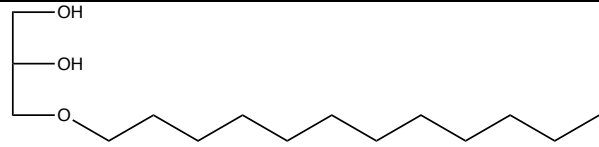
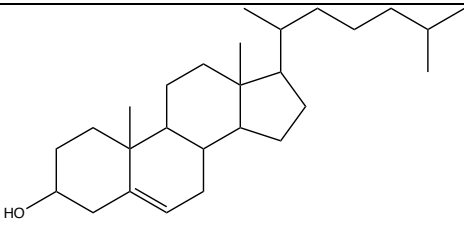


**Figure 1-3** The Prawn wasted bio-refinery



**Figure 1-4** Structure of Chitin (left) and Chitosan (Right).

**Table 1-3** Groups of lipophilic molecules detected in prawn waste lipid.

Compounds	Structures
Fatty acids	
Fatty alcohols	
Monoglycerides	
Diglycerides	
Ether of glycerols	
sterols	

The shell waste bio-refinery will definitely create new industrial opportunities in Southeast Asia and beyond. The conversion of these waste products into high value products or materials could create new employment opportunities as well as reduce the amount of industrial waste generated from shrimp farming. However, to sustainably establish a profitable industrial activity from this valuable waste resource, creativity in chemistry is required.<sup>46</sup> The use of clean chemical technologies can aid in resolving waste management issues and resource depletion through the consumption of shrimp wastes as feedstocks for industry.



## 1.5 Bio-refinery Concept

*“Biorefining is the sustainable processing of biomass into a spectrum of marketable products and energy”.*

This is the widely used definition of the concept of biorefinery, which was accomplished by the International Energy Agency (IEA).<sup>7</sup> Biorefinery concept involves a variety of technologies in order to separate biomass resources into their building blocks. Moreover, the biorefinery concept is the development of bio-based industrial products using an extensive range of combined technologies with the aim to maximise sustainable transformation of biomass into their building blocks with the concomitant production of biofuels, energy, chemicals and materials as well as minimising the generation of the waste.<sup>47</sup> Therefore, the intention to integrate Green chemistry to the bio-finery concept is of interest for scientists. Biorefineries have now been divided into 3 types as follows.

*Phase I Biorefinery* processes only one feedstock with fixed processing capacities and results in only one major product. They have been in operation and shown to be economically viable. One of the well-known examples is the production of biodiesel. Phase I Biorefineries are widely in use in Europe; the main feedstocks are vegetable oils, mainly rapeseed oil. The fixed amount of biodiesel and glycerine is produced through a single process of transesterification.<sup>48</sup> The limitation of the phase I biorefineries is the absence of flexibility to recover investment and operating costs.

*Phase II Biorefinery* is capable of using only one feedstock, similar to phase I biorefineries. However, the process is able to produce multiple final products, including energy, chemicals and materials. The phase II biorefineries are more flexible than the phase I. These can therefore be adjusted according to the market demand, prices and the size of the plants. It has been reported in recent studies that integrated biorefinery with biofuels and chemicals production was effective in generating a high return rate of return on investment and was able to meet its energy and economic targets.<sup>49</sup> Novamont plant in Italy is an example of this phase II biorefinery. Corn starch is used to produce various chemical products such as biodegradable polyesters (Origi-Bi) and starch-derived thermoplastic (Mater-Bi).<sup>5</sup>

*Phase III Biorefinery* is able to produce a variety of final products including energy, and chemicals with multiple choices of feedstocks and technologies in order to create a wide range of industrial products. This diversity builds in flexibility to meet future market demands. Therefore, high profitability and maximum investment returns can be achieved with the phase III biorefinery, which can be called the most developed type of biorefinery.<sup>50</sup> An important advantage of this type of biorefinery is its multiple feedstock option, which helps minimising the risk of feedstock shortage and offers the most profitable combination of integrated biorefinery technologies and raw material.<sup>5</sup> Most of existing biorefineries processing plants are currently in operation in single production chains. Even though, phase III biorefinery is known to be the most profitable, there is no commercial scale plant in operation at the moment. However, extensive research projects are ongoing in the EU and around the world.<sup>51</sup>

The aim of biorefinery industries is to develop industrial facilities, which are able to implement in rural areas. Unlike oil refinery, which is almost impossible to change the processing procedure as it has been proved as the most efficient process for more than 100 years.

## **1.6 Green chemistry and Biorefinery as sustainable partnership**

Biomass is consisted of different chemical products, which widely proved to be useful and profitable in various industrial applications. Through different technologies, chemicals, biofuels, materials and different forms of energy can be obtained. Conceptually, a biorefinery would apply hybrid technologies with multidisciplinary including polymer chemistry, bioengineering and agriculture. Nowadays, there are three major biorefinery platform technologies: extraction of high-value compounds, thermochemical and biochemical processes (**Figure 1-5**).<sup>52</sup>

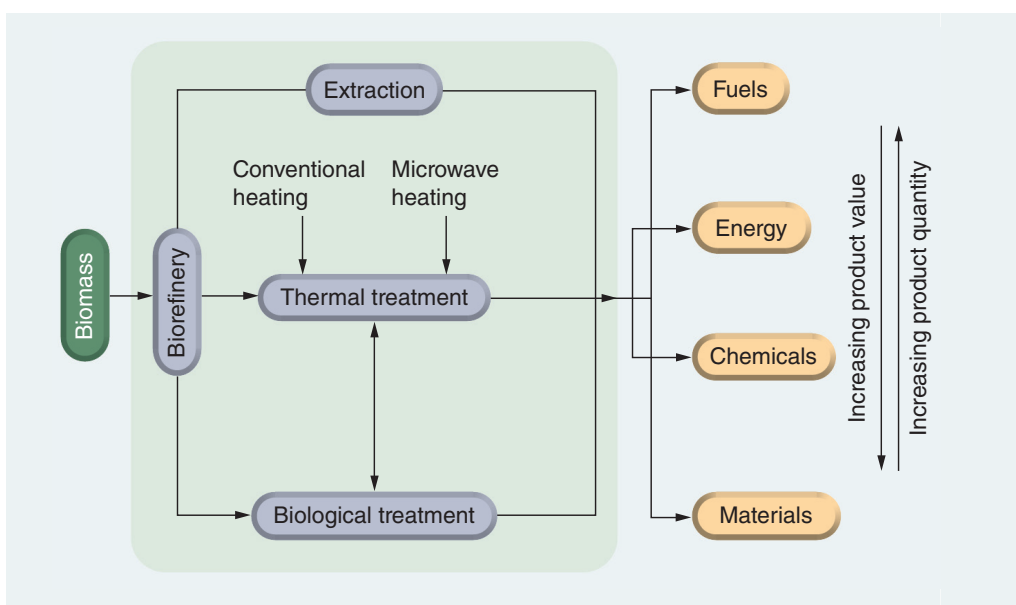


**Figure 1-5** Biorefinery treatment of biomass

(Reproduced from Future Oncol. (2007) 3(5),  
569-574 with permission of Future Medicine Ltd.<sup>52</sup>)

### 1.6.1 Extraction

Waxes and lipids are important and utilised in a wide range of industrial applications.<sup>53</sup> Our society largely depends on petroleum waxes. The reduction in fossil resources combined with a predicted growth demand may lead to supply issue. Therefore, there are opportunities for natural waxes from other sources. The current method of wax extraction from natural sources involves the use of large quantities of conventional toxic organic solvents, such as toluene, chloroform, dichloromethane and hexane causing substantial amount of solvent waste.<sup>28,53</sup> There are opportunities towards natural waxes combined with greener and sustainable processing routes. In this project, two extraction technique were used in order to compare the efficiency of the conventional and the alternative methods.

#### 1.6.1.1 Soxhlet extraction

Soxhlet extraction is classed as one of the conventional techniques for extracting metabolites from biomass. A cellulose thimble is used to load the biomass sample then place in a Soxhlet extractor, which is connected directly to a solvent reservoir (see **Figure 1-6**). Once the solvent is heated to the boiling point and it condenses into the condenser and passes through the Soxhlet extractor, which slowly fills up with solvent at the same time as the lipids are extracted by the

hot solvent. The large advantage of this method is that the fresh solvent is continually brought into contact with the biomass, which displaces the extraction equilibrium. Therefore, high yield of the metabolite can be obtained.<sup>54</sup> With the high temperature maintained throughout the extraction, there is no need for further filtration step caused by biomass leaching.<sup>54</sup> This technique is considered more efficient than other conventional solvent extraction methods. However, it is time consuming due to the high temperature required to heat the solvent to the boiling point, which might also cause thermal decomposition of the extract.<sup>55</sup> Moreover, large quantity of solvent is needed, which means the waste solvent as post extraction requires the removal of solvent.<sup>54</sup> However, Soxhlet extraction would not be suitable as part of a biorefinery approach because: (i) large amounts of solvent utilized leading to copious amounts of waste, (ii) energy intensive-process, (iii) solvents used are often toxic and (iv) biomass is wet following the extraction – these mean that an energy intensive procedure would have to be utilized to dry the biomass prior to other processes.

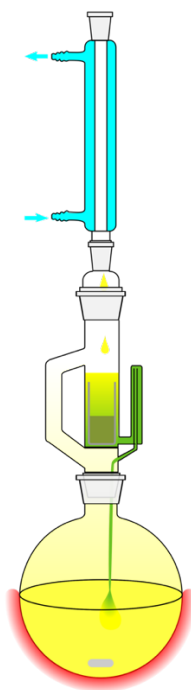


**Figure 1-6 Diagram of Soxhlet apparatus**

### 1.6.1.2 Supercritical Fluids Extraction

A supercritical fluid (SFC) is referred as a substance that possesses its pressure and temperature ( $P_c$ ,  $T_c$ ) above the critical value.<sup>56,57</sup> Pressure and temperature play important role as their variations leads to a change of properties of a substance. This phenomenon can be explained with the aid of a phase diagram, which is essentially a plot of vapour pressure vs temperature (**Figure 1-7**). All stable substances are known to have a triple point and a critical point.<sup>58</sup> The triple point represents the pressure and the temperature conditions at which the solid, liquid and gas phases coexist as there is an equilibrium between them. The line that starts from the triple point until the critical point, located between the liquid and gaseous regions, is called the gas-liquid (G-L) coexistence curve. By moving towards the critical point along the G-L line, thermal expansion results in a decrease in the density of the liquid while the increase in pressure leads to a rise in the density of the gas. The densities of the two phases are identical at the critical point, it is no longer possible to distinguish between the liquid and gas phases due to their similar properties. Consequently, the critical point, with the critical temperature and the critical pressure, can be defined as the maximum temperature and pressure applied, that leads to an equilibrium between the liquid and the gaseous phases. Beyond this point, there is no distinction between the two phases.<sup>59</sup> The Figure 15 is the phase diagram of carbon dioxide, in which the critical point in is at 73.8 bar and 31.1 °C. The critical point for common supercritical fluids can be found in **Table 1-4**.

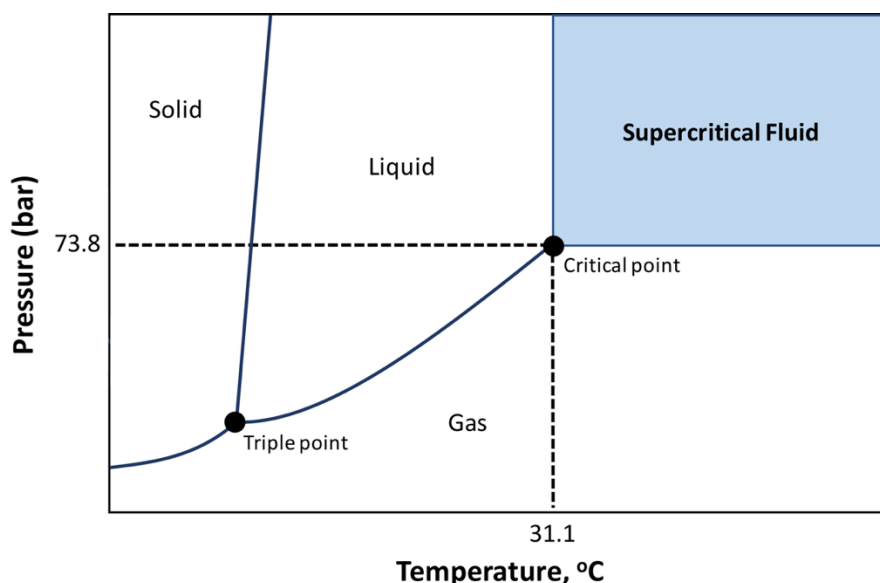


**Figure 1-7** Phase diagram for carbon dioxide.<sup>60</sup>

The most popular SCF is supercritical carbon dioxide (scCO<sub>2</sub>) as it is considered as non-polar and can be ideally used as alternative solvent for lipid extraction, especially in the food industry where solvent residues in products are strictly controlled.<sup>61</sup> The first advantage of CO<sub>2</sub> is the low operation temperature (>35°C) due to its relatively low T<sub>c</sub>. CO<sub>2</sub> is also non-toxic, inexpensive and available in large quantities with a high degree of purity. Despite of a relatively high P<sub>c</sub> (73.8 bar), which can be a limitation of the use of the CO<sub>2</sub>, it has become common in industrial processes to operate at such condition, for example in the extraction of caffeine from coffee and extraction of hops.<sup>62</sup>

**Table 1-4** Critical pressure and temperatures of various compounds.<sup>59</sup>

Compound	Pressure (bar)	Temperature (°C)
Ammonia	113.2	132.4
Carbon dioxide	73.8	31.1
Methane	46	-82.8
Ethane	48.7	32.2
Propane	42.5	96.7
Ethene	50.4	9.2
Methanol	80.9	239.5
Ethanol	61.4	240.8
Acetone	47	235
Nitrous oxide	33.4	73.5
Water	374.2	220.5

The polarity of scCO<sub>2</sub> has been reported to be quite similar to the polarity of hexane and toluene.<sup>63</sup> Moreover, it has been considered as a promising alternative for fat and oil extraction, as it leaves no solvent residue and solvent properties can be tuned by changes in the temperature and pressure of the system.<sup>53,64,65</sup>

As mentioned earlier, waxes and lipids are used in various industrial applications including candles, board sizing, coatings for paper, food packaging and pharmaceutical sectors.<sup>66,67</sup> Numerous studies have been carried out on the extraction of waxes and bioactive compounds

from biomass. In flax industries, a large number of dust were produced and added value co-product is a solution for this industry.<sup>68</sup> scCO<sub>2</sub> extraction with high pressure and temperature were used (557 bar, 60 °C) and resulted in 7.4% of crude yield, significantly higher than that of hexane (4%). Four groups of valuable main compounds were characterized: *n*-policosanols, fatty acids, fatty aldehydes and wax esters. *n*-Policosanols was the major component, 350-380 mg/g of wax, with the chain length C<sub>18</sub>-C<sub>30</sub>.<sup>68</sup> Wheat straw extraction using scCO<sub>2</sub> were investigated by Deswarte *et al.* and Sin *et al.*<sup>53,69</sup> This agricultural waste is considered as low economic value; however, it is can be a high value source of chemicals. The main group of compounds found in wheat straw wax were hydrocarbons, fatty acids, fatty alcohols, fatty aldehydes, wax esters and sterols. Moreover, β-diketones, having interesting chelating properties, 14, 16-hentriacontanedione and 16,18-tritriacontanedione, were also identified in quite large concentration. These compounds were previously found in triticale wheat straw wax extracted by scCO<sub>2</sub>.<sup>65</sup> Sugarcane residues (rind, bagasse and leaves) were also investigated using scCO<sub>2</sub> extraction by Attard *et al.*<sup>70</sup> Each residue was separately extracted and it was found that the wax composition varied for each type of residue. In sugarcane rind, long-chain fatty aldehydes and *n*-policosanols were dominated.<sup>70</sup> Miscanthus waxes from two species, *miscanthus giganteus* and *miscanthus sinensis* were obtained using a 2x2 full factorial experimental design.<sup>71</sup> it was found that pressure and temperature played important role in the extraction, with optimum conditions of 350 bar and 50 °C. The quantities of compounds found in these two species were different, which reflected the melting temperatures of the waxes. The *miscanthus sinensis* wax with higher melting temperature can be potentially used in similar application as carnauba wax.<sup>71</sup>

Not only agricultural residues, shell wastes are also of interested in terms of scCO<sub>2</sub> extraction. The by-products of Brazilian redspotted shrimp (*Farfantepenaeus paulensis*) including head, shell and tail were extracted using scCO<sub>2</sub>. Polyunsaturated fatty acids, mainly ω-3 fatty acids, docosahexaenoic acid (DHA) and eicosapentaenoic acid (EPA) were found in high concentration. The highest amount of extract was obtained at 370 bar and 43 °C.<sup>40</sup> The ω-3 fatty acids from Northern shrimp by-product were also successfully recovered by scCO<sub>2</sub> at 40 °C and 350 bar. The comparison of extraction efficiency with conventional organic solvents were conducted. Although solvent extraction (acetone and hexane) gave higher total crude yields than the scCO<sub>2</sub>, the quantities of DHA and EPA obtained were comparable to conventional extraction.<sup>44</sup>

To the best of author's knowledge, the scCO<sub>2</sub> extraction of rice straw has been investigated and only a study on different organic solvents was carried on.<sup>28</sup> Therefore, this is the first time of a systematic valorisation of rice straw in SFC. In addition, scCO<sub>2</sub> and solvent extractions of Pacific White shrimp (*Litopenaeus vannamei*), have previously been investigated.<sup>33,43,72</sup> However, these studies conducted limited optimisation and only focused on the analysis of fatty acid methyl ester (FAME) profile.<sup>33,43,72</sup>

### 1.6.2 Biochemical process

"Biochemical conversion is the process by which biomass is converted to gas (CO<sub>2</sub>/CH<sub>4</sub>), waste (compost or fertilizer) and water (ie. water or ethanol) by using microorganisms".<sup>73</sup> The process refers to i) aerobic fermentation resulting in compost, carbon dioxide and water, ii) anaerobic digestion which produces fertilizer and gas (CH<sub>4</sub>/CO<sub>2</sub>) and iii) alcoholic fermentation which produces ethanol, carbon dioxide and waste.<sup>73</sup> Biochemical processes undergo at lower temperature and have lower reaction rates, unlike thermochemical process. The most popular and common types of biochemical processes are fermentation and anaerobic digestion. The fermentation uses microorganism and/or enzymes to convert a fermentable substrate into products, usually alcohols or organic acids. Currently, ethanol is the largest volume and best studied fermentation process. Hexose, especially glucose is the most frequently used as fermentation substrates, whereas pentose (from hemicellulose) is still under investigation to find the suitable microorganism for ethanol conversion.<sup>74,75</sup> On the other hand, anaerobic digestion requires bacteria to destroy organic materials in the absence of oxygen over a temperature range from 30 to 65 °C. The major final product of the reaction in biogas, which is a mixture of methane, CO<sub>2</sub> and other impurities.<sup>76,77</sup>



### 1.6.3 Thermochemical processes

Conventionally, there are three types of thermochemical processes for converting biomass into energy and chemical products.

#### 1.6.3.1 Types of thermochemical processes

##### 1) Gasification

Gasification is considered as an efficient and environmentally friendly way to produce energy.<sup>78</sup> The gasification process is simply a conversion of a solid fuel into gaseous fuel. The overall process completely occurs at elevated temperature range of 800-1300 °C with series of chemical reactions.<sup>79</sup> Biomass as raw material is considered as more promising than coal gasification due to the low amount of sulfur and its less reactive property. The use of biomass is potentially suitable for the highly efficient power generation equipped with gasification technology as well as suitable for cogeneration.<sup>80,81</sup> The final products is an energy rich mixture of combustible gas H<sub>2</sub>, CO, CH<sub>4</sub> and other impurities such as CO<sub>2</sub>, nitrogen, sulfur, alkali compounds and tars, which a complex mixture of organics that is produced during thermochemical process.<sup>82</sup>

##### 2) Pyrolysis

Pyrolysis is the process of thermal degradation of organic matter in order to dehydrate/deoxygenate the substrate and increase the energy intensity. The resulting products become more applicable to fuels with higher commercial values.<sup>52</sup> Pyrolysis has obtained attention due to its ability to convert biomass directly into solid (char), liquid (bio oil) and gaseous (fuel gas) products in the absence of oxygen.<sup>83</sup> There are several options to categorise pyrolysis processes.

- *Torrefaction* is low temperature thermochemical process in which the biomass is heated in an inert atmosphere at temperature of 150-300 °C, usually in order to upgrade as solid biomass fuel.<sup>52</sup> Nitrogen is the most common carrier gas used in this so-called mild pyrolysis. Torrefaction is interesting as the properties of the biomass are significantly improved such as higher heating value or energy density, lower moisture content, higher hydrophobicity, improved grindability and reactivity and more uniformity of biomass.<sup>84,85</sup>

- *Slow pyrolysis* is a medium temperature process (~400 °C). The process usually yields equal quantities of bio-oil, char and gas.<sup>86</sup>
- *Fast pyrolysis* is the thermal process where biomass decompose very quickly to generate mainly bio oil, also some vapours and aerosols and some char and gas. The heating rates are high and the residence time is typically in the order of 1s.<sup>52,87</sup>

### 3) Carbonisation

Carbonisation is direct combustion of biomass, which is inconvenient and polluting due to its extensive smoke formation. Charcoal is usually used as a fuel because due to its easy handling, transportability and lower smoke production.<sup>79</sup>

#### **1.6.3.2 Microwave chemistry**

In this project, pyrolysis is the selected thermochemical process, which will be applied with biorefinery concept. The fact that thermochemical processes involve high temperature and long residual time in order to completely decompose the major biomass structural components (cellulose, hemicellulose, lignin), making a biorefinery based on these methods is potentially unprofitable. As a result, alternative promising heating method to replace conventional heating such as microwave heating is investigated in this study.

Microwave-assisted chemistry has been of interest since the late 1980s.<sup>88</sup> Microwave irradiation lies between radio and infrared in the electromagnetic spectrum in the frequency range of 0.3 to 300 GHz (**Figure 1-8**). Specialised chemistry microwave reactor operates at 2.45 GHz similar to domestic microwave. The attractive advantage of microwave chemistry is that it offers a high efficiency on heating material by “microwave dielectric heating effect”, depending on the ability of a material to absorb and interact with the microwave in order to convert it into heat.<sup>89-91</sup>

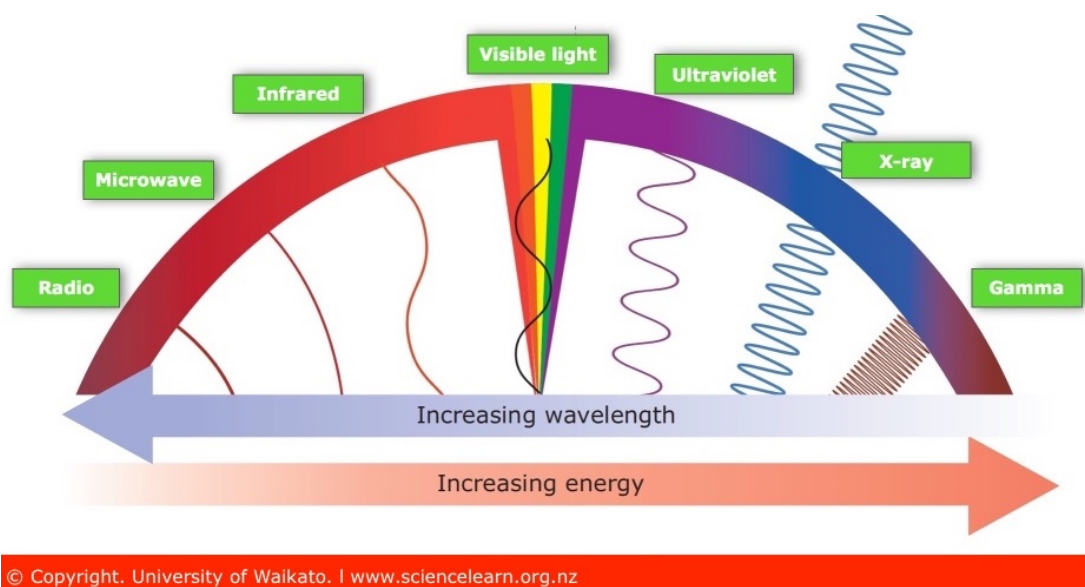


**Figure 1-8** Electromagnetic spectrum.

(Reproduced from Science Learning Hub – Pokapū Akoranga Pūtaiao, University of Waikato, with permission of [www.sciencelearn.org.nz](http://www.sciencelearn.org.nz)).

In microwave heating, there are two main mechanisms on how the interaction occurs, dipolar polarisation and ionic conduction. The moment when polar molecules are in a strong electric field, the positive and negative charges will orientate opposite to the direction of the electric field. Then, heat is dissipated as the distortions within the molecule relax to their original orientation. The ability to convert electromagnetic energy into heat under given microwave irradiation is totally dependent on the “dielectric loss factor” (a measure of the efficiency of conversion of electromagnetic energy to heat), expressed as  $\epsilon''$ . The microwave heating rate is proportional to the loss tangent which calculated as  $\tan\delta = \epsilon''/\epsilon'$ , where  $\epsilon'$  is dielectric constant (the molecule’s ability to be polarised by the electric field). **Table 1-5** shows the  $\tan\delta$  values of a different solvents, a high  $\tan\delta$  value represents efficient absorption of microwave energy and a great rate of heating. Also, microwave energy is able to cause a heating effect via ionic conduction. This occurs when free ionic ions are found in the substance; the electric field caused by microwave irradiation leads to ionic movement resulting in rapid heating.<sup>89</sup>

**Table 1-5**  $\tan \delta$  values of some solvent at 25°C

Solvent	$\tan \delta$
Ethanol	0.941
Methanol	0.659
Water	0.123
Hexane	0.02

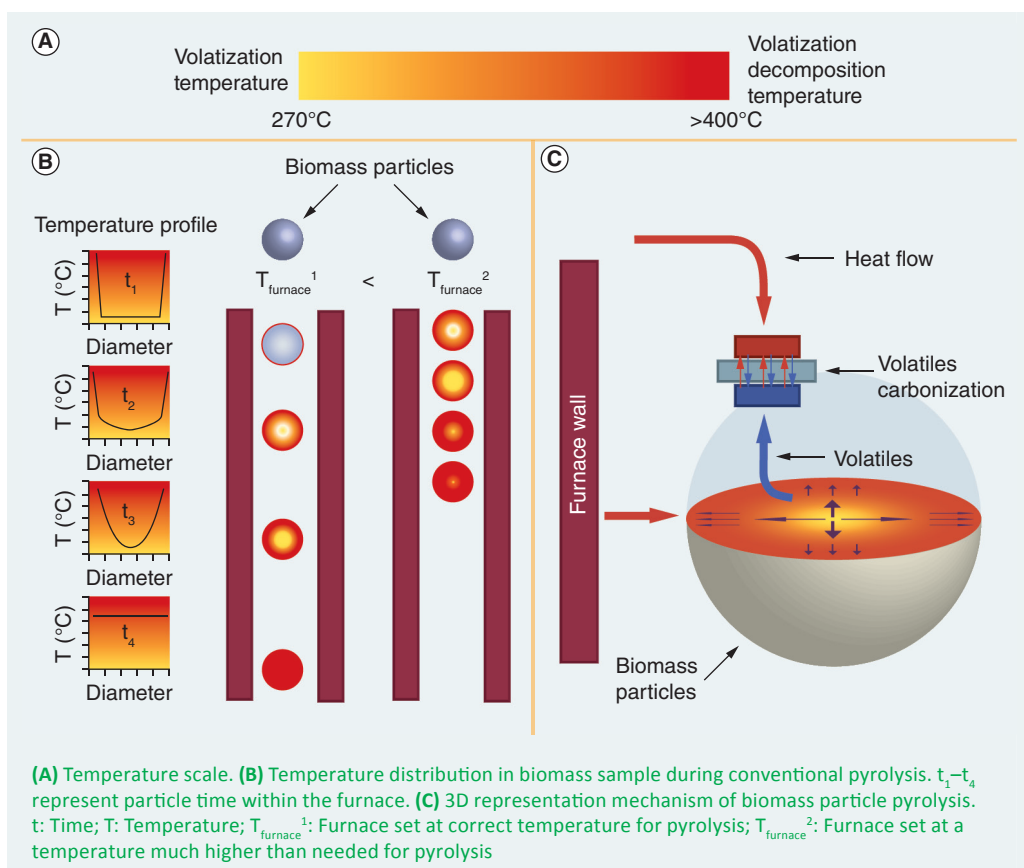


**Figure 1-9** Conventional pyrolysis process.

(Reproduced from Future Oncol. (2007) 3(5),

569-574 with permission of Future Medicine Ltd.<sup>52</sup>)

Microwave heating offers many benefits compared with conventional heating. Overall process is more energy efficient as microwave irradiation heats the whole volume of a sample, whereas conventional heating heats the reaction vessel before reaching the sample. **Figure 1-9** shows how the pyrolysis occurs using conventional heating. Only the external particle area is quickly heated due to their low rate of thermal conductivity. The internal part is therefore heated slowly

governed by thermal diffusivity of biomass. As heating the biomass in a furnace, two distinctive temperature regions of pyrolysis apparently exist; low temperature biomass vaporisation and high temperature carbonisation.<sup>52</sup>

Unlike conventional heating method, the heating effect is almost instantaneous in microwave, it is not necessary to spend time waiting for the reactor to heat up or cool down. **Figure 1-10** illustrates the microwave-assisted pyrolysis of a biomass. The material interacts directly with the microwave instead of radiant heat. The biomass itself generate heat, the heating can therefore be volumetric, very rapid and highly selective. The temperature is more uniform during the heating process.<sup>92</sup>

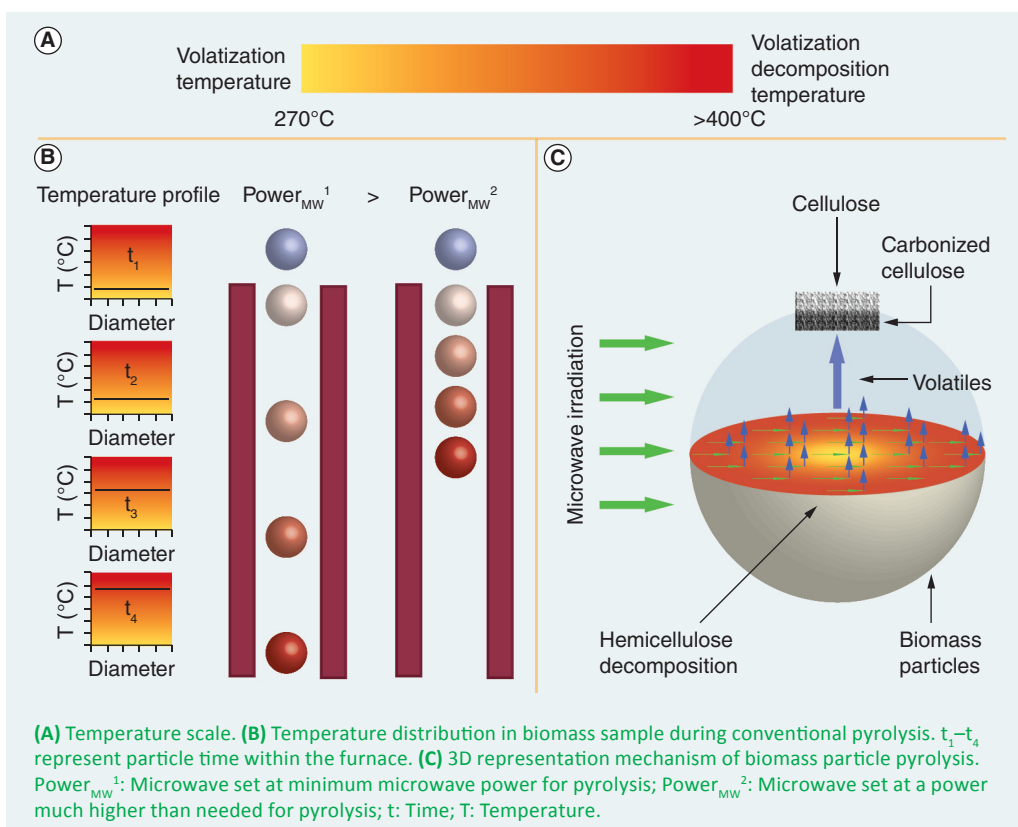


**Figure 1-10** Microwave-assisted pyrolysis process.

(Reproduced from Future Oncol. (2007) 3(5), 569-574 with permission of Future Medicine Ltd.<sup>52</sup>)

Microwave pyrolysis of biomass was well documented with lignocellulosic biomass, such as crops, wood, agricultural and forestry residues. These are mainly composed of cellulose, hemicellulose, and lignin. Microwave pyrolysis has been applied to various lignocellulosic feedstocks. Aktas *et al.* investigated microwave pyrolysis of tea wastes with a target to produce activated carbon.<sup>93</sup> As the waste was woody with high lignin content, a pre-treatment with phosphoric acid was required. The activated carbon was produced with high surface area at the temperature ranged 300-700 °C using domestic microwave.<sup>93</sup> Coffee hulls were also used as feedstock in microwave pyrolysis in the study of Menéndez *et al.*<sup>94</sup> The biomass consists predominantly of cellulose with high amount of ash. It was found that a large amount of gaseous product was obtained (>60% dry weight) in the present of char as microwave absorber over the temperature between 500-1000°C. Interestingly, the hydrogen contents were significantly higher in the microwave compared to the conventional heating.<sup>94</sup> Wheat straw was also pyrolyzed by Lanigan and Budarin.<sup>95,96</sup> The microwave pyrolysis of wheat straw occurred at relatively low temperature (below 200 °C). Subsequently, a fraction of bio oil was collected after only 2 minutes of irradiation with remarkably low water. In addition, levoglucosan was the largest component (ca. 28%) in the bio oil with benzofuran (ca. 10%) and phenol (ca. 11%).<sup>96</sup> Moreover, two publications on microwave pyrolysis of rice straw have been published. The first one investigated all the output products<sup>24</sup> (char, bio oil and gas) and the second one only focused on the production of gas.<sup>97</sup> It has been reported that increase in microwave power led to increases in both rate of heating and final temperature achieved. No microwave absorber was added in the process, the results were attributed to the high power densities available in single-mode system allowing the pyrolysis to initiate along with the production of char, which then acted as microwave absorber.<sup>24</sup> The analysis of gaseous product, the major product, showed that H<sub>2</sub> is predominant in the gas fraction (50.67%) with 22.56% of CO<sub>2</sub>, 16.09% of CO and 7.42% of methane.<sup>97</sup> Other raw materials such as oil palm,<sup>98</sup> pine wood,<sup>99</sup> rice husk,<sup>100</sup> corn stover,<sup>101</sup> and wood<sup>102</sup> were also studied and will be discussed in detail in Chapter 2 and Chapter 3.

All these methods mentioned above including extraction, biochemical and thermochemical processes have been studied individually. However, it was demonstrated that combining different green chemical technologies and integrating them to the biorefinery is more

commercially profitable for the diversity of applications and chemical output. An integrated close to zero process involving a sequential process including extraction, followed by a combination of biochemical and thermochemical methods. Extraction of bioactive compounds from biomass prior to its further decomposition either with biochemical or thermochemical processing can remarkably increase the overall investment return.<sup>103</sup> Budarin *et al.* has successfully conducted a combined system of scCO<sub>2</sub> extraction with thermochemical processing, low temperature microwave pyrolysis using wheat straw as feedstock.<sup>103</sup> High value chemicals such as fatty acids, wax esters and fatty alcohols can be obtained via scCO<sub>2</sub> extraction. The post-extraction residues then were pyrolyzed at low temperature (<200 °C) using microwave reactor. Compared with conventional heating, microwave pyrolysis was more energy efficient and able to produce higher quality bio oils and chars. High value chemicals including levoglucosan and levoglucosanone, were able recover from the bio oil fraction and the char can be potentially used in co-firing.<sup>103</sup> In addition, Attard *et al.* has investigated a miscanthus biorefinery with the use of scCO<sub>2</sub> to extract valuable lipophilic compounds, combined with subsequent enzymatic saccharification.<sup>71</sup> A wide range of high value molecules were detected including long-chain hydrocarbons, fatty acids, n-policosanols, aldehydes, wax esters, sterols and steroid ketones. Using scCO<sub>2</sub> as pre-treatment step had a positive and beneficial effect on further downstream processing of miscanthus as it was found to increase the total sugar recovery by 20% after saccharification compared to the untreated biomass.<sup>71</sup>

## **1.7 Introduction to the work within this thesis**

Firstly, an investigation of lipid profile of the selected waste biomass, rice straw and *Litopeneous vannamei* by-product has been carried on using solvent extraction and supercritical carbon dioxide (scCO<sub>2</sub>) extraction (Chapter 2 and Chapter 4).

Secondly, the microwave technology was used for the valorisation of post scCO<sub>2</sub> extraction residues in order to assess the suitability of the scCO<sub>2</sub> process as pre-treatment step in rice straw biorefinery. (Chapter 2)

Thirdly, the study of the effect of potassium ion in rice straw was investigated by a series of experiments (Chapter 3).

Fourthly the study of the enzyme within the prawn waste and their ability to enhance the extraction yield and increase the concentration of polyunsaturated fatty acids.



## **Chapter 2**

# **Supercritical carbon dioxide extraction as a first step in holistic rice straw biorefinery**

## 2 ScCO<sub>2</sub> extraction as a first step in a holistic rice straw biorefinery

### 2.1 Introduction

Natural waxes have been utilized for various applications particularly in cosmetics, food, personal care products, coatings, polishes and household products.<sup>104–106</sup> There is a high demand for natural waxes, with approximately three thousand kilotons of wax being commercially available each year in the world market.<sup>107</sup> Rice straw has been reported to contain between 0.65 and 1% by dry weight, which generally consists of a mixture of different groups of compounds including long chain fatty acids and fatty alcohols, sterols and wax esters.<sup>28,108</sup> The significant volumes of rice straw makes it attractive to exploit this waste resource.

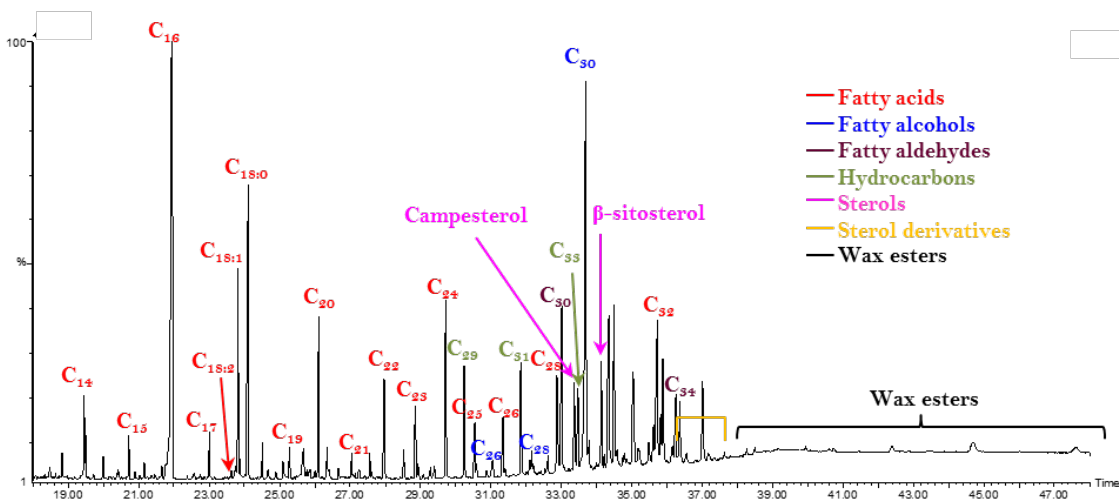
Extraction of lipophilic compounds is traditionally conducted using an organic solvent such as hexane. Extraction of vegetable oils annually requires about 8 million tons of hexane and releases more than 20 million kilograms of hexane to the atmosphere. However, there are environmental hazards and health concerns associated with the use of hexane as it is recognized as hazardous air pollutant and reported to potentially cause nervous system damage.<sup>11, 12</sup>

Conventional solvent extraction is non-selective, resulting in the necessity to further purify or extract a number of undesirable co-extractives from the waxes. Thus, it is important to consider the use of alternative greener solvents for wax extraction.<sup>53,69,111,112</sup> Supercritical fluid extraction, which is environmental friendly, efficient and often more selective,<sup>113</sup> could be an alternative path towards wax traction and a potential first step in an integrated rice straw biorefinery.

## 2.2 Characterisation of main group of compounds in rice straw waxes.

As mentioned previously many traditional solvent extractions are highly unselective, however, hexane is considered to be the most selective of traditional organic solvents for waxes. Soxhlet extraction is also amongst the most efficient of the classical extraction methods. As a result, this technique and organic solvent were selected as the extraction system of choice for lipid components from rice straw. In this current work, the typical yield for the hexane soxhlet extraction of rice straw was 1.05% of dry weight this result is consistent with previous literature findings.<sup>28</sup> The chromatogram of hexane extracted is illustrated in **Figure 2-1**.

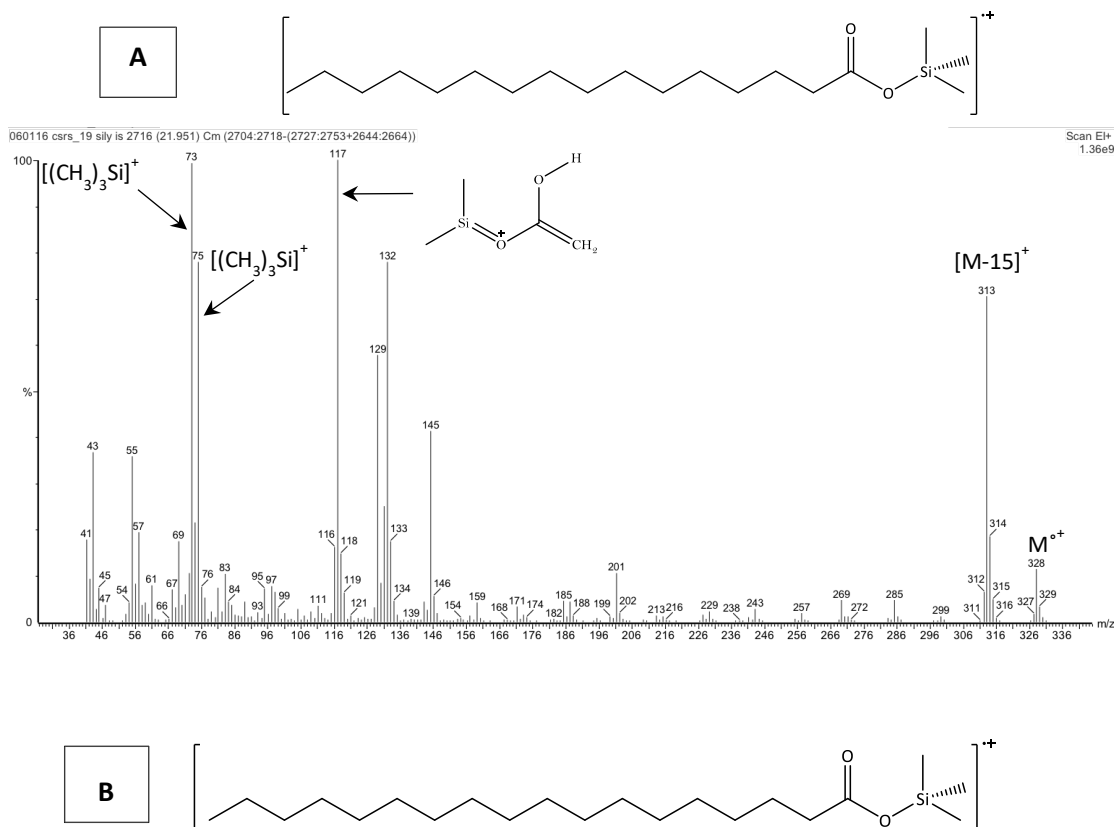
Lipid components were identified and quantified by Gas chromatography coupled to mass spectrometry and FID detector. The method was described in Chapter 6 (Materials and Methods). Wax samples were derivatised with 200  $\mu$ L bis-(trimethylsilyl)-trifluoro-acetamide (BSTFA) in order to improve the volatility of the high polarity, high molecular weight polar components. Mass spectra obtained from gas chromatography coupled to electron impact mass spectra of lipid components were analysed and compared to those of standards and a NIST library. Further investigation on mass spectra fragmentation pattern of the compounds identified were also studied and presented in this chapter. Quantification of rice straw wax extracts was achieved through the use of GC-FID and errors were calculated based on a minimum of three repetitions. The experimental and analytical procedures were described in Chapter 6, section 6.4 and 6.7.

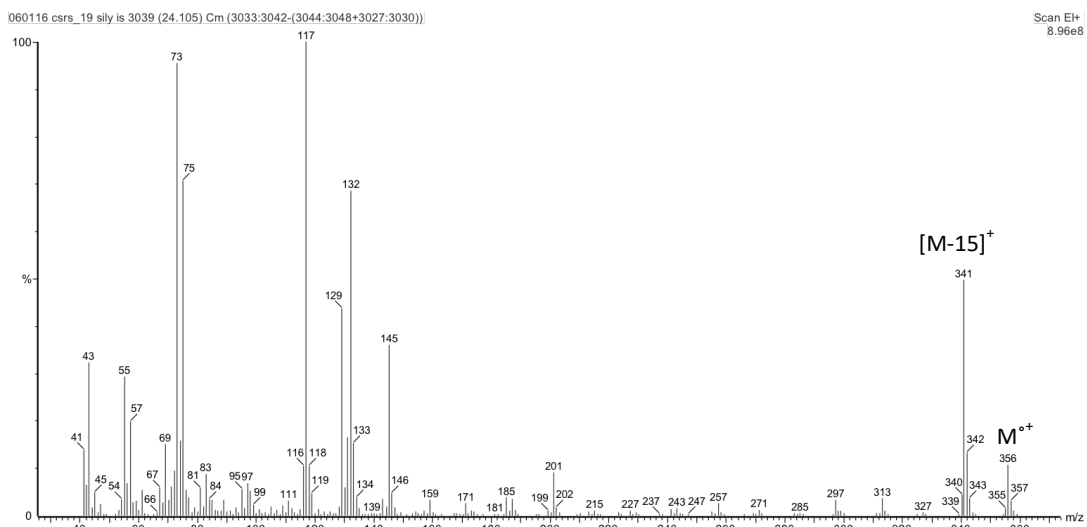


**Figure 2-1** Gas chromatogram of derivatised rice straw wax obtained from Soxhlet extraction using hexane.

### 2.2.1 Free fatty acids in rice straw

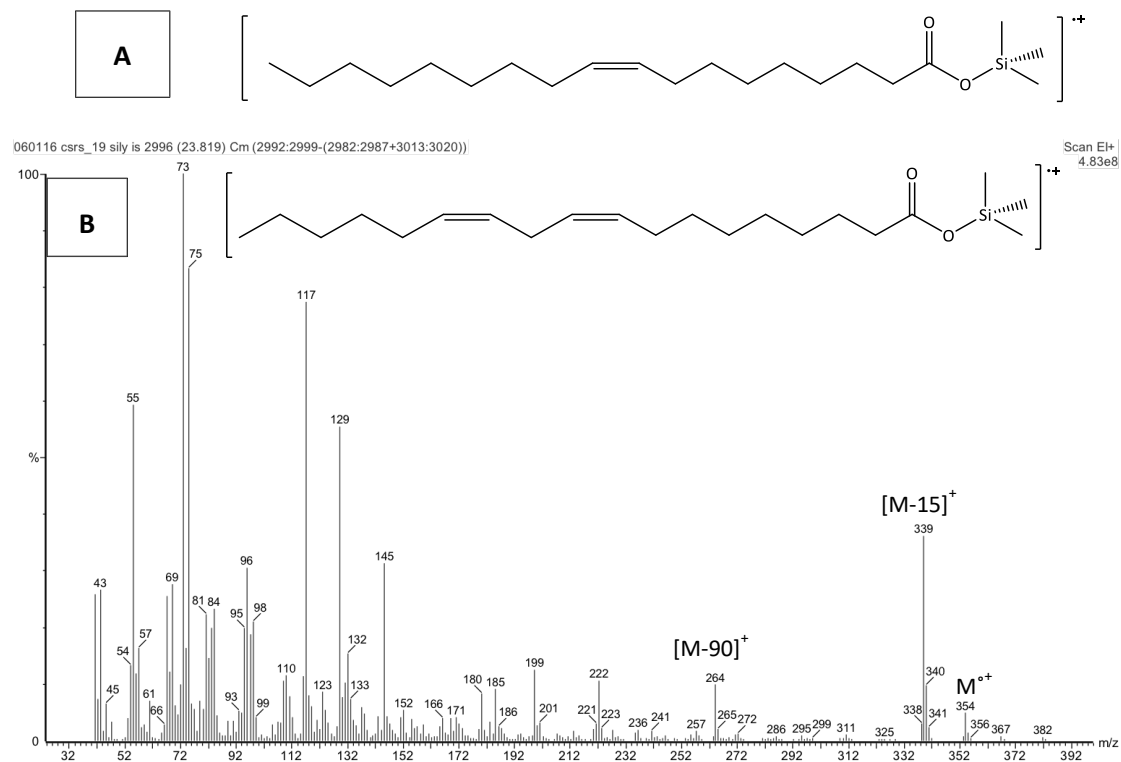
Free fatty acids with chain lengths ranging from C<sub>12</sub>-C<sub>32</sub> were identified and found to be the most abundant lipophilic family in rice straw wax obtained by hexane Soxhlet. These molecules were determined by gas chromatography coupled with electron impact mass spectrometry. **Figure 2-2 A and B** show the EI mass spectra of two predominant saturated fatty acids: palmitic acid (C<sub>16:0</sub>) and stearic acid (C<sub>18:0</sub>), which are found to be the major saturated fatty acids in plants.





**Figure 2-2** EI Mass spectra of TMS ester of A) hexadecanoic acid ( $C_{16:0}$ ) and B) octadecanoic acid ( $C_{18:0}$ )

**Figure 2-3 A and B** illustrate the EI mass spectra of oleic acid ( $C_{18:1}$ ) and linoleic acid ( $C_{18:2}$ ), the major monoenoic acid and dienoic acid in rice straw extract.<sup>108</sup>



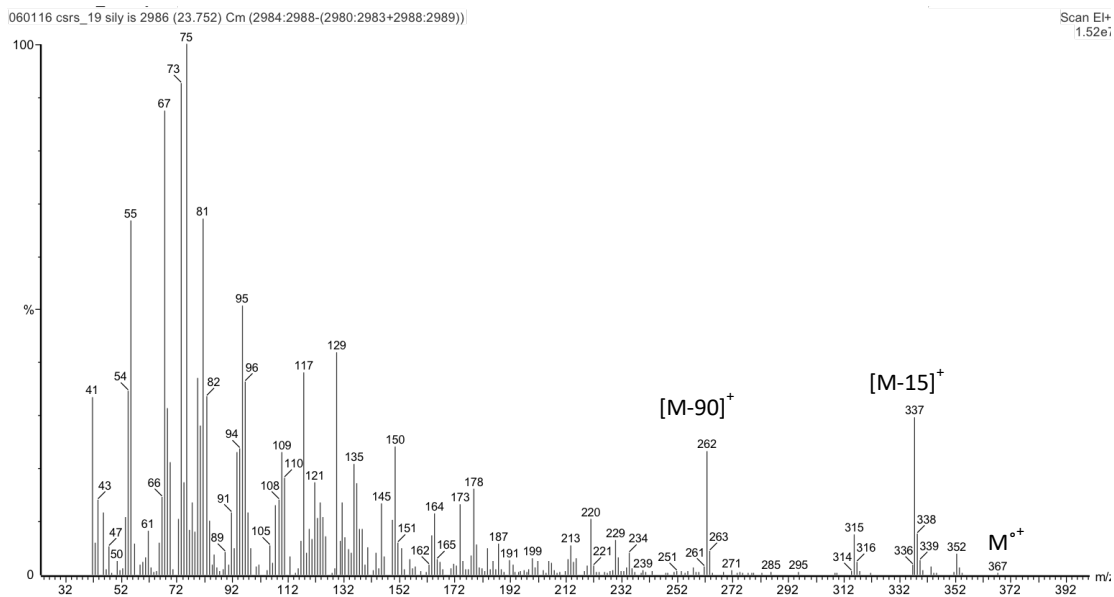


**Figure 2-3** EI Mass spectra of TMS esters of A) oleic acid ( $C_{18:1}$ ) B) linoelic acid ( $C_{18:2}$ ).

The characteristic homologue ions of the trimethylsilyl (TMS) ester of fatty acids are a base peak at  $m/z$  73  $[(CH_3)_3Si]^+$  and a high-intensity peak at  $m/z$  75  $[(CH_3)_2SiOH]^+$ , corresponding to the derivatising group. There are other abundant signals, which are common features of TMS esters of fatty acids and detected at  $m/z$  117, 129, 132 and 145 (**Figure 2-4** and **2-5**).<sup>114</sup>

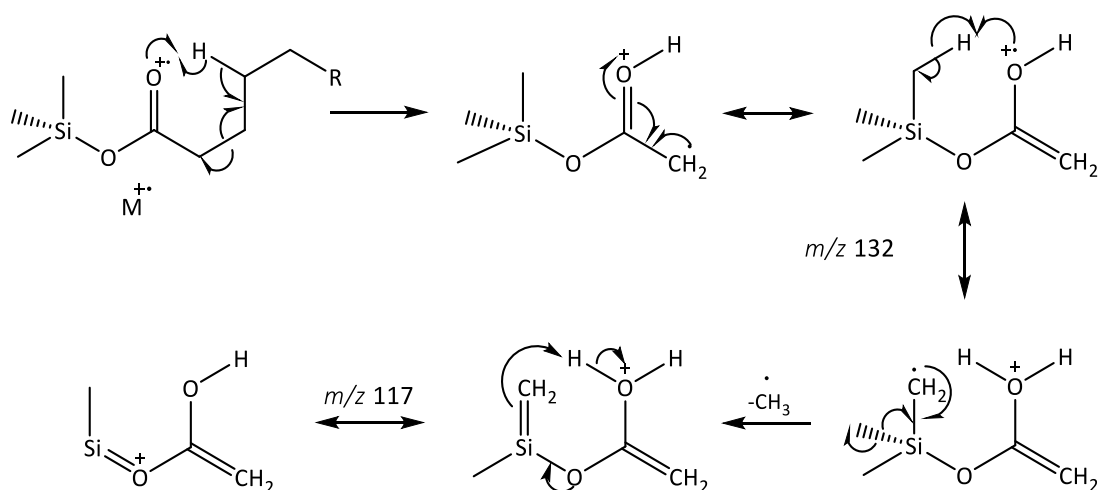


**Figure 2-4** McLafferty rearrangement occurs through a six membered transition state, resulting in  $\gamma$ H-transfer and  $\beta$ -cleavage, the formation of ions of  $m/z$  132 and 117 was observed.<sup>115</sup>

As illustrated in **Figure 2-4**, another characteristic fragment  $m/z$  132 was observed via the McLafferty rearrangement of the TMS ester of fatty acids, involving a hydrogen transfer to the carbonyl oxygen ( $\gamma$ H-transfer) followed by  $\beta$ -cleavage between C-2 and C-3. Then, elimination of methyl group resulted in ion  $m/z$  117.<sup>116</sup> The ion at  $m/z$  145 originates from the molecular ion the similar mechanism. **Figure 2-4** illustrates the formation of  $m/z$  117; however, the cleavage occurs between C-4 and C-5. The other high-intensity fragmentation at  $m/z$  129 arises from the loss of methane from the previous fragment of  $m/z$  145 (See **Figure 2-2 and 2-3** for EI mass spectra).<sup>115,117,118</sup>

Molecular ion is another characteristic fragment of the electron impact mass spectra of trimethylsilyl ester of fatty acids. However, it is either undetected or appears as a weak signal. An important ion which is most of the case abundant and used to assign the molecular weight of this family, is the  $[M-15]^+$  corresponding to the loss of a methyl group from the trimethylsilyl group. In the case of unsaturated fatty acids as illustrated in **Figure 2-3**, a well-pronounced peak,  $[M-90]^+$  was detected in accordance with the previous study of Kuksis.<sup>119</sup>

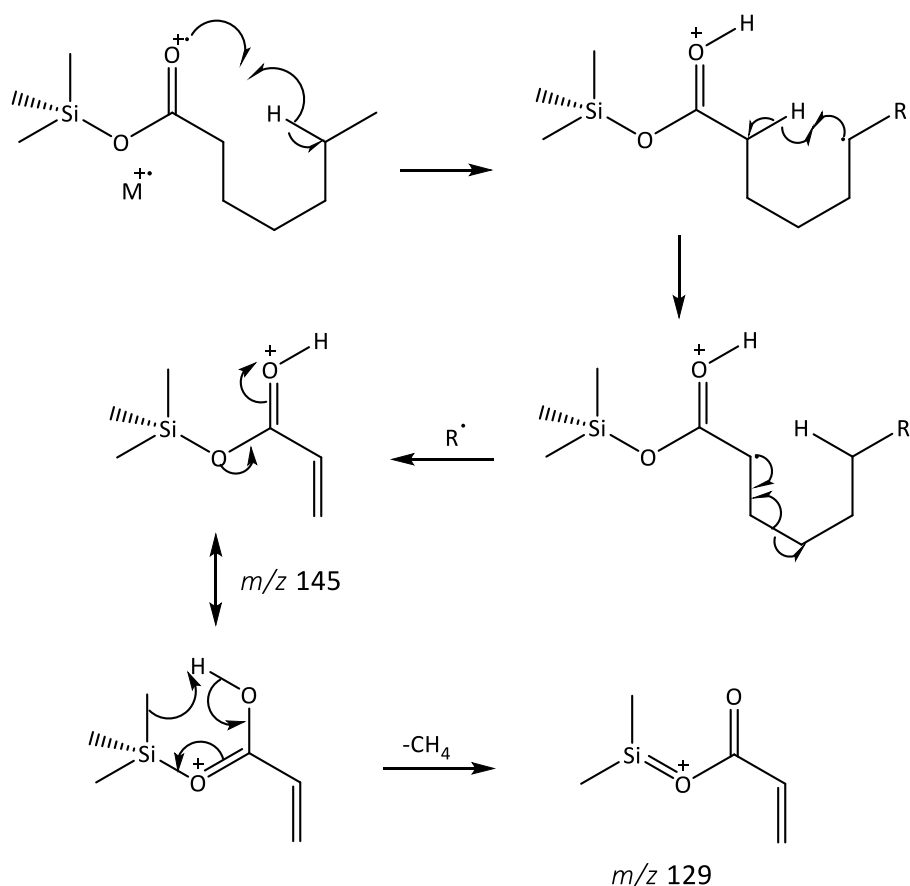


**Figure 2-5** Formation of EI fragments *m/z* 145 and 129 for TMS ester of fatty acids.<sup>115,118</sup>

A dicarboxylic acid was also identified in the rice straw extract, azelaic acid (C-9). The EI mass spectra of the silylated compound is showed in **Figure 2-6** and the formation pathway of an interesting fragment, [M-131]<sup>+</sup>. This peak was present in high intensity due to the stable radical formed during the fragmentation (**Figure 2-7**).<sup>120</sup> A small amount of the dicarboxylic acid was found with the concentration of 9.3 μg/g of plant (See **Table 2-1**). This result is consistent with previous studies using hexane to extract rice straw, which indicate that azelaic acid (C-9) is a minor component of the free fatty acid content.<sup>28</sup> Diacids, such as azelaic acid, may find important use as crosslinking agents in bio-based polymers.<sup>121</sup>



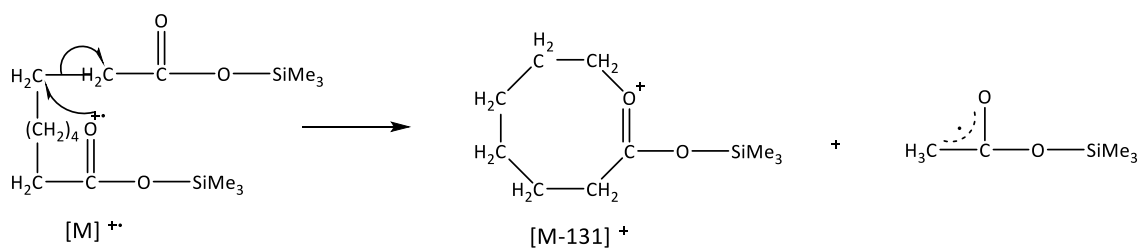


**Figure 2-6** Formation pathway of  $[M-131]^+$  of TMS of azelaic acid.<sup>120</sup>

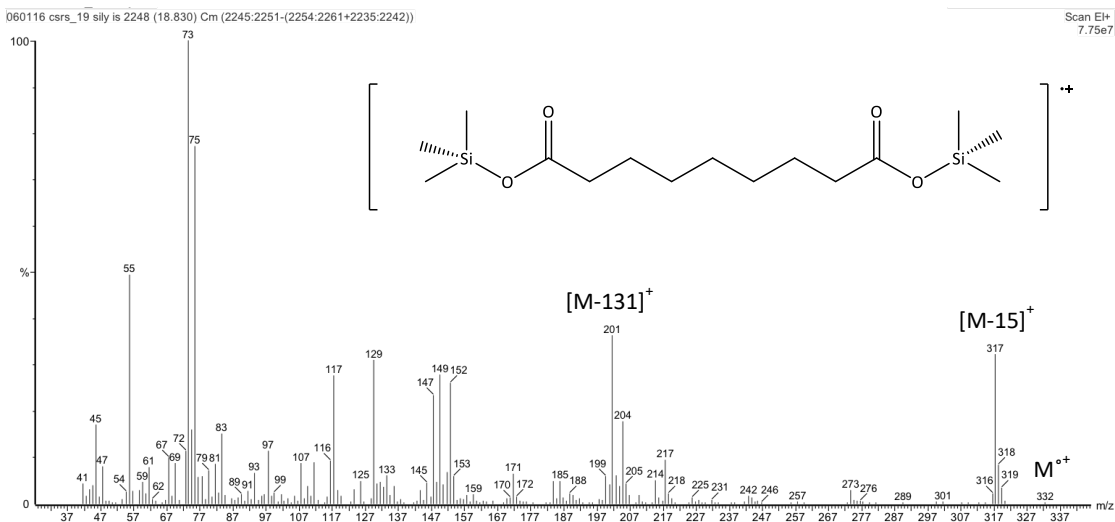


**Figure 2-7** EI mass spectra of silylated azelaic acid from rice straw.

As seen in **Table 2-1**, both odd and even-chain length free fatty acids were detected in rice straw extract by HTGC-MS, ranging from  $C_{12}$  to  $C_{32}$  with total concentration of  $1004.5 \pm 13.7 \mu\text{g/g}$  of plant. Whereas, the even-chain fatty acids were found in higher quantities. Saturated fatty acids represented the majority of group of compounds ( $977.6 \pm 13.7 \mu\text{g/g}$  of plant) and only two unsaturated fatty acids, oleic acid ( $C_{18:1}$ ) and linoleic acid ( $C_{18:2}$ ), were identified with the total of  $26.9 \pm 2.0 \mu\text{g/g}$  of plant. The quantification was carried out with three replicates in order to calculate the values of standard deviation.

**Table 2-1** List of free fatty acid present in rice straw wax extracted using hexane, molecular weight and their abundance in  $\mu\text{g/g}$  of dry plant.

Names	Molecular weight	Characteristic fragments		Abundance $\mu\text{g/g}$ dry plant
		$\text{M}^{\circ+}(\text{TMS})$	$[\text{M}-15]^+$	
<b><i>Saturated Free Fatty acids</i></b>				
Dodecanoic acid $\text{C}_{12:0}$ (lauric)	200.2	272.2	257.2	$7.4 \pm 0.2$
Azelaic acid (diacid)	188.2	332.2	317.2	$9.3 \pm 0.1$
Tetradecanoic acid $\text{C}_{14:0}$ (myristic)	228.2	300.2	285.2	$26.4 \pm 0.0$
Pentadecanoic acid $\text{C}_{15:0}$	242.2	314.3	299.2	$13.0 \pm 1.7$
Hexadecanoic acid $\text{C}_{16:0}$ (palmitic)	256.2	328.3	313.3	$410.1 \pm 0.2$
Heptadecanoic acid $\text{C}_{17:0}$ (margaric)	270.3	342.3	327.3	$16.8 \pm 0.0$
Octadecanoic acid $\text{C}_{18:0}$ (stearic)	284.3	356.3	341.3	$127.1 \pm 2.6$
Nonadecanoic acid $\text{C}_{19:0}$	298.3	370.3	355.3	$19.4 \pm 0.0$
Eicosanoic acid $\text{C}_{20:0}$ (arachidic)	312.3	384.3	369.3	$53.5 \pm 3.0$
Heneicosanoic acid $\text{C}_{21:0}$	326.3	398.4	383.3	$9.8 \pm 0.2$
Docosanoic acid $\text{C}_{22:0}$ (behenic)	340.3	412.4	397.4	$26.6 \pm 0.1$
Tricosanoic acid $\text{C}_{23:0}$	354.3	426.4	411.4	$17.3 \pm 0.0$
Tetracosanoic acid $\text{C}_{24:0}$ (lignoceric)	368.4	440.4	425.4	$50.8 \pm 0.4$
Pentacosanoic acid $\text{C}_{25:0}$	382.4	454.4	439.4	$11.8 \pm 0.3$
Hexacosanoic acid $\text{C}_{26:0}$ (cerotic)	396.4	468.4	453.4	$16.9 \pm 0.6$
Octacosanoic acid $\text{C}_{28:0}$ (montanic)	424.4	496.5	481.4	$113.1 \pm 1.0$
Dotricontanoic acid $\text{C}_{32:0}$	480.5	552.5	537.5	$48.5 \pm 3.0$
<b><i>Total saturated fatty acids</i></b>				<b><i>977.6 <math>\pm</math> 13.7</i></b>
<b><i>Unsaturated Free Fatty acids</i></b>				
Oleic acid $\text{C}_{18:1}$	282.3	354.7	339.3	$24.6 \pm 1.6$
Linoleic acid $\text{C}_{18:2}$	280.2	352.7	337.3	$2.3 \pm 0.4$
<b><i>Total unsaturated fatty acids</i></b>				<b><i>26.9 <math>\pm</math> 2.0</i></b>
<b>Total Free Fatty acids identified</b>				<b>1004.5 <math>\pm</math> 15.7</b>

**Figure 2-8** shows the percentage of composition of total free fatty acids found in rice straw wax obtained by hexane extraction. The most abundant fatty acid in rice straw was palmitic acid (C16:0) in concentration of  $410.1 \pm 0.2 \mu\text{g/g}$  of plant and 41.3% of fatty acids composition. Relatively high quantities of longer chain fatty acids were also found, stearic acid (C18:0), 12.6%, and octacosanoic acid (C28:0), 11.5%, with the amounts of  $127.1 \pm 2.6$  and  $113.1 \pm 1.0 \mu\text{g/g}$  of plant respectively. These results are consistent with previous studies that highlighted that palmitic acid (C16 : 0) was the most abundant free fatty acid, and corresponding to 3.82–8.11% of the total extract.<sup>28</sup> Saturated fatty acids such as palmitic acid (C<sub>16:0</sub>) can be used as a feedstock for the production of a wide range of home and personal care products including soaps, detergents, polishes and lubricants.<sup>122,123</sup>

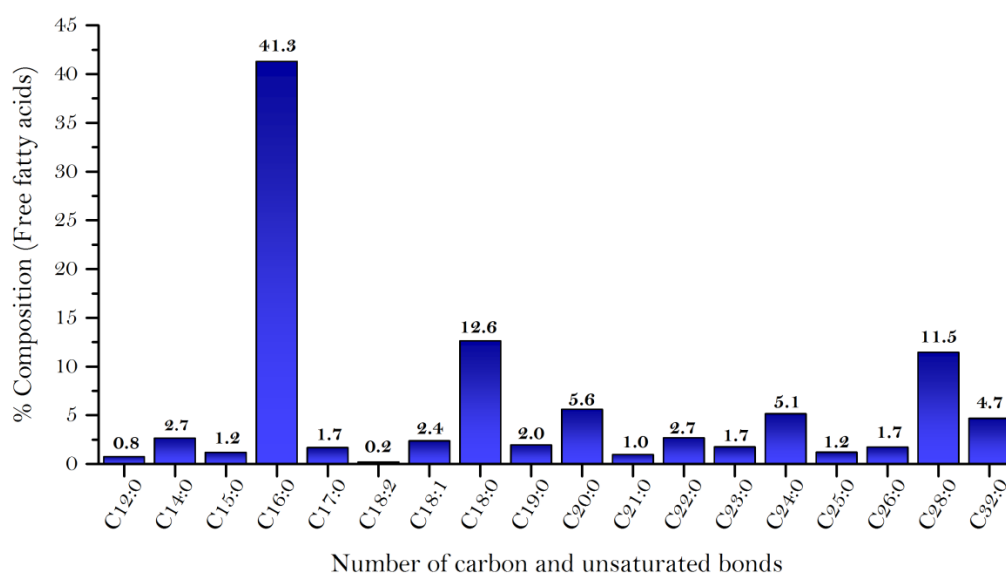


**Figure 2-8** Typical free fatty acid distribution of rice straw.

## 2.2.2 *n*-Alkane in rice straw

In lipid extract of rice straw, the identification of four long chain alkanes was conducted by HTGC-MS. The electron impact mass spectra of tritriacontane is exemplified in **Figure 2-9**. In the majority of cases of long-chain alkanes, the molecular peak in the EI mass spectra is either present as weak signal or often invisible due to the highly energetic of the technique.<sup>124</sup> Therefore, the determination of chain length of this family compounds was achieved by comparison of their retention time with those of commercial standards.

The fragmentation patterns in the EI mass spectra of *n*-alkanes consists of alkyl-type ions of the formula  $[C_nH_{2n+1}]$ . The EI mass spectrum of tritriacontane showing in **Figure 2-9** demonstrates that the characteristic loss of  $m/z$  14, corresponds to  $CH_2$  alkane via a simple cleavage of the chain. The base peak appears at  $m/z$  57 corresponding to butyl ions  $C_4H_9^+$ .<sup>115</sup> The series of alkyl ions are found at  $m/z$  43, 57, 71, 85, 99, 113, 127, 141 and those of unsaturated ions at  $m/z$  41, 55, 69, 83, 97, 111 and 125.<sup>124</sup> The peak intensities of the alkyl fragments regularly decrease with increase of carbon number.<sup>106,125,126</sup>

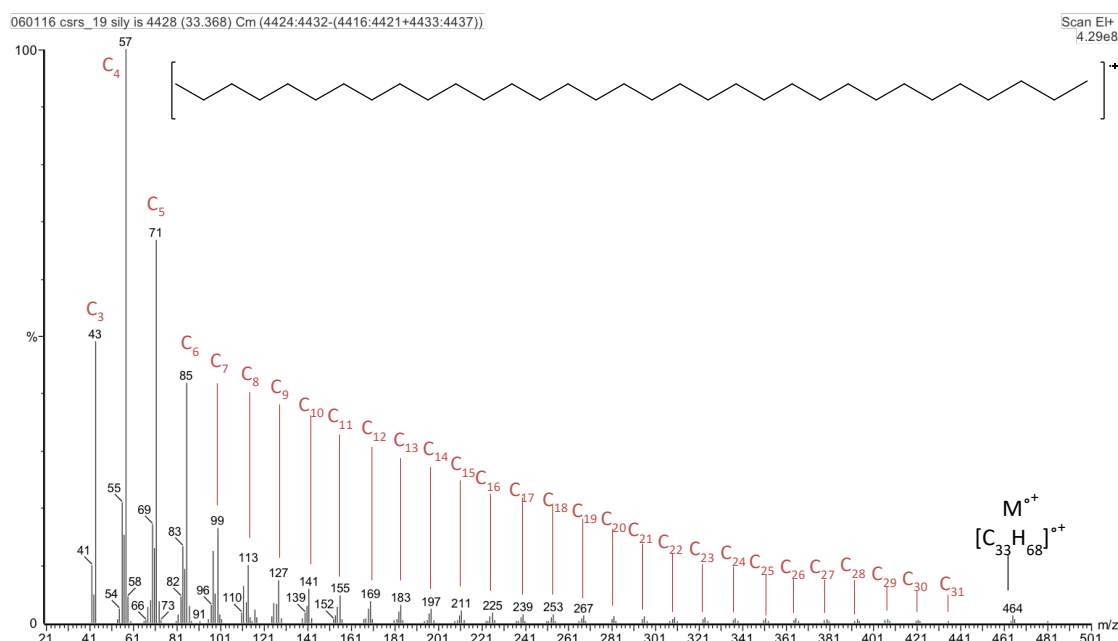


**Figure 2-9** EI mass spectra of Tritriacontane (C<sub>33</sub>)

The *n*-alkanes detected in rice straw wax possess the chain length of C<sub>27</sub> to C<sub>31</sub>, presented in. The dominant compound of the family belongs to tritriacontane (C<sub>33</sub>) with the concentration of 101.0

$\pm 0.6 \mu\text{g/g}$  of plant. Alkane distribution of rice straw is relatively insignificant with the total of  $202.2 \pm 1.1 \mu\text{g/g}$  of plant and found to be  $\text{C}_{33} > \text{C}_{31} > \text{C}_{29} > \text{C}_{27}$  (See **Table 2-2**). This alkane pattern is consistent with other agricultural residues (sugarcane and maize) that demonstrate a high abundance of  $\text{C}_{33}/\text{C}_{31}/\text{C}_{29}$  alkanes.<sup>70,104</sup> For the best of author knowledge, this is the first time that *n*-alkane is identified and quantified in rice straw extract.

**Table 2-2** List of identified *n*-alkanes with their molecular weights and abundances in  $\mu\text{g/g}$  of plant

Alkanes	Molecular weight	Abundance $\mu\text{g/g}$ of plant
Heptacosane ( $\text{C}_{27}$ )	380.7	$10.1 \pm 0.1$
Nonacosane ( $\text{C}_{29}$ )	408.8	$41.0 \pm 0.1$
Hentriacontane ( $\text{C}_{31}$ )	436.8	$50.1 \pm 0.3$
Tritriacontane ( $\text{C}_{33}$ )	464.9	$101.0 \pm 0.6$
<b>Total alkanes</b>		<b><math>202.2 \pm 1.1</math></b>

Plant alkanes such as those identified in rice straw can display semiochemical properties and provide a key role in plant-insect interactions.<sup>127</sup> Semiochemicals act as biochemical signals for living organisms such as insects.<sup>128</sup> Work by Deswarte *et al.* demonstrated that alkanes from wheat straw wax can be utilised as a natural insecticide for the control of aphids.<sup>129</sup> Further work would be needed to determine if rice straw wax could be used in such applications.

### 2.2.3 Fatty alcohols in rice straw

The trimethylsilyl ethers of fatty alcohols do not usually exhibit molecular ion in EI mass spectrometry but the peak  $[M-15]^+$  is significantly prominent. The alkane fragments, which correspond to the alkane fragmentation of the carbon chain, are dominant such as  $m/z$  57, 97 and 117 in the spectra of 1-triacontanol (**Figure 2-10**). Ions resulting from the trimethylsilyl group are  $m/z$  73, 75, 89 and 103. The high intensity ion at  $m/z$  75 relates to  $[(CH_3)_2SiOH]^+$ . The remaining ions with  $m/z$  73, 89 and 103 correspond to  $[(CH_3)_3Si]^+$ ,  $[(CH_3)_3SiO]^+$  and  $[(CH_3)_3OSiCH_2]^+$  respectively.

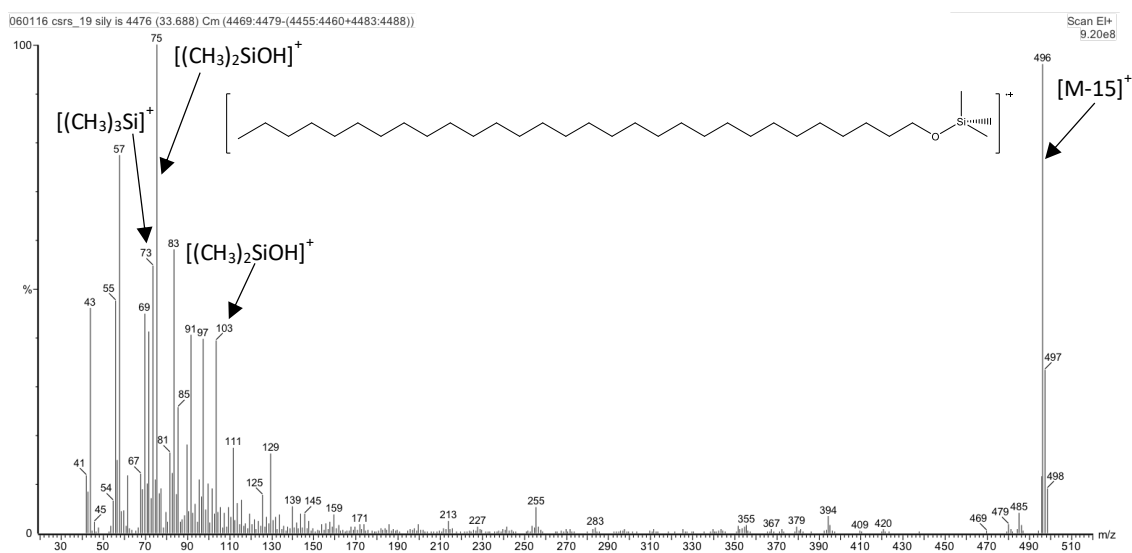


**Figure 2-10** EI mass spectra of trimethylsilyl ether of 1-Triacontanol ( $C_{30}$ )

Three long-chain fatty alcohols with even chain length,  $C_{26}$ - $C_{30}$  were identified and quantified for the first time within rice straw wax with total concentration of  $111 \pm 0.3 \mu\text{g/g}$  of dry biomass. The abundance of fatty alcohols found herein increased with the increase of number of carbon chain-length,  $C_{26} < C_{28} < C_{30}$ ,  $7.7 \pm 0.1$ ,  $19.7 \pm 0.2$  and  $83.6 \mu\text{g/g}$  of dry straw respectively (See **Table 2-3**).

**Table 2-3** List of free fatty alcohols in rice straw wax extracted with hexane and the abundance in  $\mu\text{g/g}$  dry biomass

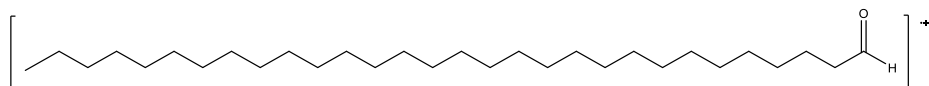
Fatty alcohols	Molecular weight	$M^{+}$ (OTMS)	$[M-15]^{+}$	Abundance
1-Hexacosanol ( $C_{26}$ )	382.4	454.5	439.4	$7.7 \pm 0.1$
1-Octacosanol ( $C_{28}$ )	410.4	482.5	467.5	$19.7 \pm 0.2$
1-Triacontanol ( $C_{30}$ )	438.5	510.5	495.5	$83.6 \pm 0.0$
<b>Total fatty alcohols</b>				<b><math>111.0 \pm 0.3</math></b>

*n*-Policosanols were found in relatively low quantity in rice straw wax. However, these hydrophobic molecules, such as hexacosanol ( $C_{26}$ ), octacosanol ( $C_{28}$ ) and triacontanol ( $C_{30}$ ), have been reported to be promising for cardiovascular disease prevention and therapy as lowering-cholesterol and increasing low-density lipoprotein (LDL) levels.<sup>28</sup>

#### 2.2.4 Fatty aldehydes in rice straw

The presence of fatty aldehydes in rice straw was not reported in previous study by Sun *et al.*<sup>130,131</sup> However, Sun did report the extraction of phenolic aldehydes including syringaldehyde and *p*-hydroxybenzaldehyde.

Analysis by gas chromatography coupled to mass spectrometry confirmed the presence of 1-triacontanal ( $C_{30}$ ) and 1-tetratricontanal ( $C_{34}$ ) in rice straw (See **Table 2-4**). Long-chain fatty aldehyde have been shown to effectively prevent and treat osteoporosis.<sup>132</sup> The EI mass spectra of 1-triacontanal (**Figure 2-11**) showed a small recognisable molecular ion at  $m/z$  436. Other diagnostic ions were  $m/z$  418  $[M-18]^{+}$  and 390  $[M-46]^{+}$  characteristic of the carbonyl group. The successive loss of hydrocarbon portion of 14 and 28 mass units were also observed.<sup>133,134</sup>



060116 csrs\_19 silyl is 4373 (33.001) Cm (4369:4376-(4378:4384+4363:4366))

Scan E1+  
4.55e8

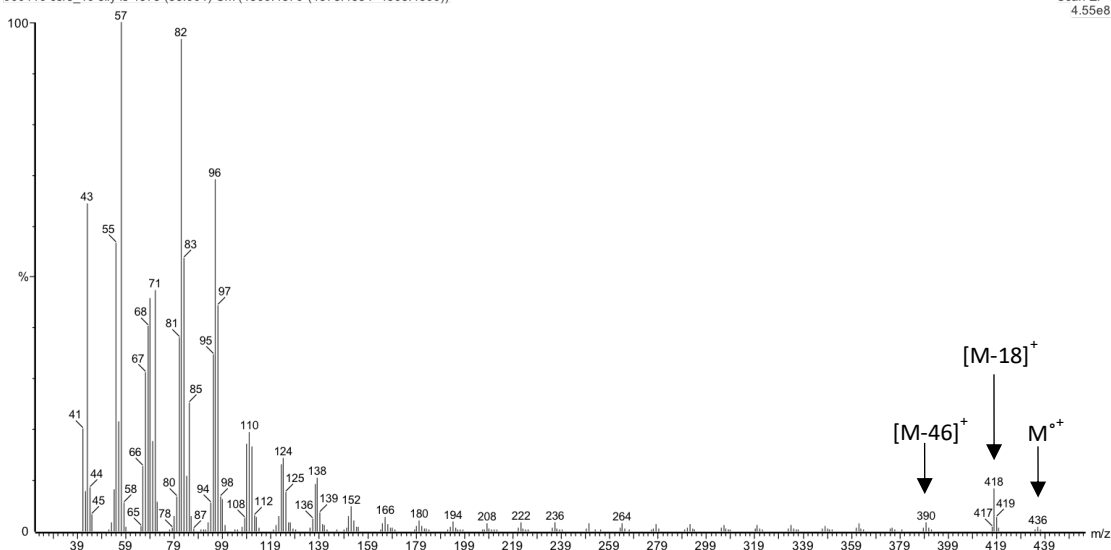


**Figure 2-11** EI mass spectra of 1- triacontanal (C30)

**Table 2-4** List of fatty aldehydes identified in rice straw extract and the abundance in  $\mu\text{g/g}$  dry plant

Aldehydes	Molecular weight	[M-18] <sup>+</sup>	[M-46] <sup>+</sup>	Abundance
1- triacontanal (C <sub>30</sub> )	436	418	390	105
1-tetratricontanal (C <sub>34</sub> )	493	474	447	176.7 ± 11.6
<b>Total aldehydes</b>				<b>281.6 ± 11.6</b>



### 2.2.5 Sterols in rice straw

Sterols present in rice straw were identified by comparison with the NIST 98 library, standard compounds and published spectra.<sup>135,136</sup> Only sterols compounds consisted of campesterol and  $\beta$ -sitosterol (**Figure 2-12**). **Figures 2-13** and **2-14** demonstrate the EI mass spectrum of trimethylsilyl ether of campesterol and  $\beta$ -sitosterol. To the best of author's knowledge, this is first reported study of phytosterols extraction by  $scCO_2$  from rice straw (please see section **2.3.3**). However, previous studies have detected  $\beta$ -Sitosterol and stigmasterol as the predominant components in the solvent extraction from rice straw, comprising over 90% of the total sterols.<sup>28</sup> This is somewhat in contrast to this current study as campesterol was previously not detected in the solvent extraction with hexane, but stigmasterol, stigmastenol, campesterol and  $\beta$ -sitosterol have all previously been detected in the particulate organic matter emitted from rice straw burning.<sup>137</sup>

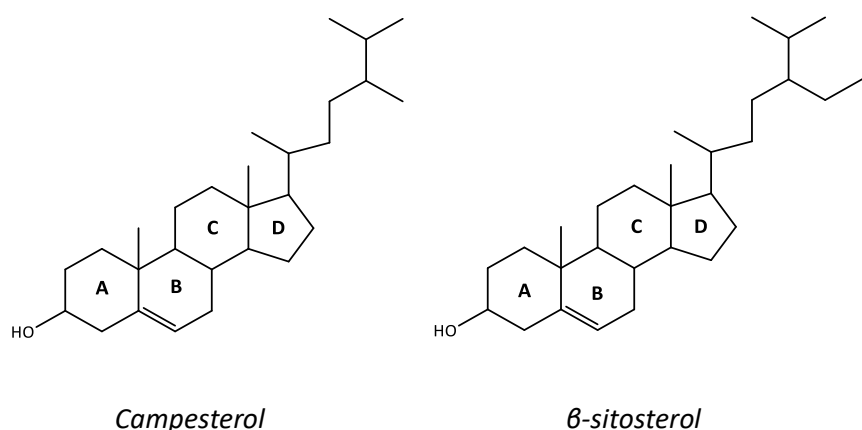


**Figure 2-12** Structure of sterols present within rice straw wax.

**Figure 2-15** illustrates the formation mechanism of fragment  $m/z$   $[M-90]^+$  resulting from the loss of trimethylsilanol (TMSOH) group, which is a common fragmentation in the EI mass spectra of these derivatives.<sup>138</sup>  $\Delta^5$ -sterols (double bond in position 5) including campesterol and  $\beta$ -sitosterol also have particularly characteristic fragmentations involving the loss of TMS-group at the same time with  $C_1$ ,  $C_2$  and  $C_3$  of the sterol A-ring as shown in **Figure 2-16** and **Figure 2-17**. This give rise to the base peak at  $m/z$  129 resulting from a  $\beta$ -cleavage in the ring followed by hydrogen migration and formation of the conjugated siliconium ion and the ion at a  $\beta$ -cleavage in the ring followed by hydrogen migration and formation of the conjugated siliconium ion and

also  $m/z$   $[M-129]^+$ . Then, the formation of  $[M-SC-TMSOH]^+$  ion is presented in **Figure 2-18**. The mechanism involves the loss of the side chain  $[M-SC]^+$  ion followed by rapid loss of a trimethylsilanol TMSOH group so that only  $m/z$  255  $[M-SC-TMSOH]^+$  was detected in the mass spectrometry.<sup>135,136,139</sup> All the characteristic fragments of trimethylsilyl ether of campesterol and  $\beta$ -sitosterol are listed in **Table 2-5**.

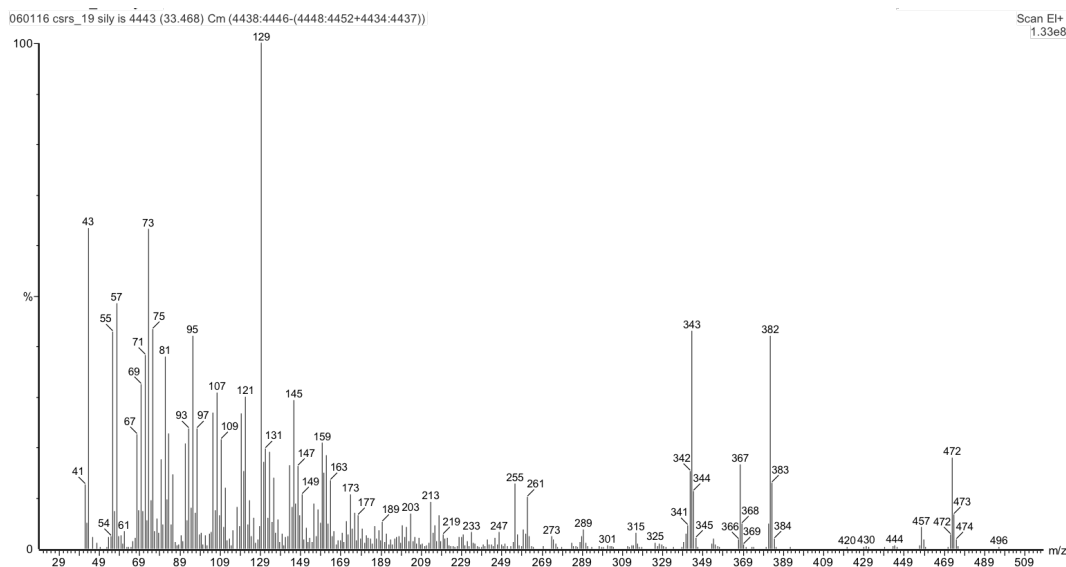


**Figure 2-13** The EI Mass spectrum of trimethylsilyl ether of campesterol.

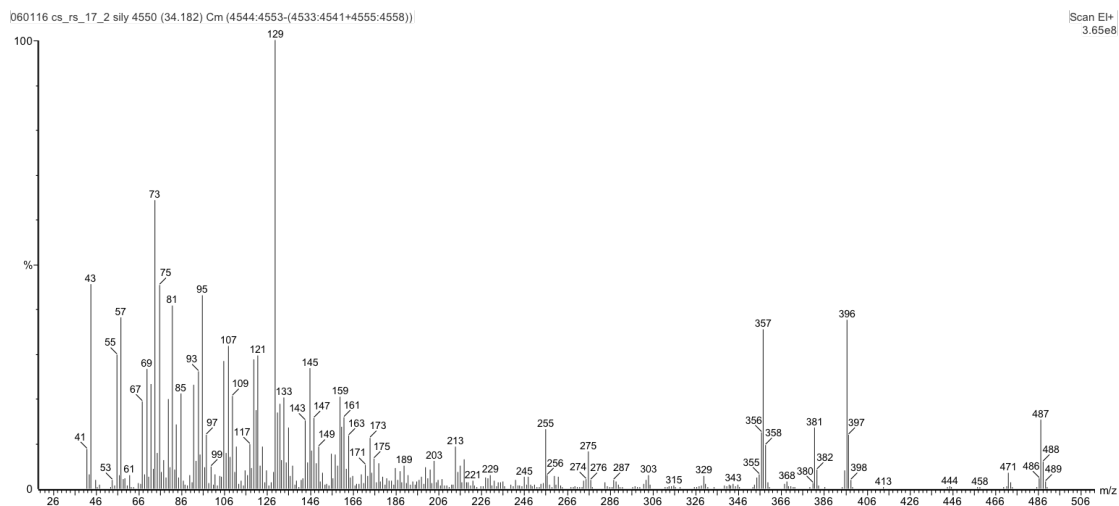


**Figure 2-14** The EI Mass spectrum of trimethylsilyl ether of  $\beta$ -sitosterol.

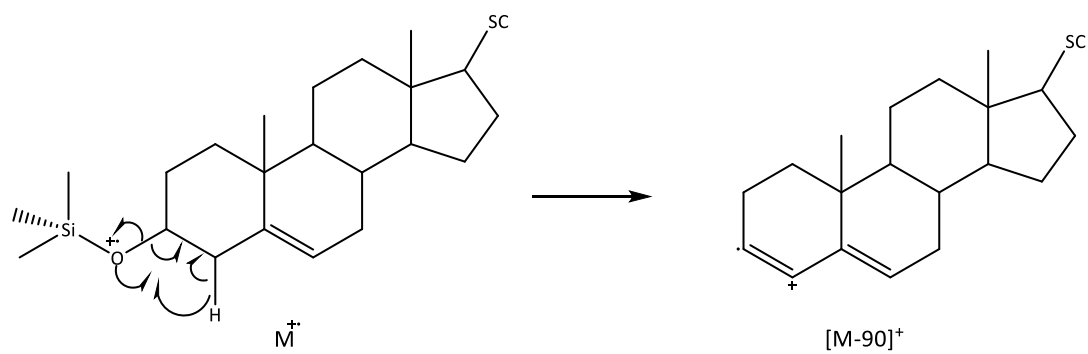


**Figure 2-15** Formation of the characteristic fragment  $m/z$   $[M-90]^+$

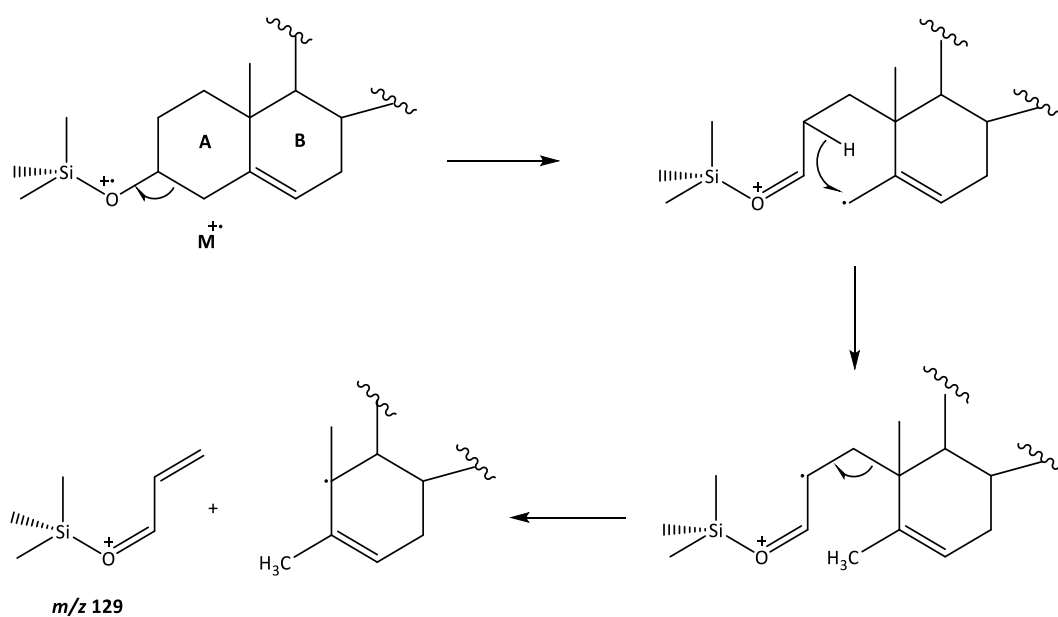


**Figure 2-16** Fragmentation of a  $\Delta^5$ -steroid TMS ether to the characteristic  $m/z$  129

$([C_1, C_3 + TMSO]^+)$ .<sup>135,136,139</sup>

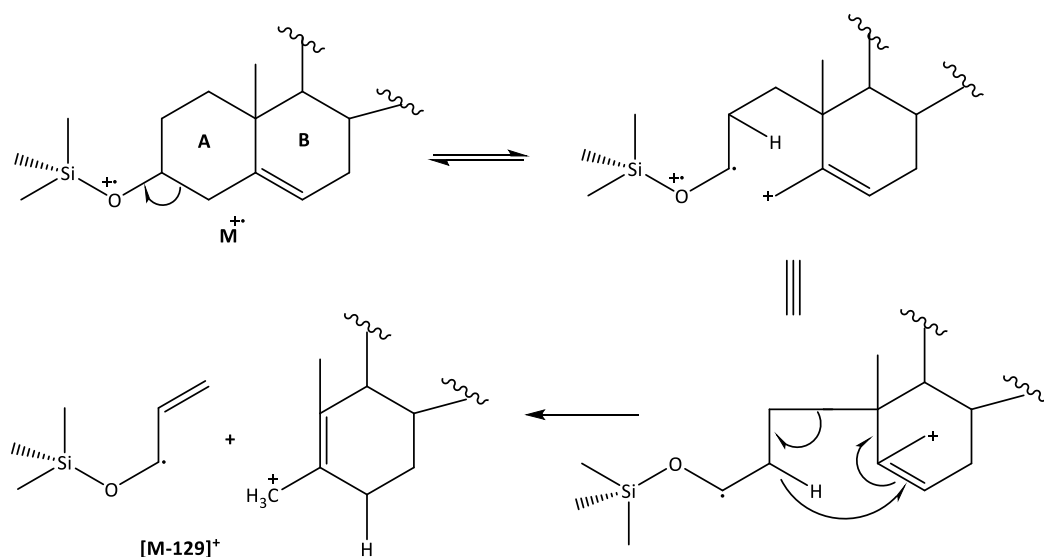


**Figure 2-17** Fragmentation  $\Delta^5$ -steryl TMS ether to the characteristic  $m/z$  [M-129]<sup>+</sup> ([M-C<sub>1</sub>,C<sub>3</sub>-TMSO]<sup>+</sup>) ions.<sup>138</sup>

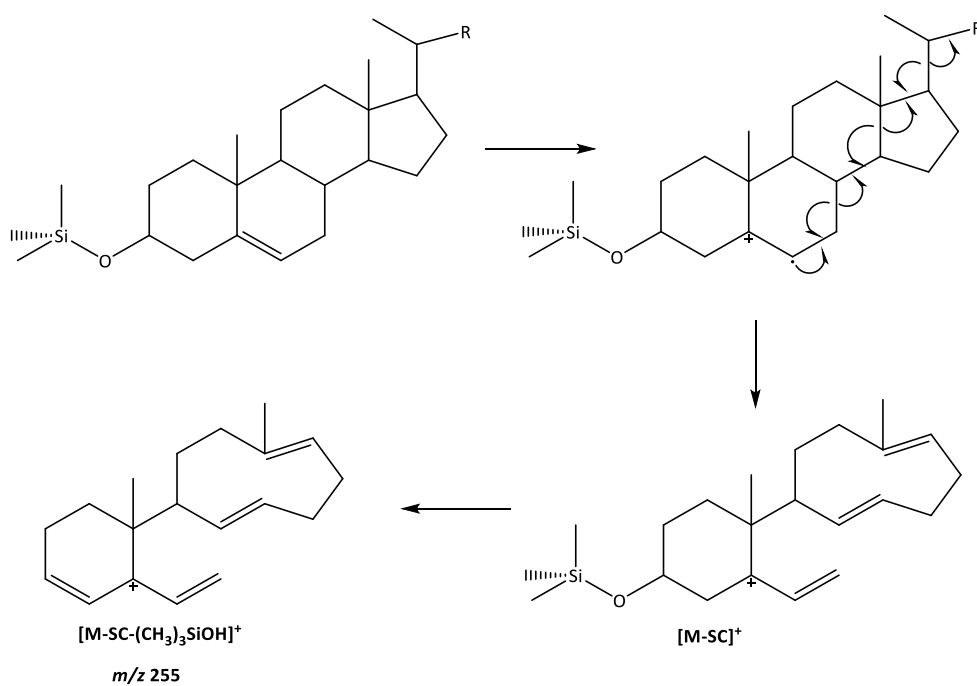


**Figure 2-18** Fragmentations of a  $\Delta^5$ -steryl TMS ether to the characteristic  $m/z$  255 ([M-SC-TMSOH]<sup>+</sup>) by loss of the side chain.<sup>140-142</sup>

**Table 2-5** Characteristic fragments of campesterol and  $\beta$ -sitosterol OTMS.

Characteristic fragments	Campesterol (C <sub>28</sub> H <sub>48</sub> O)	$\beta$ -sitosterol (C <sub>29</sub> H <sub>50</sub> O)
Molecular weight	400.4	414.4
M <sup>o+</sup>	472.4	486.4
[M-15] <sup>+</sup>	457.4	471.4
[M-CH <sub>3</sub> -TMSOH] <sup>+</sup> or [M-(15+90)] <sup>+</sup>	367.3	381.4
[M-SC-TMSOH] <sup>+</sup>	255.2	255.2
[C <sub>1</sub> ,C <sub>3</sub> + TMSO] <sup>+</sup>	129.1	129.1

The presence of both campesterol and sitosterol in rice straw was not in high concentration with the total detected  $351.9 \pm 18.7 \mu\text{g/g}$  dry straw. The abundance of campesterol was  $245.1 \pm 07 \mu\text{g/g}$  dry straw while that of sitosterol was only  $106.8 \pm 18.0 \mu\text{g/g}$  dry straw. However, these sterol molecules have valuable health benefits similar to polyosanol of possessing ability to reduce total and LDL cholesterol levels when used in conjunction with a healthy diet and exercise. With current limit supply source such as vegetable oil and pinewood, rice straw could be another door to satisfy the demand.<sup>143-145</sup>

### 2.2.6 Steroid ketone

Another class of lipid compounds identified in rice straw wax was steroid ketones. Two steroid ketones, stigmast-4-en-3-one and (5 $\alpha$ )-stigmastane-3,6-dione, were detected by GC-MS. NIST library and published papers (which will be cited later on) were used as reference to confirm the present of the components (See structures in **Figure 2-19**).

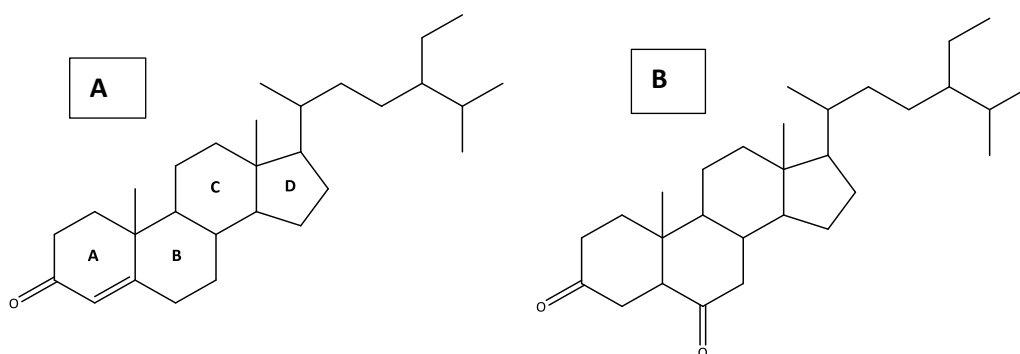


**Figure 2-19** Structure of A) stigmast-4-en-3-one and B) (5 $\alpha$ )-stigmastane-3,6-dione.

The EI mass spectra of Stigmast-4-en-3-one (**Figure 2-25**) showed  $m/z$  at 412  $[M^+]$  as the molecular ion and was consistent to the molecular formula ( $C_{29}H_{48}$ ). The molecular weight of 412 suggested that it was  $\Delta^4$ -3-keto steroid. A characteristic peak at  $m/z$  124 resulted from the B-ring cleavage and other important fragments observed in the EI mass spectra included fragments at  $m/z$  398  $[M-15]^+$ , 370  $[M-42]^+$ , 288  $[M-124]^+$ , 271  $[M\text{-side chain}]^+$ , 229  $[M-42\text{-side chain}]^+$ .<sup>144,146</sup> **Figure 2-20** show the structure and carbon atoms label.

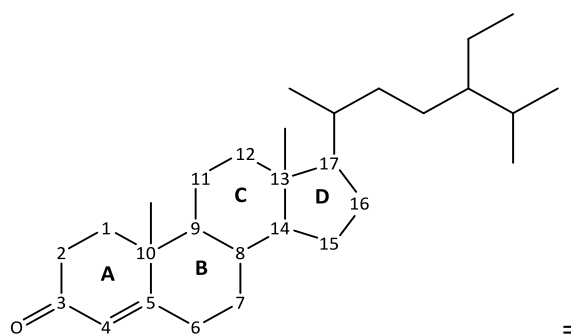


**Figure 2-20** Label of carbon atom in the structure of Stigmast-4-en-3-one.

The formation mechanism of the characteristic fragment of  $\Delta^4$ -3-ketosteroids  $m/z$  124 is shown in **Figure 2-21**. The steric effect on the A/B ring system is diminished by the fission of allylically activated  $C_9$ - $C_{10}$  bond of the ionised steroid resulting in the presence of ion A. The following formation of ion B takes place by hydrogen migration of  $C_8$  to  $C_{10}$  where the radical site is located. Then, chemical bond between  $C_6$ - $C_7$  is cleaved by the transfer of an allylic hydrogen from  $C_{11}$  to the oxygen atom giving rise to ion C of  $m/z$  124 and neutral fragment D.<sup>144</sup>

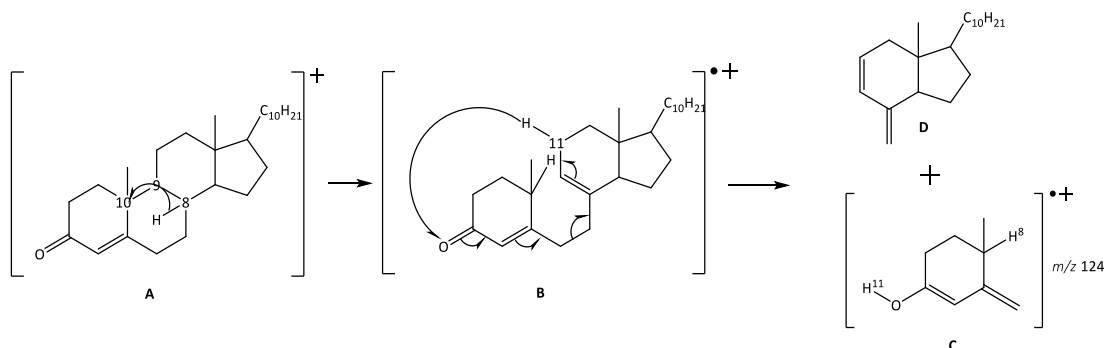


**Figure 2-21** Mechanism of formation of fragment  $m/z$  124 in steroid ketones.<sup>144</sup>

Similarly to the formation of fragment  $m/z$  124, another characteristic ion at  $m/z$  288  $[M-124]^+$  is a result of C<sub>6</sub>-C<sub>7</sub> and C<sub>9</sub>-C<sub>10</sub> cleavage. However, the positive charge is located on the rings C and D where the hydrocarbon fragment is. A hydrogen atom is migrated away from the charged molecular ion; however, migration is not specific with the possibilities of transfer from C<sub>8</sub>, C<sub>14</sub>, C<sub>15</sub> and C<sub>9</sub>. (see **Figure 2-22** for the formation of  $[M-124]^+$ ).<sup>144</sup>

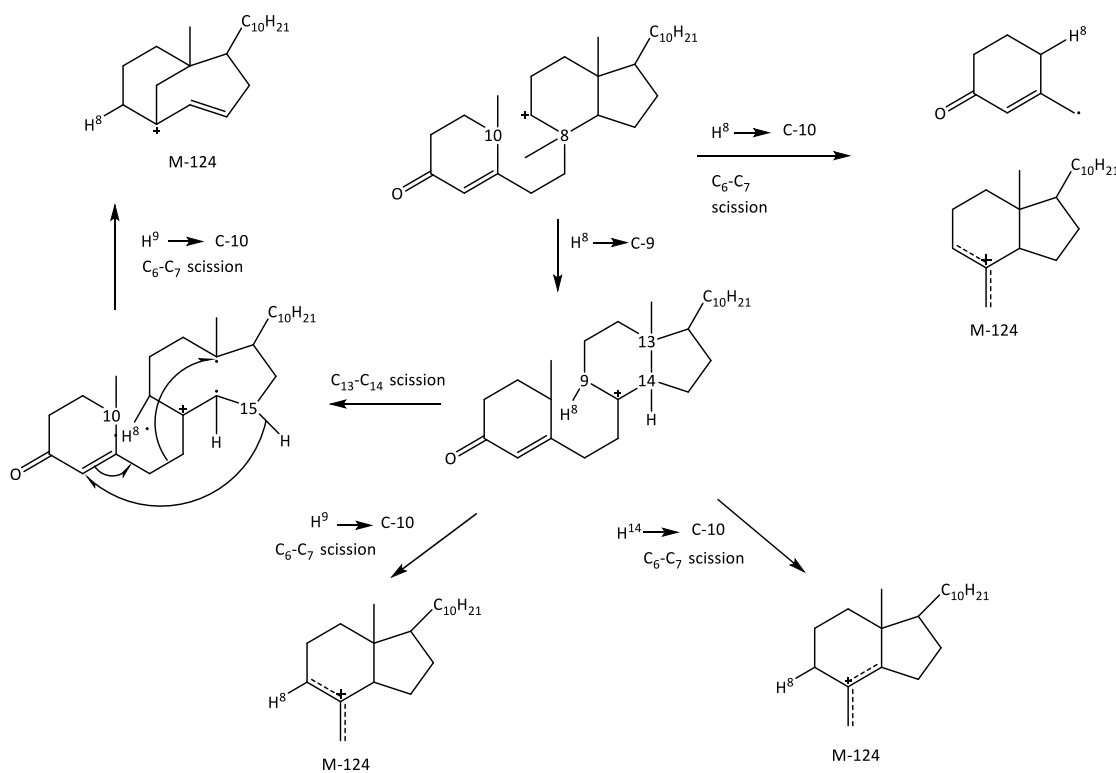


**Figure 2-22** Overall formation of  $m/z$  288  $[M-124]^+$  via hydrogen migration.<sup>143</sup>

There are other important characteristic fragments of  $\Delta^4$ -3-ketosteroids apart from  $m/z$  124 and  $[M-124]^+$ . The signal at  $m/z$  370 is produced by the loss of a ketene from ring A, the possible pathway is presented in **Figure 2-23**. The low intensity ion at  $m/z$  355 is results of the loss of ketene and a methyl radical.<sup>147</sup>

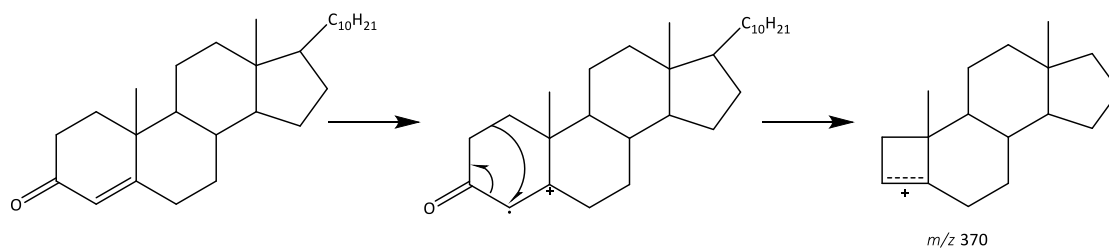


**Figure 2-23** Fragmentation of  $m/z$  370 via the loss of ketene from ring A.

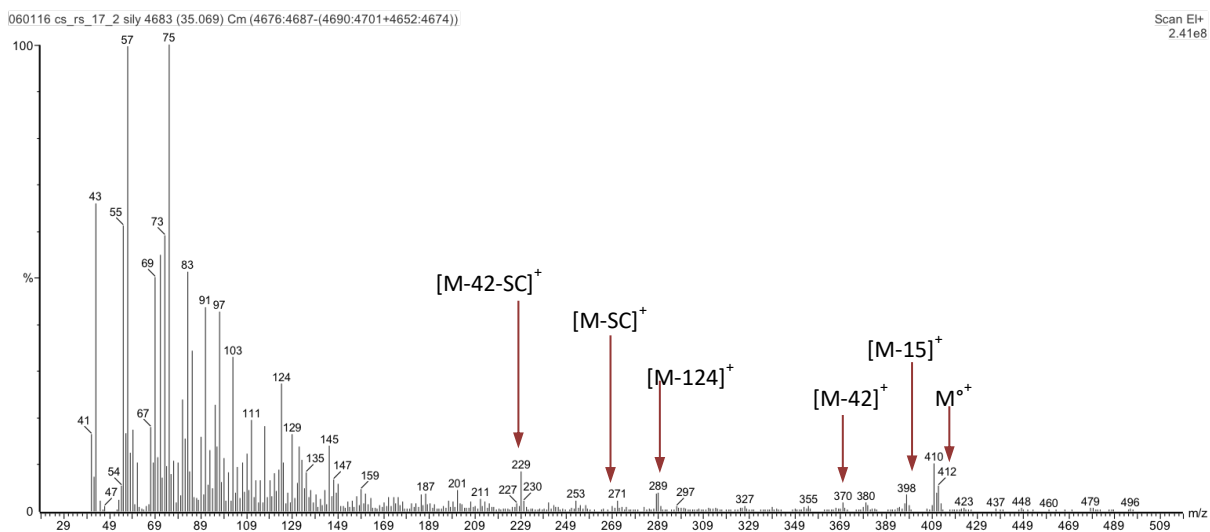


**Figure 2-24** EI mass spectra of Stigmast-4-en-3-one.

The other steroid determined in the rice straw wax was (5 $\alpha$ )-Stigmastane-3,6-dione. In **Figure 2-25**, the molecular ion at  $m/z$  428 corresponded to the molecular formula  $C_{29}H_{48}O_2$ . The other characteristic fragments were  $m/z$  413  $[M-15]^+$ , 315  $[M-C_8H_{17}]^+$ , 287  $[M-C_{10}H_{21}]^+$ , 259  $[M-C_{10}H_{21}-28]^+$ , 245  $[M-C_{10}H_{21}-C_3H_6]^+$ , 231  $[M-C_{10}H_{21}-28-28]^+$ .<sup>109,148</sup>



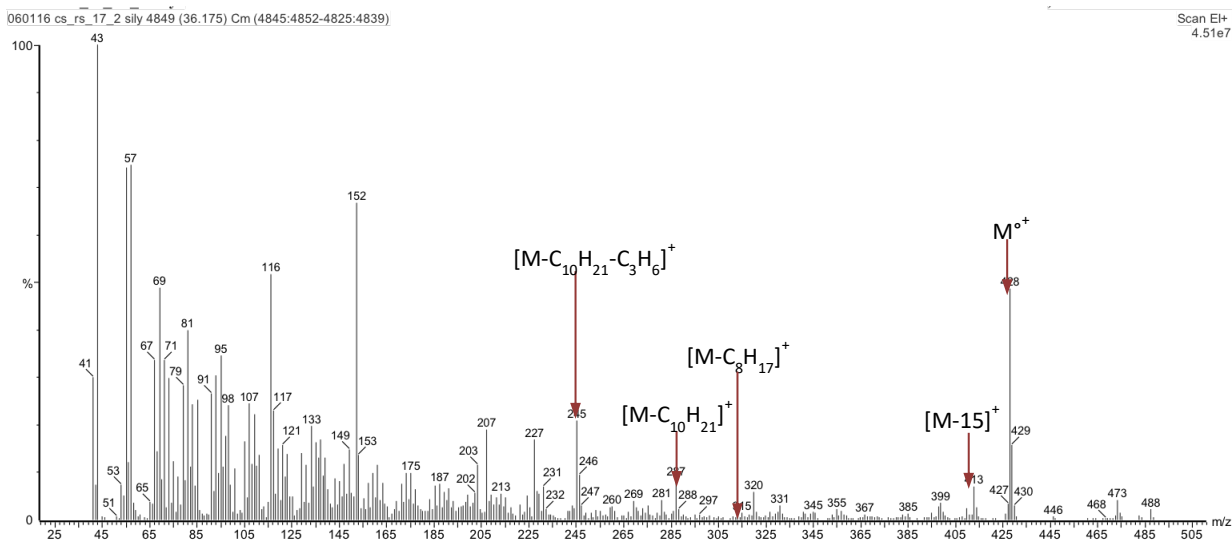


**Figure 2-25** EI mass spectra of (5 $\alpha$ )-Stigmastane-3,6-dione.

These two steroid ketones identified in rice straw wax has shown high health benefits, stigmast-4-en-3-one demonstrated hypoglycaemic effects, ability to reduce in level of blood glucose.<sup>104</sup> The extract of rice straw contained of total steroid ketones  $330 \pm 9.9 \mu\text{g/g}$  of dry straw. The abundance of (5 $\alpha$ )-Stigmastane-3,6-dione is slightly higher than stigmast-4-en-3-one with the concentrations of  $171.4 \pm 3.9$  and  $159.4 \pm 6.0 \mu\text{g/g}$  of dry straw for (5 $\alpha$ )-Stigmastane-3,6-dione and stigmast-4-en-3-one respectively. Rice straw contains low amount of steroid ketones which is in contrast to other agricultural residues such as maize husk.<sup>28</sup>

### 2.2.7 Wax esters

Wax esters were identified to be present in small quantities in rice straw and appeared at the end of the chromatogram. The determination was made with comparison of NIST library and commercial standards available. Herein, seven molecules of wax esters were characterised and identified by their electron impact mass spectra and comparison with the literature and commercial standard. These compounds detected exclusively consisted of esters of *n*-alkanoic acid and *n*-alkan-1-ol, in the range of C<sub>42</sub> to C<sub>54</sub> with odd carbon atoms. However, it was previously reported that rice straw extract contained several wax esters with the chain length of C<sub>32</sub>, C<sub>34</sub> and C<sub>36</sub>.<sup>116,149,150</sup>

Defining R' as the alkyl group in the alcohol moiety and R the alkyl group in the acid moiety. The first characteristic ion was the molecular ion M<sup>+</sup>, other intense fragment ions originating from the fatty acid moiety [RCO<sub>2</sub>H<sub>2</sub>]<sup>+</sup>, [RCO]<sup>+</sup> and [RCO<sub>2</sub>H]<sup>+</sup>. These fragments allowed to determine the chain length of acid moiety, the EI spectra also showed fragments allowing a characterisation of alcohol part, ions m/z [R'-H]<sup>+</sup>, [R'-C<sub>2</sub>H<sub>5</sub>]<sup>+</sup> and [R'-OCO]<sup>+</sup>. the EI mass spectra wax also indicated ions of aliphatic chain at low mass area, [C<sub>n</sub>H<sub>2n+1</sub>]<sup>+</sup> and [C<sub>n</sub>H<sub>2n-1</sub>]<sup>+</sup>.<sup>113,148,151</sup> Here is showed in **Figure 2-26**, the EI mass spectra of hexadecanoic acid (C<sub>16</sub>) and hexacosanol(C<sub>26</sub>), C<sub>42</sub> (C<sub>16</sub>:C<sub>26</sub>). The molecular ion was present in very low intensity at m/z 620 and characteristic fragments of the acid moiety were found at m/z 257 [RCO<sub>2</sub>H<sub>2</sub>]<sup>+</sup>, 256 [RCO<sub>2</sub>H]<sup>+</sup>, 239 [RCO]<sup>+</sup>. Other features allowing to identify the alcohol moiety of this molecule were 365 [R'-H]<sup>+</sup>, 336 [R'-C<sub>2</sub>H<sub>5</sub>]<sup>+</sup> and 409 [R'-OCO]<sup>+</sup>.

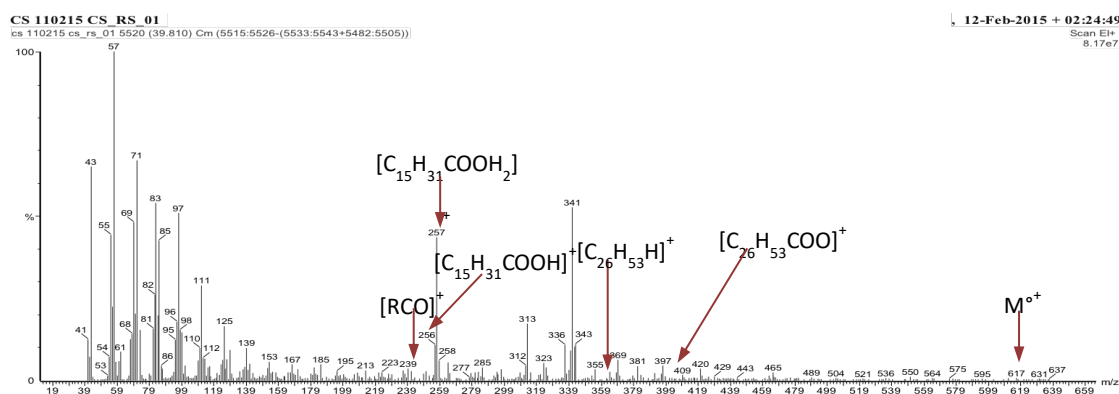


**Figure 2-26** EI mass spectra of ester of hexadecanoic acid (C<sub>16</sub>) and hexacosanol(C<sub>26</sub>): C<sub>42</sub> (C<sub>16</sub>:26).

### 2.3 Supercritical carbon dioxide (scCO<sub>2</sub>) extraction of rice straw

An attempt to optimise the total recovery of wax from rice straw was carried out by applying a factorial experimental design to the variation of temperature and pressure in the scCO<sub>2</sub> extraction. Factorial experimental designs are well documented as an efficient method for enhancing research and reduce the time for process development.<sup>104</sup> This tool aids to describe relationships which may exist between variables. In supercritical fluid extraction, there are important factors including pressure, temperature, density flow rate, duration of extraction and biomass preparation. In this study, the explanatory factors, which were temperature and pressure, were systematically investigated; hence a two-level factorial design was applied. Four extractions have been carried on to study the effect of temperature and pressure (Experiment number 1, 2, 4 and 5) and extra experiment number 3 was conducted as a check point. A variety of temperature and pressure ranges was incorporated into this study as seen in **Table 2-6** and **Figure 2-27**. Four-hour extraction times and constant flow rate of 40 g min<sup>-1</sup> of CO<sub>2</sub> were allotted for each set of experiments. The temperature and pressure ranges selected were between 35 to 65 °C and 75 to 400 bar respectively. The extracts obtained were analysed without further purification.

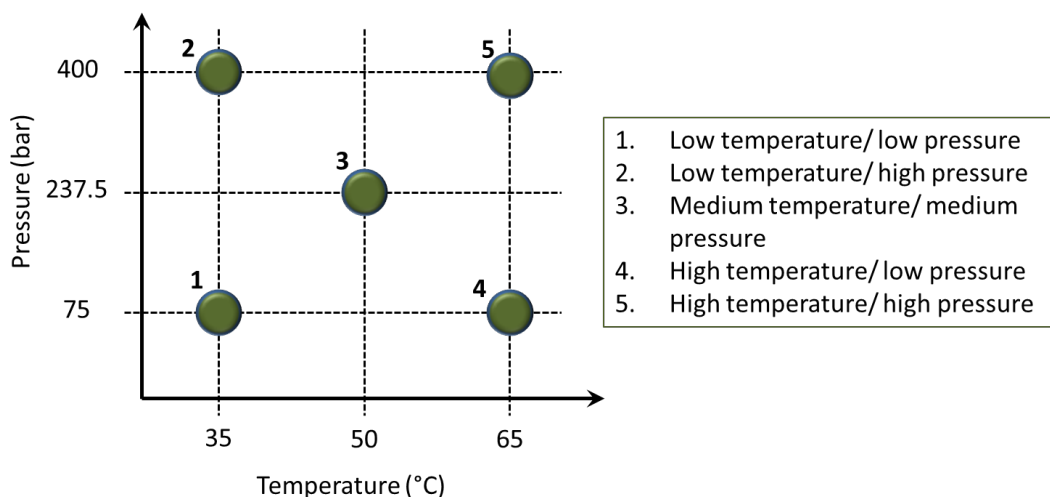


**Figure 2-27** Two-level factorial design experiments.

### 2.3.1 Extraction yields

The scCO<sub>2</sub> extracted rice straw waxes under different conditions varied from 0.01 to 0.70% of dry biomass demonstrating in **Figure 2-28**. The yields of lipophilic extractives from rice straw are summarised in **Table 2-6**. The highest yield was obtained at 65°C and 400 bar (0.70% of dry plant), which can preliminary consider as the optimal condition. These yields are consistent with those previously reported by Sun *et al.* by hexane extraction (0.65% of dry plant)<sup>28</sup> but, slightly lower than the 1% obtained for hexane extraction in this study. In contrast, the lowest yield was recovered at 65°C and 75 bar. At constant temperatures, the extraction yields increased with rising pressure, the similar trend on the yields was observed with increasing temperature at fixed pressure. It is previously seen that a relationship existed between the extraction capability of scCO<sub>2</sub> and its density. It was predicted that higher extraction yield was proportional to the increase in density of CO<sub>2</sub>.<sup>53,104</sup>

**Table 2-6** Extraction yields obtained at different pressures and temperatures for rice straw.

Experiments	Temperature (°C)	Pressure (bar)	Density of CO <sub>2</sub> (g.cm <sup>-3</sup> )	Yield (dry biomass)
1	35	75	0.27	0.05
2	35	400	0.97	0.41
3	50	238	0.82	0.52
4	65	75	0.16	0.01
5	65	400	0.87	0.70

### 2.3.2 Effect of temperature and pressure on scCO<sub>2</sub> extraction efficiency

Different temperature and pressures resulted in a change in the dielectric constant and the density of CO<sub>2</sub> which in turn led to changes in the solvation properties of CO<sub>2</sub>. This influences the solubility of compounds in CO<sub>2</sub> leading to different extraction yields and chemical composition of the extracts (See **Figure 2-28**).<sup>53,69,104</sup>

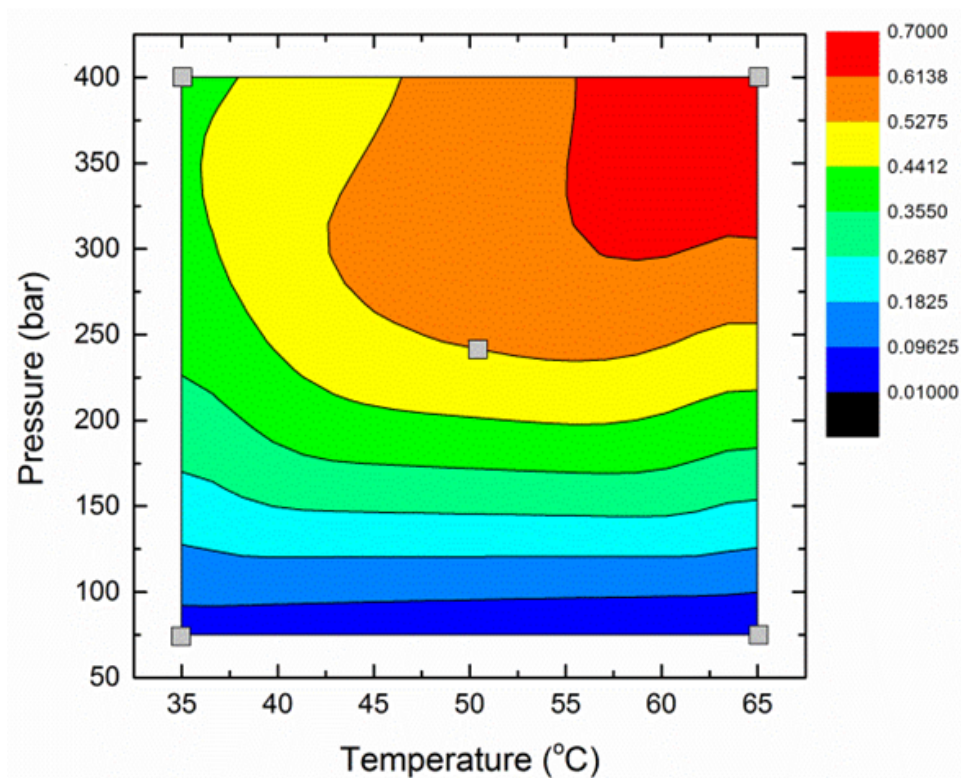


**Figure 2-28** The contour plot of wax yield under different condition of scCO<sub>2</sub> extraction as designated according to the two-level factorial design.

The yields of wax extract significantly increased with increasing pressure. At fixed temperature, a rise in pressure from 75 to 400 bar dramatically increased the extraction yield (0.05% at 35°C/75 bar compared to 0.41% at 35 °C/400 bar and 0.01% at 65°C/75 bar compared to 0.70% at 65 °C/400 bar). These results indicated that the density of CO<sub>2</sub> played an important role in the extraction efficiency as in both experiments, the density of CO<sub>2</sub> is high, 0.97 g.cm<sup>-3</sup> at 35 °C/400 bar and 0.87 g.cm<sup>-3</sup> at 65 °C/400 bar. Furthermore, the highest yield (0.70%) was achieved at 65°C and 400 bar with the density of the CO<sub>2</sub> 0.87 g.cm<sup>-3</sup>, in comparison with the yield obtained

at 35°C, 400 bar (0.41%) in which the density of CO<sub>2</sub> is the greatest, 0.97 g.cm<sup>-3</sup>. This demonstrates that although the density of CO<sub>2</sub> has an important influence, other aspects that dictate the solubility of the wax products in the CO<sub>2</sub> need to be taken into account.

Temperature is also an important factor in scCO<sub>2</sub> extraction of rice straw as higher yields were obtained at higher temperature (65°C). In contrast, the highest yield, 0.70%, was obtained. The density of CO<sub>2</sub> at 65 °C and 400 bar is 0.87 g.cm<sup>-3</sup>, which is lower than the density at 35 °C and 400 bar. The plant cuticular waxes require quite high thermal energy to increase the solubility due to their internal semi-crystalline structure. The results found herein on the influence of pressure and temperature are consistent with previous findings of the scCO<sub>2</sub> extractions of waxes from maize leaf and wheat straw.<sup>152</sup> The effect of pressure and temperature on the solubility of different wax components was in agreement with the published work investigating the extraction of lipid components from wheat straw by scCO<sub>2</sub>.<sup>152</sup> It was reported that the solubility of selected lipid molecules increases with elevated pressure; however the effect of pressure on solubility differs with nature of solutes and operating temperature. The influence of temperature at constant pressure was explained using two mechanisms. The first mechanism is increasing in temperature causes an increase in vapour pressure of CO<sub>2</sub> leading to an increasing in solubility. The second mechanism is a decrease in solvent density caused by temperature increase resulting in a decrease in solubility.<sup>153</sup> A crossover pressure value exists between these two opposing factors. At the pressure below this crossover point, solubility decreases with temperature (where the density is more important). Once this crossover has been overcome, there is an increase in solubility with temperature.<sup>53</sup> This explanation is supporting to this current work where higher yield was obtained at low pressure and temperature (0.05% at 75 bar, 35°C) compared to higher temperature (0.01% at 75 bar, 65°C). This increase of the yield is obviously due to the increase of density. However, at high pressure region, an outstanding increase of yield was achieved at higher temperature (0.70% at 400 bar, 65°C), whereas at lower temperature, 35°C, only 0.41% was yielded.

### **2.3.3 Identification and quantification of group of key compounds in scCO<sub>2</sub>-rice straw extracts.**

The different key wax components have been successfully identified with the full identification process described earlier in this chapter. The extracts obtained from scCO<sub>2</sub> extraction under

different conditions shared similar GC profile to the hexane extract (as chromatogram shown previously in **Figure 2-1**). The use of scCO<sub>2</sub> at different temperatures and pressures has been used as alternative method for traditional organic solvents. The quantification of each product was conducted to demonstrate the influence of pressure and temperature on the chemical composition.

### **2.3.3.1 Free fatty acids**

In rice straw wax, free fatty acid was previously found as the most abundant lipophilic compounds. Both odd and even-chained fatty acids were detected with the chain lengths ranging from C<sub>12</sub> to C<sub>32</sub> and were consistent with the results obtained by hexane soxhlet. Despite several odd chained acids are present, they are in smaller quantities compared to the even chained acids. The quantities of the saturated and unsaturated fatty acids found in scCO<sub>2</sub> extracted wax are summarised in **Table 2-7**.

Saturated fatty acids represented the majority of this group of compounds with hexadecanoic acid (C16:0) being the most predominant (consistent with hexane soxhlet extraction). At lower pressure condition (75 bar) where the density of CO<sub>2</sub> is relatively low, fatty acids were not successfully removed and were detected in small quantities. The highest concentration of fatty acids was found at 65 °C, 400 bar (681.5 ± 10.3 µg/g of dry plant). While a slight difference was observed at 35°C and 400 bar with 652.1 ± 8.4 µg/g of dry plant. However, unsaturated fatty acids were preferentially extracted at lower temperature, 35 °C and 400 bar, 100.4 ± 1.5 µg/g of dry plant, compared to 22.1 ± 0.2 µg/g of dry plant at 65 °C and 400 bar. The highest amount of unsaturated fatty acids was obtained at 50°C and 238 bar. This trend was also observed in the extraction of lipids from sorghum distillers grains.<sup>64,153</sup> Saturated fatty acids were selectively extracted with increased temperature; this is in contrast to the trend of unsaturated fatty acids that decreased with increasing temperature. This is consistent with previous studies that saturated fatty acids extraction efficiency increase as higher temperatures and pressures are applied.<sup>154</sup> The greatest concentration of oleic acid (C18:1), was obtained at 50 °C, 238 bar and that of linoleic acid (C18:2) were obtained by scCO<sub>2</sub> extraction at 50 °C and 238 bar 96.6 ± 0.9 and 31.2 ± 1.2. The extraction of unsaturated fatty acids by scCO<sub>2</sub> was significantly higher than that of hexane soxhlet (24.6 ± 1.6 and 2.3 ± 0.4 µg/g of dry straw for oleic and linoleic acids respectively).

**Table 2-7** Type and quantity of saturated and unsaturated fatty acids in rice straw waxes obtained from different conditions using scCO<sub>2</sub> extraction for 4 hours.

Free fatty acids	Abundance in the extracts in µg/g of dry plant				
	35°C, 75 bar	35°C, 400 bar	50°C, 238 bar	65 °C, 75 bar	65°C, 400 bar
Dodecanoic acid (C <sub>12:0</sub> )	1.0 ± 0.0	3.8 ± 0.0	3.4 ± 0.5	0.3 ± 0.0	4.8 ± 0.1
Azelaic acid	0.7 ± 0.0	2.6 ± 0.0	1.4 ± 0.0	0.2 ± 0.0	3.5 ± 0.0
Tetradecanoic acid (C <sub>14:0</sub> )	6.3 ± 0.0	17.6 ± 0.0	15.7 ± 0.0	4.8 ± 0.0	20.9 ± 0.0
Pentadecanoic acid (C <sub>15:0</sub> )	1.4 ± 0.0	7.0 ± 0.1	6.1 ± 0.0	0.4 ± 0.0	7.7 ± 0.0
Hexadecanoic acid (C <sub>16:0</sub> )	30.7 ± 0.0	252.0 ± 0.4	236.9 ± 0.1	7.2 ± 0.0	267.6 ± 0.6
Heptadecanoic acid (C <sub>17:0</sub> )	0.9 ± 0.0	9.1 ± 0.3	8.1 ± 0.1	0.2 ± 0.0	10.3 ± 0.8
Linoleic acid (C <sub>18:2</sub> )	0.3 ± 0.0	21.4 ± 0.6	31.2 ± 1.2	0.2 ± 0.0	2.1 ± 0.1
Oleic acid (C <sub>18:1</sub> )	0.8 ± 0.0	79.0 ± 1.0	96.6 ± 0.9	0.2 ± 0.0	20.0 ± 0.1
Octadecanoic acid (C <sub>18:0</sub> )	4.5 ± 0.0	78.0 ± 2.7	70.9 ± 0.0	2.7 ± 0.0	81.3 ± 0.3
Nonadecanoic acid (C <sub>19:0</sub> )	4.3 ± 0.0	12.2 ± 0.3	11.6 ± 1.0	1.1 ± 0.0	14.2 ± 1.4
Eicosanoic acid (C <sub>20:0</sub> )	1.0 ± 0.0	33.3 ± 0.1	29.8 ± 0.5	0.4 ± 0.0	36.7 ± 1.8
Heneicosanoic acid (C <sub>21:0</sub> )	1.7 ± 0.0	6.2 ± 0.3	5.7 ± 0.1	0.2 ± 0.0	9.1 ± 0.3
Docosanoic acid (C <sub>22:0</sub> )	0.4 ± 0.0	15.5 ± 0.3	13.6 ± 0.4	0.1 ± 0.0	18.0 ± 0.1
Tricosanoic acid (C <sub>23:0</sub> )	0.5 ± 0.0	10.9 ± 0.1	10.8 ± 0.0	0.1 ± 0.0	11.7 ± 0.5
Tetracosanoic acid (C <sub>24:0</sub> )	0.5 ± 0.0	27.1 ± 0.1	29.2 ± 0.5	0.4 ± 0.0	37.6 ± 0.7
Pentacosanoic acid (C <sub>25:0</sub> )	0.2 ± 0.0	5.3 ± 0.0	6.2 ± 0.2	0.1 ± 0.0	8.4 ± 0.4
Hexacosanoic acid (C <sub>26:0</sub> )	0.2 ± 0.0	6.9 ± 0.2	9.0 ± 0.3	0.1 ± 0.0	12.2 ± 0.2
Octacosanoic acid (C <sub>28:0</sub> )	0.3 ± 0.0	35.0 ± 1.2	64.1 ± 0.5	0.2 ± 0.0	78.9 ± 0.5
Dotriacontanoic acid (C <sub>32:0</sub> )	0.7 ± 0.0	29.2 ± 0.7	23.4 ± 8.6	0.1 ± 0.0	36.5 ± 2.4
<i>Total saturated fatty acids</i>	55.3 ± 0.0	551.7 ± 6.9	545.9 ± 12.8	18.6 ± 0.0	659.4 ± 10.1
<i>Total unsaturated fatty acids</i>	1.1 ± 0.0	100.4 ± 1.5	127.8 ± 2.1	0.4 ± 0.0	22.1 ± 0.2
<b>Total Fatty acids identified</b>	<b>56.4 ± 0.0</b>	<b>652.1 ± 8.4</b>	<b>673.7 ± 14.9</b>	<b>19.0</b>	<b>681.5 ± 10.3</b>



As shown in **Figure 2-29**, in comparison with the result obtained with hexane, the traditional solvent extraction was a more effective method in terms of total free fatty acid recovery as it was able to extract  $1004.5 \pm 15.7 \mu\text{g/g}$  of dry straw, whereas the maximum concentration obtained by  $\text{scCO}_2$  at  $65^\circ\text{C}$  and 400 bar was  $681.5 \pm 10.37 \mu\text{g/g}$  of dry straw. However,  $\text{scCO}_2$  was clearly seen to be the more selective method towards unsaturated fatty acids,  $127.8 \pm 2.1$  and  $26.9 \pm 2.0 \mu\text{g/g}$  of dry straw obtained by  $\text{scCO}_2$  at  $50^\circ\text{C}$  and 238 bar and hexane soxhlet respectively. Such difference might be due to the fact that  $\text{scCO}_2$  protects these components from further oxidation. However, further experiment need to be carried on to verify this assumption.

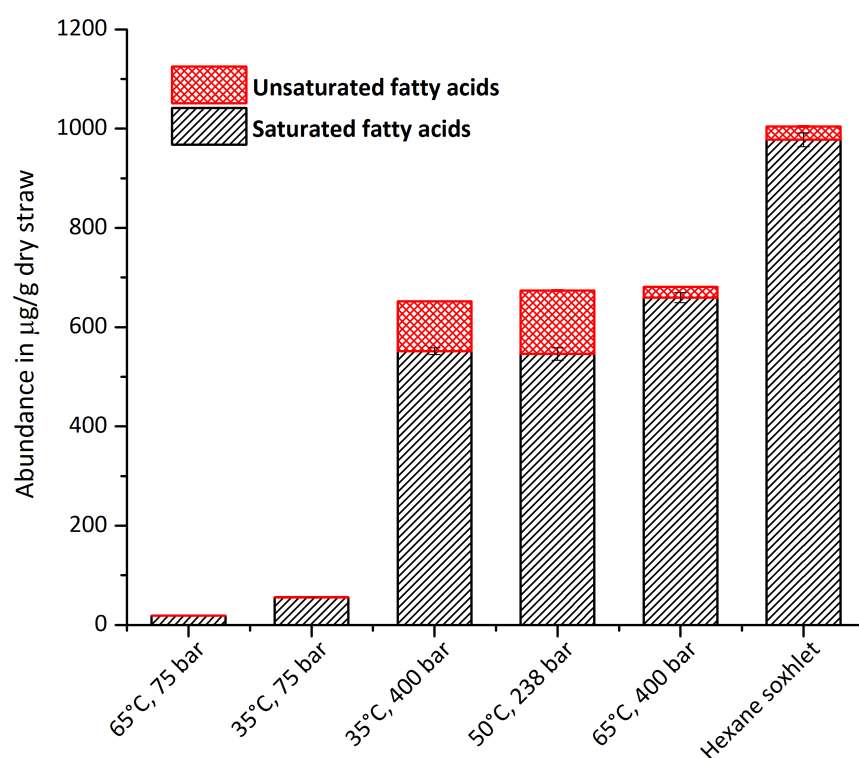


**Figure 2-29** Comparison on concentration of free fatty acids in rice straw waxes extracted using  $\text{scCO}_2$  and hexane Soxhlet for 4 hours.

### 2.3.3.2 Alkanes

As identified earlier in this chapter, the hydrocarbons in hexane extract were all exclusively *n*-alkanes with odd-numbers due to the wax biosynthetic pathway.<sup>155</sup> There were four *n*-alkanes detected, heptacosane ( $\text{C}_{27}$ ), nonacosane ( $\text{C}_{29}$ ), hentriacontane ( $\text{C}_{31}$ ) and triatriacontane ( $\text{C}_{33}$ ), which were also identified in the hexane extract. **Table 2-8** summarised the concentration of the main long chain hydrocarbon in rice straw wax extracted using  $\text{scCO}_2$ . The experiments at low pressure were not effective to extract those lipophilic compounds as only small amounts, 1-2

$\mu\text{g/g}$  of dry straw, were detected in the extracts obtained at 75 bar, 35 °C and 65 °C, which belonged to the low density of  $\text{CO}_2$  region (see **Table 2-6** for the list of density of  $\text{CO}_2$  for each condition). On the other hand, higher concentrations of hydrocarbons were identified in the other three conditions, 35°C, 400 bar, 50°C, 238 bar and 65°C, 400 bar. There was no significant difference among them in terms of concentration; however, the greatest amount of *n*-alkanes was obtained at 65 °C, 400 bar with  $197.8 \pm 1.8 \mu\text{g/g}$  of dry biomass, followed by sc $\text{CO}_2$  extraction at 50°C, 238 bar with  $193.3 \pm 0.7 \mu\text{g/g}$  of dry biomass and then 35°C, 400 bar with  $182.6 \pm 1.0 \mu\text{g/g}$  of dry biomass. Not only density of  $\text{CO}_2$  played important role in the amount of hydrocarbon extracted, but the temperature was also another key factor, which was in agreement with the study of extraction efficiency of aromatic hydrocarbon in sc $\text{CO}_2$ .<sup>156</sup> The comparison of extraction efficiency towards *n*-alkanes of sc $\text{CO}_2$  and hexane soxhlet is shown in **Figure 2-30**. The concentration of *n*-alkanes identified in hexane extract was completely comparable to that of sc $\text{CO}_2$  at 65°C, 400 bar,  $197.8 \pm 1.8$  and  $202.2 \pm 1.1 \mu\text{g/g}$  of dry straw.

**Table 2-8** Types and quantity of main hydrocarbons in rice straw waxes obtained from different conditions using scCO<sub>2</sub> extraction for 4 hours.

<i>n</i> -Alkane	Abundance in the extracts in µg/g of dry plant				
	35°C, 75 bar	35°C, 400 bar	50°C, 238 bar	65 °C, 75 bar	65°C, 400 bar
Heptacosane (C <sub>27</sub> )	0.7 ± 0.0	6.2 ± 0.4	6.4 ± 0.0	0.2 ± 0.0	7.7 ± 0.1
Nonacosane (C <sub>29</sub> )	0.8 ± 0.1	22.4 ± 0.2	27.9 ± 0.0	0.3 ± 0.0	34.1 ± 0.1
Hentriacontane (C <sub>31</sub> )	0.6 ± 0.0	23.9 ± 0.2	33.0 ± 0.1	0.2 ± 0.0	36.6 ± 1.5
Tritriacontane (C <sub>33</sub> )	0.4 ± 0.0	130.1 ± 0.2	126.0 ± 0.6	0.3 ± 0.0	119.3 ± 0.1
<b>Total <i>n</i>-alkanes</b>	<b>2.5 ± 0.1</b>	<b>182.6 ± 1.0</b>	<b>193.3 ± 0.7</b>	<b>1.0 ± 0.0</b>	<b>197.8 ± 1.8</b>

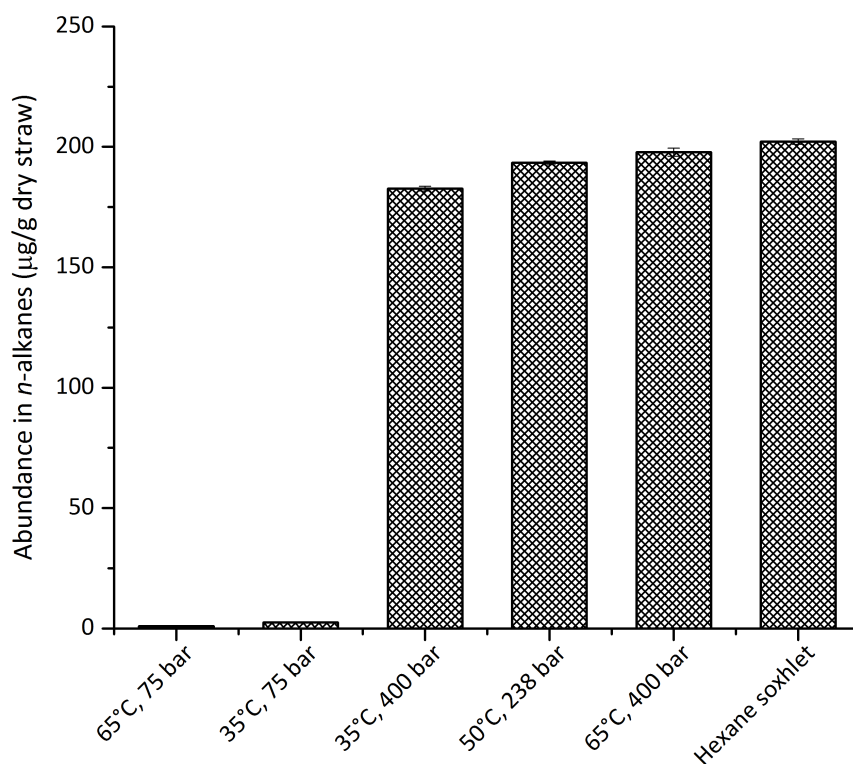


**Figure 2-30** Comparison on concentration of free fatty acids in rice straw waxes extracted using scCO<sub>2</sub> and hexane Soxhlet for 4 hours.

### 2.3.3.3 Long-chain fatty alcohols

Free fatty alcohols were identified in relatively low quantity in rice straw extract. The total concentration of fatty alcohols in lipid extract as obtained through the use of hexane soxhlet was  $111.0 \pm 0.4 \mu\text{g/g}$  of rice straw, this concentration was lower compared to the supercritical extract at  $35^\circ\text{C}$ , 400 bar,  $50^\circ\text{C}$ , 238 bar and  $65^\circ\text{C}$ , 400 bar with  $154.6 \pm 0.4$ ,  $145.8 \pm 2.1$  and  $129.3 \pm 0.8 \mu\text{g/g}$  of rice straw respectively (see **Table 2-9** and **Figure 2-31**). The results in this study were in line with the comparative study of flax dust using hexane and  $\text{scCO}_2$  extraction, the yield of alcohols in  $\text{scCO}_2$  extract was higher than that of hexane.<sup>65,157</sup>

The predominant fatty alcohols in  $\text{scCO}_2$  extracts was 1-triacontanol as found in hexane extract. At low pressure, almost none of fatty alcohol was extracted; however, at high pressure and low temperature, at  $35^\circ\text{C}$ , 400 bar, the greatest amount of total fatty alcohol was recovered. It was also reported that long chain fatty alcohols were effectively obtained when applying high pressure to a supercritical system.<sup>158</sup>

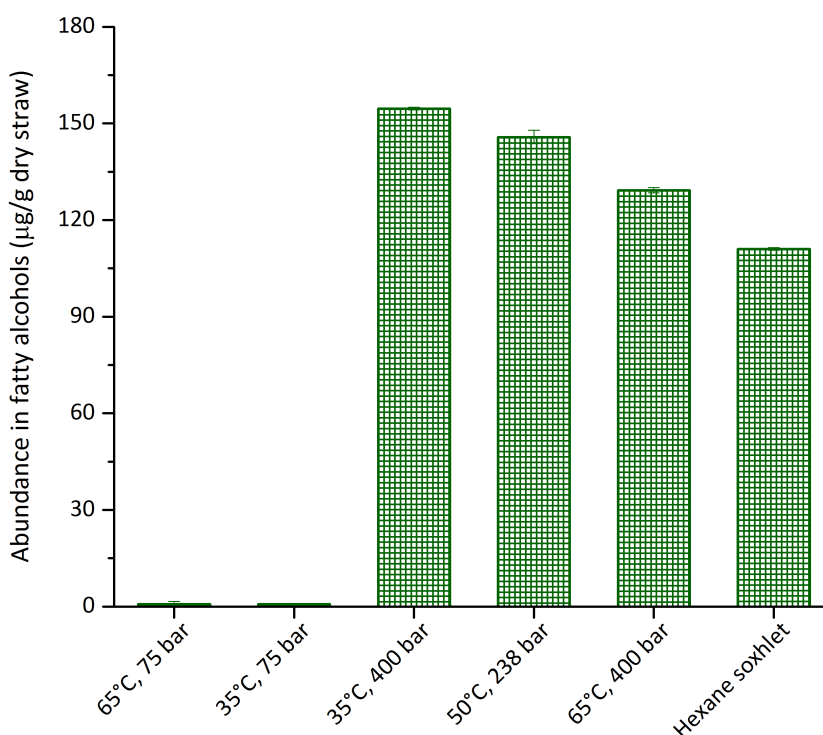


**Figure 2-31** Comparison on concentration of free fatty alcohols in rice straw waxes extracted using  $\text{scCO}_2$  and hexane Soxhlet for 4 hours.

**Table 2-9** Types and quantities of long chain fatty alcohols in rice straw waxes obtained from different conditions using scCO<sub>2</sub> extraction for 4 hours.

Fatty alcohols	Abundance in the extracts in µg/g of dry plant				
	35°C, 75 bar	35°C, 400 bar	50°C, 238 bar	65 °C, 75 bar	65°C, 400 bar
1-Hexacosanol	0.1 ± 0.0	4.4 ± 0.0	5.4 ± 0.0	TR	6.3 ± 0.0
1-Octacosanol	0.1 ± 0.0	7.4 ± 0.3	13.1 ± 0.2	TR	15.6 ± 0.6
1-Triacontanol	0.6 ± 0.0	142.8 ± 0.1	127.3 ± 1.9	0.8 ± 0.0	107.4 ± 0.2
<b>Total Fatty alcohol</b>	<b>0.8 ± 0.0</b>	<b>154.6 ± 0.4</b>	<b>145.8 ± 2.1</b>	<b>0.8 ± 0.0</b>	<b>129.3 ± 0.8</b>

\* TR = *trace* amount

#### 2.3.3.4 Fatty aldehydes

Long chain fatty alcohols, Triacontanol (C30) and Dotriacontanol (C32), were identified in rice straw extract in both hexane and scCO<sub>2</sub> extracts. In scCO<sub>2</sub> extraction, these two compounds were barely extractable in low pressure. However, in high pressure experiments, 35 °C, 400 bar and 50°C, 238 bar and 65°C, 400 bar, the total concentration obtained were completely comparable, 253.7 ± 2.7, 257.5 ± 5.0 and 257.4 ± 16.7 in µg/g of dry rice straw respectively (see Table 2-10).

**Table 2-10** Types and quantities of long chain fatty aldehydes in rice straw waxes obtained from different conditions using scCO<sub>2</sub> extraction for 4 hours.

Aldehydes	Abundance in the extracts in µg/g of dry plant				
	35°C, 75 bar	35°C, 400 bar	50°C, 238 bar	65 °C, 75 bar	65°C, 400 bar
Triacontanal (C30)	0.1 ± 0.0	197.0 ± 2.0	177.9 ± 4.4	0.2 ± 0.0	149.8 ± 6.6
Dotriacontanal (C32)	0.9 ± 0.2	56.7 ± 0.7	79.6 ± 0.6	0.8 ± 0.0	107.6 ± 10.1
<b>Total fatty aldehydes</b>	<b>1.0 ± 0.2</b>	<b>253.7 ± 2.7</b>	<b>257.5 ± 5.0</b>	<b>1.0 ± 0.0</b>	<b>257.4 ± 16.7</b>

In comparison with hexane extract as shown in **Figure 2-32**, there was no significant difference in terms of total fatty aldehydes presented in both extraction methods, hexane extraction yielded a little higher concentration in fatty aldehydes, which was in agreement with previously study.<sup>159</sup> However, it was interesting to analyse each fatty aldehyde separately, as each

condition yielded different concentration of these compounds. In all extracts, from hexane and scCO<sub>2</sub>, triacontanal (C30) was largely predominant; however, at 65°C and 400 bar, higher concentration of dotriacontanal (C32) was detected. Therefore, it was advantageous to selectively extract a component only by changing the temperature. The solubility of fatty aldehyde increased with temperature and pressure, as it was observed in the scCO<sub>2</sub> of saw dust.<sup>53,65</sup>

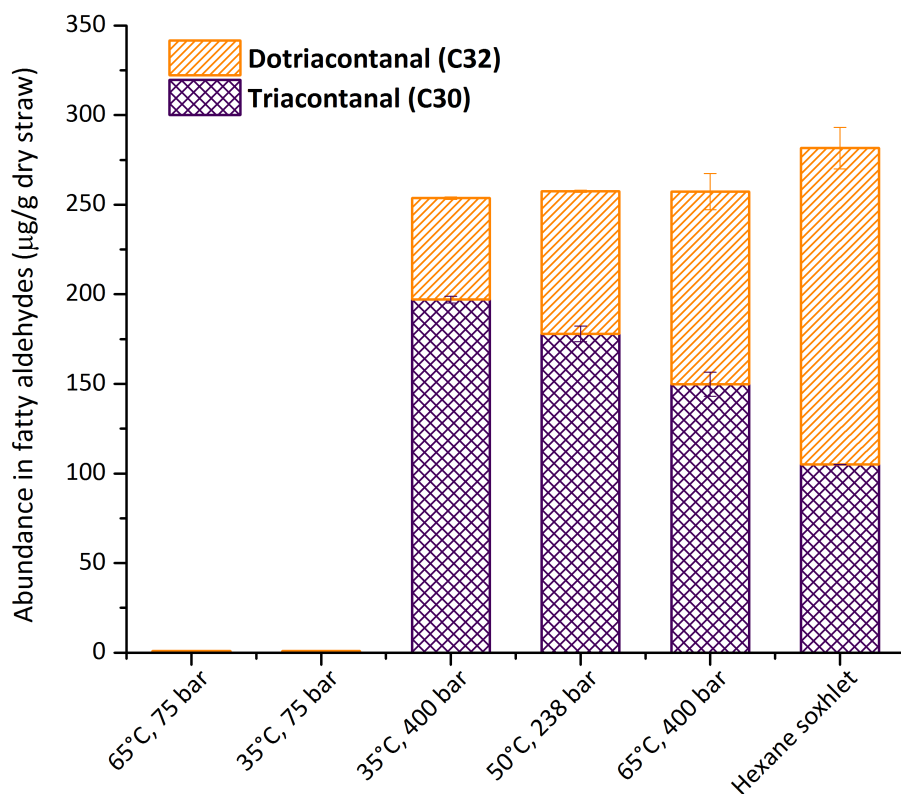


**Figure 2-32** Comparison on concentration of fatty aldehydes in rice straw waxes extracted using scCO<sub>2</sub> and hexane Soxhlet for 4 hours.

### 2.3.3.5 Sterols

Similarly, campesterol and  $\beta$ -sitosterol were identified in scCO<sub>2</sub> extracts as in hexane extract. Sterols were not extractable at low pressure; only about 1  $\mu\text{g/g}$  of dry straw was detected at 35°C and 65°C at 75 bar. The highest concentration identified among all the scCO<sub>2</sub>-extracts were obtained at 65°C, 400 bar, with  $205.8 \pm 0.7 \mu\text{g/g}$  of dry straw, followed by the extract recovered at 50°C, 238 bar with  $148.0 \pm 0.4 \mu\text{g/g}$  of dry straw. This result was in a good agreement with optimisation of scCO<sub>2</sub> of triticale straw and wheat straw (See **Table 2-11**).<sup>53,65</sup>

**Table 2-11** Types and quantities of long chain fatty aldehydes in rice straw waxes obtained from different conditions using scCO<sub>2</sub> extraction for 4 hours.

Sterols	Abundance in the extracts in $\mu\text{g/g}$ of dry plant				
	35°C, 75 bar	35°C, 400 bar	50°C, 238 bar	65 °C, 75 bar	65°C, 400 bar
Campesterol	1.0	$67.2 \pm 0.9$	$148.0 \pm 0.4$	0.1	$205.8 \pm 0.7$
$\beta$ -sitosterol	0.4	$30.2 \pm 4.3$	$32.4 \pm 19.4$	0.3	$60.9 \pm 1.1$
<b>Total sterols</b>	<b>1.4</b>	<b><math>97.4 \pm 5.2</math></b>	<b><math>180.4 \pm 19.8</math></b>	<b>0.4</b>	<b><math>266.7 \pm 1.8</math></b>

As seen in **Figure 2-33**, hexane showed to be more efficient in order to obtain high amount of sterols from rice straw. This comparison in this study was in line with the previous results obtained in other studies.<sup>159</sup>

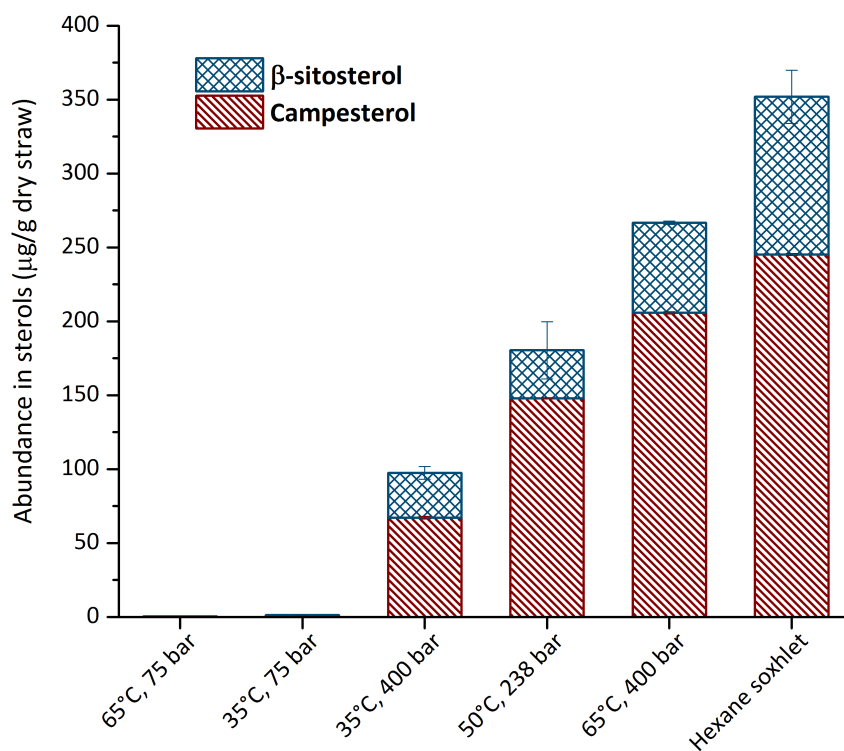


**Figure 2-33** Comparison on concentration of fatty aldehydes in rice straw waxes extracted using scCO<sub>2</sub> and hexane Soxhlet for 4 hours.

### 2.3.3.6 Steroid ketones

Steroid ketones including stigmast-4-en-3-one and 5 $\alpha$ -stigmastane-3,6-dione, were identified and obtained with the highest concentration,  $330.7 \pm 9.9$   $\mu\text{g/g}$  of dry straw with hexane soxhlet extraction (see **Figure 2-34** for comparison). In scCO<sub>2</sub> extraction, the greatest yield for steroid ketones was 65°C, 400 bar was  $224.4 \pm 6.1$   $\mu\text{g/g}$  of dry straw (see **Table 2-12** for the summary of quantities steroid ketones from all scCO<sub>2</sub> condition).



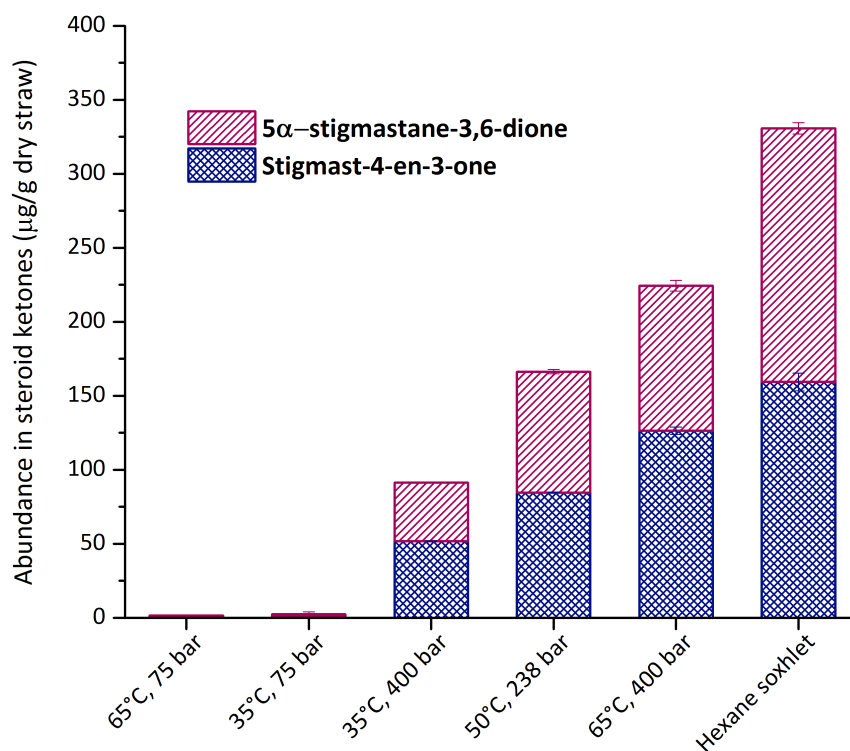


**Figure 2-34** Comparison on concentration of steroid ketones in rice straw waxes extracted using scCO<sub>2</sub> and hexane Soxhlet for 4 hours.

**Table 2-12** Types and quantities of steroid ketones in rice straw waxes obtained from different conditions using scCO<sub>2</sub> extraction for 4 hours.

Steroid ketones	Abundance in the extracts in µg/g of dry plant				
	35°C, 75 bar	35°C, 400 bar	50°C, 238 bar	65 °C, 75 bar	65°C, 400 bar
Stigmast-4-en-3-one	0.8	51.7 ± 0.2	84.6 ± 0.3	0.5	126.4 ± 2.4
5α-Stigmastane-3,6-dione	1.7 ± 1.5	39.5 ± 0.2	81.7 ± 1.5	1.1	98.0 ± 3.7
<b>Total steroid ketones</b>	<b>2.5 ± 1.5</b>	<b>91.2 ± 0.4</b>	<b>166.3 ± 1.8</b>	<b>1.6</b>	<b>224.4 ± 6.1</b>

### 2.3.3.7 Wax esters

In rice straw extract, the predominant wax ester molecule was C46, which was similar to the stem extract of maize.<sup>68</sup> Wax esters were detected in low concentration in rice straw as in hexane and scCO<sub>2</sub> extractives. The greatest concentration was usually at 65 °C and 400 bar using scCO<sub>2</sub> extraction, 255.3 ± 0.8 µg/g of dry straw (see **Figure 2-35**). The conditions at low pressure were reconfirmed to be unsuitable to extract lipophilic compounds from rice straw, including wax esters (see **Table 2-13**). Morrison *et al.* also demonstrated that wax esters were successfully extracted at approximately the same range of temperature and high pressure, 60 °C and 552 bar.<sup>159</sup>

**Table 2-13** Types and quantities of wax esters in rice straw waxes obtained from different conditions using scCO<sub>2</sub> extraction for 4 hours.

Wax esters	Abundance in the extracts in µg/g of dry plant				
	35°C, 75 bar	35°C, 400 bar	50°C, 238 bar	65 °C, 75 bar	65°C, 400 bar
Wax C42	0.1	10.8	18.2 ± 1.0	TR	22.5
Wax C44	0.3	23.7	47.8 ± 0.1	0.1	56.2 ± 0.1
Wax C46	0.7	21.5 ± 0.1	49.6 ± 0.8	0.3	60.6 ± 0.2
Wax C48	0.6	12.0 ± 0.2	32.5	0.4	47.0 ± 0.2
Wax C50	0.4	7.4	20.6	0.3	37.2 ± 0.2
Wax C52	0.3	3.2	8.0 ± 0.1	0.2	21.5 ± 0.1
Wax C54	0.1	1.3	1.2 ± 0.1	4.5 ± 0.1	10.3
<b>Total wax esters</b>	<b>2.5</b>	<b>79.9 ± 0.3</b>	<b>177.9 ± 2.1</b>	<b>5.8 ± 0.1</b>	<b>255.3 ± 0.8</b>

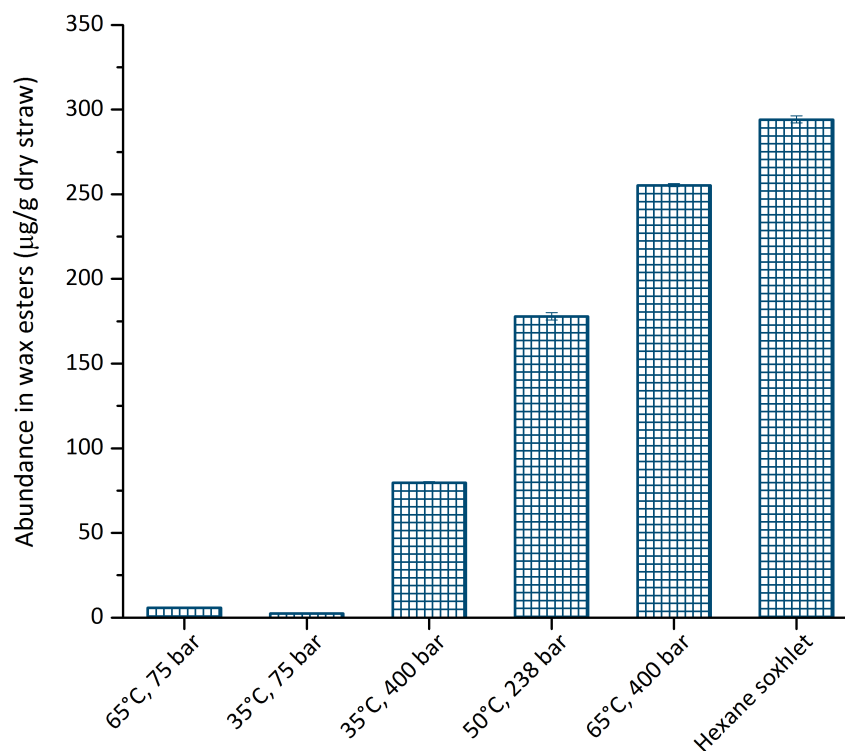


**Figure 2-35** Comparison on concentration of wax esters in rice straw waxes extracted using scCO<sub>2</sub> and hexane Soxhlet for 4 hours.

### 2.3.4 Time optimization study

The time optimisation experiment was performed in order to determine the suitable extraction time for scCO<sub>2</sub> extraction of rice straw wax using lab-scale supercritical unit. The scCO<sub>2</sub> of rice straw was carried using a 500 ml extractor containing 90 g of milled rice straw. The CO<sub>2</sub> flow rate was 40 g/min and the extraction was carried out for 6 hours using the optimum scCO<sub>2</sub> condition previously determined, at 60°C and 400 bar. The extract was collected at 30, 60, 120, 180, 240, 300 and 360 minutes in order to look at the extraction kinetics. **Figure 2-36** illustrates the extraction curve obtained for the extraction of wax from rice straw.

In general, there are three linear steps in the extraction plot profile in a supercritical fluid extraction process. In **Figure 2-36**, the first purple line at the beginning of the process is referred to the constant extraction rate (CER) corresponding to the extraction of easily accessible compounds. Consequently, convection in solvent film, which surrounds the raw material, dominates the mass transport. The second dash line represents the falling rate period (FER) and

during this period both convection and diffusion effects are crucially responsible for mass transport. The red third line referred to a stage, which is completely diffusion controlled. The moment where all of easily extractable solute has been obtained and the mass transfer depends totally on the diffusion of particle from inside of the biomass, as a result, the rates of extraction are typically low.<sup>105</sup> The evolution of total accumulated yield during scCO<sub>2</sub> extraction at 65 °C and 400 bar. It was found that 74% of the total extractive was recovered within the first 30 minutes, 87% and 94% were collected after 1 hour and 2 hours respectively. Therefore, an hour of extraction time provides a reasonable balance between yield and duration, as such there is no need to prolong the extraction time. This is significantly beneficial from an economical point of view and advantageous over the conventional solvent extraction.

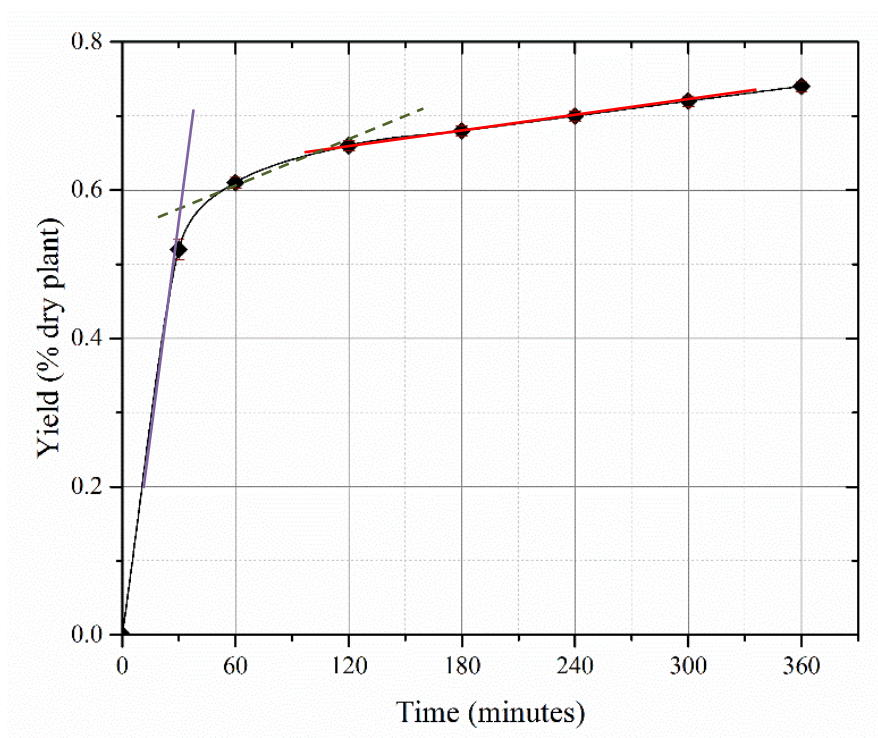


**Figure 2-36** Variation in total accumulated crude extract against extraction times by scCO<sub>2</sub> extraction at 65 °C and 400 bar.

### 2.3.5 Differential scanning calorimetry (DSC)

The melting profile is normally used to define the application area of waxes. The DSC thermograms in **Figure 2-37** illustrates the melting range of waxes obtained from hexane, scCO<sub>2</sub> (at the optimal condition) and also commercial waxes such as candelilla wax and beeswax. The melting profiles of hexane and scCO<sub>2</sub> were respectively ranged from 66 to 81 °C, with no sharp peak observed, and 58 to 70 °C with an endothermic minimum at 67 °C. Wax extracted using hexane was reported to have a high melting profile as in grain sorghum<sup>104,160</sup> and triticale straw<sup>136,139</sup> as hexane co-extracts complex lipids such as glycerides and phospholipids. As natural waxes contain a wide range of different hydrophobic molecules with complex composition, it is rare to observe a sharp signal to define the melting point.<sup>68</sup> The wider ranged melting profile of the hexane wax also indicated low selectivity of the conventional extraction method compared to scCO<sub>2</sub> which showed a well-defined melting profile. In comparison to the melting range of commercial candelilla wax and beeswax which were found to be 59 - 72 °C and 51 - 63 °C respectively, rice straw wax from scCO<sub>2</sub> could potentially be used in similar applications to these commercial waxes. The elevated melting point range observed for supercritical extracted wax may make it a suitable replacement for candelilla or carnauba wax.

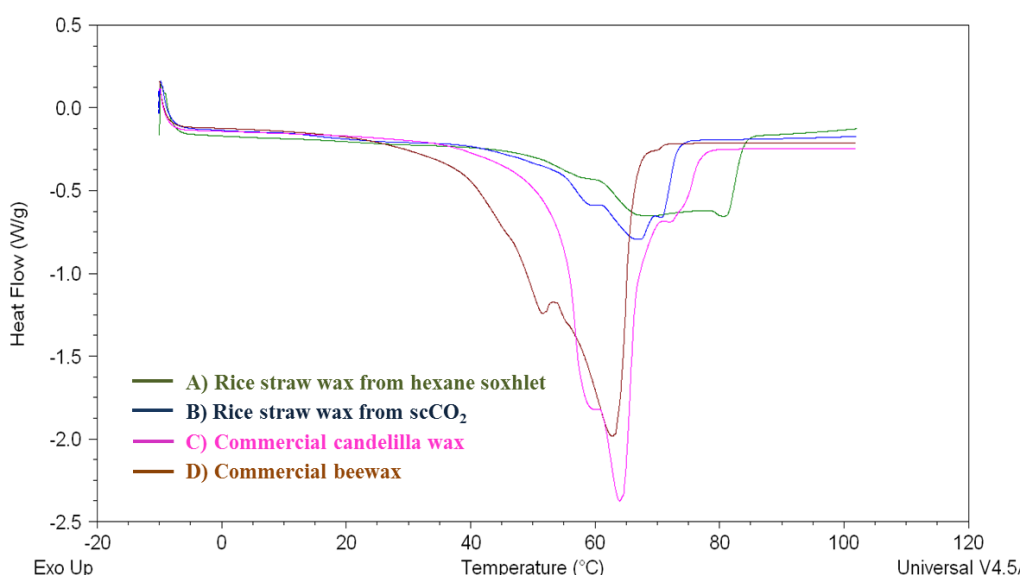


**Figure 2-37** DSC plot showing the melting profiles for different waxes (A) hexane soxhlet (B) scCO<sub>2</sub> at 65 °C and 400 bar for 4 hours (C) Commercial candelilla wax (D) Commercial beeswax

### 2.3.6 Scanning electron microscopic (SEM)

The SEM micrograms, **Figure 2-38**, demonstrated changes in the surface morphology of rice straw before and after scCO<sub>2</sub> extraction at 65 °C and 400 bar. The surface of the untreated rice straw (a) was coated with the epicuticular wax. However, that of the scCO<sub>2</sub> extracted one was clearly smooth (b), which confirmed that the wax was efficiently removed during the extraction. ScCO<sub>2</sub> extraction has been reported in earlier studies to be an alternative method of pre-treatment prior to enzymatic hydrolysis in ethanol production, as it increased the availability and permeability of the surface of the biomass, which means the sugar production was also improved after the enzymatic process.<sup>71,104,161</sup>

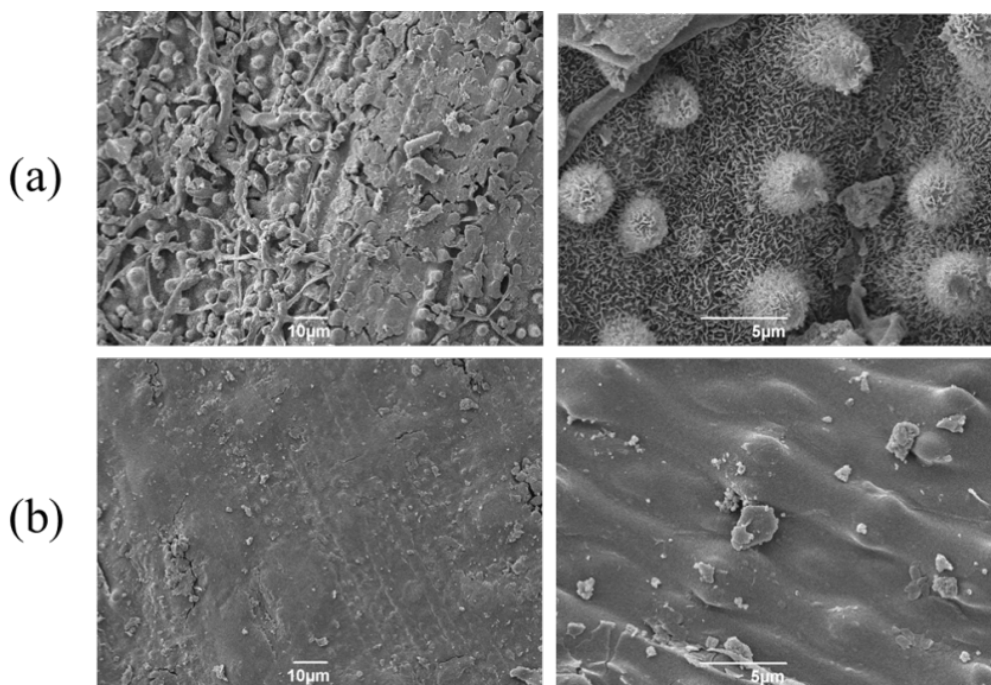


**Figure 2-38** SEM micrograms of rice straw (a) before scCO<sub>2</sub> extraction (b) after scCO<sub>2</sub> extraction at 65 °C, 400 bar for 4 hours

### **2.3.7 Application to biorefineries**

This study has demonstrated that supercritical extraction can be an effective method for the extraction of waxes from rice straw wax. In addition, a recent study has demonstrated that scCO<sub>2</sub> pre-treatment of rice straw lead to improved yields of glucose on enzymatic hydrolysis of the resulting biomass.<sup>160</sup> scCO<sub>2</sub> was found to create fluffy and soft fibres, which enhanced cellulase enzymatic hydrolysis. Such a development provides significant advantages for the use of scCO<sub>2</sub> as a first step of a rice straw biorefinery. To date, no study has investigated if pre-treatment with scCO<sub>2</sub> would have a positive effect on the conversion of biomass via thermal decomposition methods. As such, section 2.4 investigates the application of supercritically extracted biomass in microwave assisted pyrolysis.

## **2.4 A comparison of the microwave assisted pyrolysis of rice straw and supercritical extracted rice straw**

Only a handful of studies have investigated the effects of supercritical extraction on the downstream processing of biomass, and in all previous studies conventional hydrolysis for sugar release was investigated.<sup>103</sup> To date no previous studies have focused on the effects of supercritical extraction on microwave pyrolysis of biomass. Budarin *et al.* looked at combining supercritical extraction and microwave pyrolysis of wheat straw, however, the effect that supercritical extraction had on the microwave process was not investigated.<sup>162</sup> Furthermore, no previous studies have conducted microwave pyrolysis on rice straw following supercritical extraction. Therefore, for the first time, an attempt to combine two green technologies for an integrated rice straw study was investigated, whereby the effects of supercritical extraction on the rate of heating and reaction time were studied by comparing the results obtained with non-scCO<sub>2</sub> extracted rice straw. Furthermore, the effect of particle size on the microwave pyrolysis of rice straw was studied, something which has not been previously investigated in microwave pyrolysis processes.

ScCO<sub>2</sub> demonstrated a high efficiency and selectivity to remove valuable phytochemicals without leaving any solvent residue in the rice straw. Therefore, the extracted straw is suitable for further uses in various applications. A combination of scCO<sub>2</sub> extraction with a thermochemical process such as microwave pyrolysis of the scCO<sub>2</sub> treated rice straw could offer others high-value outcomes as it results in liquid, solid and gaseous products.<sup>24,163</sup>

The microwave pyrolysis of untreated and scCO<sub>2</sub> treated rice straw was investigated using fixed power mode at 300W in closed vessel. As stated previously, the aim was to study the effect of scCO<sub>2</sub> extraction on the resulting products and thermal behaviour towards the microwave heating of untreated and scCO<sub>2</sub> treated feedstocks. Moreover, the effect of particle size was also investigated in this study. The products, including char, bio-oil and gas, were analysed and thermogravimetric analysis (TGA) was also used to compare conventional and microwave heating. The detail theory of microwave chemistry was previously mention in Chapter 1.

### 2.4.1 Temperature and Pressure profiles

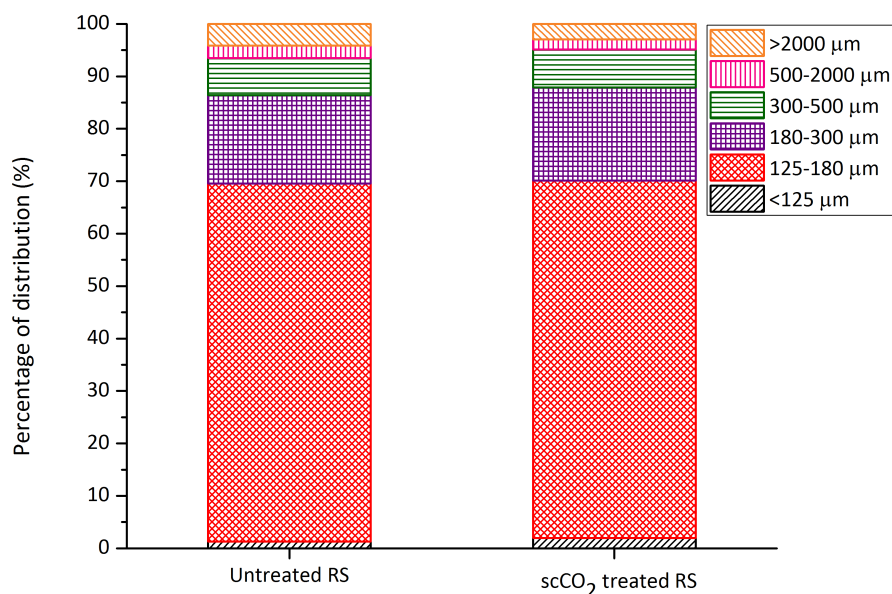


**Figure 2-39** Particle size distribution of untreated and scCO<sub>2</sub> treated rice straw after milling.



To understand the thermal behaviour of rice straw in the microwave pyrolysis, reaction temperature is one of the essential factors that must be taken into account. Other factors such as the particle size may also have an effect on the pyrolysis process and this was therefore investigated. **Figure 2-39** shows the distribution of particle sizes of the untreated and scCO<sub>2</sub> treated raw materials after milling.

**Figure 2-40** illustrates the temperature profile of microwave pyrolysis of untreated and scCO<sub>2</sub> treated rice straw with six different particle sizes, <125 μm, 125-180 μm, 180-300 μm, 300-500 μm, 500-2000 μm and >2000 μm. The patterns of reaction temperature were identical in the two raw materials. Interestingly, there was a difference in the temperature profiles among the different particle sizes. In the case of the smaller particles sizes (particle sizes smaller than 500 μm), there was a sharp temperature increase in the first 100 seconds which plateaued at around 125 – 140 seconds. Final temperatures of above 250 °C were obtained.

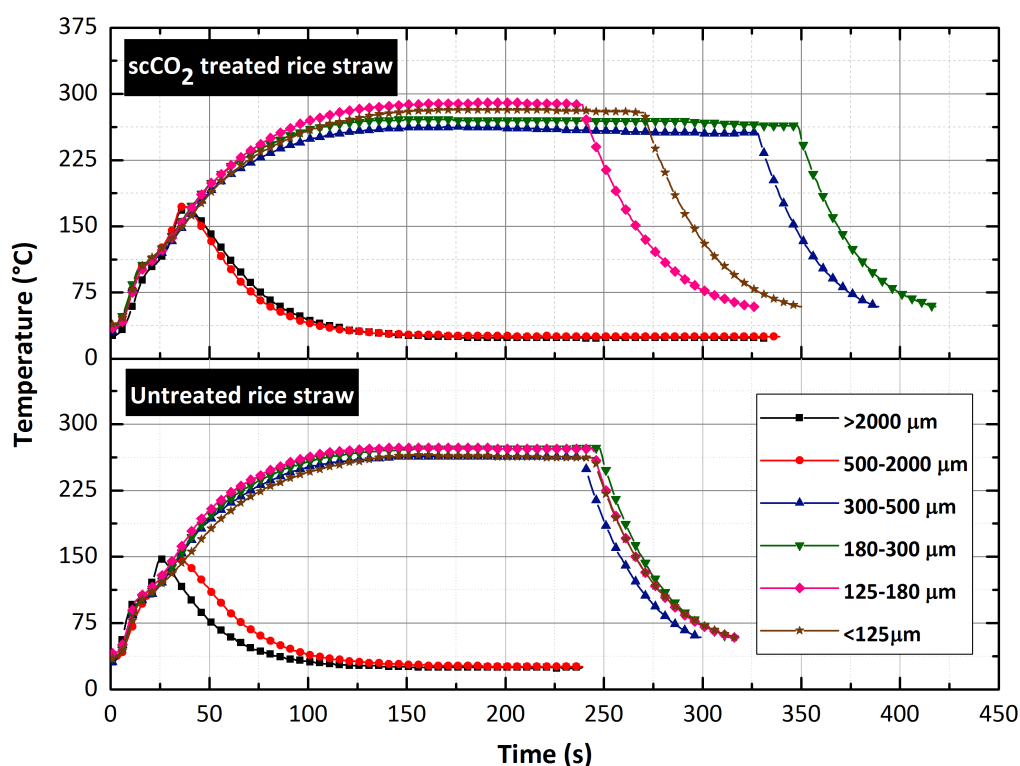


**Figure 2-40** Temperature profiles of microwave pyrolysis of untreated and B) scCO<sub>2</sub> treated rice straw with different particle sizes.

(Sample mass 0.3g, closed vessel, 300W, fixed power mode)

In contrast, the pyrolysis temperatures of the larger particle sizes (of the two materials,  $\geq 500\mu\text{m}$ ) were terminated at early heating stage (around  $125\text{ }^\circ\text{C}$ ) due to a rapid increase in pressure (surpassing the safety pressure limit of 280 PSI) (**Figure 2-41**). This spontaneous increase of pressure was attributed to the generation of incondensable gases during the microwave pyrolysis process. Consequently, it can be concluded that particle size played an important role not only in reaction temperature, but also in the end products of the microwave pyrolysis of rice straw.

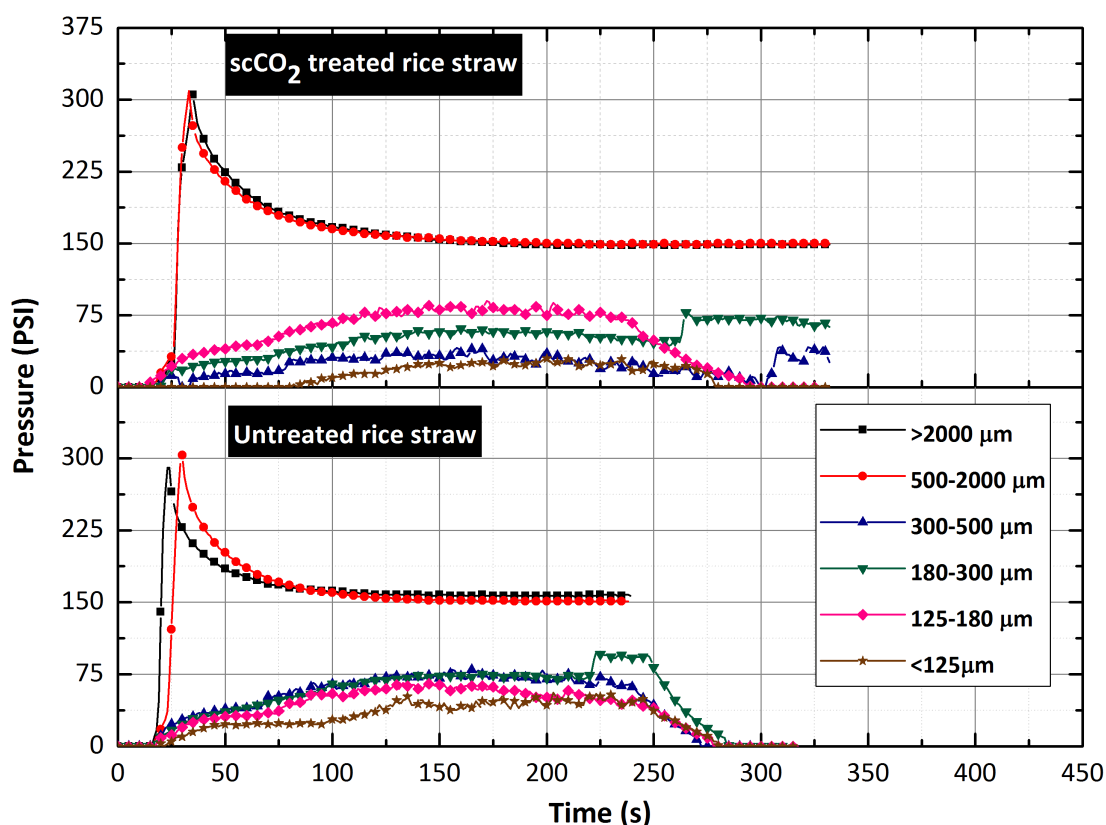


**Figure 2-41** Pressure profiles of microwave-assisted pyrolysis of untreated and  $\text{scCO}_2$  treated rice straw with different particle sizes.

(Sample mass 0.3g, closed vessel, 300W, fixed power mode)

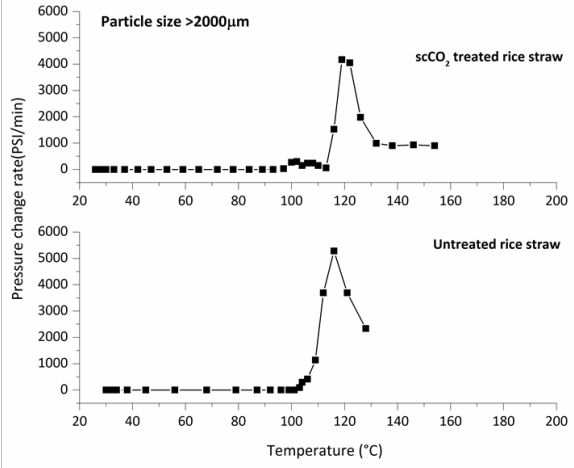
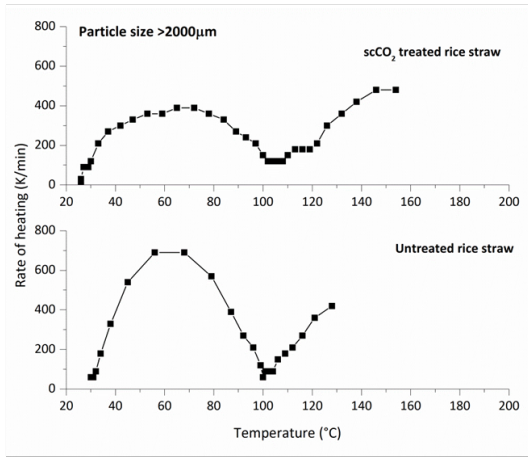
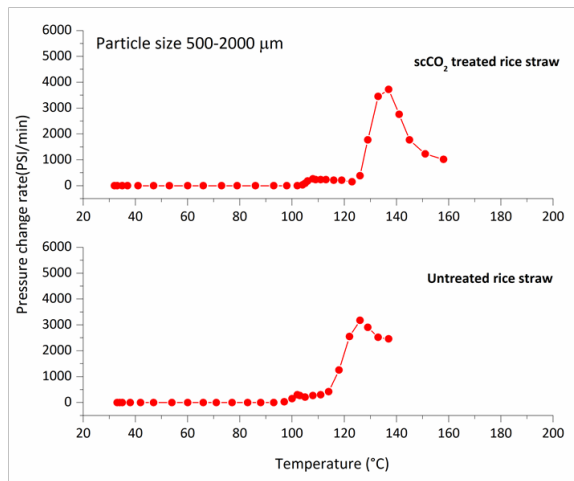
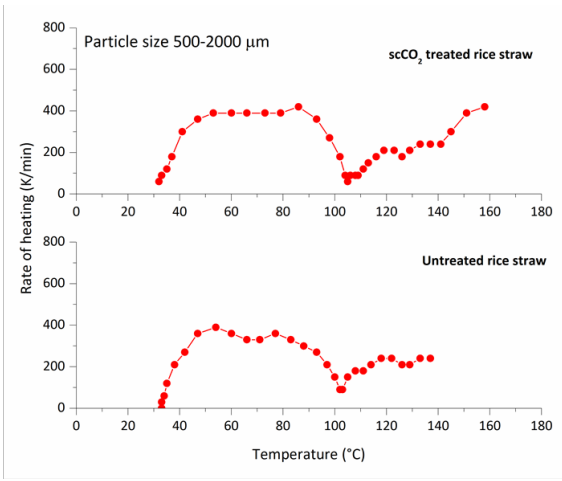
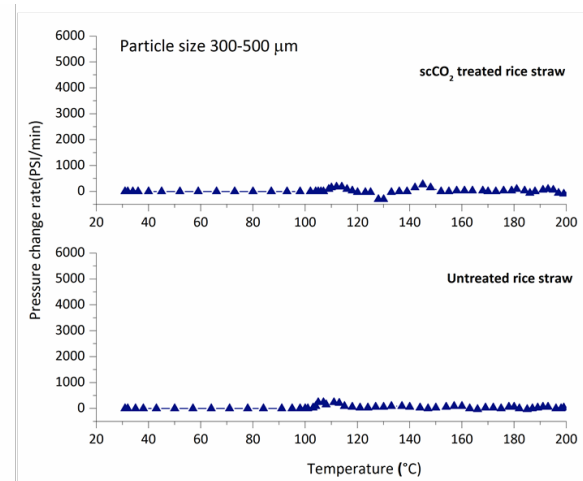
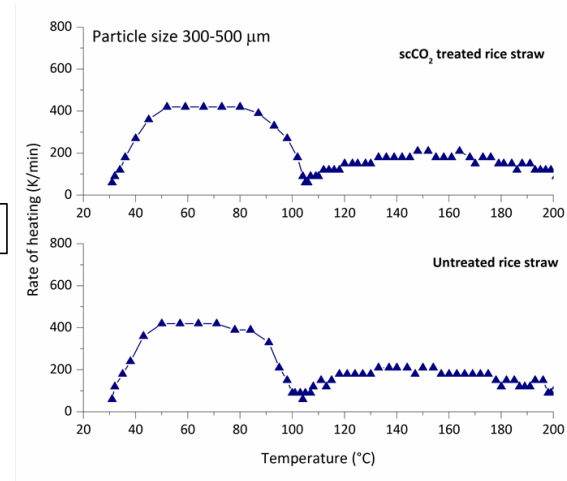
## 2.4.2 Heating and pressure change rates

The full comparison and the evolution of the heating rates and pressure change rates were illustrated in **Figure 2-42** with the variation of particle size. The summary of the heating rate and maximal temperature of microwave pyrolysis for untreated and scCO<sub>2</sub> treated rice straw are listed in **Table 2-14**. It was observed that the highest temperatures were reached with the particle size of <125µm scCO<sub>2</sub> treated rice straw, followed by 125-180 µm and 180-300 µm with the highest temperature attained at 272-273 °C for both untreated and scCO<sub>2</sub> treated rice straw. For the particle size smaller than 500 µm, there was no significant in terms of heating behaviours for both untreated and scCO<sub>2</sub> treated rice straw during microwave irradiation.

**Table 2-14** Heating rates and maximum temperatures during microwave pyrolysis.

Particle size (µm)	Heating rate (K min <sup>-1</sup> )		Maximum temperature (°C)	
	Untreated	scCO <sub>2</sub> treated	Untreated	scCO <sub>2</sub> treated
<125	180	180	265	282
125 - 180	180	180	273	272
180 - 300	210	210	272	273
300 - 500	210	240	262	263
500 - 2000	240	420	137	158
>2000	420	480	128	154

Similar to the pressure change rates, as shown in **Figure 2-42**, the samples having the particle size smaller than 500 µm resulted in relative low pressure change rates due to the absence of incondensable gas production during the process. The pressure change rate indicated the rate of decomposition of the biomass at the specific temperature. The untreated and scCO<sub>2</sub> treated rice straw with the particle size larger than 500 µm, including 500-200 and >2000 µm, possessed special thermal behaviour towards the microwave irradiation resulting in not only high heating rates, but also high pressure change rates. The pressure change rates and their corresponding temperatures were summarised in **Table 2-15**.

**A****B****C**

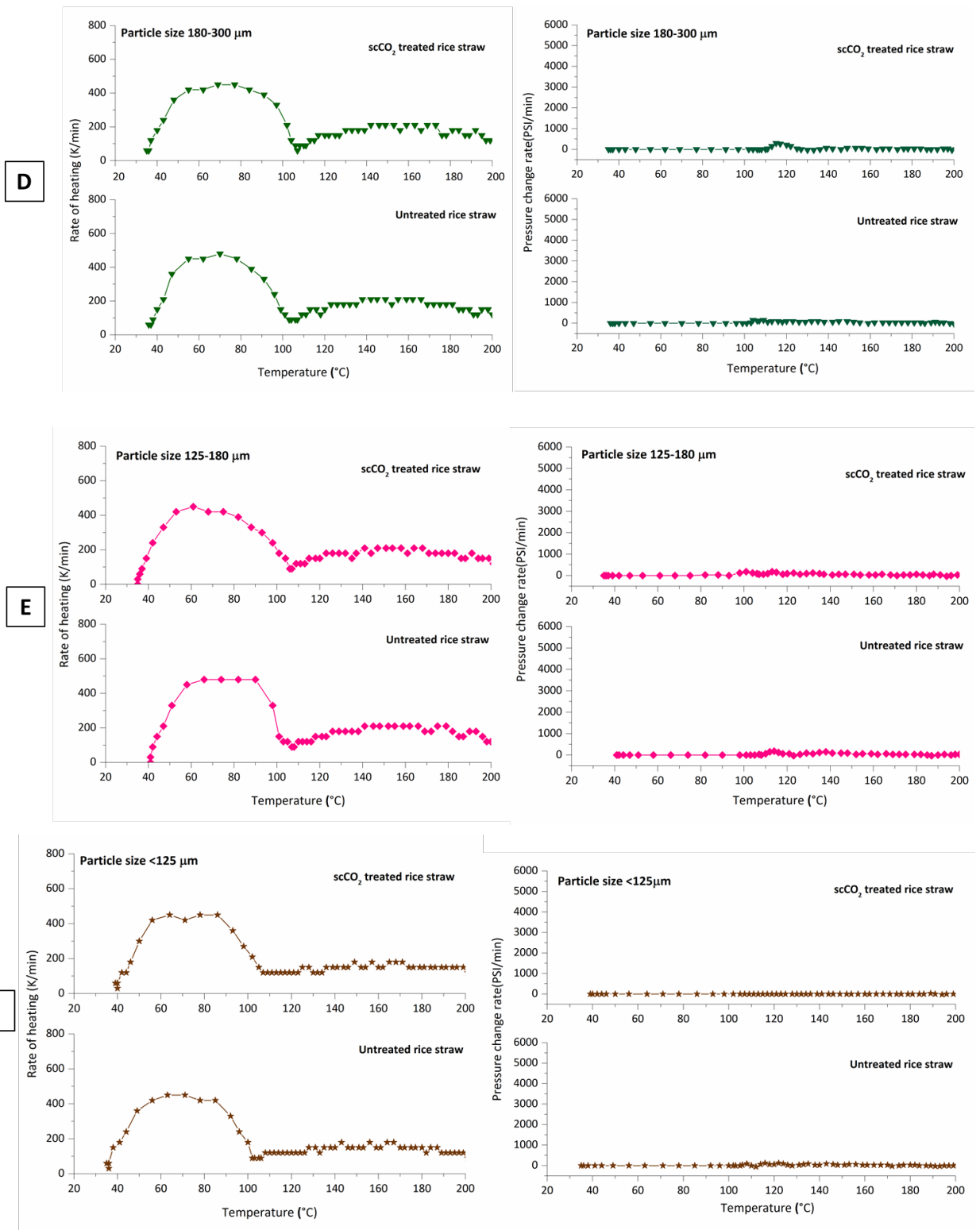


**Figure 2-42** The comparison and the evolution of heating rates and pressure change rates of untreated and scCO<sub>2</sub> treated rice straw according to particle sizes A) >2000  $\mu\text{m}$ , B) 500-2000  $\mu\text{m}$ , C) 300-500  $\mu\text{m}$ , D) 180-500  $\mu\text{m}$ , E) 125-180  $\mu\text{m}$  and F) <125  $\mu\text{m}$ .

**Table 2-15** Pressure change rates and temperature at maximum pressure change rates during microwave pyrolysis.

Particle size ( $\mu\text{m}$ )	Max pressure change rate (PSI $\text{min}^{-1}$ )		Temperature at max pressure change rate ( $^{\circ}\text{C}$ )	
	Untreated	scCO <sub>2</sub> treated	Untreated	scCO <sub>2</sub> treated
<125	180	180	255	245
125 - 180	180	180	272	272
180 - 300	150	150	263	263
300 - 500	210	210	224	232
500 - 2000	3180	3720	126	137
>2000	5280	4170	116	119

It can be seen in this study that the overall trend of heating rate increased with increasing particle size. For the feed sizes of <125  $\mu\text{m}$ , 125 -180  $\mu\text{m}$ , 180 - 300  $\mu\text{m}$ , 300 - 500  $\mu\text{m}$ , 500-2000  $\mu\text{m}$  and >2000  $\mu\text{m}$ , the rates of heating were 170, 210, 210, 210, 270 and 480  $\text{K}\cdot\text{min}^{-1}$  respectively for untreated rice straw and 170, 210, 210, 240, 420 and 480  $\text{K}\cdot\text{min}^{-1}$  respectively for scCO<sub>2</sub> treated rice straw. Importantly, the rate of heating in the microwave pyrolysis of rice straw was found to be exceptionally high, with a typical heating rate of 480  $\text{K}\cdot\text{min}^{-1}$  in the largest feed size (>2000  $\mu\text{m}$ ). On the other hand, for the smaller sample size <500  $\mu\text{m}$ , the heating performances were identically lower (150 - 240  $\text{K}\cdot\text{min}^{-1}$ ) than those of the larger sizes. Interestingly, the scCO<sub>2</sub> extracted biomass, sized 500-2000  $\mu\text{m}$ , was capable of retaining high rates of heating at 420  $\text{K}\cdot\text{min}^{-1}$ , which is the largest particle size distribution, while that of the untreated straw substantially dropped down to 270  $\text{K}\cdot\text{min}^{-1}$ . Therefore, this demonstrates that the extraction of waxes has a significant effect on the rate of heating and therefore on the efficiency of microwave pyrolysis process. It can be concluded that certain wax fractions may inhibit the rate of pyrolysis within the rice straw.

It has been shown in previous studies that the final temperature and the heating rate of microwave pyrolysis increased when the particle size decreased. This was due to the increase of bulk density and the contact area, which enhance heat transfer.<sup>164,165</sup> In contrast, in this study, the heating rate observed was in the opposite direction and the maximal temperature was irrespective of size. It was also clearly seen that scCO<sub>2</sub> treated biomass could reach higher

temperatures when compared size by size with the untreated rice straw. In addition, greater heating rates were recorded in experiments in the case of scCO<sub>2</sub> treated rice straw. These results indicate that the wax removal by scCO<sub>2</sub> has an influence on the dielectric property of the rice straw, as the scCO<sub>2</sub> treated rice straw became a better microwave absorber with a constant high heating rate and higher final temperature. This therefore shows that scCO<sub>2</sub> extraction has a positive effect on the microwave pyrolysis process, further illustrating the benefits of introducing this technology within a holistic biorefinery.

### 2.4.3 Comparison of Conventional and Microwave heating.

Thermogravimetric analysis (TG) of untreated and scCO<sub>2</sub> treated rice straw having different particle sizes was conducted in this study as a conventional heating pyrolysis process. This was done in order to compare the thermal behaviour and decomposition of the biomass when using conventional pyrolysis with that of microwave pyrolysis. Generally, there are three main stages of decomposition in biomass pyrolysis; moisture evaporation, main devolatilisation and continuous devolatilisation.<sup>166-168</sup> Rice straw is a lignocellulosic biomass consisting mainly of the three types of biopolymers; hemicellulose, cellulose and lignin. The composition of cellulose, hemicellulose and lignin of the rice straw in study was 34%, 19% and 13% respectively. The hemicellulose of rice straw is generally the first to decompose up to a temperature of 250°C, followed by the breakdown of cellulose at about 250-350 °C, both with significant mass loss rates. The decomposition of lignin is the most complex as it occurred slowly from the initial stages of the heating process to 900 °C with a very low mass loss rate.<sup>167,168</sup> The TG and DTG curves of untreated and scCO<sub>2</sub> treated rice straw, **Figure 2-43**, showed a similar pattern. The first mass loss is a result of water evaporation. The decomposition of hemicellulose occurred at approximately 180 °C followed by cellulose decomposition to approximately 350 °C. The hemicellulose decomposition could not be clearly observed as it overlapped with the cellulose decomposition peak as seen in previous studies.<sup>91</sup> The TG and DTG curves for all particle sizes (for both the untreated and scCO<sub>2</sub> treated rice straw) were found to be similar. A maximum decomposition rate at 320 - 330 °C was observed (for all feed sizes), attributed to the decomposition of cellulose (main component of the rice straw). This indicates that the particle

size has no influence on the pyrolysis temperature in conventional heating. However, the weight loss rate was slightly affected.

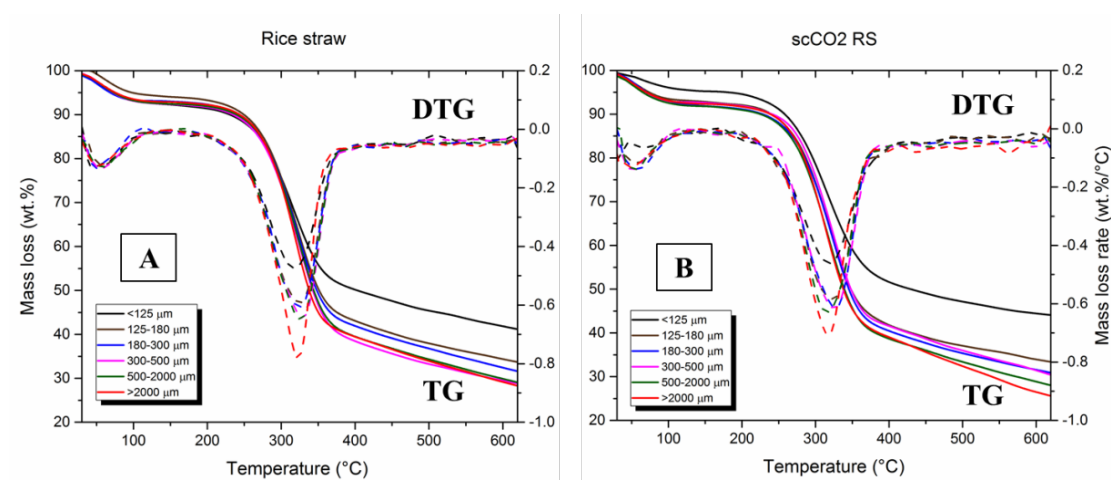


**Figure 2-43** TG and DTG curves of the raw materials A) Untreated B) scCO<sub>2</sub> Treated rice straw

As stated previously, the cellulose decomposition (of the two feedstocks) occurred at very low temperature during the microwave pyrolysis (indicated by the production of incondensable gas). The decomposition occurred at  $\sim 120^\circ\text{C}$  (size  $>2000\ \mu\text{m}$ ) and  $\sim 130^\circ\text{C}$  (size  $500\text{--}2000\ \mu\text{m}$ ), which was exceptionally low compared to the conventional pyrolysis in the TG ( $320^\circ\text{C}$ ). Such a reduction in temperature may lead to the use of less energy and quicker pyrolysis, which could improve the economic viability of the process. In order to confirm that microwave heating is a promising alternative thermal method to conventional heating in a rice straw biorefinery, the solid chars were also analysed by TG to compare the thermal behaviour of the biomass before and after microwave pyrolysis. The untreated and scCO<sub>2</sub> treated rice straw demonstrated identical TG and DTG curves and will therefore be discussed together. In the case of feed size  $>500\ \mu\text{m}$ , the TG of the solid char showed that the peak of cellulose decomposition,  $\sim 320^\circ\text{C}$  was no longer present (See **Figure 2-44**). In contrast, in the case of particle size  $<500\ \mu\text{m}$ , it was clearly visible even though the intensity sharply decreased. This finding is very interesting as it indicates that, with microwave pyrolysis, the decomposition of cellulose happened at a low temperature, at  $120\text{--}130^\circ\text{C}$  ( $\sim 200^\circ\text{C}$  lower than conventional heating), for particle sizes larger



than 500  $\mu\text{m}$ . However, further investigation is needed for a better understanding of this from a mechanistic point of view.

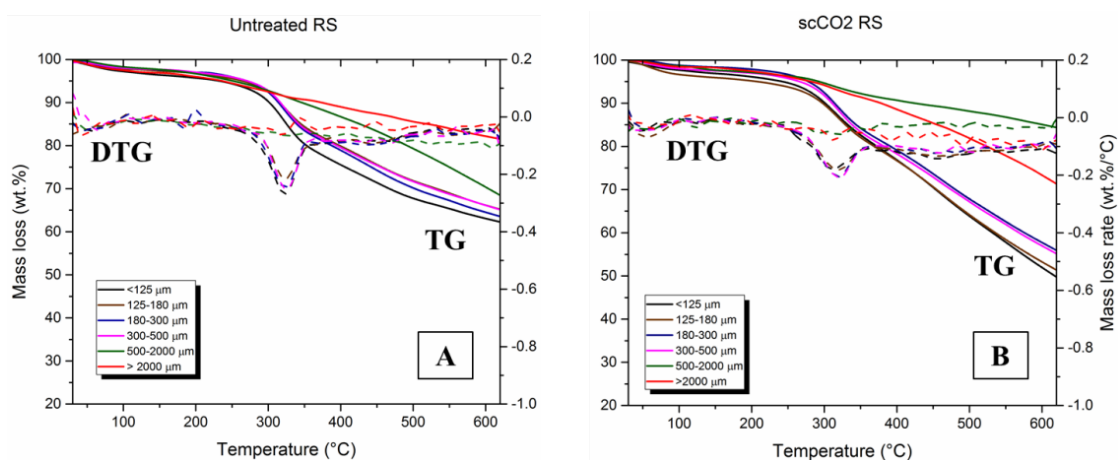


**Figure 2-44** TG and DTG curves of solid chars from A) Untreated B)  $\text{scCO}_2$  Treated rice straw

#### 2.4.4 Products distribution

Pyrolytic products typically consist of bio-oil, char and gas, with each product yield depending on the biomass type and experimental conditions implemented. In this study, microwave pyrolysis of untreated and  $\text{scCO}_2$  treated rice straw showed that particle size significantly affected the product yields. **Figure 2-45** shows the significant influence of particle size on product distribution. In the case of small feed sizes ( $<500 \mu\text{m}$ ), bio-char was predominantly produced during microwave pyrolysis, yielding 50-60% dry weight, for both the  $\text{scCO}_2$  treated and untreated materials. The yields of bio-oil were low, 6-9% dry weight and there were no incondensable gas generated during this thermal process. However, in contrast to this, the main product obtained following pyrolysis of the large particles sizes ( $\geq 500 \mu\text{m}$ ) was the gas, with yields of 56-59% dry weight. This was coupled with significant decreases in solid char (approximately 25-32%) and a slight increase in bio-oil production (10-12%) (for both untreated and  $\text{scCO}_2$  treated rice straw sized 500-2000 $\mu\text{m}$  and  $>2000\mu\text{m}$ ).

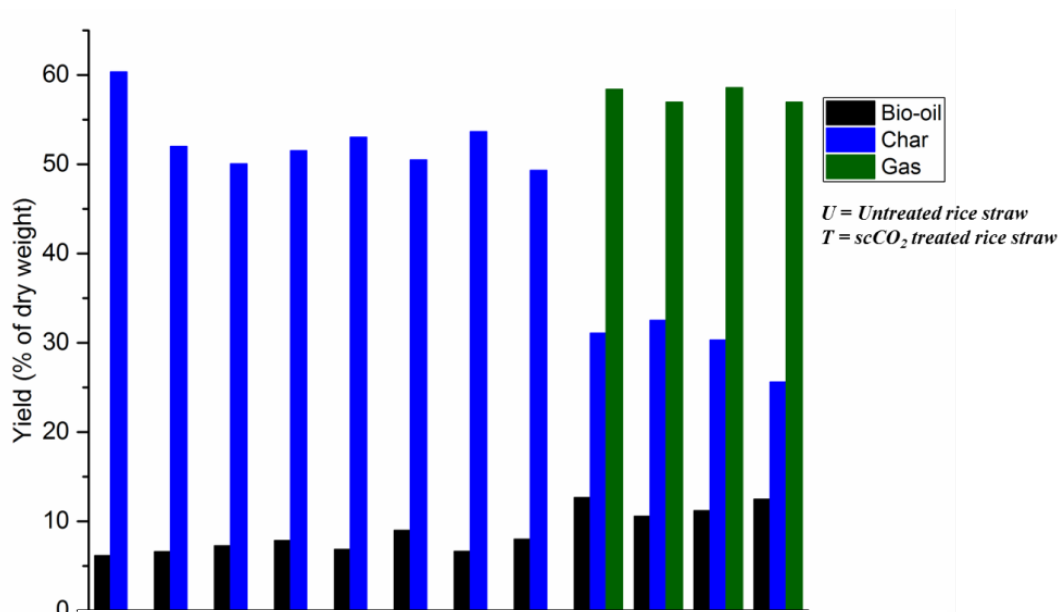


**Figure 2-45** Pyrolytic Product distribution of untreated (U) and scCO<sub>2</sub> treated (T) rice straw.

## 2.4.5 Product analysis

The most distributed particle size after sieving, 500 - 2000  $\mu\text{m}$ , was used for qualitative analysis for both untreated and scCO<sub>2</sub> treated rice.

### 2.4.5.1 Gaseous products

The incondensable gaseous products generated were collected in a syringe and then analysed by FTIR. The composition of gas products from microwave pyrolysis of biomass such as wheat straw,<sup>100</sup> coffee hulls,<sup>169</sup> rice husk<sup>24</sup> and rice straw<sup>167,168</sup> is primarily composed of H<sub>2</sub>, CH<sub>4</sub>, CO, CO<sub>2</sub> and some short chain hydrocarbons.

**Figure 2-46** shows the FTIR spectra of the gas phases of the two feedstocks, the major components of product gases from rice straw microwave pyrolysis were CO, CO<sub>2</sub>, CH<sub>4</sub>, C<sub>1</sub>-C<sub>2</sub> hydrocarbons, and some carbonyl-containing gases. The result obtained was in agreement with previous studies with conventional heating<sup>24</sup> and with microwave heating.<sup>24,166-168</sup> The gas composition of the untreated and scCO<sub>2</sub> treated rice straw were completely identical, which confirmed that scCO<sub>2</sub> extraction has no adverse effect on the biomass and can be used as a pre-treatment step in a holistic biorefinery of rice straw. Interestingly, certain gases such as CH<sub>4</sub> and some light hydrocarbons were detected at low-temperature microwave pyrolysis in this study, which was previously reported to be obtained at higher temperatures (>400°C).<sup>101,102,168</sup>

The detail explanation of the specific low-temperature interaction of microwave with rice straw at 120°C will be shown in Chapter 3. The interpretation of this phenomenon based on the assumption that microwave interacts with a deprotonated cellulose- potassium complex. In this complex potassium cation directly bonded to oxygen. Therefore, it could be presumed that at the first stage of the microwave pyrolysis, oxygen will be predominately removed from the rice straw, accumulating hydrogen content in the solid residue and increasing probability of methane production at the second stage of pyrolysis which take place between 120 and 137°C.<sup>170,171</sup>

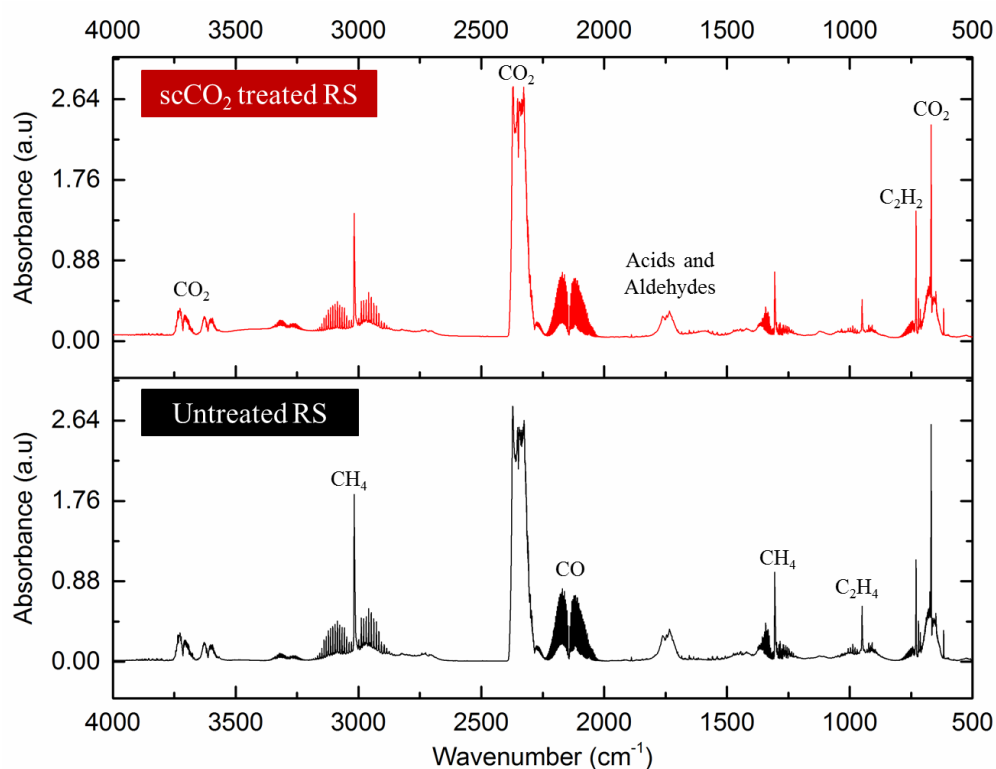


**Figure 2-46** FT-IR gas product from microwave pyrolysis of scCO<sub>2</sub> treated (above) and untreated rice straw (below).

### 2.4.5.2 Liquid fraction

The liquid fractions, obtained from sample size 500-2000  $\mu\text{m}$ , were analysed by HT-GC-MS without further purification. **Figure 2-47** illustrates the chromatograms of the acetone-soluble fractions of the bio-oil for the untreated and  $\text{sc-CO}_2$  treated rice straw. The two samples of bio-oil from microwave pyrolysis showed similar chromatographic profiles. A range of phenolic compounds (products of lignin decomposition) were identified based on GC-MS data such as 2-methoxy-phenol, 2- and 3-methyl-phenol, 2,6-dimethyl-phenol and 4-vinyl-2-methoxy-phenol. Moreover, it has been confirmed that some aromatic and polycyclic aromatic compounds included naphthalene, anthracene and phenanthrene were identified in the microwave pyrolysis oil. The presence of these molecules are in good agreement with the results of previous studies.<sup>122,123</sup> The non-acetone-soluble liquid fraction contained a range of anhydride sugars and cellulose breakdown products. Further investigation of the bio-oil and the distribution of other pyrolysis products will be the focus of future work.

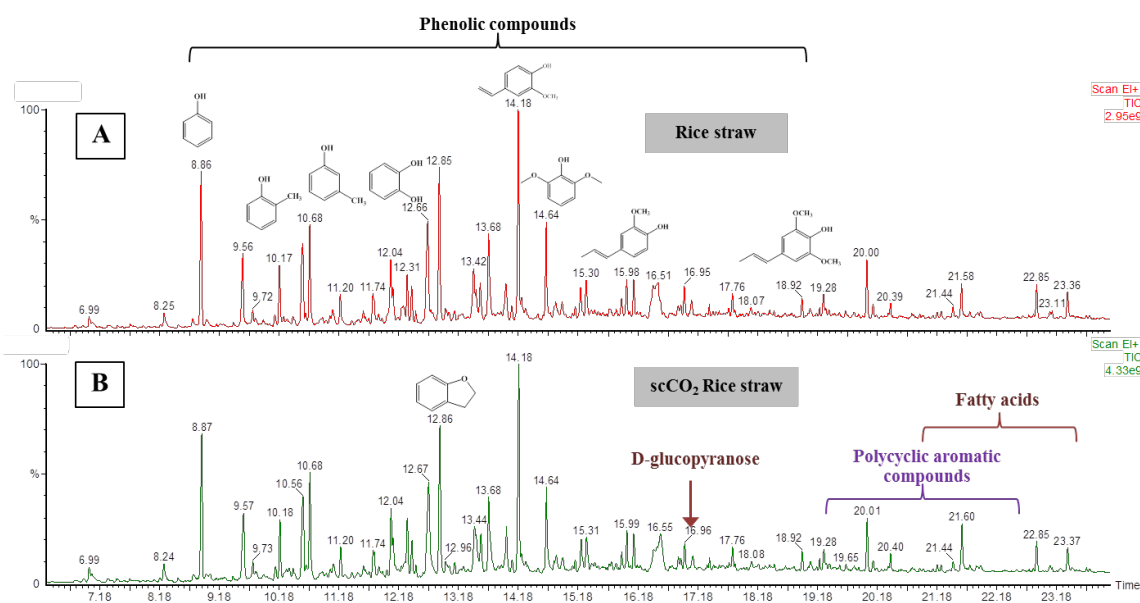


**Figure 2-47** HT-GC-MS chromatograms of bio oil of liquid fractions of A) Rice straw and B) Extracted rice straw.

### 2.4.5.3 Solid analysis

The analysis of solid residues, from the raw materials sized 500-2000  $\mu\text{m}$ , is presented in **Table 2-16**. The elemental analysis of the biomass showed a significant increase in the percentage of carbon and a decrease in hydrogen. However, there was no significant difference between the untreated and  $\text{scCO}_2$  extracted rice straw.

**Table 2-16** Characteristics of untreated and  $\text{scCO}_2$  extracted rice straw pre and post microwave pyrolysis.

Elemental analysis (wt.%)	Before pyrolysis		After pyrolysis	
	Untreated RS	$\text{scCO}_2$ extracted RS	Untreated RS	$\text{scCO}_2$ extracted RS
C	38.9	40.5	48.5	51.1
H	5.2	5.3	1.9	1.6
N	0.3	0.3	0.2	0.3
Calorific value (MJ $\text{kg}^{-1}$ )	15.8	15.5	18.7	18.5

The gross caloric value of the solid residues were 18.7 and 18.5  $\text{MJ kg}^{-1}$  in untreated and  $\text{scCO}_2$  treated rice straw respectively, which were notably higher when compared to the starting biomasses (typically 15  $\text{MJ kg}^{-1}$ ) making them useful for large scale energy production. This demonstrates that microwave pyrolysis could be a viable technology for the production of chemicals and fuels within a rice straw biorefinery.

## 2.5 Conclusion and Future work

It can be concluded that supercritical carbon dioxide extraction is a suitable technology for the extraction of lipids from rice straw. Yields of waxes from the supercritical extraction of rice straw were comparable to hexane soxhlet, with yields of 0.7% by dry weight at 65 °C and 400 bar. The extracts were identified by GC-MS, with the use of commercial standards, NIST library and use of published data. Extracts consists of a mixture of different groups of compounds including long chain fatty acids and fatty alcohols, sterols and wax esters. Quantification was achieved through the use of GC-FID, in triplicate.

This extraction method also serves as a pre-treatment step to provide enhanced interactions between microwaves and the resulting extracted biomass. In addition, greater heating rates were recorded in experiments in the case of scCO<sub>2</sub> treated rice straw. These results indicate that the wax removal by scCO<sub>2</sub> has an influence on the dielectric property of the rice straw, as the scCO<sub>2</sub> treated rice straw became a better microwave absorber with a constant high heating rate and higher final temperature. This therefore shows that scCO<sub>2</sub> extraction has a positive effect on the microwave pyrolysis process, further illustrating the benefits of introducing this technology within a holistic biorefinery.

In the case of particle size <500 µm, it was found that with microwave pyrolysis, the decomposition of cellulose happened at a low temperature, at 120 - 130 °C (~ 200 °C lower than conventional heating). This could lead to significant reduction in energy usage for the decomposition of cellulose in rice straw. However, further investigation is needed for a better understanding of this from a mechanistic point of view. The products obtained from microwave assisted pyrolysis of rice straw including gas, bio oil and char have potentially high market values. However, further study on upgrading and improving qualities of products are needed.

## **Chapter 3**

# **The influence of potassium ions in microwave-assisted pyrolysis of rice straw**

## 3 The influence of potassium ions in microwave-assisted pyrolysis of rice straw

### 3.1 Introduction

As previously discussed in Chapter 2 (scCO<sub>2</sub> extraction as pre-treatment step in the biorefinery of rice straw), the decomposition of the biomass especially cellulose and hemicellulose in rice straw occurred in microwave-assisted pyrolysis at around 120 °C, which is 200 °C earlier than in the conventional heating. To the best of author's knowledge, such low-temperature decomposition has not been observed for rice straw and has only been reported in a limited number of investigations of other biomasses.<sup>103</sup> Consequently, it is worthwhile to have a better understanding of what is the chemistry behind this process as this could be beneficial in terms of energy economy and efficiency in the downstream processes within the concept of the biorefinery. To investigate the processes systematically, a series of hypotheses were proposed, followed by experiments and further analysis, with the aim to understand why this relative lower temperature of decomposition of cellulose is observed within the rice straw.

Microwaves are a type of electromagnetic wave lying in frequency between 300 MHz and 300 GHz by general definition. Not all sources of materials can absorb microwaves depending on their nature of interaction with microwaves, which means they must be absorptive or dielectric. Microwaves primarily heat matter through two mechanisms, one the interaction for rotational energy levels of dipolar molecules (as seen in heating water molecules), the other ionic conduction whereby the alternating electromagnetic field interacts with mobile ions. In both cases the molecules or ions need to also subsequently dissipate to surrounding matter the energy absorbed (e.g. water molecules heating starch polymers in food). Rice straw has been reported in previous study as non-dielectric biomass.<sup>24,172-175</sup> However, it was believed that there should be at least in rice straw a key component (a microwave absorber), which promotes the early decomposition of cellulose in microwave pyrolysis.



### 3.2 The study on effect of moisture content in microwave-assisted pyrolysis

Not all the materials can be heated by microwave irradiation, since some materials are transparent or non-absorbing to microwaves (e.g. no rotating or non-polar). Water could be the first microwave absorber that can be considered due to its availability in plants and its dielectric and polar properties its dielectric and polar properties.<sup>24,162,172-175</sup> Therefore, water could play an important role on initiating the pyrolysis within rice straw as illustrated in **Figure 3-1**, the structure of cellulose is used due to its highest abundance in rice straw, about 35% wt dry basis. In order to investigate the effect of water on microwave-assisted decomposition of rice straw both untreated rice straw and the same batch of rice straw, dried in the oven for 24 hours at 105 °C to ensure that minimal moisture content remains in the biomass prior to the microwave pyrolysis, were used in this study. In addition, water was re-added to the dried rice straw to reach the same moisture content (~8%), and the same method of microwave-assisted pyrolysis was subsequently applied. The moisture content of the dried rice straw was assumed to be minimal (<1% of dry plant) compared to the untreated straw (~8% of dry plant). The rice straw samples used in this study were not sieved and the mass used for each experiment was 0.265 g. Therefore, the results obtained were not identical and cannot be compared with the results reported in Chapter 2 and onwards where the biomass has been sieved to demonstrate the effect of particle size on the microwave pyrolysis of rice straw. In addition, the results from this study will only be used to qualitatively explain the effect of water in microwave-assisted pyrolysis of rice straw. The same method of microwave was applied as described in Experimental chapter.

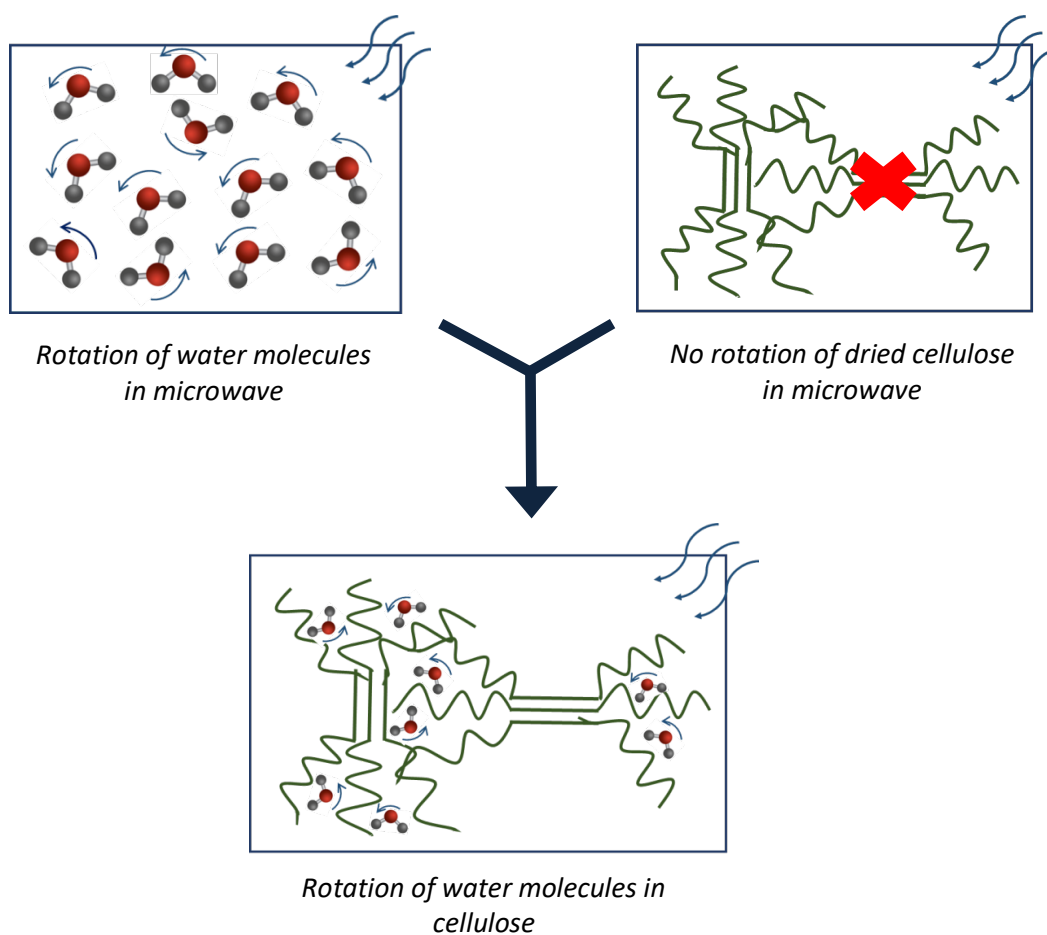


**Figure 3-1** Interaction of water in cellulose.

### 3.2.1 Temperature and pressure profiles

**Figure 3-2** depicts the real time temperature and pressure profiles of untreated rice straw, oven-dried rice straw at 105°C and dried rice straw with re-addition of water in microwave-assisted pyrolysis (without the addition of other microwave absorbers). The real-time pressure profiles of the three samples showed dramatic increase of pressure, which indicated the production of gas after 30 seconds of the microwave irradiation. These three samples produced large amount of incondensable gases as the pressure remained high after the microwave was turned off. As previously discussed in Chapter 2, incondensable gases such as CO, CO<sub>2</sub>, CH<sub>4</sub> and H<sub>2</sub> were mainly produced during the microwave pyrolysis of rice straw of rice straw.<sup>24,98,162</sup> The temperature profiles illustrated significant difference in heating behaviour of these three samples, which is

obviously due to the presence of water in the biomass. The rate of heating and pressure change rate will be discussed in detail later in this chapter. At the beginning, the temperature of the re-added water rice straw rose first followed by the untreated and the dried rice samples. At the early stage of the process, the increase of temperature normally corresponds to evaporation step, as the moisture contents of the untreated and the rehydrated water samples were higher. As a consequence, the water evaporation was dramatically noticed in this case.

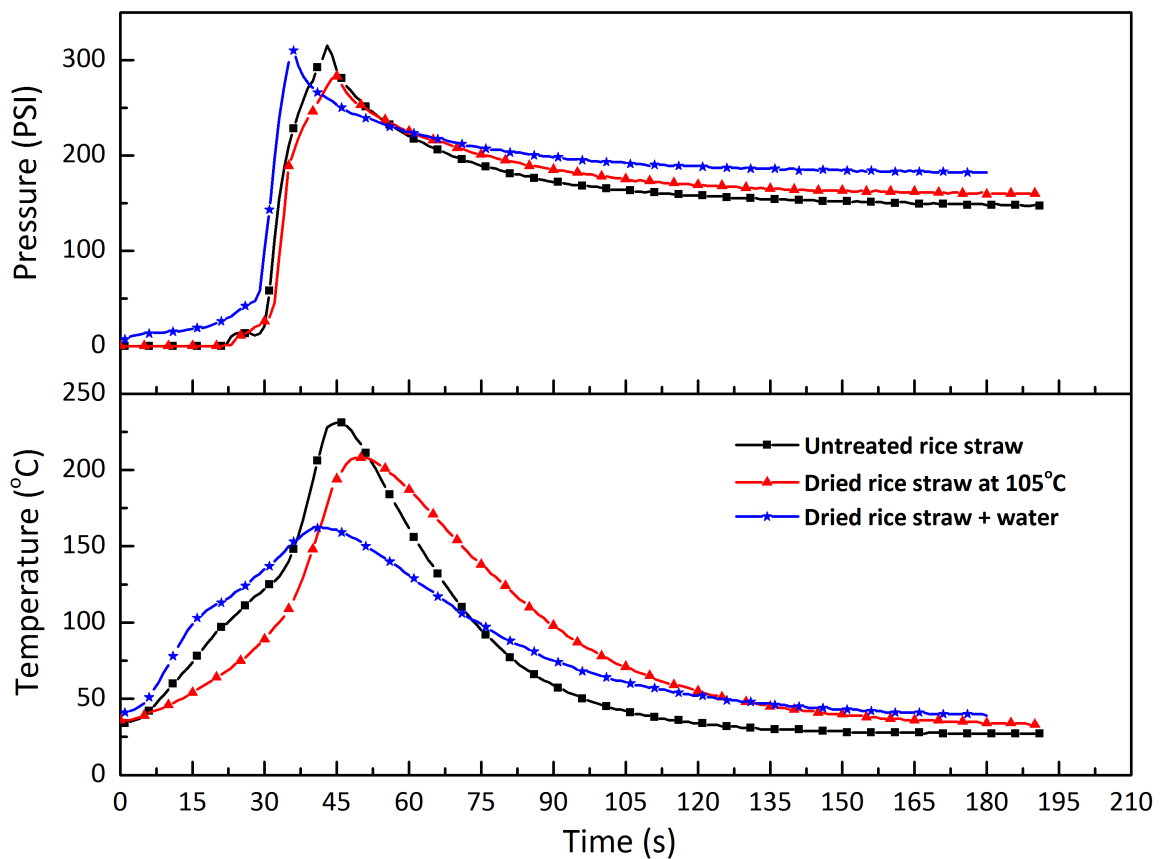


**Figure 3-2** Comparison of temperature and pressure profiles of untreated, oven-dried and rehydrated rice straws in MAP (0.265g, 300W, closed vessel, Fixed power mode, MW power).

### 3.2.2 Heating and pressure change rates

Heating and pressure changes rates are very informative experimental parameters representing intensity of interaction of MW irradiation with biomass. The microwave heating rate is proportional to dielectric loss and is a good indicator of efficiency sample-microwave interaction.<sup>176</sup> Higher rate of MW heating is corresponded to more efficient interaction. Therefore, the heating rate analysis could generate additional information about mechanism of MW activation. In addition to the heating rate the pressure changes rate is a strong indicator of gas production rate demonstrating intensity of MW assisted biomass pyrolysis.

The comparison of the heating rates of untreated, oven-dried and rehydrated samples in **Figure 3-3** confirmed that these three straws behaved differently towards microwave irradiation. At the temperature below 100°C, the highest heating rate recorded belonged to the rice straw with the re-addition of water, 360 K/min at 78°C. In contrast, the lowest heating rate in this temperature range was that of the oven-dried rice straw with 146 K/min at 78°C and the intermediate was the untreated rice straw, 240 K/min at 78°C. This result is in agreement with the study of previous studies in which it was found that water had important effect on the heating profile of raw material. Moreover, lower heating rate was recorded at below 100°C with vacuum dried cellulose compared with the wet sample.<sup>98,162,177</sup>

The results were split into two discussions to highlight the influence of water in microwave-assisted pyrolysis of rice straw. Firstly, the comparison of untreated and oven-dried raw materials during the process clearly indicated non-identical heating rate profiles. At the first, low temperature (<100°C), stage of the process water significantly increases heating rate of the sample showing that in this temperature range water is the major factor of the MW-biomass interaction. The absence of moisture content resulted in the lower heating rate at the evaporation stage, this agreeing with the hypothesis that residual water molecules absorb and dissipate the microwave energy. Alternatively, at temperatures higher than 100 °C the initial water content does not have any systematically influence on the MW-biomass interaction. On the one hand, at this temperature range untreated straw demonstrates the highest heating rate around 780 K/min at 193 °C, while the heating rate of the dried sample achieved only 630 K/min at 177 °C. Contrariwise, the sample with high water content after rehydration significantly reduces the heating rate maximum (200 K/min, 150 °C).

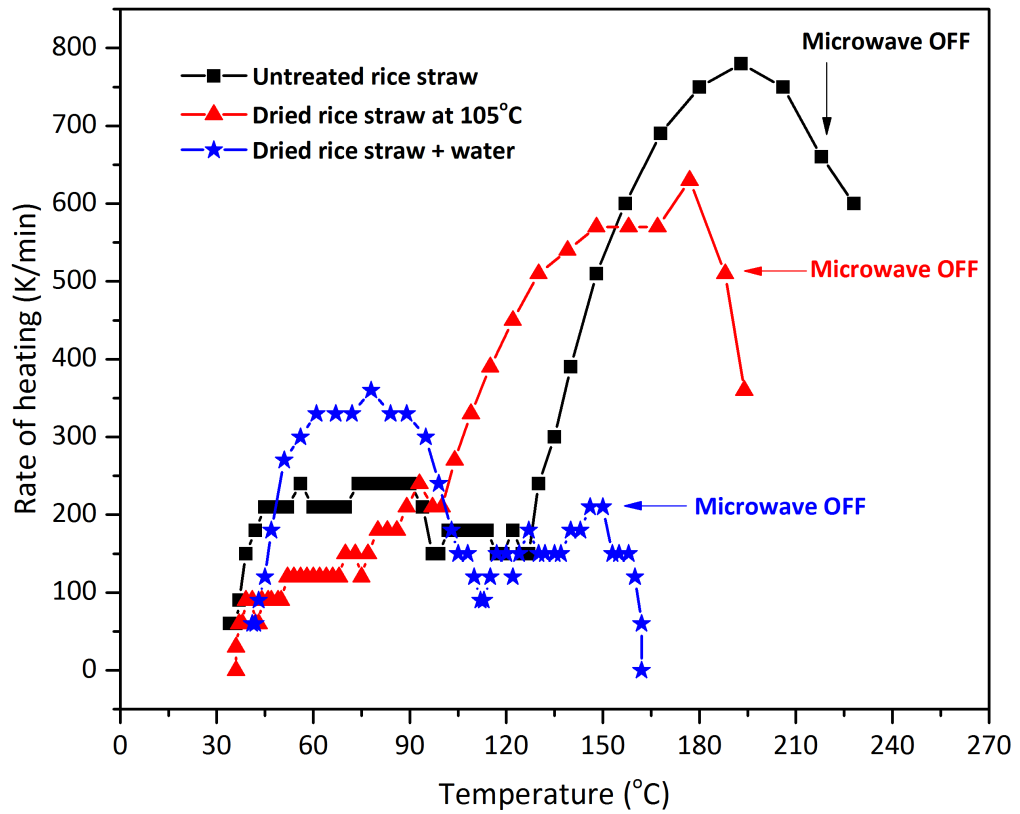


**Figure 3-3** Comparison of rate of heating of untreated rice straw, dried rice straw and rehydrated rice straw in microwave pyrolysis.

As was mentioned before, pressure is another crucial indicator to assess the pyrolysis process as it indicates the decomposition of the biomass as well as the pyrolysis process. **Figure 3-4** illustrates the evolutions of pressure and the pressure change rates against temperature during the microwave-assisted pyrolysis of untreated, oven-dried and rehydrated rice straws.

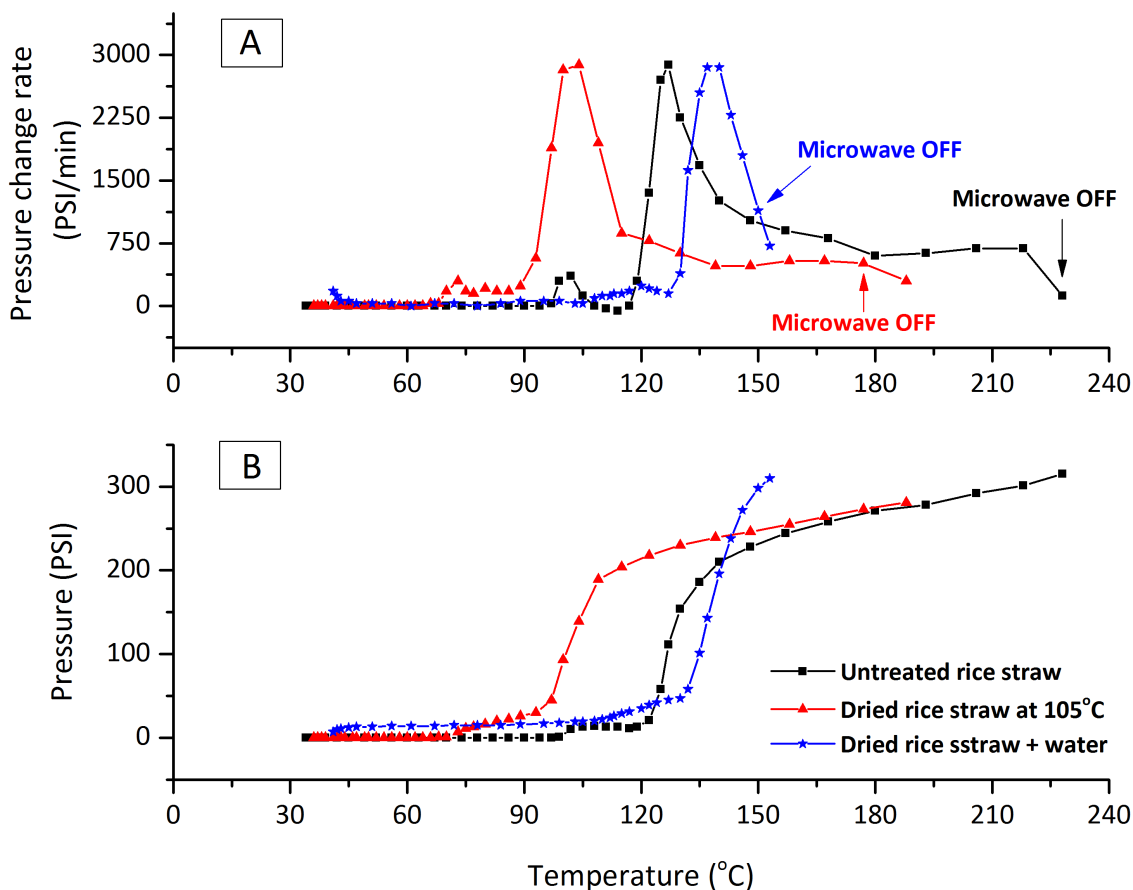


**Figure 3-4** Pressure change rates (A) and total pressure evolution (B) of untreated, oven-dried and rehydrated rice straw in microwave pyrolysis. (0.265g, 300W, closed vessel, fixed power mode).

It was clearly seen that the decomposition of each rice straw occurred at completely different temperature. The pressure evolution of the untreated and oven-dried samples (see **Figure 3-4B**) shared an identical pattern with a sharp increase of pressure followed by a plateau, whereas the rehydrated rice straw possessed individual characteristics. The increase of pressure, which referred to the production of gas, occurred at lower temperature for the oven-dried sample than in the untreated straw. In the untreated rice straw, the pressure started increasing at 120 °C and the highest rate of pressure change (2880 PSI/min) was recorded at 127 °C. On the other hand, in case of the dried sample, the pressure change initiated at 95 °C and the pressure change rate reached the peak of 2880 PSI/min at 104 °C. After reaching the peak point, the pressure change

rates of the untreated and the oven-dried samples dropped dramatically and stabilized until the microwave automatically stopped, which signified the slower rate of decomposition. The trivial level of moisture content in the dried straw effectively enhanced the pyrolysis process by decreasing the temperature from 120 °C to 95 °C. In the case of rehydrated rice straw a comparable result with the untreated rice straw was expected as these samples had the same moisture content (~8% of dry weight). However, the pyrolysis was surprisingly delayed as pressure started rising at 130°C and the pressure change rate reached its maximum of 2850 PSI/min at 140 °C. The pressure evolution did not follow similar pattern of the other two samples, a plateau has not been seen clearly due to the automatic cut of the microwave.

This can be drawn to the conclusion in the first place that the initial water content has an important effect on the microwave pyrolysis of rice straw. Moreover, the near absence of moisture in the dried sample enhanced the process by shortening the time for the biomass to reach the temperature below 100 °C and decreasing the pyrolysis temperature with the similar rate of pressure change to the untreated sample. Gasification was still observed either with or without the presence of moisture during the pyrolysis process of these three samples, which means water does not catalyse the gasification of microwave pyrolysis of rice straw and is not responsible for early decomposition of the biomass.

**Table 3-1** The rates of heating and pressure change of untreated, dried and remoistened rice straw during MW pyrolysis.

Raw materials	Temperature at beginning of microwave interactions and rapid increase of heating rate (°C)	Temperature of maximum pressure change rate(°C)
Untreated RS	125	127
Dried RS	100	104
Rehydrated RS	137	140

Results of analysis of the heating and pressure change rates are summarized in **Table 3-1**. In this study, the temperature of the maximum pressure change occurs 3-4 °C after the initial start of

microwave biomass interaction. The pressure increases in the system strongly correlated with the beginning of rapid increase in heating rate and microwave interaction with the biomass.

### 3.2.3 Thermogravimetric analysis (TGA)

As stated previously in Chapter 2, the rice straw decomposition occurred at very low temperature (at 120 °C) during the microwave pyrolysis of rice straw. To be able to systematically assess the pyrolysis process, thermogravimetric analysis was used in order to compare the thermal behaviour of the raw materials in the conventional heating method to the microwave heating. The comparison of TGA of the three raw materials is illustrated in **Figure 3-5**, and of first major note is that decomposition under conventional heating clearly occurs at a higher bulk temperature than for microwaves, supporting the view of differing effects between microwave and conventional heating.

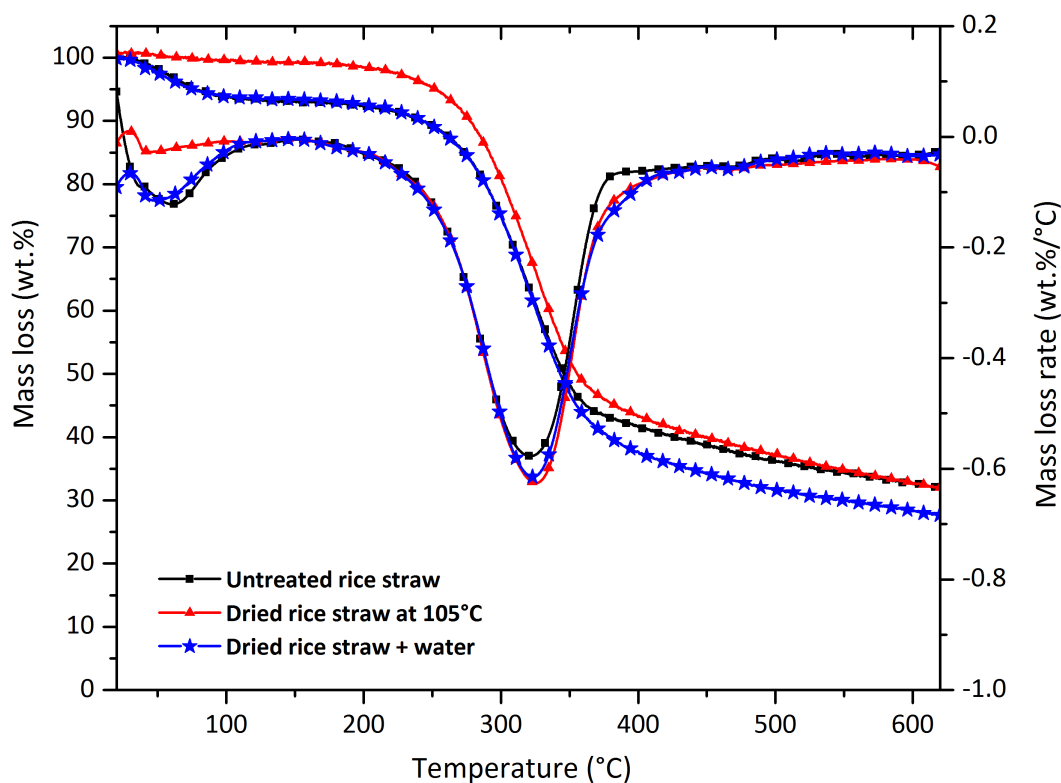


**Figure 3-5** TGA of raw materials before microwave-assisted pyrolysis.



In the TGA plot of the untreated rice straw (in black), the predominant weight loss from 200 to 380°C should be contributed to decomposition of hemicellulose and cellulose with the highest mass loss rate (DTG) of 0.57 wt.%/°C at 320°C, then the decomposition was insignificant. On the hand, the thermal properties of the oven-dried (in red) and the rehydrated (in blue) rice straw are obviously non-identical to that of the untreated straw. There was no obvious difference between these three biomasses, apart from the evaporation stage at the beginning. The oven-dried and rehydrated biomasses possess two main stages of thermal decomposition, the first decomposition with the highest mass loss rate belongs to hemicellulose and cellulose and the second broad signal should reasonably correspond to the decomposition of lignin, which was not been described before in previous Chapter 2.<sup>162,177</sup> As mentioned previously, untreated, oven-dried and rehydrated rice straws degraded at totally different temperature during the microwave pyrolysis. However, the conventional heating shows a slight shift in decomposition temperature. The oven-dried and rehydrated samples appeared to decompose a little earlier than the untreated with the maximal mass loss rate of 0.62 and 0.57 wt.%/°C, respectively. In addition, water might not be located at the same position in the biomass (i.e. inside or out of the cell wall). As a result, the rehydrated rice straw behaved differently in the microwave compared with the untreated rice straw.

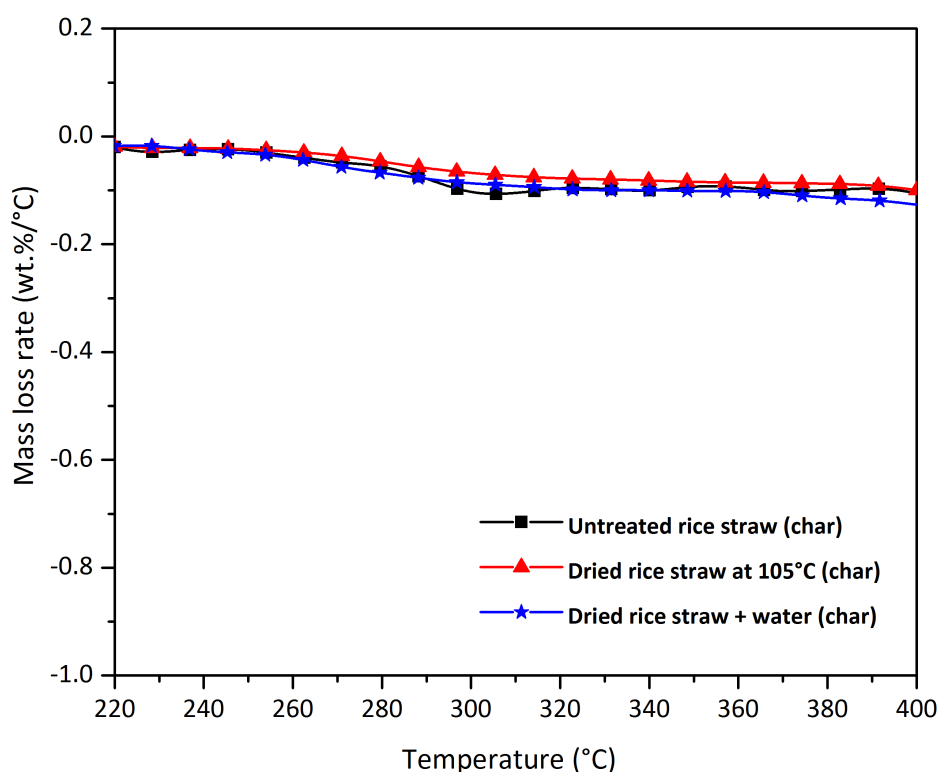


**Figure 3-6** TGA of solid products after microwave-assisted pyrolysis.

The TGA analysis (See **Figure 3-6**) of bio-chars of untreated, oven-dried and rehydrated rice straws after microwave pyrolysis highlighted that the decomposition of cellulose previously seen at  $\approx 310^\circ\text{C}$  was no longer observed. This confirmed that decomposition of cellulose occurred at very low temperature whether water is in the structure of the biomass or not.

The influence of water on the behaviour of rice straw in microwave pyrolysis can be explained by the dielectric property of water and the hydrogen bonding in cellulose structure. **Figure 3-7** indicates that the dielectric loss ( $\epsilon''$ ) and dielectric constant ( $\epsilon'$ ) of water decreased with increasing temperature. Note that the dielectric loss factor ( $\epsilon''$ ) is a measure of the efficiency of conversion of electromagnetic energy to heat and the dielectric constant ( $\epsilon'$ ) represents the molecule's ability to be polarized by the electric field.<sup>178</sup>

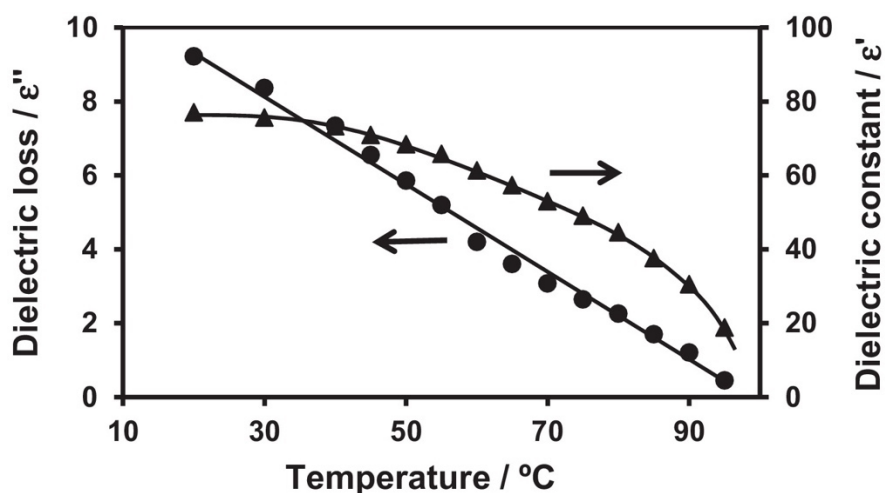


**Figure 3-7** Profiles of the changes in the dielectric loss ( $\epsilon''$ ) and dielectric constant ( $\epsilon'$ ) of water with changes in temperature.

Reprinted from *Applied Catalysis A: General*, 460-461, S. Horikoshi, A. Osawa, S. Sakamoto and N. Serpone, Control of microwave-generated hot spots. Part V. Mechanisms of hot-spot generation and aggregation of catalyst in a microwave-assisted reaction in toluene catalyzed by Pd-loaded AC particulates, 52-60, Copyright 2013, with permission from Elsevier 2018.<sup>11</sup>

According to the published paper,<sup>11</sup> at the beginning of the microwave irradiation (lower temperature), the dielectric loss of water was 9.2 at  $20^\circ\text{C}$ , whereas it decreased dramatically to 0.45 when the temperature reached  $95^\circ\text{C}$ . This means water is heated preferentially as the

microwave precisely focused on water rather than cellulose. However, when the temperature of water increased, the dielectric loss of water dropped so that the electric field radiation was able to concentrate itself on cellulose.<sup>178,179</sup> This phenomenon could be followed by specific microwave effect which is the formation of hotspot as the heating rate recorded was surprisingly high.<sup>178</sup> This can clearly explain why the microwave pyrolysis of the oven-dried straw occurred at the lowest temperature compared to the other higher moisture content rice straws.

This observation can also be explained by the interaction of hydroxyl groups and water in cellulose with various degree of hydrogen bonding (See **Figure 3-8**).<sup>180</sup> Cellulose possesses dielectric properties, with dielectric constant of cellulose is  $\approx 10$  at  $90^\circ\text{C}$ , due to its  $-\text{OH}$  groups and each glucose unit in the chain is able to move at the oxygen bond  $-\text{O}-$  that supposes to held them together.<sup>25,181</sup> However, when moisture is present, the dielectric properties of cellulose are affected due to the unavailability of  $-\text{OH}$  groups.<sup>15</sup> Once the microwaves interact with the biomass, the moisture starts absorbing the microwaves and build up a dielectric polarisation, which results in rotation of water molecules, with dielectric constant  $\approx 60$  at  $90^\circ\text{C}$ , in order to align themselves to the radiation accordingly. This leads to the friction and collision between the molecules, and then energy is consequently generated in the form of heat, which causes increase in temperature during this stage.<sup>15,25</sup> In the absence of water, microwave can interact with biomass, especially cellulose, directly that could explain why the decomposition of the biomass occurred at lower temperature. Alternatively, it may be that the “dried” biomass still contains a small amount ( $<1\%$ ) of water, but that this remains located within areas of the biomass where its absorption and dissipation of microwave energy is particularly effective in assisting biomass degradation.

With all this evidence, it can be concluded that water molecule as microwave absorber has a crucial effect on the microwave pyrolysis of rice straw. The microwave pyrolysis occurred at lower temperature in the absence of moisture content, which means the energy efficiency was improved. However, water is not solely responsible for the decomposition of rice straw at low temperature as the same behaviour toward microwave was still observed in the dried and wet

rice straw. Therefore, other key component within rice straw will be investigated in the next step.

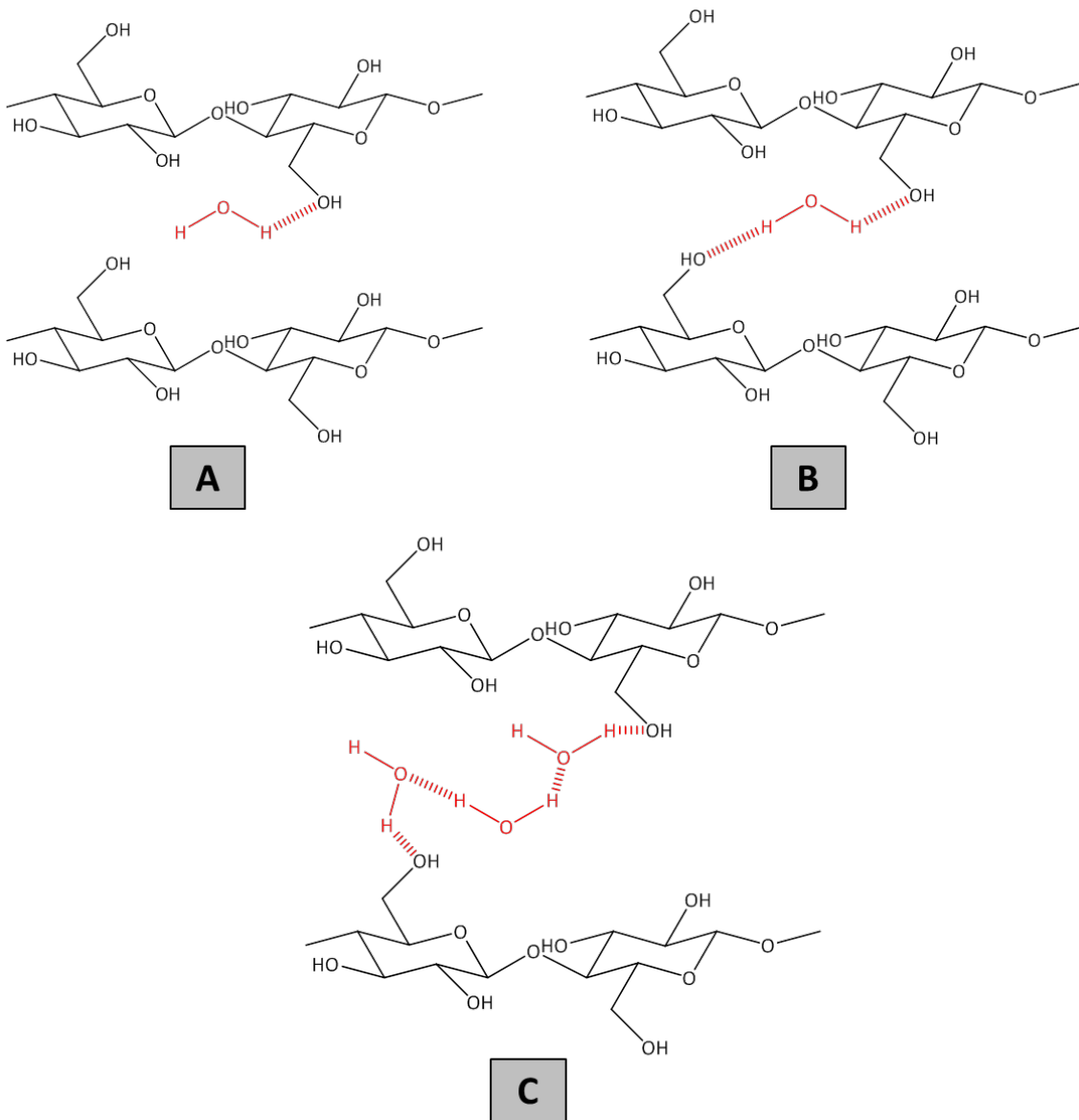


**Figure 3-8** Hydrogen bonding of hydroxyl groups and water between cellulose units A) Single hydrogen bonded water B) Double bonded and C) Multi-layer hydrogen bonding between water molecules and cellulose.<sup>182</sup>

### 3.3 The influence of silicate ions in microwave pyrolysis of rice straw

In living plants, silicon is found in three basic forms; insoluble silica, colloidal silicic acid and silicate ions. The rice plant absorbs silicon in the form of silicic acid from soil; however, nearly 90% of silicon is stored in the form of insoluble silica.<sup>183</sup> Although silicates are not present in high concentration in rice straw, they have a crucial metabolic effects as they help to increase grain yield in rice.<sup>184</sup> In addition, this low amount of silicate ions could play an important role as microwave absorber in the microwave pyrolysis of rice straw. To effectively extract silicates, diluted solution of NaOH should be used as silicates ions such as sodium silicate is stable at pH 11-12.<sup>178</sup> Acid wash is another effective method; however, it is very likely to alter the degree of polymerization and crystallinity of the biomass.<sup>185</sup>

The experiments in this study were originally designed for an investigation of the effect of water. Water was chosen in the first place to avoid the minimal disruption of the internal structure of rice straw. However, the results obtained were able to provide information not only on the concentrations of silicate ions, but also that of minerals presenting within rice straw. The experiment involved a pre-treatment of rice straw in hot water for 10 minutes. Figure 3-9 (left) is the image of rice straw after the pre-treatment in water, with brownish aqueous solution and rice straw at the bottom of the beaker. Then the treated rice was filtered using Buchner funnel and gently oven-dried the biomass at 50 °C for 72 hours. The aqueous fraction was directly boiled in order to remove maximum of water, the 2 volumes of ethanol were added to the remaining aqueous solution, finally the mixture ethanol-water was evaporated under vacuum. The solid obtained after water removal was then dried at 105 °C in the oven for 24 hours and the final picture of solid shows in **Figure 3-9** (right), which yielded 9.7% of dry rice straw.

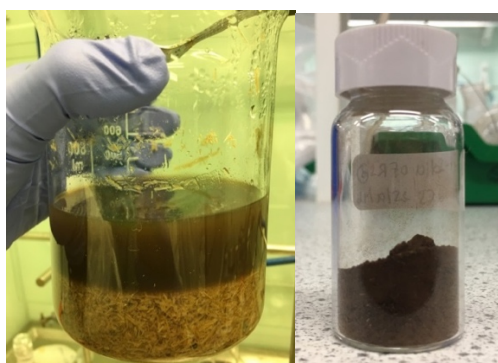


**Figure 3-9** Pre-treatment of rice straw with water

### 3.3.1 Temperature and pressure profiles

Figure 3-10 illustrates the temperature and pressure profiles of the untreated and water treated biomass. The final temperature of the treated straw was higher than that of the untreated, 271 °C and 134 °C respectively. The pressure profiles of these raw materials are non-identical, the rapid increase in pressure during the pyrolysis process was no longer observed.

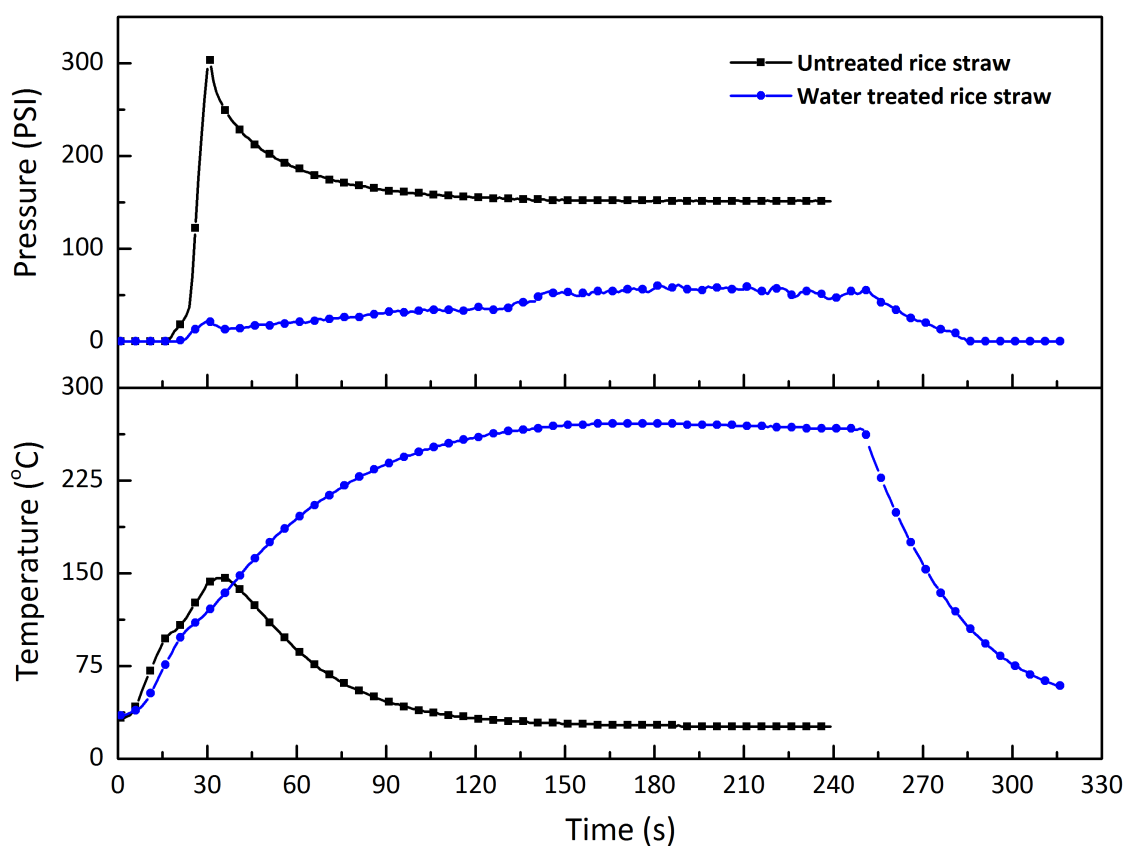
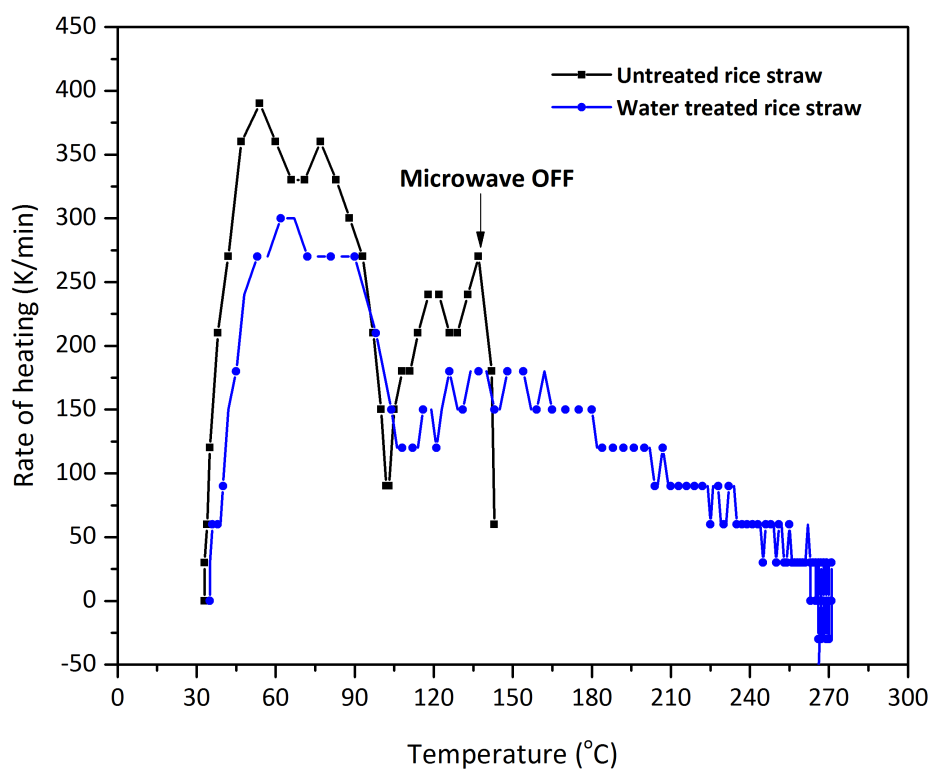


Figure 3-10 Temperature and pressure profile of untreated and water treated rice straw.

(sample mass 0.3 g, closed vessel, 300 W, fixed power mode).

### 3.3.2 Heating and pressure change rates

In **Figure 3-11**, the rate of heating of the treated straw dramatically decreased ( $150 \text{ K}\cdot\text{min}^{-1}$ ) compared to that of the untreated ( $270 \text{ K}\cdot\text{min}^{-1}$ ). These two raw materials behaved completely differently under microwave irradiation, indicating the rice straw became essentially more transparent or less active to the microwaves after being washed with water.



**Figure 3-11** Heating rates of untreated and water treated rice straw during microwave pyrolysis.

The comparison of pressure change rates in **Figure 3-12** clearly also indicates the different behaviour of the washed and untreated rice straw. After being treated in water, gasification during microwave pyrolysis was no longer observed. Its pressure and pressure change rate stayed indifferent during the irradiation of the sample.

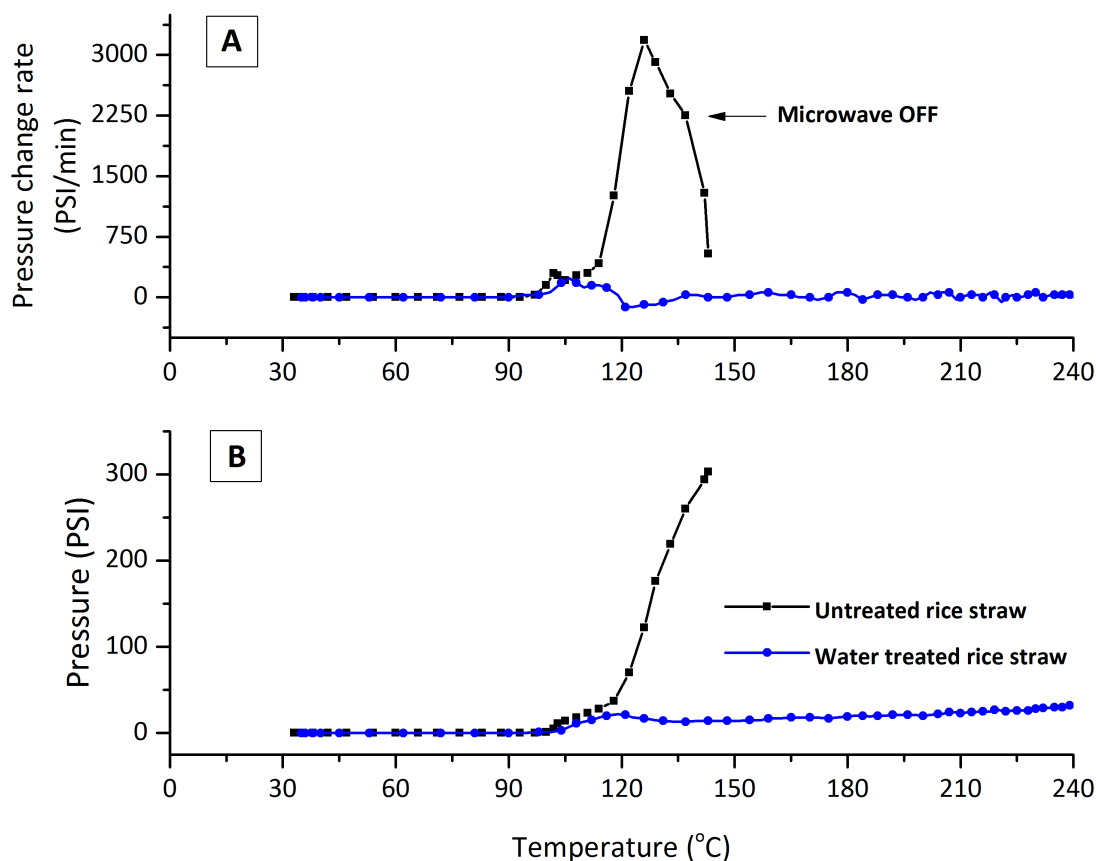


**Figure 3-12** Pressure change rate (A) and Pressure evolution (B) of untreated and water treated rice straw during microwave pyrolysis.

(sample mass 0.3 g, closed vessel, 300 W, fixed power mode)

### 3.3.3 Thermogravimetric analysis (TGA)

In **Figure 3-13A** shows thermogravimetric analysis (TGA) of the raw materials before and after washing with water. In the case of washed straw, the decomposition of cellulose was slightly shifted to higher temperature, 350 °C, while the cellulose of the untreated degraded at about 320 °C. Therefore, water washing did seem to affect the decomposition behaviour of rice straw pyrolysis under conventional heating. Moreover, in the DTG of the raw material, hemicellulose (the signal at 300 °C) and cellulose (the signal at 350 °C) independently decomposed of one another in washed rice straw, unlike in the untreated straw. The peak of cellulose decomposition was well sharpened with higher weight loss rate. This result is completely in agreement with what



was observed in water washed rice hull and wheat straw.<sup>185,186</sup> The pyrolytic behaviour was significantly influenced by water wash prior to pyrolysis. The water pre-treatment elevated the peak temperature and the activation energy for the decomposition of the main components of rice hull.<sup>180,186–188</sup> The delayed decomposition was also observed in the microwave with more pronounced temperature shift.

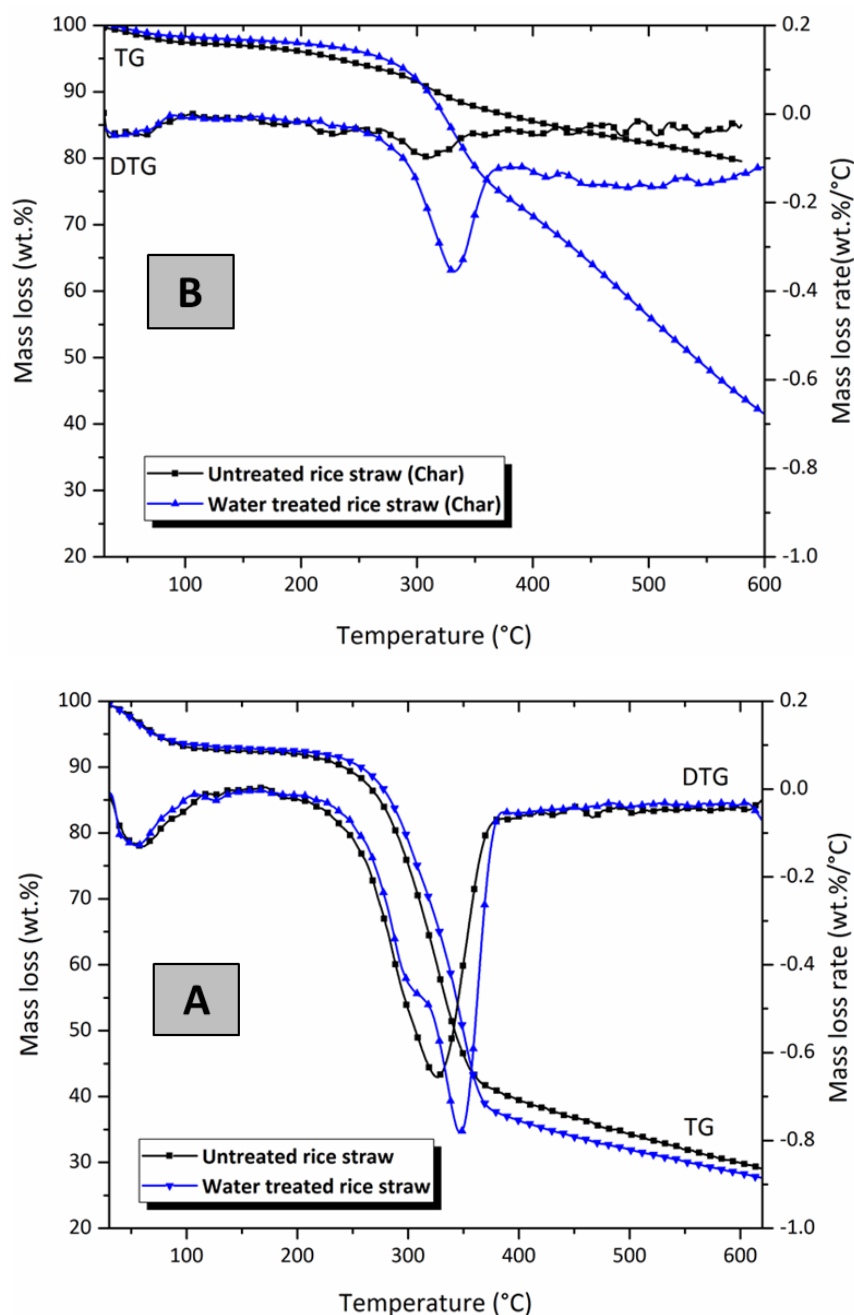


**Figure 3-13** Thermogravimetric analysis (TG) of Raw materials (A) and Chars (B).

After microwave pyrolysis (See **Figure 3-13B**), the peak that indicates the decomposition of cellulose clearly disappeared in the case of untreated rice straw, whereas in the water washed

rice straw the DTG peak of cellulose remained, although it was not of the same intensity indicating that part of cellulose was degraded during the microwave irradiation. The results strongly suggest that the water-soluble mineral matter in rice straw played the role of catalyst for the decomposition of cellulose during the microwave-assisted pyrolysis of rice straw. The presence of the water-soluble mineral component demonstrated the similar effect on thermal behaviour both in conventional and microwave heating. However, the influence in the microwave was dramatically more significant in terms of lowering the decomposition temperature.

### **3.3.4 Elemental surface analysis of untreated and water-washed rice straw**

It was very likely that the so-called microwave absorber were washed out with the water, as they would be polar or ions. To verify the hypothesis about the role of silicates, further analysis was carried out using X-ray photoelectron spectroscopy (XPS), the Inductive Coupled Plasma Atomic Emission (ICP-AES), *Scanning electron microscopy (SEM) and Scanning electron microscope coupled with Energy-dispersive X-ray spectroscopy (SEM/EDX) were used in this study.* The results of XPS was obtained from University of Newcastle. In **Figure 3-14** and **Figure 3-15**, it can be seen that the atomic concentration of silicon stayed almost unchanged in the water treated rice straw (3.7%) compared with the untreated (3.82%). Thus, silicon has not been washed out with hot water, which also means silicates in rice straw do not seemingly play an important role in microwave pyrolysis of rice straw in order to produce the major gaseous product. Since the XPS is the surface analysis technique which has limitation in case the soluble silicon is not located in the surface, the ICP-AES was used to support the XPS. The ICP results are in good agreement with the XPS (See **Table 3-2**), the concentrations of Si in untreated and washed rice straw are slightly different, 59.82 and 44.01  $\mu\text{g/g}$  biomass respectively. It can be concluded that silicates in the biomass are not the key compounds to catalyse the microwave pyrolysis of rice straw. However, it could be other components which were washed out with water.

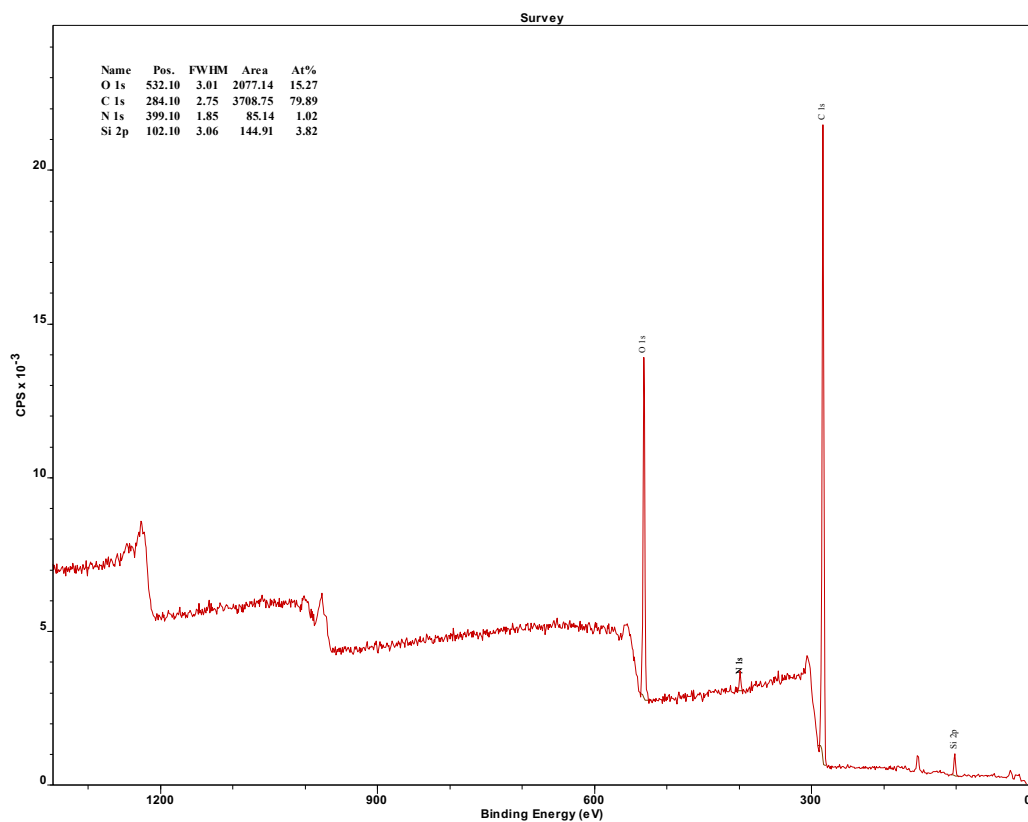


**Figure 3-14** XPS of untreated rice straw.

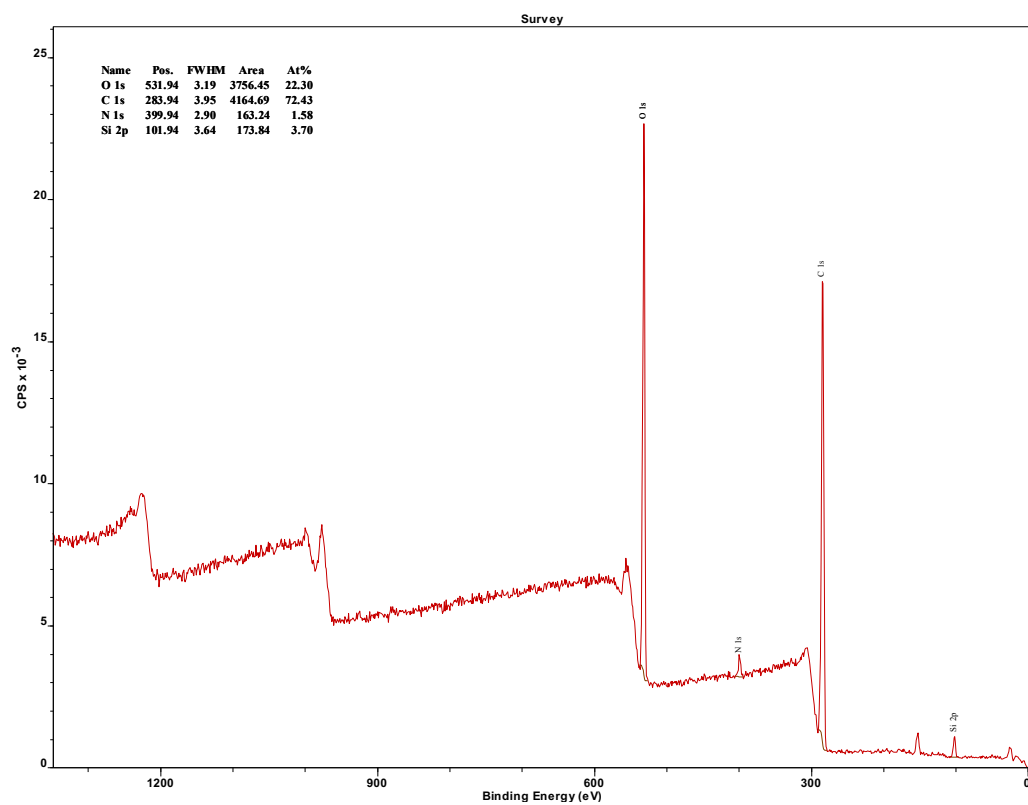


**Figure 3-15** XPS of water treated rice straw

**Table 3-2** ICP results of untreated and water treated rice straws in  $\mu\text{g/g}$  of biomass.

Elements	Concentration ( $\mu\text{g/g}$ of biomass)	
	Untreated rice straw	Water treated rice straw
Al	13.4	14.9
Ba	164.5	170.4
Ca	3019.5	3222.2
Fe	61.6	63.4
K	5108.0	1780.3
Mg	522.9	398.6
Mn	398.7	318.0
Na	94.1	60.0
P	106.0	45.5
S	273.0	185
Si	59.82	44.10
Zn	12.04	12.04

The results of SEM and SEM/EDX were obtained in collaboration from College of Nanotechnology, King Mongkut's Institute of Technology Ladkrabang, Thailand. The SEM images of untreated and water washed rice straw was, **Figure 3-16**, indicated only a slight change in morphology unlike acid washing, which was previously reported as an effective method to reduce ash content.<sup>189</sup> The water treated rice straw became more fragile and easier to crack compared to the untreated straw. The smooth surface of untreated rice straw, in **Figure 3-16A**, disappeared. The broken surface of the water washed sample was well spotted in **Figure 3-16B**.

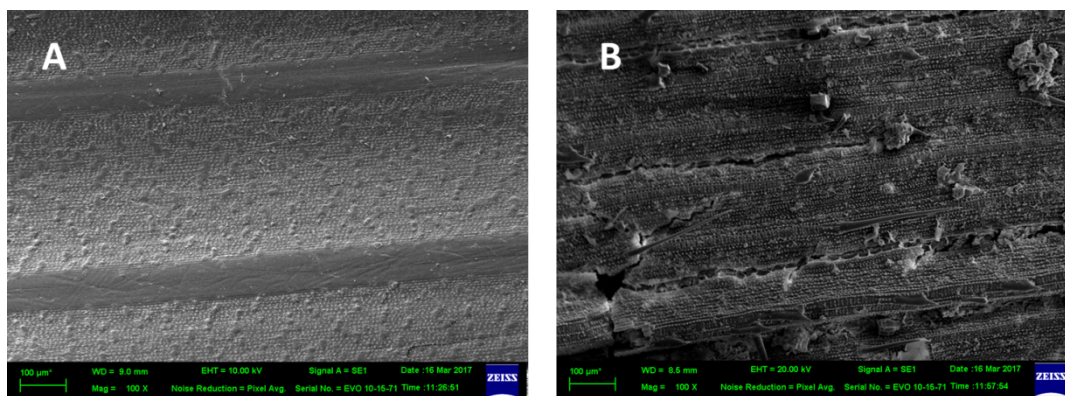


**Figure 3-16** SEM of A) untreated rice straw and B) water treated rice straw.

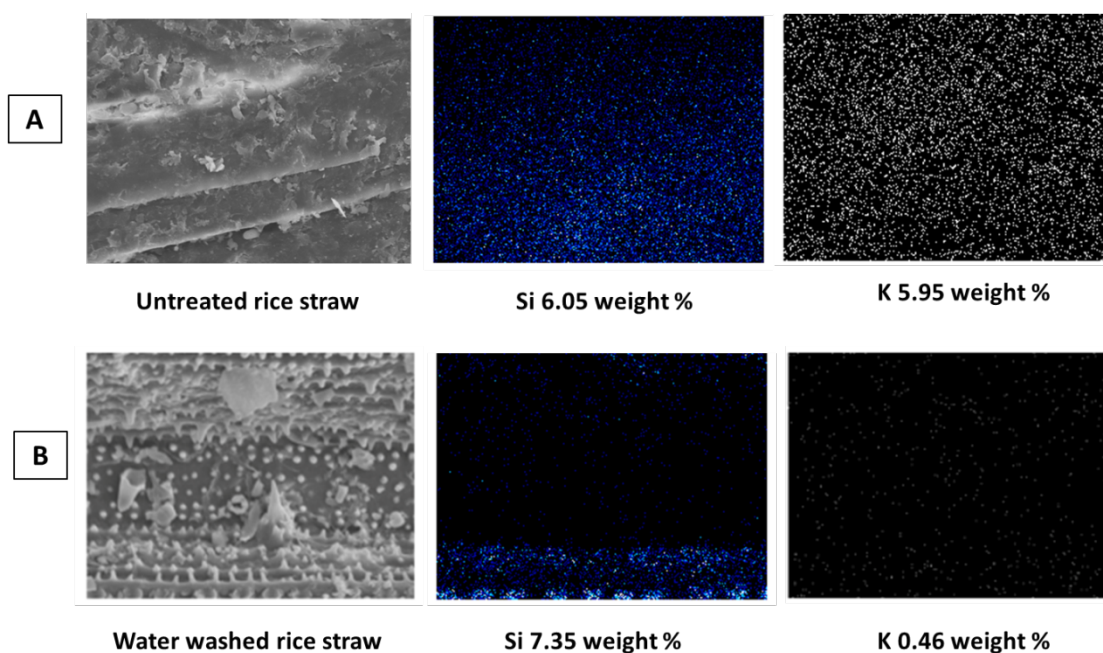


**Figure 3-17** Elemental mapping analysis using SEM/EDS mapping of Si and K of A) untreated rice straw and B) water washed rice straw.

Further comparing the results of the surface morphology of untreated and water washed rice straw was carried on using SEM/EDX for elemental mapping analysis. The difference between these two biomasses can be clearly seen in **Figure 3-17**. A coloured area indicated a higher concentration element of element in question than a dark black area.<sup>190</sup> **Figure 3-17A** shows a great distribution and high amount in silicon (Si) and potassium (K) with 6.05% and 5.95% of

total element for Si and K respectively. In water treated rice straw, the availability of Si remained high, 7.35% of total element; however, that of K dramatically decreased to 0.46% of total element (see **Figure 3-17B**). This result from SEM/EDS indicated that practically large amount of K was effectively removed by water washing, which was also in agreement with the data from ICP and XPS analysis.

In this study, the XPS, ICP and SEM/EDX results strongly confirmed that leaching rice straw with water was not effective to remove silicon-containing compounds and did not decompose organic matters. However, it was able to remove some inorganic components including alkali metals from rice straw. The finding from other studies were supportive, soaking the biomass in water, flushing water through them and leaving the straw exposed in the field to natural precipitation were also able to wash out minerals effectively.<sup>27,191</sup>

Calcium and potassium are two inorganic elements that are of significant abundance in rice straw. The concentration of calcium remained the same after washing, whereas, that of potassium decreased dramatically. This might be due to the fact that calcium is double positively charged, as consequent, it bonds quite strongly to the biomass, which makes it harder to remove compared with potassium, this only singly charged (**Figure 3-18**). Moreover, to remove K and Ca from its anion, requires a replacement ion or another form of complex maybe formed with cellulose.

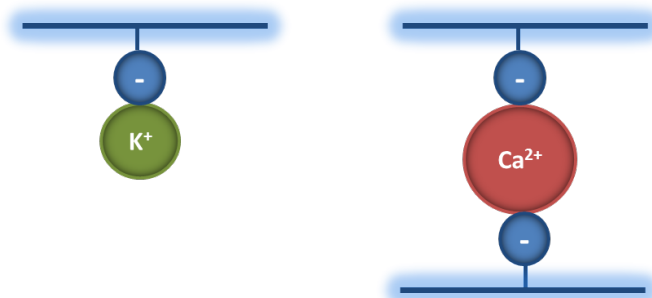


**Figure 3-18** Chemical bonding of potassium and calcium ions.

With all the analytical data discussed in this topic, it is conclusive that silicates do not play an important role on catalysing either the early decomposition of cellulose or the rapid self-gasification during the MW pyrolysis of rice straw. However, the water-soluble mineral matter including especially potassium can potentially be the answer of this phenomenon. Therefore, further investigation specifically into the influence of potassium salts was systematically studied in order to comprehend and to propose the mechanism of the reaction.

### **3.4 The study on the effect of potassium ions by potassium salt impregnation.**

The results obtained previously indicate that some mineral components can be easily washed out with water. These compounds could be either microwave absorbers or a catalyst, which turned cellulose to active cellulose. The most potential according to the ICP analysis (**Table 3-2**) is potassium ions as the concentration of potassium alters significantly compared to the other elements after being washed with water. Therefore, the concentration would also play important role.

It is worth to note that the content of alkali metal of plant biomass such as potassium and sodium changes naturally depending on how the plant exposes to agricultural factors including type of plant, soil conditions, the use of fertilisation and amount of precipitation.<sup>192</sup> Potassium is a crucial nutrient for plants since it is easily mobile; it is usually absorbed via the root system and transported through all the areas of the plant. In an agricultural point of view K-fertiliser helps improving rice yields, ameliorating the effect of nutritional disorders and increasing plant resistance to certain pests and diseases.<sup>190</sup> Upon the physiological changes of biomass, especially on drying, some potassium ions precipitate to form salts such as chloride, hydroxide, carbonate, phosphate, oxalate and sulphate. Moreover, some potassium ions stably integrate into the plant structure as it can be bound to the organic matrix by associating themselves with oxygen-containing functional groups.<sup>186,191,193</sup> Potassium is known as an interesting metal in biomass pyrolysis and combustion.<sup>193,194</sup> It plays the role of catalyst for pyrolysis process and raises the rate of decomposition. In addition, it has influence on varying the production distribution by changing the reaction mechanism.<sup>195-197</sup> It was found from fixed-bed batch reactor or

thermogravimetric studies that potassium salts enhanced the gaseous products and decreased the decomposition of tar products.<sup>193</sup> Moreover, the potassium remaining in the char is considered to be an effective catalyst for increasing rate of conversion for char combustion.<sup>193</sup>

It is assumed that potassium salts could be candidates to play a crucial role in gasification during the microwave pyrolysis of rice straw due to their high solubility in water, meaning that the ionic heating mechanism could additionally contribute to the microwave process. Moreover, potassium salts including potassium chloride (KCl), potassium phosphate ( $K_3PO_4$ ) and potassium sulphate ( $K_2SO_4$ ), are widely used as fertiliser in Thailand. Therefore, six potassium salts were selected based on the ICP results and the use of these compounds in rice cultivation to perform the impregnation study. These six potassium salts were: potassium chloride (KCl), potassium carbonate ( $K_2CO_3$ ), potassium acetate ( $CH_3COOK$ ), potassium hydroxide (KOH), potassium phosphate ( $K_3PO_4$ ), potassium formate (HCOOK) and potassium sulphate ( $K_2SO_4$ ). Each salt was weighed accordingly to meet the concentration of potassium ( $K^+$ ) in the untreated rice straw (20 mg/g of biomass, the concentration of K was kept constant). The pre-weighed salts were dissolved in 5 mL of deionised water and 1g of water treated rice straw was used for each sample. The samples were left rotating for 72 hours then oven-dried for 72 hours at 50°C. Microwave-assisted pyrolysis was then performed in power fixed mode with the sample mass 0.3 g, 300 W.



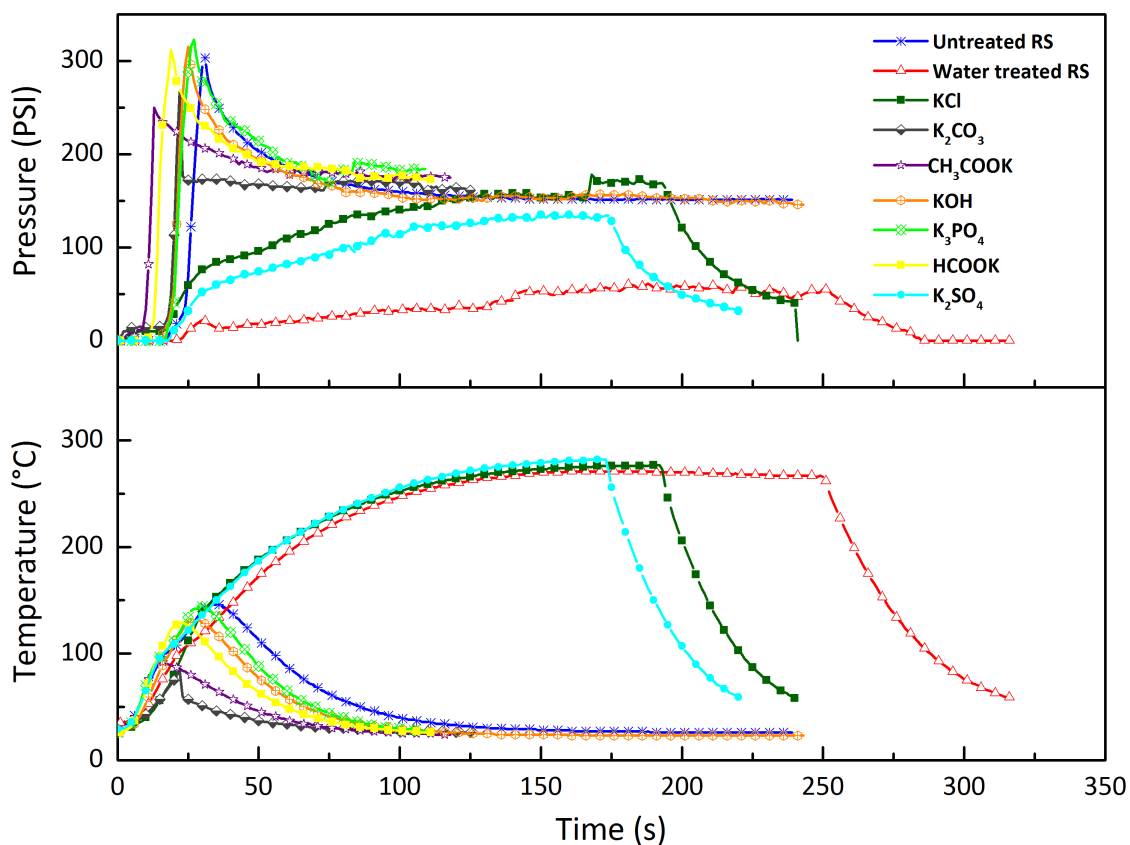


**Figure 3-19** Temperature and Pressure profiles of the impregnation study of potassium compounds with 20 mg of  $K^+$  per 1 g of washed rice straw.

### 3.4.1 Temperature and pressure profile after salt impregnations.

**Figure 3-19** illustrates the temperature and pressure profiles of each impregnated rice straw compared with the untreated and washed rice straw. According to the temperature and pressure profile in **Figure 3-19**, the behaviour towards the microwave of those samples can be categorised into two groups. The first category is when they behaved similar to the untreated rice straw in the microwave, which means the decomposition of biomass occurred spontaneously at very low temperature and produced a lot of incondensable gas, this included impregnating rice straw with  $K_2CO_3$ ,  $CH_3COOK$ ,  $KOH$ ,  $K_3PO_4$  and  $HCOOK$ . The second category is when the samples followed the behaviour pattern of the water treated rice straw, which included impregnating samples with  $KCl$  and  $K_2SO_4$ . The latter refers to the absence of production of gas during the microwave irradiation.

### 3.4.2 The comparison of pressure change rates of impregnated rice straw.

The rates of pressure change in **Figure 3-20**, confirmed that in the first category of raw material, potassium salts played an important role of either microwave absorber or cellulose activator since the spontaneous gasification and the decomposition of cellulose at lower temperature compared to the untreated rice straw was observed. Even though  $K_2CO_3$ ,  $CH_3COOK$ ,  $KOH$ ,  $K_3PO_4$  and  $HCOOK$  successfully catalysed the gasification of washed rice straw, each impregnated sample possessed its own characteristic towards the microwave irradiation. The pressure started changing at  $60^\circ C$  and the rate of pressure change was the highest in the case of potassium acetate. However, potassium phosphate showed comparable characteristics to the natural untreated rice straw in term of decomposition temperature. The pressure change also occurred at early temperatures in the case of  $KCl$  and  $K_2SO_4$  impregnated samples due to the evaporation of water; however, there was not incondensable gas produced. The maximal pressure change rates and the corresponding temperatures of each sample are listed in **Table 3-3**.

**Table 3-3** The maximal temperature change rate and its corresponding temperature of each rice straw

Raw materials	Temperature at max pressure change rate ( $^\circ C$ )	Max Pressure Change rate (PSI/min)
Untreated RS	126	3180
Water treated RS + $K_3PO_4$	116	3960
Water treated RS + $KOH$	113	4500
Water treated RS + $HCOOK$	95	4620
Water treated RS + $K_2CO_3$	80	4620
Water treated RS + $CH_3COOK$	88	5460
Water treated RS + $KCl$	80	540
Water treated RS + $K_2SO_4$	107	330
Water treated RS	106	240

Furthermore, the ICP result in **Table 3-2** confirmed that washing the rice straw with water removed not only potassium but also phosphorus. The phosphorus is mainly in the form of phosphate ions as derived from the typically used P fertiliser. It is totally possible that K-component mainly existed in the form of potassium phosphate, this being the logical reasoning for the presence of both elements.

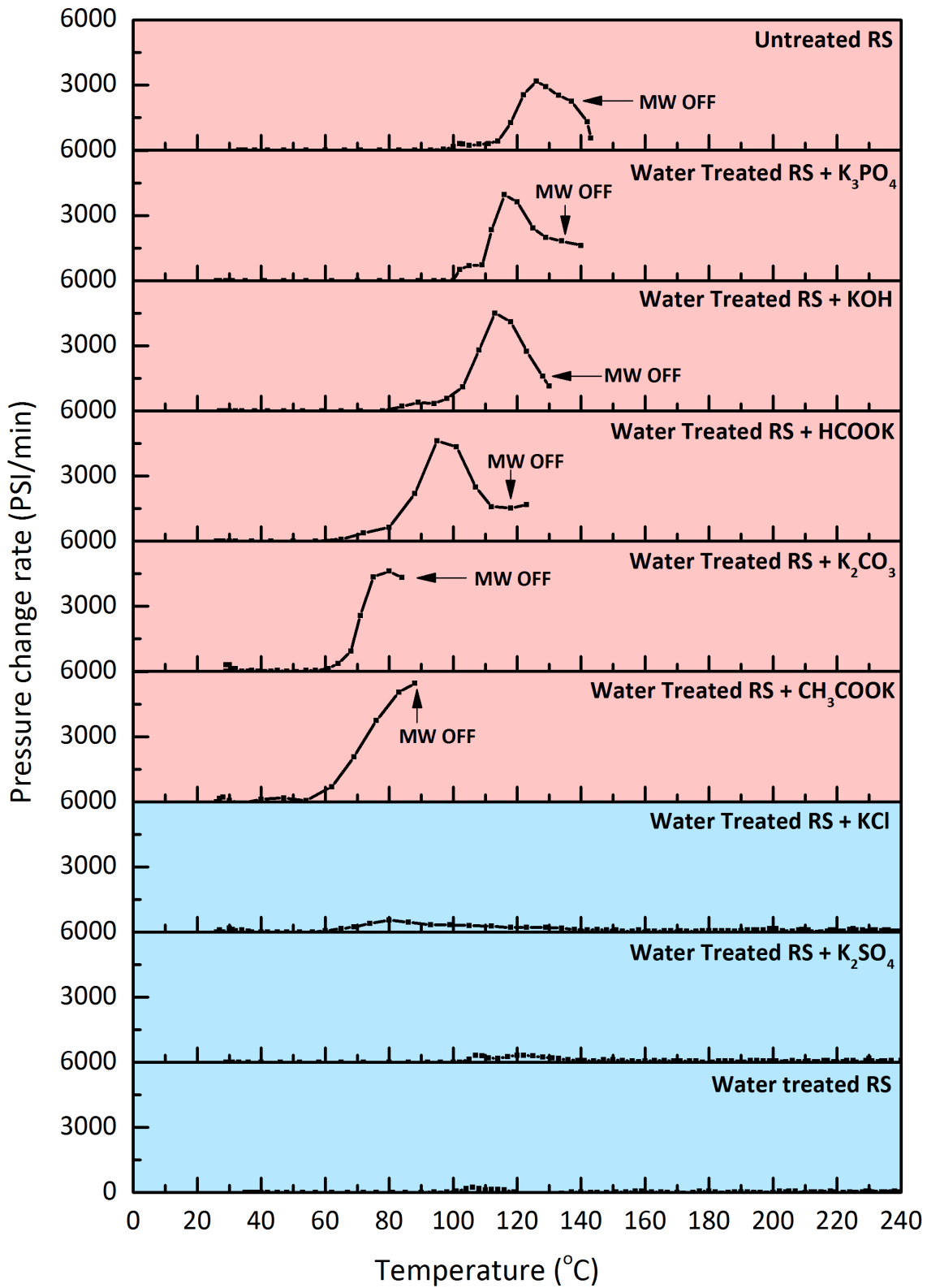


**Figure 3-20** Pressure change rates of untreated, water treated and impregnated rice straw during MAP.

Therefore, it is quite conclusive that it was the potassium phosphate that catalysed the gasification and early decomposition of rice straw during the microwave-assisted pyrolysis. The result is completely in line with the study of K-impregnated willow, which indicated that the devolatilisation occurred faster when potassium was present in biomass. Also, addition of potassium to demineralised willow results the same behaviour as the untreated willow.<sup>193</sup> It is important to bear in mind that uncontrolled factors such as seasonal variations, harvesting locations and the weather just before harvesting must be taken into account as different batches of rice straw exhibited contrasting behaviour in the microwave during this study. For example, a second batch of rice straw was collected in Khon Kaen, Thailand, closely following heavy rain. This resulted in lower amounts of potassium present, 1086 µg/g of dry biomass, and a significant decrease in the production of gas.

### 3.4.3 Influence of acid-base properties and concentration of potassium in thermal behaviour of impregnated rice straw

As previously mentioned, rice straw microwave decomposition behaviour was different depending on which potassium salt was used for impregnation. This interesting phenomenon can be explained by the acidity and basicity of the K-salts and their conjugated acids and the concentration of K in the rice straw. Firstly, the acid-base properties of salts and relationship between  $pK_a$  and  $pK_b$  were fitted perfectly in order to explain the behaviour of rice straw in MW pyrolysis. **Figure 3-21** illustrates the influence of the strength of alkaline solutions explained by  $pK_b$ . It was found that the seven potassium salts, KOH,  $K_2CO_3$ ,  $K_3PO_4$ ,  $CH_3COOH$ ,  $HCOOH$ ,  $K_2SO_4$  and KCl, selected were also divided into similar two categories to the behaviour towards the microwave. The first group belongs to the gasification region where the  $pK_b$  value of the conjugate bases ranged between -1.7 to 11.9 including  $H_2O/OH^-$ ,  $HPO_4^{2-}/PO_4^{3-}$ ,  $HCO_3^-/CO_3^{2-}$ ,  $CH_3COOH/CH_3COO^-$  and  $HCOOH/HCOO^-$ . The second group is the non-gasification region including  $HSO_4^-/SO_4^{2-}$  and  $HCl/Cl^-$  with the  $pK_b$  values of 12.1 and 21 respectively. The  $pK_b$  of the conjugate base sensitively played an important role on the catalytic ability of potassium salt. As seen in the pink gasification zone, the corresponding acids such as  $CH_3COOH$  ( $pK_a = 4.7$ ),  $HCO_3^-$  ( $pK_a = 10.3$ ),  $HPO_4^{2-}$  ( $pK_a = 12.3$ ),  $HCOOH$  ( $pK_a = 3.8$ ) and  $H_2O$  ( $pK_a = 15.7$ ), are all weak acids, which mean their conjugate bases are relatively strong,  $CH_3COO^-$  ( $pK_b = 9.3$ ),  $CO_3^{2-}$  ( $pK_b = 3.7$ ),  $PO_4^{3-}$  ( $pK_b$

= 1.7),  $\text{HCOO}^-$  ( $\text{pK}_b = 11.2$ ) and  $\text{OH}^-$  ( $\text{pK}_b = -1.7$ ). In contrast, in the blue non-gasification region, the  $\text{HCl}$  ( $\text{pK}_a = -7$ ) and  $\text{HSO}_4^-$  ( $\text{pK}_a = 1.9$ ) are strong acids with low  $\text{pK}_a$  values. Therefore, the conjugate bases are very weak with the  $\text{pK}_b$  value of 21 and 12.1 for  $\text{Cl}^-$  and  $\text{SO}_4^{2-}$  respectively. It is important to note that the catalytic power of each potassium salt is very sensitive to the efficiency of the conjugate base although  $\text{HCOO}^-$  ( $\text{pK}_b = 11.2$ ) and  $\text{SO}_4^{2-}$  ( $\text{pK}_b = 12.1$ ) are not significantly different in terms of  $\text{pK}_b$ , their catalytic properties towards the microwave irradiation are completely different.

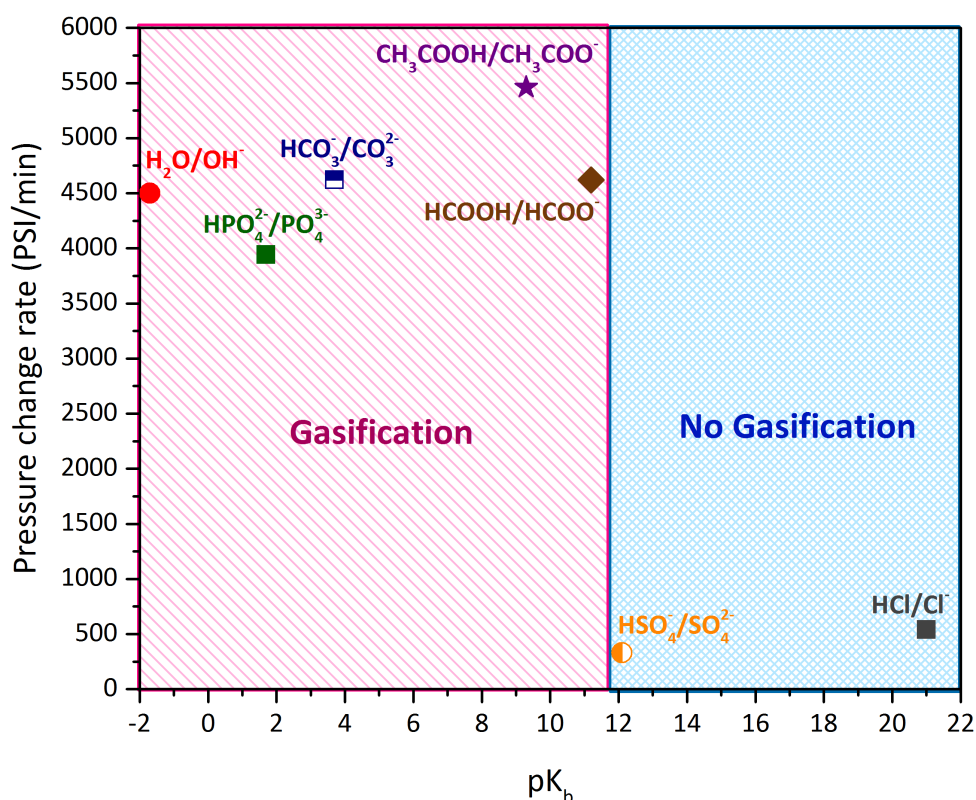


**Figure 3-21** Influence of  $\text{pK}_b$  of potassium salts in the gasification of during the microwave pyrolysis rice straw.

It has been discussed earlier in this chapter that either with or without the presence of water in the rice straw, the self-catalytic property of rice straw resulting in gasification and decomposition of cellulose at a very low temperature during microwave-assisted pyrolysis of rice was still observed. The presence of water apparently delayed the decomposition process and washing rice straw with water completely suppressed the auto-catalytic property of rice straw in the microwave. Between cellulose layers there is strong self-association due to the multiple intermolecular hydrogen bonds as shown in **Figure 3-22**. The microwave active region is located between the layers of amorphous cellulose and the inactive region is the crystalline cellulose. During the microwave process, the increased temperature reduced the crystallinity within the cellulose, increasing the freedom of movement and polarisability of groups within the chains.<sup>184</sup> **Figure 3-23** shows a possible structure of cellulose in the presence of  $K^+$  in the structure of cellulose.<sup>190</sup> It is possible that potassium ions are able to coordinate with the hydroxyl groups and ether  $-O-$  atoms within the structure of cellulose to form a complex of deprotonated cellulose within the microwave active region.<sup>190</sup> As a consequence, the base should be strong enough to deprotonate the hydroxyl group to allow the K-complex to form.

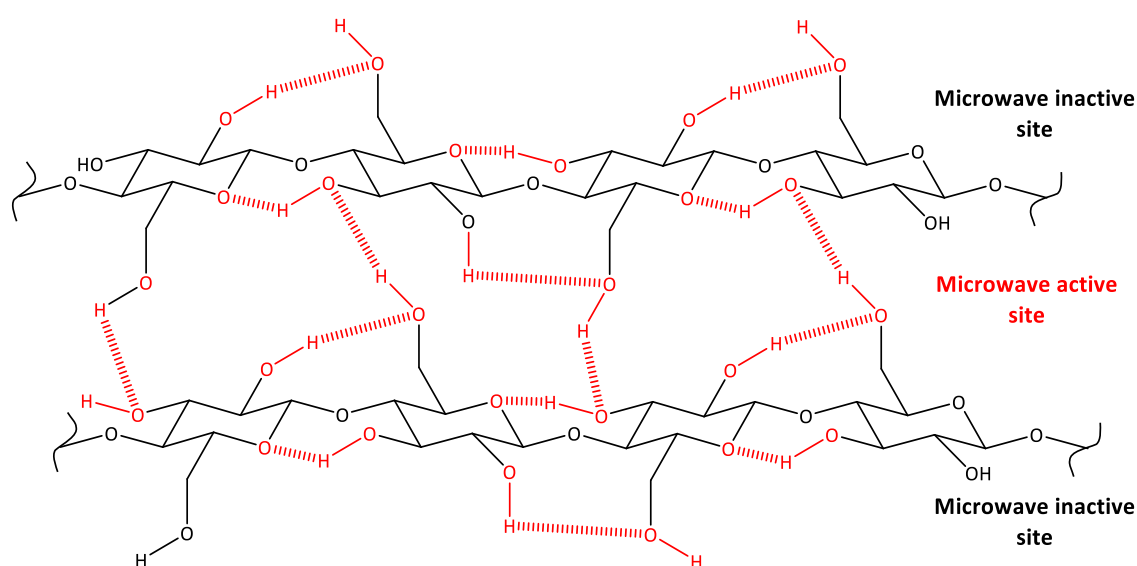


**Figure 3-22** Self-association cellulose due to the presence of H-bonding.<sup>184</sup>

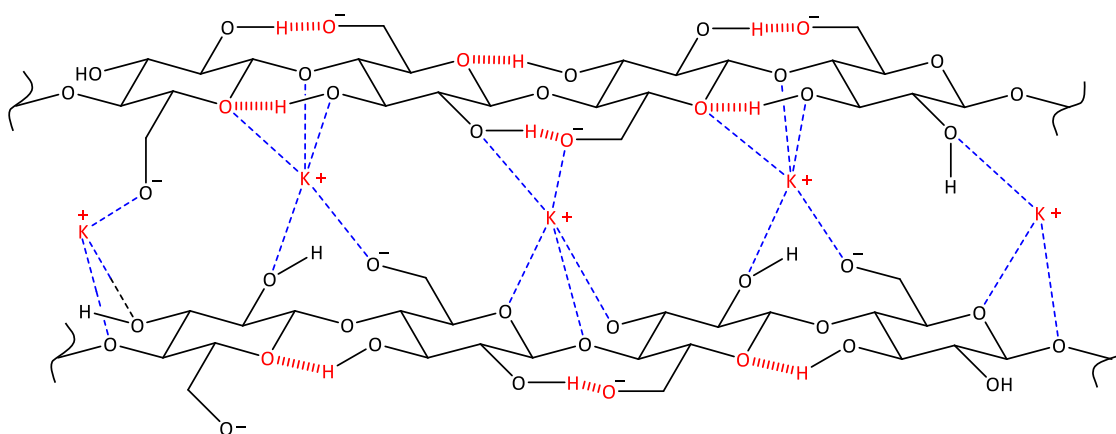


**Figure 3-23 A propose structure of the complex of deprotonated cellulose, after impregnated in potassium salt solution.<sup>190</sup>**

As previously mentioned, there were two important factors, which were keys to explain the behaviour of rice straw towards the microwave radiation. The first one was the  $pK_b$  of the K-salts, which was discussed earlier. The second essential factor was the concentration of the potassium salt in the rice straw. **Table 3-4** shows the concentration of the elements originally presented in high concentration in rice straw and the inorganic salts selected including K, Na, P and S. Water washed rice straw was impregnated in previously selected K-salts to obtain High (10-fold of the untreated RS) and Low (same concentration of untreated RS) concentration of K and then were conducted the microwave pyrolysis using the same experimental conditions as previous discussions. The results always split into two categories as before. Impregnation with  $K_3PO_4$  and KOH were chosen for ICP as their impregnated rice straw behaved similarly to the untreated straw. Also, KCl and  $K_2SO_4$  were selected to ensure that both two factors;  $pK_b$  and concentration of K needed to be met to obtain identical behaviour to untreated rice straw in MW pyrolysis. The pink highlighted zone belonged to the self-gasification zone behaving like the untreated rice straw. This zone included the impregnated rice straw with high concentration of K using  $K_3PO_4$  and KOH. The concentration of K should be at least  $5018 \mu\text{g/g}$  of straw to initiate the gasification. Therefore, impregnated samples with high concentration of  $K^+$  using  $K_3PO_4$  and KOH met the requirement perfectly with  $8640.5$  and  $8806.7 \mu\text{g/g}$  of straw for  $K_3PO_4$  and KOH impregnated straw respectively. However, high concentrations of K were also detected in the blue area of non-gasification belonging to KCl and  $K_2SO_4$  impregnated rice straw. Even though

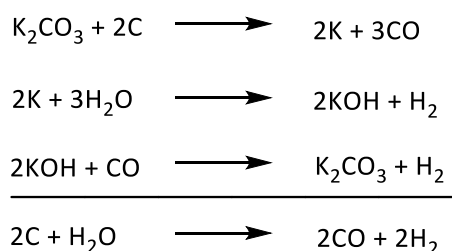


the high concentration of 9334.9 and 8666.2  $\mu\text{g/g}$  of straw for KCl and  $\text{K}_2\text{SO}_4$  impregnated rice straw respectively, were reached, they did not possess catalytic properties for self-gasification. Moreover, the qualified salts with suitable  $\text{pK}_b$  as  $\text{K}_3\text{PO}_4$  and KOH with impregnation in low concentration of K solutions, did not catalyse gasification in MW pyrolysis due to their low concentration 3050.3 and 2185.5  $\mu\text{g/g}$  of straw. The concentration of Na seemed to vary while the K-salts were used, which might due to the impurities of the chemicals. Therefore, sodium carbonate ( $\text{Na}_2\text{CO}_3$ ) was used for impregnation of Na-salts as the  $\text{pK}_b$  condition should be met. 10-fold of the concentration of the untreated rice straw was applied. The concentration of Na in the untreated rice straw was 94.1  $\mu\text{g/g}$  of straw, whereas the concentration of the Na-impregnated straw was 463.9  $\mu\text{g/g}$  of straw. However, the self-gasification was not observed. With all the evidence, K ion was the key factor of self-gasification at low temperature during the MW pyrolysis of rice straw based on the results obtained herein.

**Table 3-4** ICP results of impregnated rice straw in K-salt and Na-salt solution with high and low concentration.

Raw materials	Concentration ( $\mu\text{g/g}$ of straw)				
	K	Na	P	S	
Untreated RS	5108.0	94.1	106.0	273.0	
Water treated RS + $\text{K}_3\text{PO}_4$	H	8640.5	186.9	1998.2	214.0
Water treated RS + KOH	H	8806.7	193.8	39.7	210.0
Water treated RS		1780.3	60.0	45.5	185
Water treated RS + KCl	H	9334.9	149.0	66.8	200.0
Water treated RS + $\text{K}_2\text{SO}_4$	H	8666.2	123.3	52.7	4389
Water treated RS + $\text{K}_3\text{PO}_4$	L	3050.3	165.6	265.3	213.0
Water treated RS + KOH	L	2185.5	124.5	82.6	195.0
Water treated RS + $\text{Na}_2\text{CO}_3$	H	1796.6	463.9	84.2	208.0

The reaction of alkali catalysed gasification of char has been proposed by Mckee but the mechanism is still uncertain.<sup>198</sup> Potassium carbonate increased the rate of gasification involving carbothermic reduction of alkali carbonates to alkali metal vapours.<sup>199</sup>



Alkali catalysts were used in wood gasification by wet impregnation; the production of H<sub>2</sub> was significantly higher compared with the uncatalysed reaction.<sup>186</sup> In addition, impregnation of K<sub>3</sub>PO<sub>4</sub> to poplar wood resulted in phenolic rich bio-oil via fast catalytic pyrolysis.<sup>200</sup>

#### 3.4.4 Thermal analysis

The comparison of the DTG plots of the rice straw samples before and after the microwave pyrolysis are shown in **Figure 3-24** and **Figure 3-25** respectively. **Figure 3-24** demonstrates potassium salt impregnations affected thermal behaviour of rice straw in the conventional heating. As the water treated rice straw was used in these experiments, the presence of potassium in all samples enhanced the cellulose decomposition towards lower temperature. Therefore, the relationship between pK<sub>a</sub> and pK<sub>b</sub> did not affect this behaviour as KCl and K<sub>2</sub>SO<sub>4</sub> showed the same results in lowering the temperature.

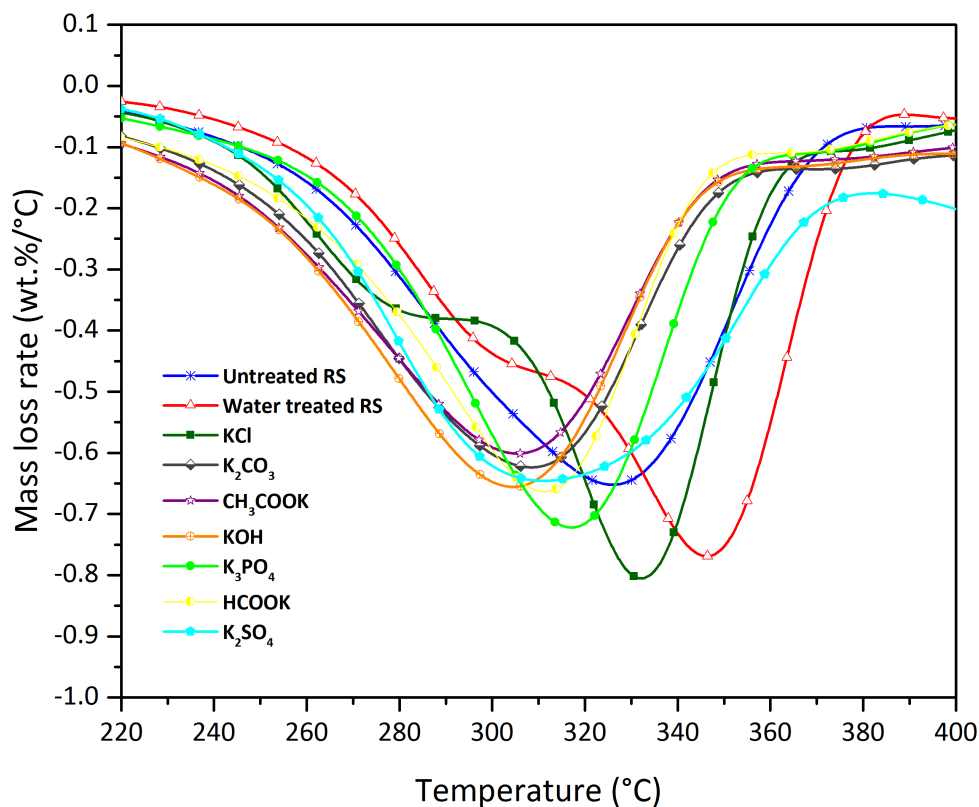


**Figure 3-24** Zoomed in DTG of the raw materials cellulose decomposition region.

It was also confirmed in **Figure 3-25** that  $K_2CO_3$ ,  $CH_3COOK$ ,  $KOH$ ,  $K_3PO_4$  and  $HCOOK$  were effective microwave energy absorbers and able to catalyse the gasification and enhanced the decomposition of cellulose in rice straw as in the untreated rice straw. The peak of maximal mass loss rate ranged from 300-330 °C disappeared completely. However, cellulose decomposition signals are still present in the case of  $KCl$  and  $K_2SO_4$  even though the final temperature reached was 280 °C.

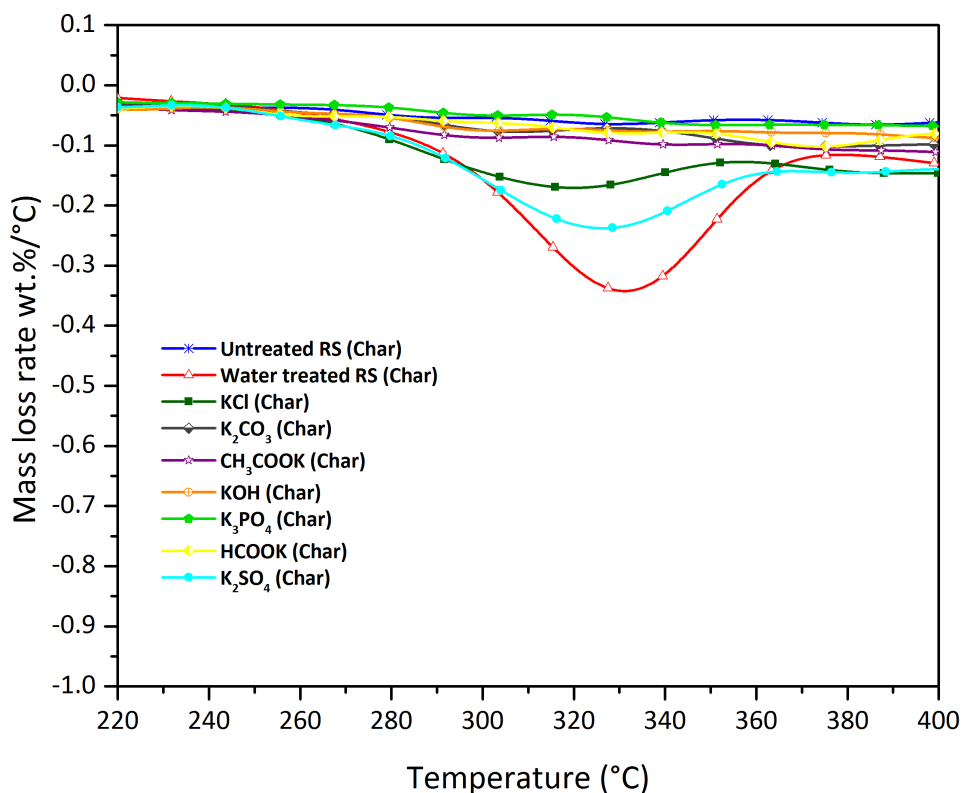


**Figure 3-25** DTG of Chars at cellulose decomposition region.

### 3.5 Conclusion and Future work

A study of the key factors that influenced and enhanced on self-gasification during the microwave-assisted pyrolysis of rice straw have been systematically assessed. Three hypotheses on potential microwave energy absorbers present in the biomass were proposed for further investigation. Water was the first microwave absorber in question due to its high availability in plant and its dielectric and polar properties. Surprisingly, not only the absence of moisture content did not have any adverse effect, but it also positively enhanced the process as the decomposition of cellulose occurred significantly at lower temperature (95°C) compared with the untreated rice straw (120°C). The second microwave absorber to be investigated was silicate compounds as the rice straw is considered as high silicon-containing biomass and some of them are stored in silicate form. As such, rice straw was treated (washed) in hot water to remove soluble silicates prior to the microwave pyrolysis. The result of untreated biomass was considered as control experiment. The water-washed rice straw behaved totally different during

the microwave irradiation, there was no incondensable gas produced during the process unlike in the case of the control. Therefore, it can be concluded that the important component was washed out with water. These water-soluble components were likely to be mineral inorganic salts, potentially potassium containing, but impossible to be the silicate as the concentration in the biomass was unchanged after washing (as determined by ICP-MS). The third microwave absorber is K-containing compound. In plants, potassium usually stays in the form of salts after the biomass is dried. Consequently, potassium salt impregnation was carried out to see if enhanced microwave pyrolysis could be returned to the previously water washed material. Six commercially available potassium salts including potassium chloride (KCl), potassium carbonate ( $K_2CO_3$ ), potassium acetate ( $CH_3COOK$ ), potassium hydroxide (KOH), potassium phosphate ( $K_3PO_4$ ), potassium formate (HCOOK) and potassium sulphate ( $K_2SO_4$ ) were screened for their impact on impregnation into the washed rice straw. K-impregnated rice straw with  $K_2CO_3$ ,  $CH_3COOK$ , KOH,  $K_3PO_4$  and HCOOK demonstrated the catalytic effect of gasification during the pyrolysis, which have similar behaviour to the untreated rice straw. In contrast, KCl and  $K_2SO_4$  impregnation sample did not result any gas production. This phenomenon can be explained by the relationship between  $pK_a$  and  $pK_b$ . To be able to catalyse the gasification, the  $pK_b$  of the conjugate bases needed to be ranged between -1.7-11.9 in order to protonate the hydroxyl group within the cellulose. Moreover, the concentration of K should be at least 5100  $\mu\text{g/g}$  of straw in order to catalyse self-gasification. Therefore, the deprotonated cellulose became microwave active after K-impregnation. Among all the alkali catalysts, potassium phosphate impregnated straw had a much closer behaviour to the untreated rice straw in term of initial temperature of pyrolysis and the pressure change rate even though the other salts were also effective catalysts. Our conclusion is drawn to potassium phosphate being the main salt responsible due to the strong correlation with the earlier obtained ICP-MS data that showed high levels of K and P in the active untreated rice straw, and reduced levels of both in the inactive washed material.

Within the concept of biorefinery it would be sustainably beneficial to investigate the product distribution and composition of the pyrolysis oil, gas and char to give a better understanding about using potassium salts in the catalytic pyrolysis process. The optimisation of the concentration of alkali metal catalyst could also be of interest in terms of energy efficiency. Product selection with the gas and oil could potentially be possible as different salts results in

different behaviour in microwave. Moreover, potassium salts are cheap and widely available, which has a positive practical economic point of view, though concerns around the availability of phosphorous should be considered carefully. Further work is needed to quantify the gaseous component. Crucially, this study provides important information for Thailand and how rice straw can be microwave treated to yield a significant quantity of gas, which maybe potentially used as synthesis gas for the production of fuels and chemicals.

## **Chapter 4**

# **Prawn waste residues as a source of valuable lipophilic compounds**

## 4 Prawn waste residues as a source of valuable lipophilic compounds

### 4.1 Introduction

Polyunsaturated fatty acids (PUFAs) are globally in high demand due to their health benefits and various industrial applications such as use in infant formula, fortified foods and beverages, nutritional supplements, pharmaceuticals, clinical nutrition and pet food, treats and supplements.<sup>201</sup> In 2011, global consumers spending on PUFAs, especially EPA/DHA fortified products across those categories reached 24.4 billion US dollars with the annual growth rate of 6.4%.<sup>202</sup> Traditional sources of omega-3s PUFAs include fish oils from anchovy or cod livers.<sup>202</sup> As consequence, alternative sources of these lipophilic compounds are needed to meet the future global demand.

Prawn Waste is one possible source of fatty acids including PUFAs, EPA (C<sub>20:5(n-3)</sub>), ARA (C<sub>20:4(n-6)</sub>) and DHA (C<sub>22:6(n-3)</sub>).<sup>203</sup> This study focuses on Pacific white shrimp (*Litopenaeus vannamei*) residues, this species is widely farmed and exported from Thailand (about 500,000 tonnes exported in 2012).<sup>33</sup> Most shrimps are de-shelled then prepared as frozen or canned meat for export. During industrial process, shells are removed as by-products including cephalothorax (shrimp heads), which account for approximately 40-50% of total weight.<sup>40,41</sup> Not only PUFAs are present, but valuable products such as astaxanthin and others valuable molecules were also identified in this prawn residues.<sup>204,205</sup>

Crustacean shells consist of three primary chemicals, which are of interest in industrial applications, calcium carbonate (20-50%), chitin (15-40%) and protein (20-40%). The traditional extraction methods of these chemicals as well are destructive, wasteful and expensive.<sup>206-208</sup> For lipid extraction, organic solvents such as hexane are widely used since they result in high percentage of crude yield.<sup>69</sup> The use of organic solvents is become restricted due to their toxicological and environmental concerns.<sup>62</sup> Supercritical carbon dioxide (scCO<sub>2</sub>) is an excellent



alternative solvent for natural products, since carbon dioxide is non-flammable, non-toxic and readily available.<sup>209–211</sup>

In this study, the supercritical extraction of hydrophobic compounds from prawn residue (*Litopenaeus vannamei*) was investigated in order to valorise this waste stream. The optimisation of lipid extraction from prawn cephalothorax (heads) by scCO<sub>2</sub> was undertaken and added-value components were characterised, quantified and their potential applications were identified.

## **4.2 Solvent extraction of Pacific white shrimp waste residues.**

A number of studies into lipid composition of prawn including the waste by-products have been investigated.<sup>34,207,212</sup> Hexane is one of the most commonly selected organic solvents of lipid extraction, as it is highly selective, however, hexane is recognized as a harmful air pollutant by the US EPA, with more than 20,000 tonnes annually released to the atmosphere from extractions alone.<sup>109</sup> Conventional solvent extraction was carried out to obtain the complete lipid profile of the waste biomass and was used as a bench mark to systematically assess the efficiency of the alternative extraction process.

Hexane and heptane were used as solvents in the Soxhlet extraction of ground prawn cephalothorax for 2 hours. The total extract yields for hexane and heptane are 8.4% and 12.4% respectively. Heptane was a more effective solvent in terms of total lipid content recovery due to the high temperatures required and was regarded as suitable to replace hexane in conventional extractions despite still being fossil derived. However, heptane does require significantly higher temperatures compared to scCO<sub>2</sub> extraction study (40-60°C) since the boiling point of heptane is 98 °C, while that of hexane is 68 °C. Temperature plays important role in the resulting lipid composition and quantity, as such, hexane is chosen in order to avoid this problem.

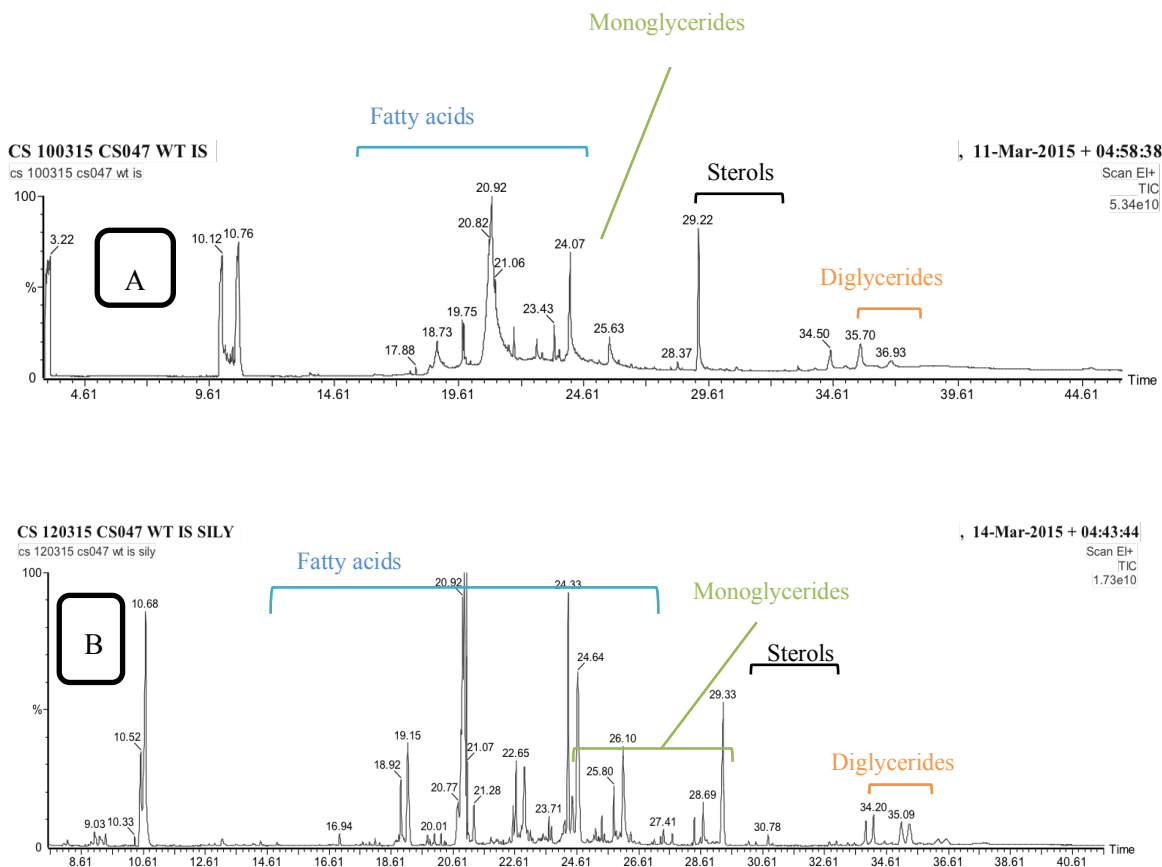


**Figure 4-1** Gas chromatogram of *Litopenaeus vannamei* from hexane extract  
 A) Without Derivatization B) with trimethylsilyl derivatization.

The fresh biomass with the moisture content of 70% by weight was utilised to avoid energy intensive drying processes, as the aim was to minimise use of energy and reduce the number of process steps. The extract was analysed by GC-MS without further purification. **Figure 4-1** illustrates gas chromatograms of prawn by-product extract using hexane. **Figure 4-1A** is the chromatogram of the underivatized extract, in which most components overlapped and resulted in poor separation due to the non-polar nature of the lipophilic compounds in the extract. However, the chromatogram of the derivatised sample in **Figure 4-1B** was found to significantly improve the separations. Silylation of the polar functional groups such as hydroxyl and carboxylic acid groups allowed identifying and characterising the long-chain lipid compounds having the chain length of  $C_{22}$ , which were not detected in underivatized samples, in addition to low-molecular lipid components and odd chain fatty acids.

#### 4.2.1 Fatty acids in Pacific white shrimp by-product as extracted by hexane Soxhlet.

Silylation of free fatty acids exhibited the molecular ion of the TMS-ester derivative, which enabled assigning molecular weights to the higher-chain fatty acids. **Figure 4-2** includes EI mass spectra of silylated  $C_{16:0}$  and  $C_{18:0}$  fatty acids. The characteristic fragmentations of fatty acids including the McLafferty rearrangement were previously discussed in details and listed in Chapter 3.

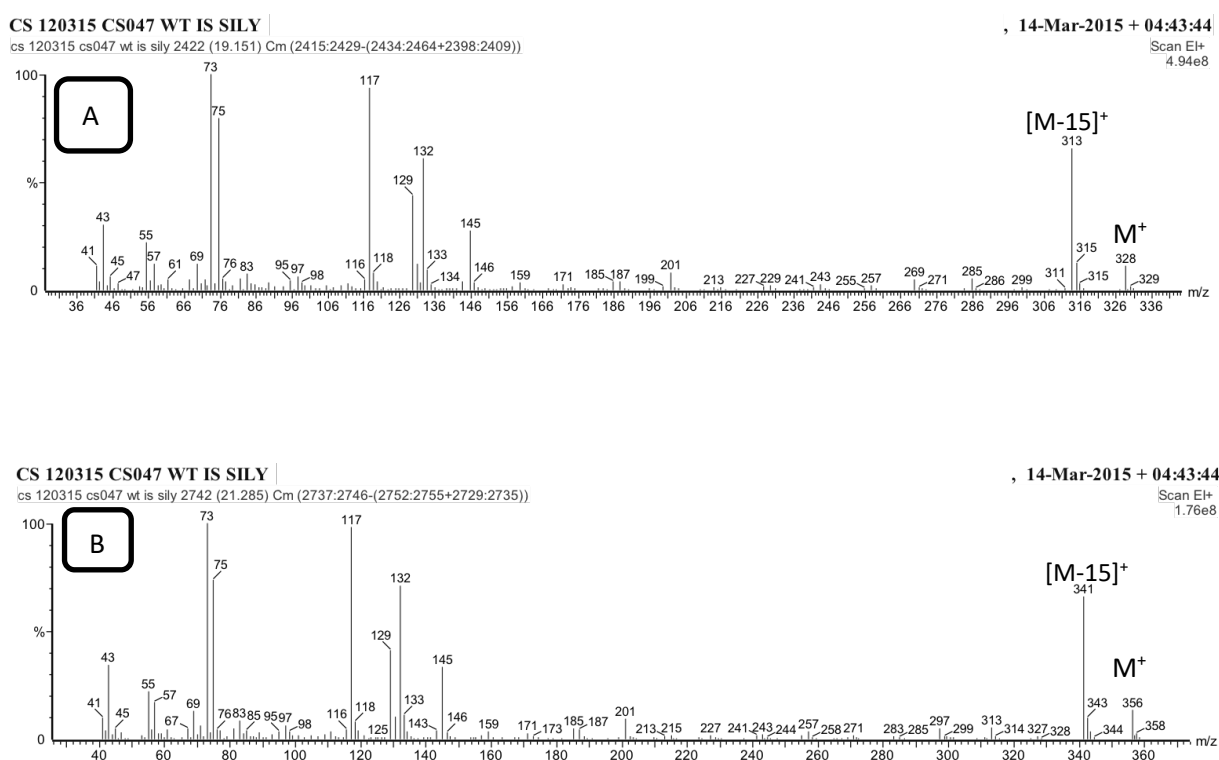
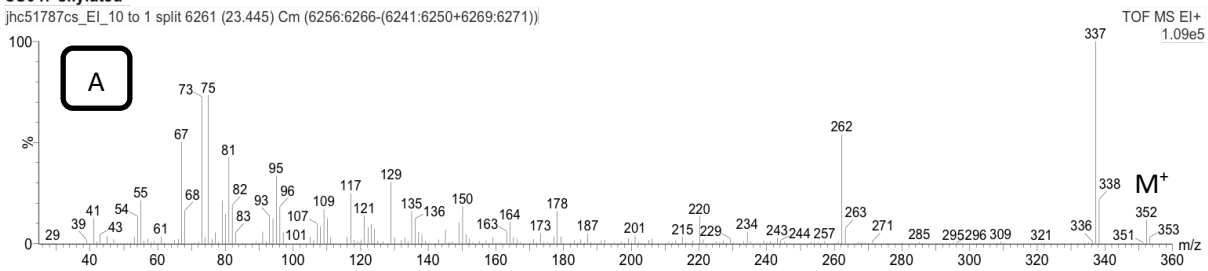


**Figure 4-2** EI mass spectra of A) hexadecanoic acid ( $C_{16:0}$ ) trimethylsilyl ester B) octadecanoic acid ( $C_{18:0}$ ) trimethylsilyl ester

Silylated oleic and linoleic acids were found co-eluted in the GC-MS, therefore, it was difficult for further quantify these two fatty acids. The GC-EI (Electron Ionization) and GC-FI (Field Ionization) were used to confirm the presence of linoleic acid and oleic acid. The GC-EI gave the full fragmentation, which matched with our previous analyse on the GC-MS of rice straw (Chapter 2) and the GC-FI allowed us to see the molecular ions of these two fatty acids, therefore, their presence was concluded (**Figure 4-3** and **Figure 4-4**). Moreover, the presence of these two free fatty acids was confirmed by the use of commercial standards.

**CS047 silylated**

jhc51787cs\_EI\_10 to 1 split 6261 (23.445) Cm (6256:6266-(6241:6250+6269:6271))



**CS047 silylated**

jhc51787cs\_FI 870 (23.549) Cm (869:870-865:866)

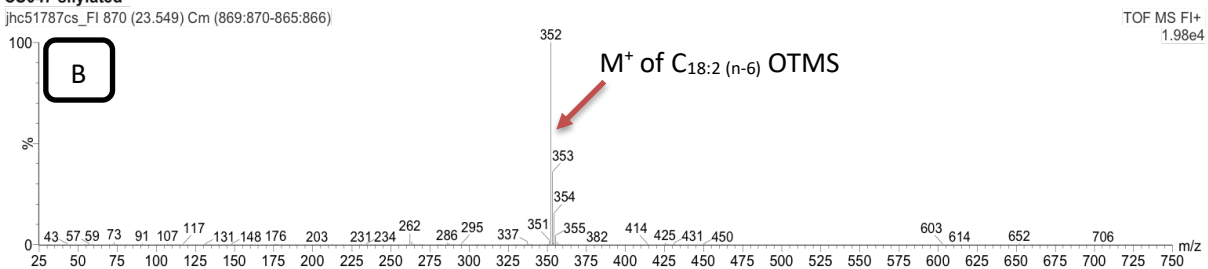


**Figure 4-3** The mass spectrum of linoleic acid trimethylsilyl ester (C<sub>18:2</sub>(n-6)) A) EI mass spectra B) FI mass spectra

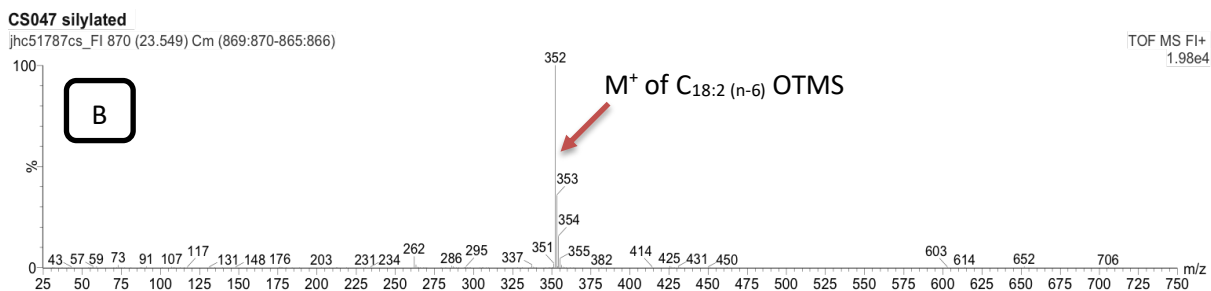
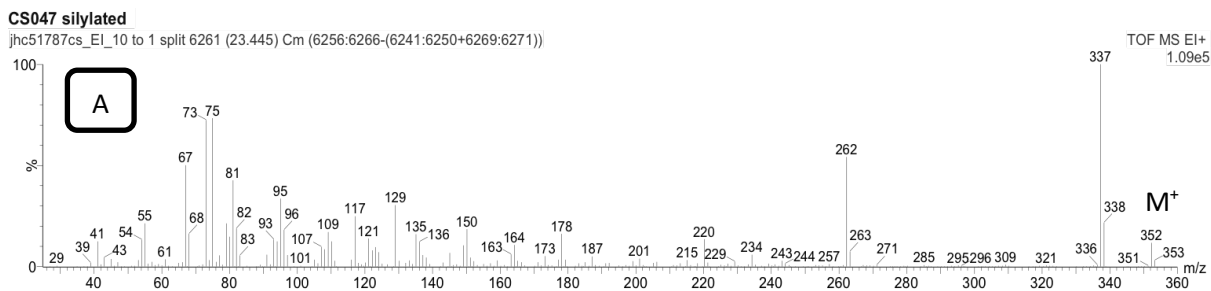


**Figure 4-4** The mass spectrum of linoleic acid trimethylsilyl ester ( $C_{18:1(n-9)}$ ) A) EI mass spectra B)

FI mass spectra

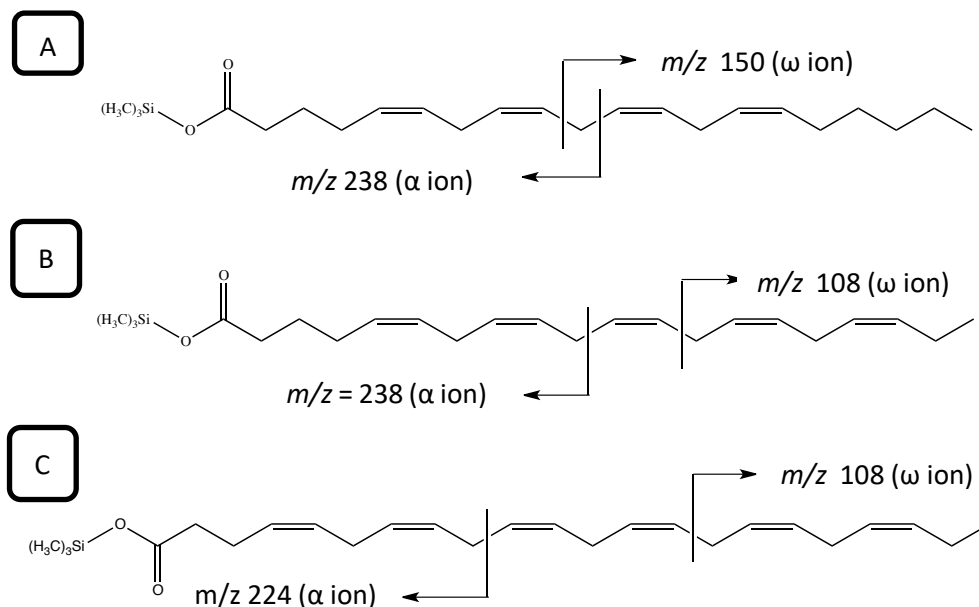


**Figure 4-5** Characteristic fragmentation of  $\omega$  ion and  $\alpha$  ion for A) n-6 terminal ( $\omega_6$ ) in ARA

( $C_{20:4(n-6)}$ ) B) and C) n-3 terminal ( $\omega_3$ ) in EPA ( $C_{20:5(n-3)}$ ) and DHA ( $C_{20:6(n-3)}$ ) respectively

Polyunsaturated fatty acids fragment in a much more complex manner in the mass spectrometer. Mass spectra of polyunsaturated fatty acid trimethylsilyl esters obtained with electron-impact ionization provide greater information due to the enhanced volatility of the substrates. On the other hand, there are some key fragmentations, methylene-interrupted unsaturation, which can be used to identify common polyenoic fatty acid such as biologically important (n-6) and (n-3) families.<sup>209,213,214</sup> The ion at  $m/z$  150 is characteristic for (n-6) fatty acids, while, the one at  $m/z$  108 is for (n-3) family ( $\omega$  ion). The  $\omega$  ion contains the first two double bonds from the extremity (or end) of the chain. There is also the presence of an  $\alpha$  ion, which contains the carboxylic group and the first two double bonds. Although it is often recognized and tends to be very small, it is equally important for the identification (**Figure 4-5**).<sup>215,216</sup>

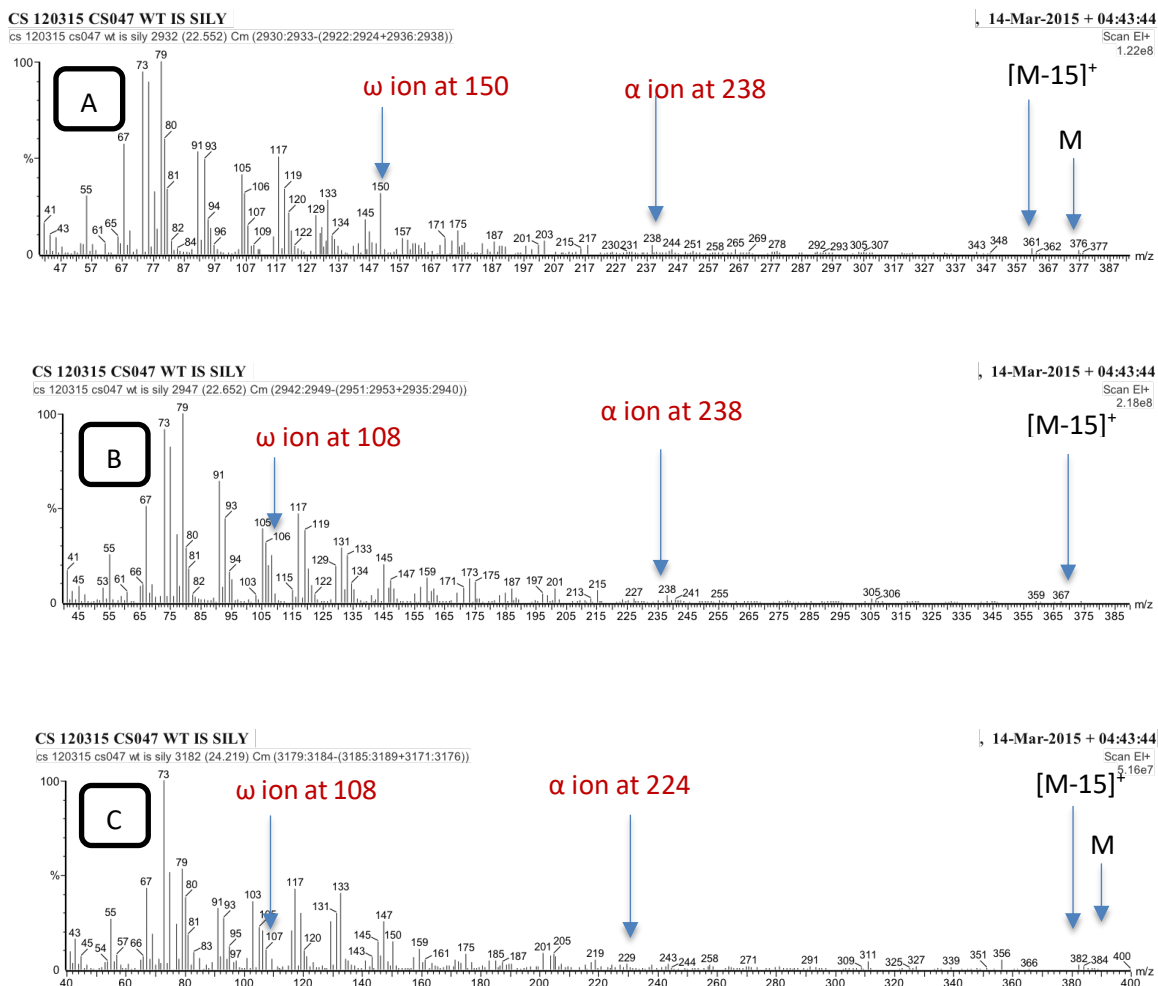


**Figure 4-6** EI mass spectra of trimethylsilyl ester of PUFAs A) ARA B) EPA C) DHA.

Lipid extract of *Litopenaeus vannamei* by-product was found to demonstrate both odd and even chain lengths of fatty acids, but, the latter are dominant in this species, which can be explained by the biosynthetic route.<sup>33,43,72</sup> The detailed free fatty acid profile of *Litopenaeus vannamei* by-product has not been reported in previous studies, only their derivatives such as fatty acid methyl ester, have been analyzed.<sup>217</sup>

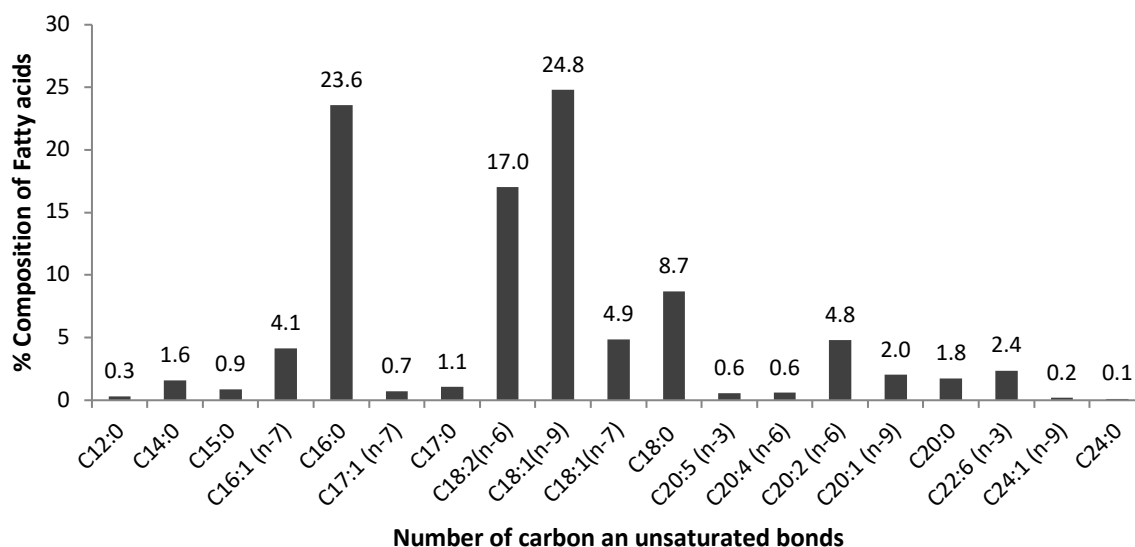


**Figure 4-7** Typical free fatty acid distribution of *L. vannamei* cephalothorax by hexane Soxhlet extraction in 2 hours.

The percentage composition of free fatty acids is illustrated in **Figure 4-7**. The hexane extract of the cephalothorax of Pacific white shrimp contained 38% of saturated fatty acids (SFAs), 36.7% of monounsaturated fatty acids (MUFAs) and 25.3% of polyunsaturated fatty acids (PUFAs). Among all the fatty acids present, oleic acid (C<sub>18:1(n-9)</sub>) and palmitic acid (C<sub>16:0</sub>) were predominant presenting in 24.8% and 23.6% of total fatty acids respectively. Linoleic acid (C<sub>18:2(n-6)</sub>) was also identified in relatively high amount of 17%. However, eicosapentaenoic acid or EPA (C<sub>20:5(n-3)</sub>) and docosahexaenoic acid or DHA (C<sub>22:6(n-3)</sub>) were not detected in high quantities in hexane extract. This is consistent with the reported method of Bligh and Dyer for the study of prawn paste extract (*L. vannamei*).<sup>218</sup>

The total abundance of free fatty acids (FFA) was the greatest of all compound classes in the hexane extract, with  $20789.8 \pm 257.3 \mu\text{g/g}$  of dry biomass. As previously mentioned, SFAs were predominant with the concentration of  $7889.7 \pm 62.2 \mu\text{g/g}$  of dry biomass, followed by MUFAs with a high distribution at  $7634.4 \pm 150.9 \mu\text{g/g}$  of dry biomass and PUFAs were the lowest in concentration with  $5265.7 \pm 44.1 \mu\text{g/g}$  of dry weight. The fatty acid abundance pattern was found SFAs > MUFAs > PUFAs (**Table 4-1**).

The three most abundant FFAs in the hexane extract were even, oleic acid ( $\text{C}_{18:1(n-9)}$ ) followed by hexadecanoic acid ( $\text{C}_{16:0}$ ) and linoleic acid ( $\text{C}_{18:2(n-6)}$ ) with the concentrations of  $5155.2 \pm 100.3 \mu\text{g/g}$  of dry biomass,  $4905.8 \pm 10.3 \mu\text{g/g}$  of dry biomass and  $3537.7 \pm 18.0 \mu\text{g/g}$  of dry biomass respectively. The focus of this current study was on PUFAs due to their high value and health benefits.<sup>219</sup> PUFAs have importantly been shown to reduce cardiovascular disease and improve cognitive development.<sup>219,220</sup> Linoleic acid was found to be highest in concentration among all others PUFAs with  $1805.1 \pm 6.1 \mu\text{g/g}$  dry biomass. However, docosahexaenoic acid (DHA), eicosapentaenoic acid (EPA) and arachidonic acid (ARA) were found in relatively low concentrations in hexane extract,  $489.0 \pm 10.4$ ,  $118.2 \pm 0.8$  and  $124.3 \pm 5.1 \mu\text{g/g}$  dry biomass respectively. By observation of **Table 4-1**, it is obvious that the hexane crude lipid is quite rich in saturated fatty acid.

**Table 4-1** Abundance (in  $\mu\text{g/g}$  dry biomass) of free fatty acids in *L. vannamei* by-product extract using hexane Soxhlet for 2 hours.

Free fatty acids		Abundance in <i>L. vannamei</i> ( $\mu\text{g/g}$ dry biomass)
Dodecanoic acid	$\text{C}_{12:0}$	$62.8 \pm 4.0$
Tetradecanoic acid	$\text{C}_{14:0}$	$326.4 \pm 1.1$
Pentadecanoic acid	$\text{C}_{15:0}$	$183.0 \pm 0.5$
Hexadecanoic acid	$\text{C}_{16:0}$	$4905.8 \pm 10.3$
Hexadecenoic acid	$\text{C}_{16:1(n-7)}$	$856.9 \pm 8.6$
Heptadecanoic acid	$\text{C}_{17:0}$	$221.1 \pm 0.8$



Heptadecenoic acid	C <sub>17:1 (n-7)</sub>	146.3 ± 0.3
Octadecanoic acid	C <sub>18:0</sub>	1805.1 ± 6.1
Octadecenoic acid	C <sub>18:1(n-7)</sub>	1014.1 ± 16.6
Oleic acid	C <sub>18:1(n-9)</sub>	5155.2 ± 100.3
Linoleic acid	C <sub>18:2(n-6)</sub>	3537.7 ± 18.0
Eicosenoic acid	C <sub>20:0</sub>	364.2 ± 38.4
Eicosenoic acid	C <sub>20:1 (n-9)</sub>	420.3 ± 25.1
Eicosadienoic acid	C <sub>20:2 (n-6)</sub>	996.5 ± 9.9
Arachidonic acid (ARA)	C <sub>20:4 (n-6)</sub>	124.3 ± 5.1
Eicosapentaenoic acid (EPA)	C <sub>20:5 (n-3)</sub>	118.2 ± 0.8
Docosahexaenoic acid (DHA)	C <sub>22:6 (n-3)</sub>	489.0 ± 10.4
Tetracosanic acid	C <sub>24:0</sub>	21.3 ± 1.0
Tetracosenoic acid	C <sub>24:1 (n-9)</sub>	41.5 ± 0.1
<i>Total saturated free fatty acids</i>		<i>7889.7 ± 62.2</i>
<i>Total monounsaturated free fatty acids</i>		<i>7634.4 ± 150.9</i>
<i>Total polyunsaturated free fatty acids</i>		<i>5265.7 ± 44.1</i>
<b>Total free fatty acids</b>		<b>20789.8 ± 257.3</b>

#### 4.2.2 Fatty alcohol in *L.vannamei* waste by-product.

The identification of fatty alcohol trimethylsilyl ether previously been discussed from rice straw extracts in Chapter 2. The EI mass spectra of the only fatty alcohol detected in pacific white shrimp waste is illustrated in **Figure 4-8**.

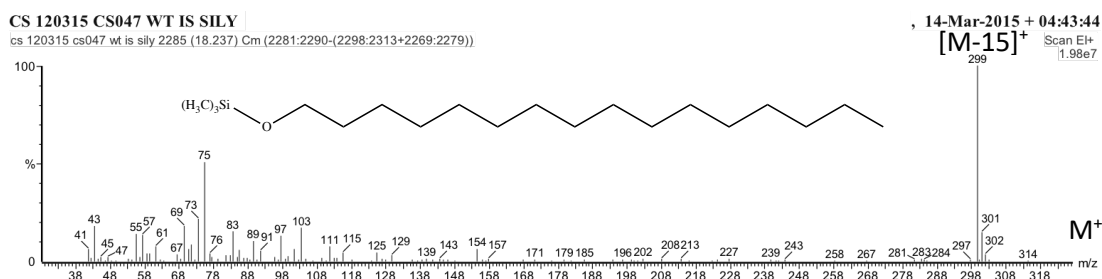


**Figure 4-8** Mass spectra of 1-hexacosanol trimethylsilyl ether (C16 fatty alcohol) from *L. vannamei* by-product

To the best of author's knowledge, this is the first time that the presence of fatty alcohol was reported in this prawn species, although, 1-hexadecanol is present in very low quantity with  $35.7 \pm 2.0 \mu\text{g/g}$  dry biomass (See **Table 4-2**).

**Table 4-2** Abundance (in  $\mu\text{g/g}$  dry biomass) of 1-hexacosanol in *L. vannamei* by-product from hexane extract in 2 hours.

Fatty alcohol	Abundance in <i>L. vannamei</i> ( $\mu\text{g/g}$ dry biomass)	
1-hexacosanol	35.7	$\pm 2.0$

#### 4.2.3 Monoglycerides

Mono- and diglycerides play an important role in the metabolism of plant and animals. They are also widely used in different sectors of industry for example as emulsifiers to oils and fats, as

aroma stabilizers in cosmetics and as antistatic agents for thermoplastic polymers.<sup>221</sup> Isomeric saturated monoglyceride trimethylsilyl ethers, 1- and 2-monopalmitin TMS spectra are sufficiently different and allow identification of these compounds. Even though the molecular ions are usually absent or present in very low intensities, the ions  $[M-15]^+$  are observed in both spectra, which can be used to assign the molecular weight of compounds. The ions  $[RCO]^+$  and  $[RCO+74]^+$  are also commonly formed.<sup>217,221</sup> The latter is due to the rearrangement between acyl chain and trimethylsilyl ether group.

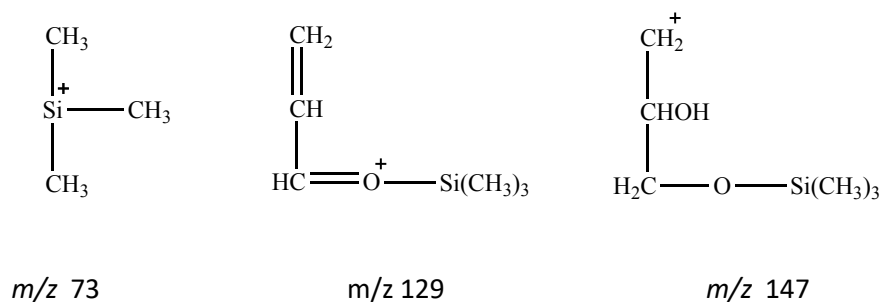


**Figure 4-9** Characteristic fragments of monoglycerides trimethylsilyl ethers.

In 1-monoglycerides, except 1-monosterin, the base peak corresponds to the fragments caused by the loss of methylene trimethylsilyl ether radicals,  $-\text{CH}_2\text{OSi}(\text{CH}_3)_3$ , from the molecular ions.<sup>217,221</sup>

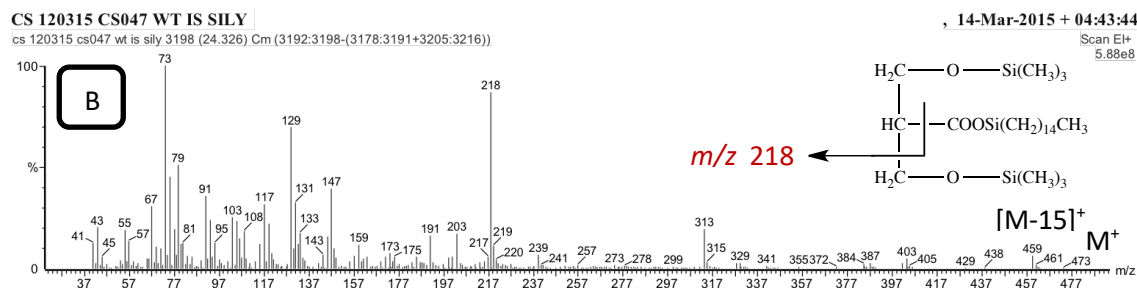
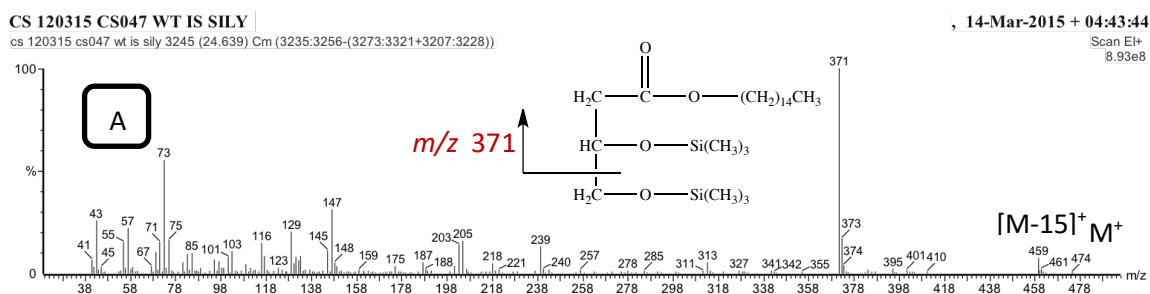


**Figure 4-10** EI mass spectra of A) Hexadecanoic acid, 2,3 bis-(OTMS) propyl ester (α-glyceryl palmitate) B) Hexadecanoic acid, 1,3 bis-(OTMS) propyl ester (β-glyceryl palmitate)

Therefore, the ions  $m/z$  371 was observed in the spectra of 1-monopalmitin. In the spectra of TMS derivatives of 2-monoglycerides, the base peak is the ion at  $m/z$  73 which is the trimethylsilyl radical, however, it is also seen in relatively high intensity in the spectra of 1-monoglycerides derivatives (**Figure 4.10**). The ion at  $m/z$  218 due to the loss of acyloxy group is more prominent in the spectra of 2-monoglycerides.<sup>72</sup>

The ion  $[RCO]^+$  is important to identify the structure of fatty acid, for instance the ions at  $m/z = 239$  are observed in the spectra of 1- and 2-monopalmitin TMS ethers.

Monoglycerides were found about 1.3% in total crude lipid extracted by hexane. This family lipid compound has not been profiled and quantified in *L. vannamei* by-product. However, Takeungwongtrakul *et al.* measured the content of monoglyceride, 0.84% in total lipid content in cephalothorax of *L. vannamei*, which was quite in agreement with the results of the current study.<sup>222</sup> The most dominant monoglyceride in *L.vannamei* by-product was  $\alpha$ -glyceryl palmitate, palmitic acid at C1 of the glycerol skeleton, with 61.8% of the composition. The second and third most abundant belonged to  $\alpha$ -glyceryl oleate, oleic acid at C1 of the glycerol skeleton, and  $\beta$ -glyceryl oleate, oleic acid at C2 of the glycerol skeleton, with the concentration of 18.4% and 5.9% of the composition, respectively (**Figure 4-11**).

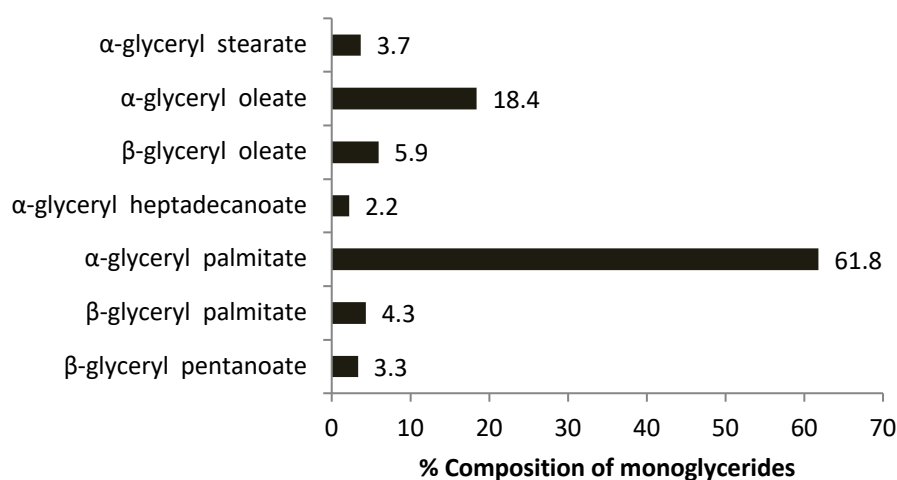


**Figure 4-11** Percentage of composition of monoglycerides in *L. vannamei* from Soxhlet extraction with hexane.

The total quantity of monoglycerides detected in this extract was  $807.0 \pm 15.9 \mu\text{g/g}$  dry biomass, while the most abundance  $\alpha$ -glyceryl palmitate was found with the concentration of  $500.3 \pm 7.9 \mu\text{g/g}$  dry biomass, followed by  $\alpha$ -glyceryl oleate with the concentration of  $149.0 \pm 1.5 \mu\text{g/g}$ . The list of monoglycerides identified is presented in **Table 4-3**.

**Table 4-3** Abundance (in  $\mu\text{g/g}$  dry biomass) of monoglycerides in *L. vannamei* waste from hexane extract.

Monoglycerides	Abundance in <i>L. vannamei</i>
$\beta$ -glyceryl pentanoate	$27.0 \pm 0.3$
$\beta$ -glyceryl palmitate	$34.9 \pm 0.5$
$\alpha$ -glyceryl palmitate	$500.3 \pm 7.9$
$\alpha$ -glyceryl heptadecanoate	$17.8 \pm 0.6$
$\beta$ -glyceryl oleate	$48.1 \pm 4.8$
$\alpha$ -glyceryl oleate	$149.0 \pm 1.5$
$\alpha$ -glyceryl stearate	$29.8 \pm 0.3$
<b>Total monoglycerides</b>	<b><math>807.0 \pm 15.9</math></b>

#### 4.2.4 Diglycerides

1,2- and 1,3-diglycerides such as 1,2- and 1,3- dipalmitin, having identical substituent fatty acids, giving virtually identical spectra when they are introduced directly into the mass spectrometer without prior derivatization to their trimethylsilyl derivatives.<sup>223</sup> The mass spectra of trimethylsilyl ether of 1,2- and 1,3-dipalmitin are also distinguished, although most of the fragments are due to the same ions (**Figure 4-12**).

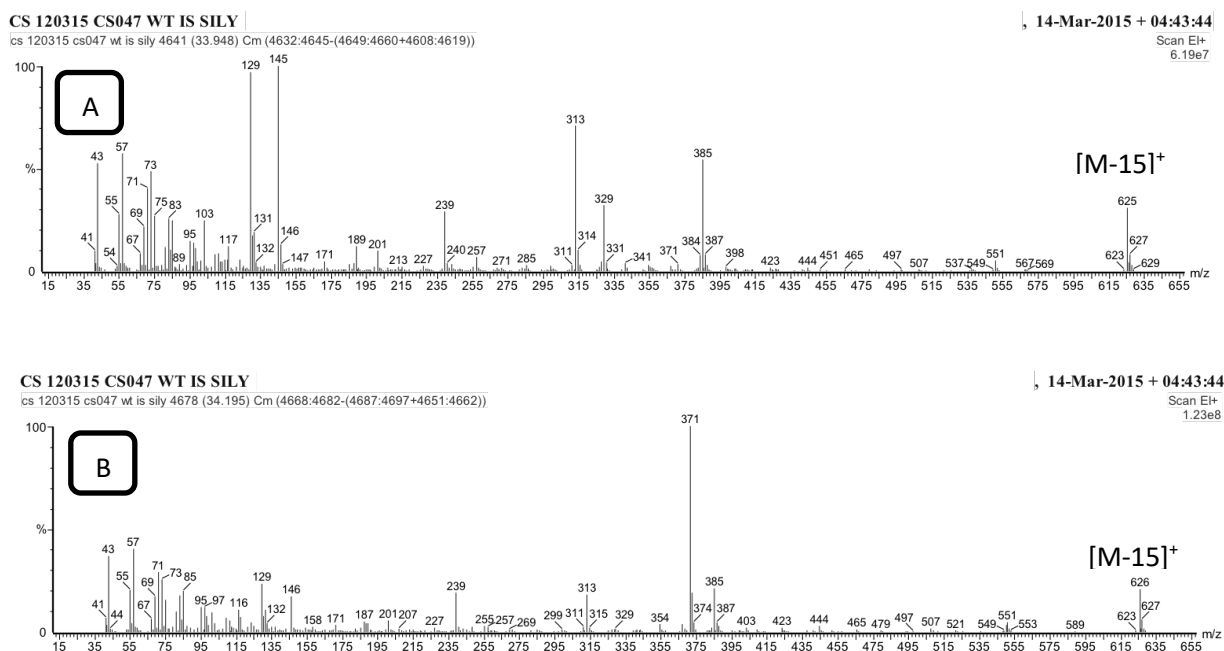


**Figure 4-12** EI mass spectra of trimethylsilyl ethers of A) 1,2 Dipalmitin and B) 1,3 Dipalmitin

The molecular ions are not seen, but the molecular weight can be determined by the ion at [M-15]<sup>+</sup>, this ion is formed by elimination of a methyl radical from the trimethylsilyl group.<sup>217</sup> The characteristic ions of 1,2- and 1,3- dipalmitin OTMS are the peaks of intensities at  $m/z$  313 and 371 respectively (**Figure 4-13**).<sup>224</sup> The ion at  $m/z$  313, [RCO+74]<sup>+</sup>, is formed by a rearrangement between the acyl and trimethylsilyl group. The other high intensity peak at  $m/z$  385 which is likely to a characteristic peak for 1,2-dipalmitin results of the loss of acyloxy group, RCOO-, from the molecular ion. The following structures are suggested:

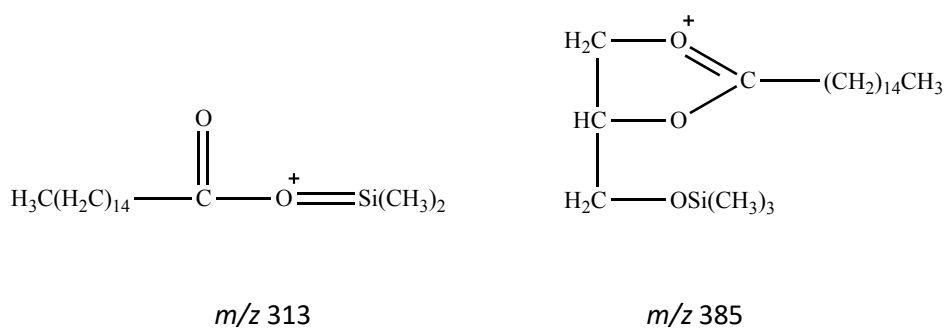


**Figure 4-13** EI mass spectra potential fragments from trimethylsilyl ethers of 1,2 Dipalmitin and 1,3 Dipalmitin

The ion at *m/z* 371,  $[\text{M}-\text{RCOOCH}_2]^+$ , the base peak for trimethylsilyl ether of 1,3-dipalmitin, is formed by cleavage between C1 and C2 or C2 and C3 of the glycerol moiety. The structure is presented below (**Figure 4-14**).

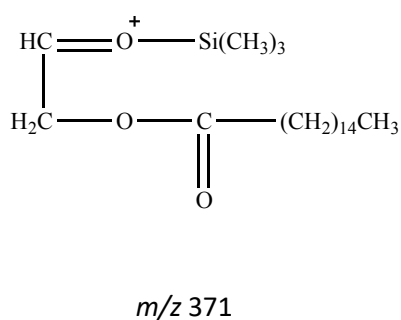


**Figure 4-14** EI mass spectra potential fragment of *m/z* 371 from trimethylsilyl ethers of 1,2 Dipalmitin and 1,3 Dipalmitin

The ions at *m/z* 129 and 145 are common in both isomers but higher intensities are clearly observed in 1,2-diglycerides OTMS. These two ions are formed by arrangement between glycerol skeleton and trimethylsilyl groups with the structures as follows (**Figure 4-15**).



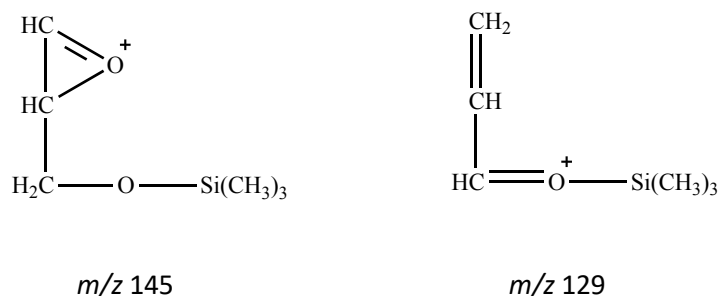


**Figure 4-15** EI mass spectra potential fragments of  $m/z$  145 and 129 from trimethylsilyl ethers of 1,2 Dipalmitin and 1,3 Dipalmitin

**Table 4-4** Abundance (in  $\mu\text{g/g}$  dry biomass) of diglycerides in *L. vannamei* by-product.

Diglycerides	Abundance in <i>L. vannamei</i> ( $\mu\text{g/g}$ dry biomass)
Glycerol 1,2-dipalmitate	$27.3 \pm 0.0$
Glycerol 1,3-dipalmitate	$52.2 \pm 0.2$
<b>Total diglycerides</b>	<b><math>79.5 \pm 0.2</math></b>

Takeungwongtrakul *et al.* stated that *Litopenaeus vannamei* by-product contained about 5% of diglycerides in total lipid content, however, in the current study, only 0.1% of diglycerides were detectable including 1,2-and 1,3-dipalmitin. Potentially more diglycerides and triglycerides could be identified from this biomass at higher temperature in the GC-MS and GC-FID or by conversion into more volatile fatty acid methyl esters. Such activities could be addressed in future work. In term of abundance in dry biomass, the total diglycerides identified is  $79.5 \pm 0.2$   $\mu\text{g/g}$  of dry biomass with the concentration of 27.3 and  $52.2 \pm 0.2$   $\mu\text{g/g}$  dry biomass for 1,2-dipalmitate and 1,3-dipalmitate respectively.

#### 4.2.5 1-O-Alkylglycerol ether lipids

Glycerol ethers including those of chimyl and batyl alcohols, are potentially beneficial in industrial sector as they have bacteriostatic and fungistatic properties, anti-inflammatory activities and hemopoietic effects <sup>225</sup> (**Figure 4-16**). Previous studies showed that they are also able to protect against radiation damage and to exhibit antitumor properties. <sup>225</sup>

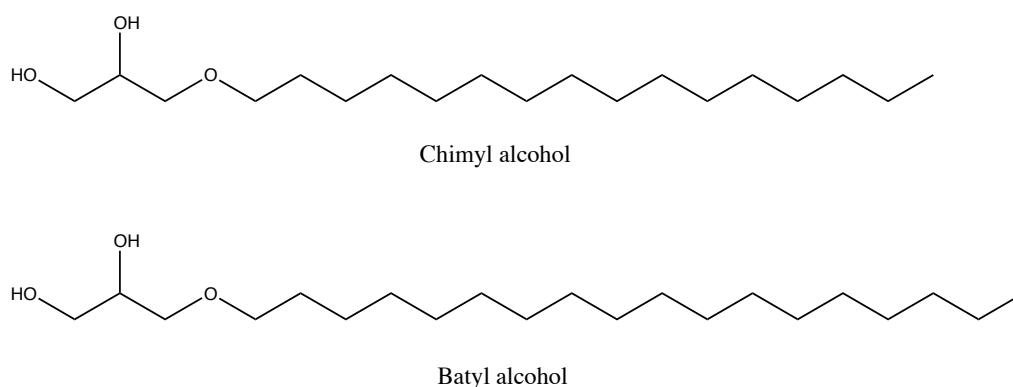


**Figure 4-16** Structure of Chimyl alcohol (1-O-Hexadecylglycerol) and Batyl alcohol (1-O-Octadecylglycerol)

1-O-hexadecyl-2,3-di-O-trimethylsilyl glycerol and 1-O-octadecyl-2,3-di-O-trimethylsilyl glycerol have been found in small quantities in the silylated sample of crude lipids obtained from *L. vannamei* by-product by hexane Soxhlet extraction (**Figure 4-17**).

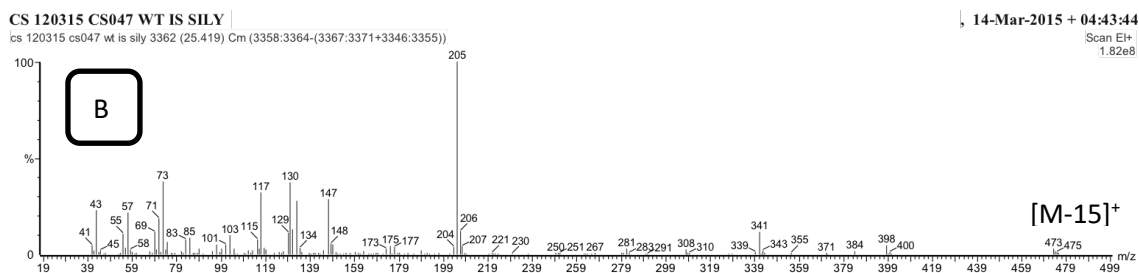
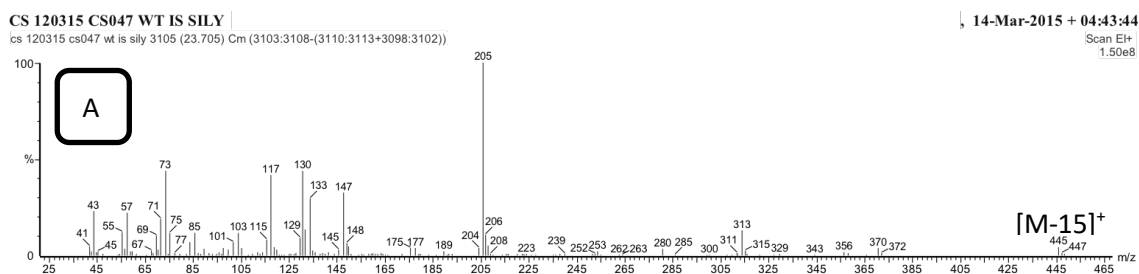


**Figure 4-17** EI mass spectra of A) 1-O-hexadecyl-2,3-di-O-TMS-glycerol B) 1-O-octadecyl-2,3-di-O-TMS glycerol

The base peak of this family compounds are ions at  $m/z = 205$ , which correspond to trimethylsilyl moiety (**Figure 4-18**). Additionally, ions at  $m/z = [M-90]^+$ ,  $[M-104]^+$ ,  $[M-147]^+$ ,  $[M-180]^+$  are important to determine the number of carbon in alkyl chain.

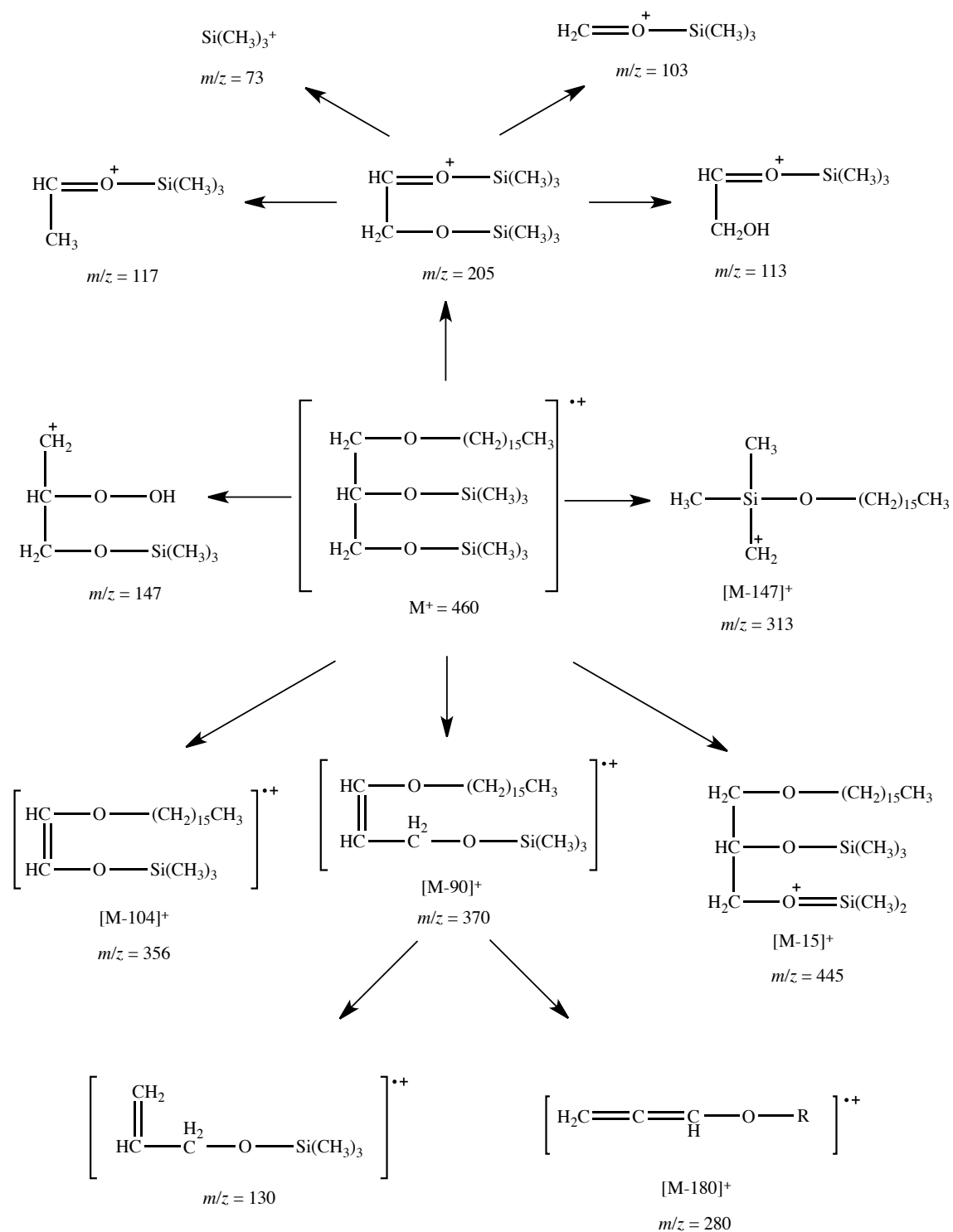


**Figure 4-18** Scheme of fragmentation of 1-O-hexadecyl-2,3-di-O-TMS-glycerol 1-O-hexadecylglycerol (chimyl alcohol)

There are also some others peaks due to the TMS radicals, which appear in all cases in relatively high intensity such as ions at  $m/z = 73, 103, 117, 130, 133$  and  $147$ . The molecular ion is usually absent, however, the ion  $[M-15]^+$  is always present in the higher-mass area. In lower mass range, the alkyl ions with  $m/z = 43, 57, 71$  and  $85$  for saturated compounds are clearly seen in significant proportions (**Figure 4-17**).

**Table 4-5** Abundance (in  $\mu\text{g/g}$  dry biomass) of ethers of glycerol in *L. vannamei* by-product

1- <i>O</i> -alkylglycerols	Abundance in <i>L. vannamei</i> ( $\mu\text{g/g}$ dry biomass)
1- <i>O</i> -heaxadecylglycerol (Chimyl alcohol)	$23.5 \pm 0.4$
1- <i>O</i> -octadecylglycerol (Batyl alcohol)	$18.0 \pm 0.0$
<b>Total 1-<i>O</i>-alkylglycerols</b>	<b><math>41.5 \pm 0.4</math></b>

The presence of 1-*O*-alkylglycerols has not been reported for *L. vannamei* by-product in previous studies; however, these two compounds were detected in this current experiment. Despite being detected in low concentration (0.03% in total lipid content), these molecules are still of interest to the industry. The total abundance of 1-*O*-alkylglycerols is  $41.5 \pm 0.4 \mu\text{g/g}$  of dry biomass corresponding to  $23.5 \pm 0.4$  and  $18 \mu\text{g/g}$  of dry biomass for chimyl and batyl alcohol respectively (**Table 4-5**).

## 4.2.6 Sterols

Cholesterol, stigmasterol, campesterol and  $\beta$ -sitosterol were found in this study. These  $\Delta^5$ -sterols are found in plants and also crustaceans consumed in the United States such as shrimp, blue crab and lobster.<sup>208</sup> According to Mika *et al.*, these chemicals were also found in brown shrimp *Crangon crangon* from Baltic sea.<sup>139,226</sup>

The mass spectra recorded for the trimethylsilyl ether of cholesterol is shown in **Figure 4-19**.

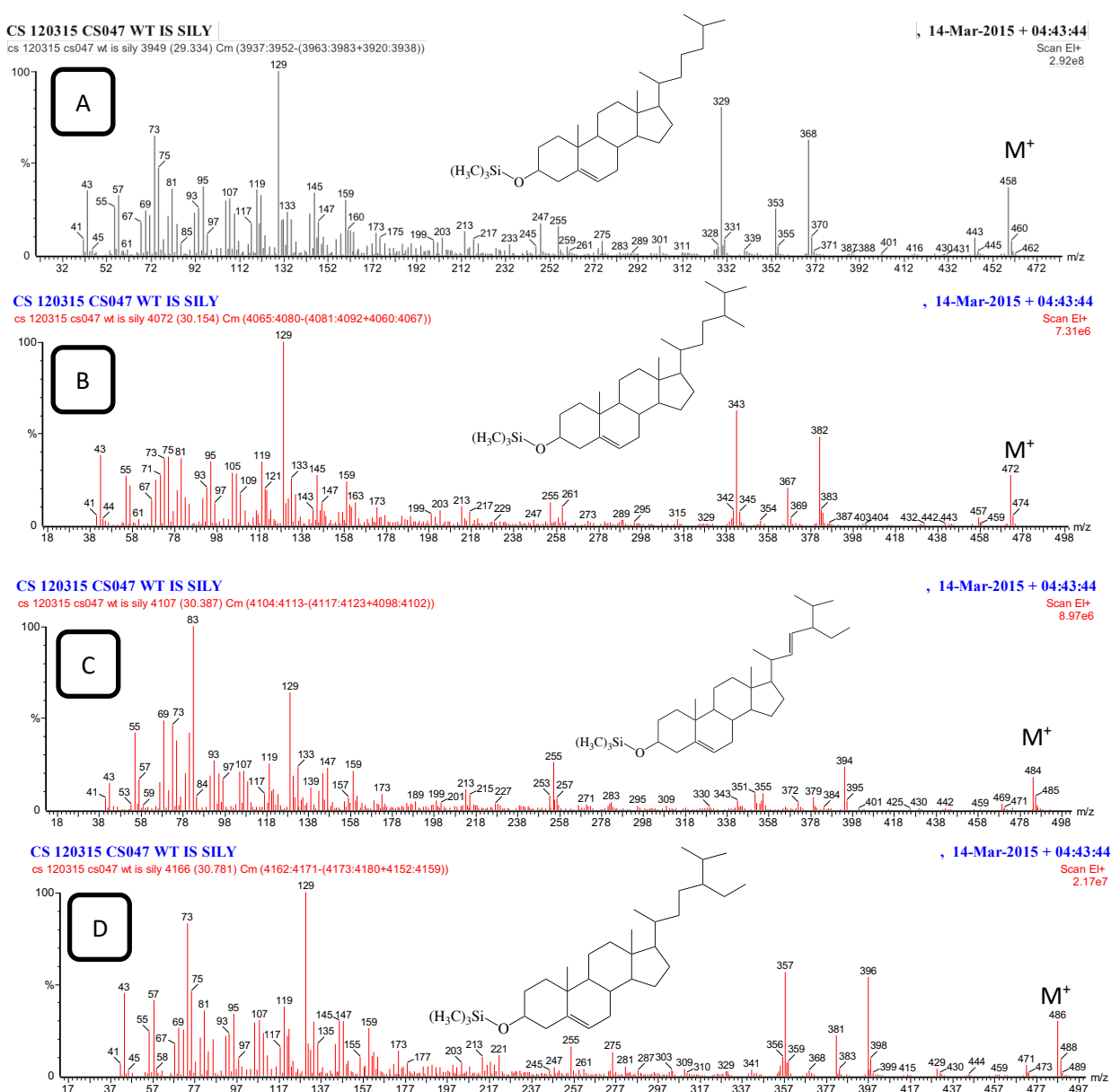


**Figure 4-19** EI mass spectra of A) Cholesteryl trimethylsilyl ether B) Campesteryl trimethylsilyl ether C) Stigmasteryl trimethylsilyl ether D)  $\beta$ -sitosteryl trimethylsilyl ether

A characteristic peak are found at  $m/z$  458  $[M]^+$ , 368  $[M-90]^+$  corresponding to the loss of trimethylsilanol,  $[(CH_3)_3SiOH]$ , 353  $[M-(90+15)]^+$ , 329  $[M-129]^+$ , 255  $[M-(90, \text{side chain } C17 + 90)]$  and 129 (**Table 4-6** and **Figure 4-20**). The latter ion is the base peak in cholesterol and all other spectra obtained from 3-trimethylsilyl ethers of  $\Delta^5$ -sterols including campesterol, stigmasterol and  $\beta$ -sitosterol.<sup>43,72</sup> The detail mechanisms of important fragmentations were previously present in Chapter 2.

**Table 4-6** Characteristic fragmentations of  $\Delta^5$ -sterols

Sterol	Mw	Mw + TMS	Characteristic fragments			
			$[M-90]^+$	$[M-$	$[M-129]^+$	$[M-$
Cholesterol	386	458	368	353	329	255
Campesterol	400	472	382	367	343	255
Stigmasterol	412	484	394	379	355	255
$\beta$ -sitosterol	414	486	396	381	357	255

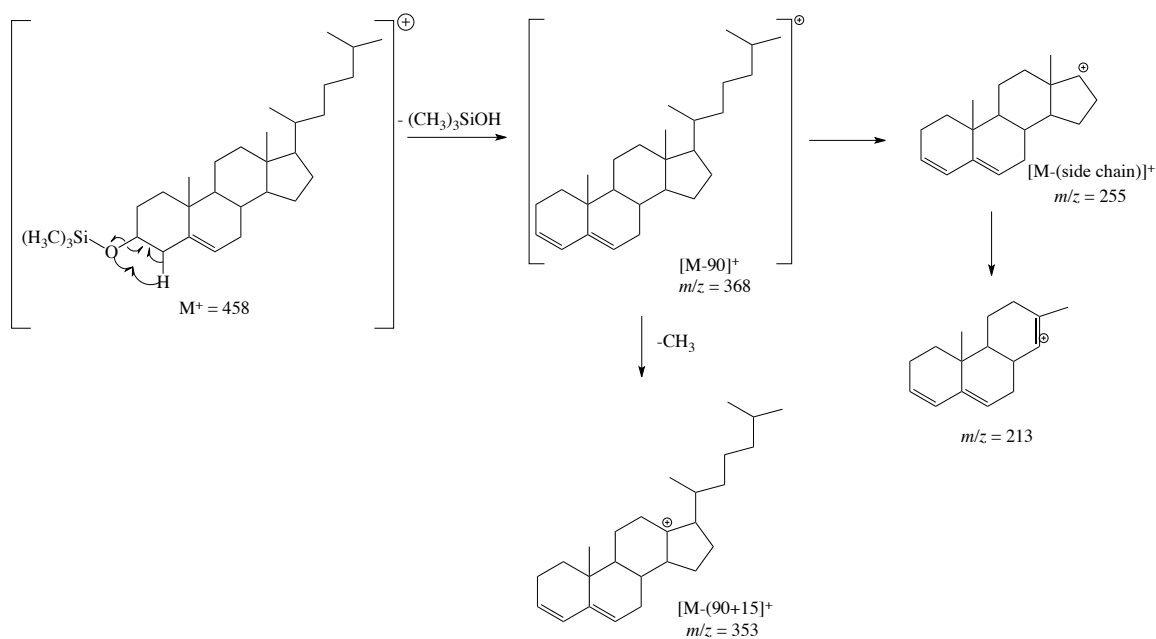


**Figure 4-20** Fragmentation scheme of Cholesteryl trimethylsilyl ether.

Sterol profile has not been reported in previous studies.<sup>43</sup> In this study, cholesterol, campesterol, stigmasterol and  $\beta$ -sitosterol were detected; these compounds present 1.3% of the total lipid content. The most abundant is cholesterol with the concentration of  $1538.0 \pm 11.6$   $\mu\text{g/g}$  of dry biomass followed by campesterol, stigmasterol and  $\beta$ -sitosterol  $75.8 \pm 3.0$ ,  $42.9 \pm 2.1$  and  $39.5 \pm 1.3$   $\mu\text{g/g}$  of dry biomass respectively (**Table 4-7**).

**Table 4-7** Abundance (in  $\mu\text{g/g}$  dry biomass) of ethers of sterols in *L. vannamei*.

Sterols	Abundance in <i>L. vannamei</i>
Cholesterol	$1538.0 \pm 11.6$
Campesterol	$75.8 \pm 3.0$
Stigmasterol	$42.9 \pm 2.1$
$\beta$ -sitosterol	$39.5 \pm 1.3$
<b>Total sterols</b>	<b><math>1696.2 \pm 18.0</math></b>

### 4.3 Supercritical extraction of lipid from Pacific white shrimp by-product

A 2 x 2 factorial design was also used for the optimization of supercritical extraction of prawn waste as in that of rice straw (**Figure 4-21**). Temperature and pressure were two variables adopted, the temperature range was selected to be between 40-60 °C and the selected pressure range was between 75-400 bar.

The compositions of the extracts were analysed by gas chromatography and gas chromatography coupled with EI mass spectrometry, without further purification.



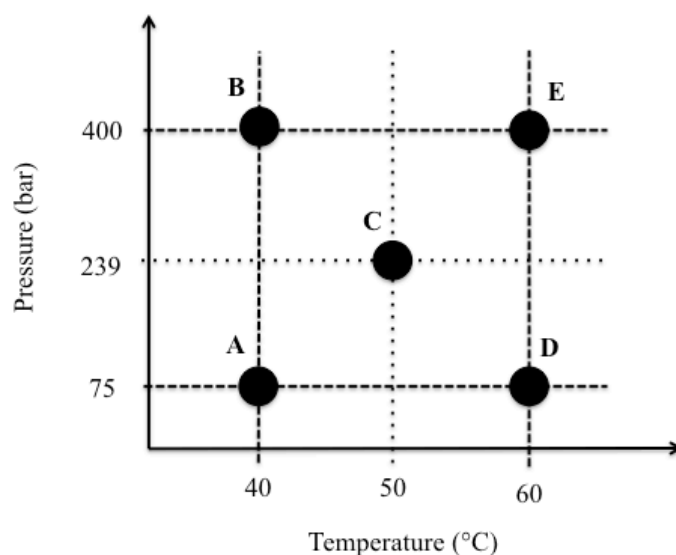


**Figure 4-21** Experimental design for optimization of supercritical CO<sub>2</sub> extraction

The percentage of crude yields of different conditions varies as temperature and pressure changed, which resulted the difference in density of carbon dioxide during extraction. The experiment B afforded the highest yield of 1.14% of dry biomass. The second and third best conditions in term of percentage of crude lipid were Experiment E and C with 0.49% and 0.38% of dry biomass respectively (**Table 4-8** and **Figure 4-22**). The pressure played more important role as the yield increased when the pressure increased at a constant temperature.

**Table 4-8** Experimental conditions, densities and yields for extractions of *L. vannamei* by-product

Experiment	Extraction conditions	Density of CO <sub>2</sub> (g/cm <sup>3</sup> )	Yield (dry biomass)
A	40°C, 75 bar and 2 hours	0.23	0.25
B	40°C, 400 bar and 2 hours	0.96	1.14
C	50°C, 237.5 bar and 2 hours	0.82	0.38
D	60°C, 75 bar and 2 hours	0.17	0.34
E	60°C, 400 bar and 2 hours	0.89	0.49

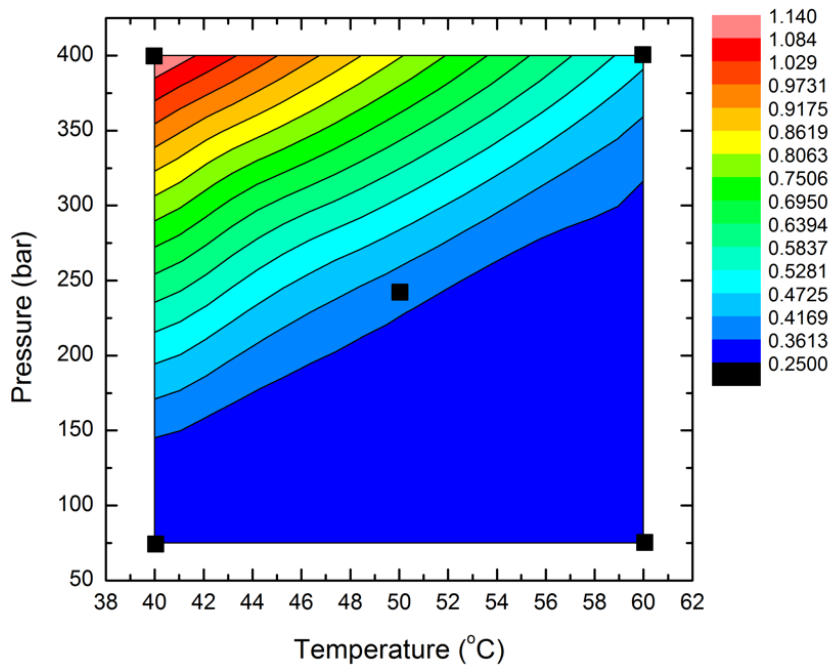


**Figure 4-22** Percentage crude yields of Pacific white shrimp lipid from scCO<sub>2</sub> extraction

**Figure 4-23** demonstrates a relationship between density of CO<sub>2</sub> and percentage of crude yield obtained. The highest yield obtained (1.14%) corresponded to the highest density of CO<sub>2</sub>, 0.96 g/cm<sup>3</sup> (**Figure 4-23B**). The experiment A and D, the two smallest yields obtained corresponded to low density of CO<sub>2</sub>. Therefore, it can be concluded that the density of the CO<sub>2</sub> in the most important factor for the scCO<sub>2</sub> extraction of the pacific white shrimp waste.

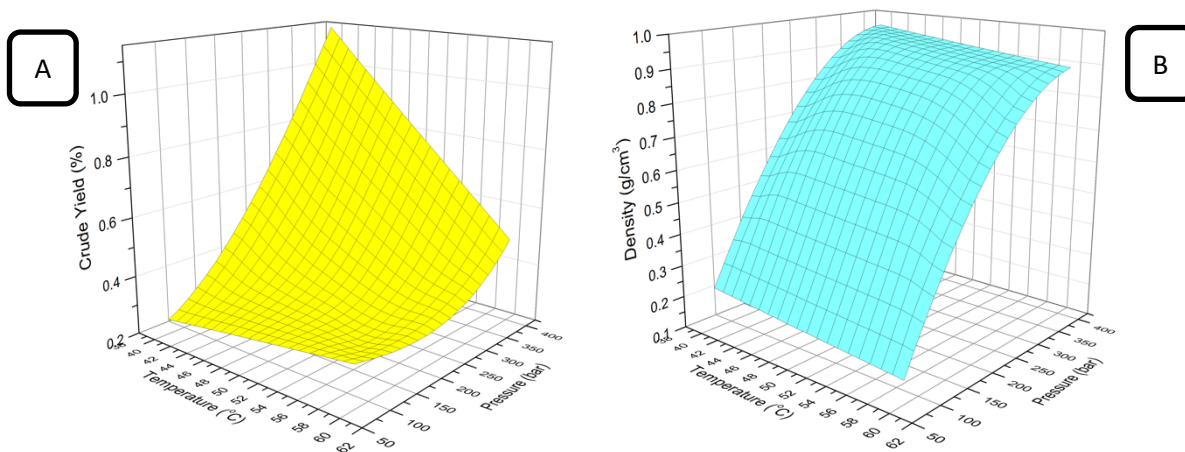


**Figure 4-23** A) A depiction of yield of lipid extractives as a function of temperature and pressure. B) A depiction of density of carbon dioxide as a function of temperature and pressure

## 1.1 Composition of extracted lipids

The quantification of the components in the lipid extracts allowed the direct comparison between the extracts of experiments A-E. Identification has been carried on the same way as for rice straw extraction in Chapter 2. The identified groups of compounds were free fatty acids, monoglycerides, diglycerides, fatty alcohol, ethers of glycerol and sterols. **Figure 4-24** shows the composition of each main group of compounds in crude yield. Free fatty acids were the most abundant in all experiments.

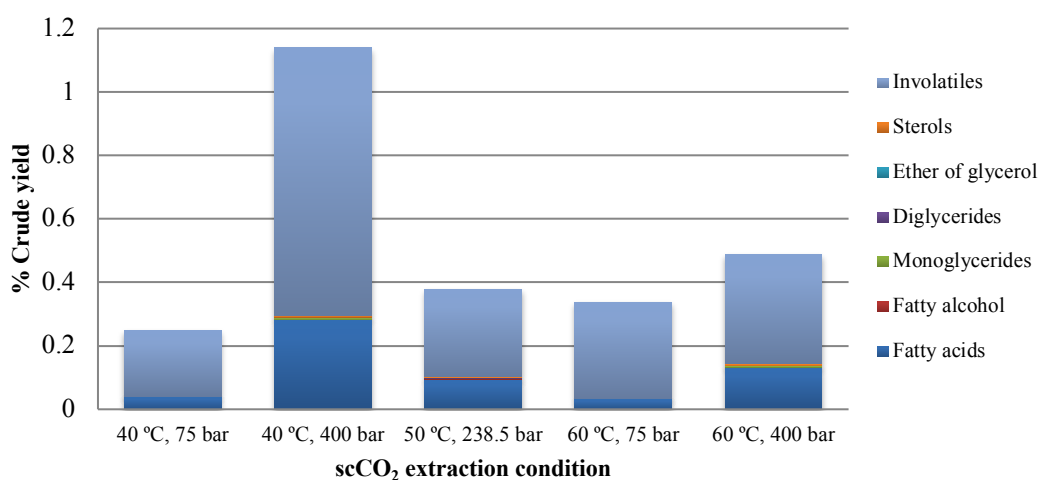


**Figure 4-24** Breakdown of main groups on Pacific white shrimp by-product extract from scCO<sub>2</sub> extraction

The experiment B (at 40°C, 400 bar) resulted the highest composition of free fatty acids, however, it displayed that the highest proportion of non-volatiles, which could not be analysed by the same method in the GC-FID and GC-MS (**Figure 4-25**). Further work would be needed to analyse such fractions by HPLC or HPLC-MS.

The results obtained in this study were different to that of Corra *et al.* on the scCO<sub>2</sub> extraction of cephalothorax of *Litopenaeus vannamei*. The highest yield obtained in this publication was 1.7% of dry weight at 50°C, 150 bar in 30 minutes and the second best condition was at 40°C,

200 bar with the lipid yield of 1.52% dry weight in 30 minutes. However, the free fatty acid profile including PUFAs was not reported, only fatty acid methyl ester profile was described.<sup>227</sup>

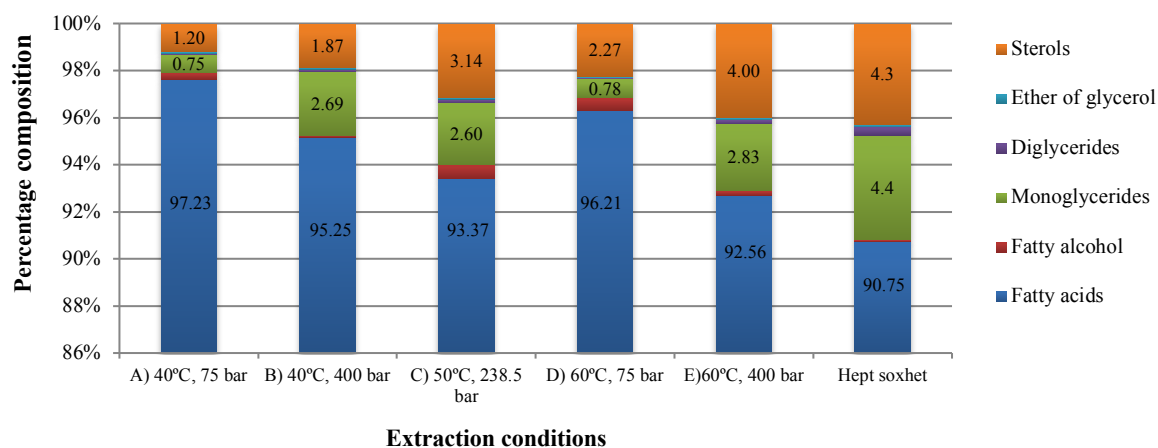


**Figure 4-25** Percentage composition of lipids compounds for *L. vannamei* as extracted in five different conditions by supercritical carbon dioxide for 2 hours and hexane Soxhlet extraction for 2 hours

Free fatty acids are the most interesting among all other compounds identified, as they were not only the majority compound in total lipid content but they are also consisted of PUFAs, which have high value. Hexane Soxhlet previously showed the presence of some polyunsaturated fatty acids such as linoleic acid, C18:2<sub>n-6</sub>, arachidonic acid (ARA), C20:4<sub>n-6</sub>, eicosapentaenoic acid (EPA), C20:5<sub>n-3</sub> and docosahexaenoic acid (DHA), C22:6<sub>n-3</sub>. In Figure 5-21, although the total yield extracted at 40°C, 400 bar, Experiment B, was greater than the similar extraction conducted at 75 bar (Experiment A). The abundance of free fatty acids was actually greater at low pressure condition, also with the presence of less higher molecular weight compounds such as monoglycerides, diglycerides and sterols. On the other hand, at high pressure and temperature (Experiment E), the composition changed, the high molecular weight molecules were obtained and the yield of fatty acid in crude lipid decreased. At high pressure and temperature, it is possible to obtain higher molecular weight extract and compounds with greater polarity.<sup>228</sup> The result obtained was also in agreement of that of Turgut *et al.*, by analyzing the concentration of FFA in crude oil, it was observed that the FFA content of the extract increased with decreasing pressure. Higher concentration of FFA of the extract obtained at low temperature due to the lower molecular weight of FFA compared to the others such as glycerides and sterols. As pressure increased, the solubility of larger molecules especially triglycerides increased.<sup>72</sup> The

results demonstrate that scCO<sub>2</sub> extraction is better than solvent extraction in term of selectivity towards free fatty acid. Although, heptane Soxhlet extraction afforded greater crude oil yield, high amount of co-extracts, which could potentially include molecules such as amino acids and polycyclic compounds.

#### **4.4 Comparison of supercritical carbon dioxide extracts and hexane Soxhlet of *Litopenaeus vannamei* by-product**

To be able to effectively evaluate the supercritical extraction technique, the lipid extracts resulted from the Experiment A-E were directly compared to that of hexane Soxhlet extraction. In all the cases, the waste biomass was obtained in January 2015, and was processed identically prior to the extraction. The summary of the abundance (in µg/g dry biomass) of fatty acids, fatty alcohol, monoglycerides, diglycerides, ether of glycerol and sterols is presented in **Table 4-9**.

**Table 4-9** Typical abundances (in  $\mu\text{g/g}$  dry biomass) of lipid as extracted by hexane Soxhlet in 2 hours and supercritical carbon dioxide in 2 hours of *L.vannamei* by-product

Compound names	Hexane	scCO <sub>2</sub> extraction conditions				
		40°C, 75 bar	40°C, 400 bar	50°C, 238 bar	60°C, 75 bar	60°C, 400 bar
<b>Free fatty acids</b>						
C12:0	62.8 ± 4.0	1.1±0.1	3.6±0.2	0.8±0.1	1.6±0.1	0.8±0.1
C14:0	326.4 ± 1.1	8.2±0.2	2.6±0.1	12.7±0.4	6.1±0.4	14.1±0.2
C15:0	183.0 ± 0.5	3.5±0.2	13.4±1.2	1.7±2.3	2.9±2.3	0.9±0.2
C16:0	856.9 ± 8.6	98.4±2.1	395.7±0.8	167.5±6.1	73.6±6.1	201.8±2.1
C16:1 (n-7)	4905.8 ± 10.3	23.4±0.9	90.4±0.4	38.8±2.5	14.3±2.5	53.9±0.9
C17:0	146.3 ± 0.3	1.8±1.0	17.0±2.4	6.5±0.8	2.0±0.8	7.3±1.0
C17:1 (n-7)	221.1 ± 0.8	3.1±0.2	16.1±1.4	7.3±0.3	2.4±0.3	9.2±0.2
C18:0	3537.7 ± 18.0	20.8±1.0	123.6±1.8	50.8±0.5	17.4±0.5	61.7±1.0
C18:1 (n-7)	5155.2 ± 100.3	20.1±1.1	114.9±3.7	38.2±0.4	15.3±0.4	46.8±1.1
C18:1 (n-9)	1014.1 ± 16.6	144.7±14.5	800.5±25.4	234.4±4.9	103.1±4.9	276.5±14.5
C18:2 (n-6)	1805.1 ± 6.1	62.4±31.8	763.7±16.4	300.2±12.4	78.0±12.4	491.7±31.8
C20:0	118.2 ± 0.8	0.8±0.2	12.1±0.2	6.1±0.4	1.1±0.4	7.1±0.2
C20:1(n-9)	124.3 ± 5.1	2.3±1.2	53.1±2.0	19.8±0.9	5.1±0.9	27.4±1.2
C20:2 (n-6)	996.5 ± 9.9	0.7±0.9	71.7±3.7	24.7±1.1	5.9±1.1	37.7±3.9
C20:4 (n-6) (ARA)	420.3 ± 25.1	7.6±1.0	29.7±1.5	8.0±0.3	1.8±0.3	23.5±1.0
C20:5 (n-3)(EPA)	364.2 ± 38.4	7.6±1.9	84.8±10.5	12.2±1.0	2.7±1.0	10.9±1.9
C22:6 (n-3)(DHA)	489.0 ± 10.4	1.5±0.3	195.3±114.8	21.6±1.0	1.7±1.0	50.9±7.3
C24:0	41.5 ± 0.1	0.3±0.2	5.2±1.1	0.8±0.2	1.3±0.2	0.9±0.2
C24:1 (n-9)	21.3 ± 1.0	0.2±0.1	2.5±0.2	0.3±0.1	0.4±0.1	0.4±0.1
<i>Total SFAs</i>	<i>7889.7 ± 62.2</i>	<i>134.9±5.0</i>	<i>596.6±7.8</i>	<i>247.0±10.8</i>	<i>106.0±10.8</i>	<i>294.6±5.0</i>
<i>Total MUFAs</i>	<i>7634.4 ± 150.9</i>	<i>193.8±18.0</i>	<i>1077.6±33.1</i>	<i>338.6±9.1</i>	<i>140.7±9.1</i>	<i>414.3±18.0</i>
<i>Total PUFAs</i>	<i>5265.7 ± 44.1</i>	<i>79.7±35.8</i>	<i>1145.2±46.9</i>	<i>366.8±15.8</i>	<i>90.1±15.8</i>	<i>613.7±45.9</i>
<b>Total Free fatty acids</b>	<b>20789.8 ± 257.3</b>	<b>408.3 ± 58.8</b>	<b>2819.4 ± 87.8</b>	<b>952.4 ± 35.6</b>	<b>336.7 ± 35.6</b>	<b>1323.6 ± 68.8</b>
<b>Free fatty alcohol</b>						
1-hexadecanol	35.7 ± 2.0	1.3 ± 0.1	2.5 ± 0.7	1.2 ± 1.5	1.9 ± 0.5	2.9 ± 0.1
<b>Total free fatty alcohol</b>	<b>35.7 ± 2.0</b>	<b>1.3±0.1</b>	<b>2.5±0.7</b>	<b>1.2±1.5</b>	<b>1.9±0.5</b>	<b>2.9±0.1</b>
<b>Monoglycerides</b>						
β-glycerol pentadecanoate	27.0 ± 0.3	0.5±0.0	0.7±0.2	0.5 ± 0.1	0.2±0.1	0.9

$\beta$ -glyceryl palmitate	34.9 $\pm$ 0.5	1.2 $\pm$ 0.3	38.1 $\pm$ 6.6	8.9 $\pm$ 1.4	0.9 $\pm$ 0.2	8.9 $\pm$ 0.7
$\alpha$ -glyceryl palmitate	500.3 $\pm$ 7.9	0.9 $\pm$ 0.3	13.6 $\pm$ 1.8	8.1 $\pm$ 0.4	0.5 $\pm$ 0.1	22.5 $\pm$ 0.3
$\alpha$ -glyceryl heptadecanoate	17.8 $\pm$ 0.6	0.3 $\pm$ 0.1	2.6 $\pm$ 0.8	1.0 $\pm$ 0.0	0.2 $\pm$ 0.0	1.4 $\pm$ 0.1
$\alpha$ -glyceryl stearate	48.1 $\pm$ 4.8	Trace	0.4 $\pm$ 0.2	0.3 $\pm$ 0.1	0.2 $\pm$ 0.1	0.6
$\beta$ -glyceryl oleate	149.0 $\pm$ 1.5	0.1 $\pm$ 0.0	18.3 $\pm$ 0.5	5.0 $\pm$ 0.1	0.4 $\pm$ 0.1	5.5 $\pm$ 0.3
$\alpha$ -glyceryl oleate	29.8 $\pm$ 0.3	0.2 $\pm$ 0.2	6.0 $\pm$ 3.1	2.8 $\pm$ 0.2	0.3 $\pm$ 0.2	0.7 $\pm$ 0.2
<b>Total monoglycerides</b>	<b>807.0 <math>\pm</math> 15.9</b>	<b>3.1 <math>\pm</math> 0.9</b>	<b>79.8 <math>\pm</math> 13.2</b>	<b>26.6 <math>\pm</math> 2.3</b>	<b>2.7 <math>\pm</math> 0.8</b>	<b>40.5 <math>\pm</math> 1.6</b>
<b>Diglycerides</b>						
Glycerol 1,2-dipalmitate	27.3 $\pm$ 0.0	0.1 $\pm$ 0.1	2.7 $\pm$ 0.0	1.3 $\pm$ 0.2	0.1 $\pm$ 0.1	1.7 $\pm$ 0.1
Glycerol 1,3-dipalmitate	52.2 $\pm$ 0.2	0.1 $\pm$ 0.0	0.6 $\pm$ 0.0	0.4 $\pm$ 0.0	0.1 $\pm$ 0.0	0.9 $\pm$ 0.0
<b>Total diglycerides</b>	<b>79.5 <math>\pm</math> 0.2</b>	<b>0.2<math>\pm</math>0.1</b>	<b>3.3<math>\pm</math>0.0</b>	<b>1.7<math>\pm</math>0.2</b>	<b>0.2<math>\pm</math>0.1</b>	<b>2.6<math>\pm</math>0.1</b>
<b>Ethers of glycerol</b>						
1-O-hexadecylglycerol	23.5 $\pm$ 0.4	0.1 $\pm$ 0.1	0.8 $\pm$ 0.4	0.4 $\pm$ 0.1	0.1 $\pm$ 0.1	0.5 $\pm$ 0.1
1-O-octadecylglycerol	18.0 $\pm$ 0.0	0.2 $\pm$ 0.0	1.3 $\pm$ 0.2	0.3 $\pm$ 0.1	0.1 $\pm$ 0.1	0.5 $\pm$ 0.0
<b>Total ethers of glycerol</b>	<b>41.5 <math>\pm</math> 0.4</b>	<b>0.3<math>\pm</math>0.1</b>	<b>2.1<math>\pm</math>0.6</b>	<b>0.7<math>\pm</math>0.2</b>	<b>0.2<math>\pm</math>0.2</b>	<b>1.0<math>\pm</math>0.1</b>
<b>Sterols</b>						
Choleterol	1538.0 $\pm$ 11.6	3.9 $\pm$ 1.6	45.0 $\pm$ 16.3	29.2 $\pm$ 0.3	3.4 $\pm$ 0.3	51.7 $\pm$ 1.6
Campesterol	75.8 $\pm$ 3.0	0.5 $\pm$ 0.1	3.5 $\pm$ 1.3	0.8 $\pm$ 0.2	1.7 $\pm$ 0.2	1.6 $\pm$ 0.1
Stigmasterol	42.9 $\pm$ 2.1	0.4 $\pm$ 0.0	2.4 $\pm$ 0.5	0.7 $\pm$ 0.1	1.8 $\pm$ 0.1	1.3 $\pm$ 0.0
$\beta$ -sitosterol	39.5 $\pm$ 1.3	0.3 $\pm$ 0.3	4.4 $\pm$ 0.0	1.3 $\pm$ 1.2	1.1 $\pm$ 0.6	2.6 $\pm$ 0.6
<b>Total sterols</b>	<b>1696.2 <math>\pm</math> 18.0</b>	<b>5.1<math>\pm</math>2.1</b>	<b>55.3<math>\pm</math>18.1</b>	<b>32.1<math>\pm</math>1.8</b>	<b>7.9<math>\pm</math>1.2</b>	<b>57.1<math>\pm</math>2.3</b>
<b>Total identified</b>	<b>23449.7 <math>\pm</math> 293.8</b>	<b>418.3 <math>\pm</math> 62.1</b>	<b>2962.3<math>\pm</math> 120.4</b>	<b>1014.5 <math>\pm</math> 40.6</b>	<b>349.6 <math>\pm</math> 38.4</b>	<b>1427.7 <math>\pm</math> 73.1</b>

According to the studies of Takeungwongtrakul *et al.*<sup>33</sup> and Senphan *et al.*<sup>64</sup> the major constituent in the extracted lipids from cephalothorax and hepatopancreas of Pacific white shrimp (*L. vannamei*) are phospholipid (PL) and triglycerides (TG).

In cephalothorax, PL was accounted about 82.5% of total lipid content and TG and DG were measured at 8.9% and 5.1% respectively. In hepatopancreas, there were 43.4% and 38% of PL and TG respectively and also contained 8.7% of FFAs. The mixture of cephalothorax and hepatopancreas in raw material are rich in FFA, PL, and TG, however, the latter two (PL and TG) not extracted in this current work due to the non-polar nature of the scCO<sub>2</sub>.

#### **4.4.1 Comparison of fatty acids between hexane extract and scCO<sub>2</sub> extracts from *L. vannamei* by-product.**

The free fatty acid profile of the supercritical extract was found to be dramatically different to that of the Soxhlet. Firstly, a greater abundance of this compound family was found in the hexane Soxhlet extraction over 2 hours, 20789.8 ± 257.3 µg/g of dry biomass compared to 2819.4 ± 87.8 µg/g of dry biomass by supercritical carbon dioxide extraction at 40°C, 400 bar, which is the optimised condition in this study. This is likely due to a number of factors that could influence the efficiency of the supercritical extraction. The fact that the operating temperatures of the two experiments were significantly different 40°C in scCO<sub>2</sub> and 68 °C in hexane Soxhlet, (however the temperature of the extracting solvent in the Soxhlet was approximately 50 °C). The higher temperature of hexane can result in free fatty acid formation from triglycerides, which was not the case in scCO<sub>2</sub>.<sup>33,72,229</sup>

It has been reported that an internal organ called hepatopancreas located in the cephalothorax of *L. vannamei* contains an active enzyme that could play an important role in the amount of free lipids available to extract. Such enzymes can cause hydrolysis of ester bonds in triglycerides, thus leading to an increased yield of free lipids to extract.<sup>230</sup> It has also been demonstrated that scCO<sub>2</sub> can effectively remove water from the active sites of enzymes, thus reducing their activity.<sup>231</sup> Crucial control of the amount of water is therefore essential for maintaining activity of such enzymes. One potential explanation for the dramatic difference in extraction yield between hexane and scCO<sub>2</sub> could be that hydrolysis continues to take place in hexane (a solvent which will not effectively extract the water), but the activity is significantly reduced in the supercritical system, where water can be extracted. Further discussion on the active enzyme in the cephalothorax of *L. vannamei* and the implications on lipid yield will be presented in Chapter 5.



Comparing abundance of FFAs obtained from five scCO<sub>2</sub> extraction conditions, as previously mentioned, the optimal condition resulted the highest FFA concentration was at 40°C, 400 bar, 2819.4 ± 87.8 µg/g of dry biomass, followed by the experiments at 60°C, 400 bar and 50°C, 237.5 bar with 1323.6 ± 68.8 and 952.4 ± 35.6 µg/g of dry biomass. It was interesting that PUFAs were the majority fatty acids in this extraction, which was in agreement with previous studies.<sup>232</sup> This is in contrast to the results of hexane extraction, where the SFAs were the most abundant. The most dominant fatty acid was oleic acid (C18:1<sub>n-9</sub>), followed by linoleic acid (C18:2<sub>n-6</sub>) in all experiments. The PUFAs including ARA, EPA and DHA were also obtained in high amount from the Soxhlet and scCO<sub>2</sub> at 40°C, 400 bar. The results from the scCO<sub>2</sub> extractions showed the relationship between the density of the supercritical fluid and the solubility of the fatty acids in the carbon dioxide, which was in agreement with the study of Maheshwari *et al.*<sup>44</sup> The density of the supercritical carbon dioxide is maximal at 40°C, 400 bar and minimal at 60°C, 75 bar. Thus, the results obtained totally supported previously conclusion on the influence of the density of CO<sub>2</sub>.

The optimal condition of supercritical extraction of fatty acid that we have adopted, 40°C, 400 bar, were quite similar to the study of Treyvaud *et al.*, the fatty acid profile including PUFAs was reported at 40°C, 300 bar, for Northern shrimp (*Pandalus borealis* Kreyer) by-product.<sup>40</sup> Brazilian redspotted shrimp (*Farfantepenaeus paulensis*) was also investigated at 40°C, 300 bar for lipid profile.<sup>233</sup> Therefore, it can be concluded that it was suitable to extract fatty acids at quite high pressure and low temperature for shrimp by-products.

The fatty alcohol was present in very small quantities but noticeable amount in all extractions. The hexane Soxhlet extraction still demonstrated the highest abundance of fatty alcohol in Pacific white shrimp's cephalothorax and hepatopancreas. Although, there was a small quantity, in high-pressure condition (higher density of scCO<sub>2</sub>), fatty alcohols were obtained in greater abundance. Therefore, the density still played important role in this case.<sup>64</sup>

The quantity of mono- and diglycerides were dramatically higher in hexane Soxhlet extracts, 807.0 ± 15.9 and 79.5 ± 0.2 µg/g of dry biomass for mono- and diglycerides respectively. This was due to the fact that triglycerides were broken down during the high temperature process of the hexane Soxhlet (potentially due to enzymatic hydrolysis). Thus, such a process will result in higher concentrations of mono- and diglycerides. Whereas, the same approach could not

applied to scCO<sub>2</sub> extraction with the operating temperature ranged between 40°C to 60°C, the lower concentration of the compounds were apparently obtained.<sup>234</sup>

The characterisation and quantification of ether of glycerols or 1-*O*-Alkylglycerols have not been reported in previous studies. Herein, the best method of 1-*O*-Alkylglycerols still remained to the hexane Soxhlet extraction, 41.5 ± 0.4 µg/g dry biomass. In the scCO<sub>2</sub> extraction, the density of CO<sub>2</sub> plays a key role with the highest concentration obtained at 40°C, 400 bar, 2.1 ± 0.6 µg/g of dry biomass.

Cholesterol showed the highest concentration among all sterols identified with the most abundant 1696.2 ± 18.0 µg/g of dry biomass from hexane Soxhlet extraction. ScCO<sub>2</sub> extraction was found to be an alternative method to remove cholesterol from food. Guangmin *et al.* demonstrated that cholesterol from goat placenta could be effectively removed by scCO<sub>2</sub> extraction at the range of temperature and pressure of 40-62.5 °C and 300 and 450 bar respectively.<sup>208</sup> Their results and those obtained in this current work were in agreement, as higher concentration of cholesterol were observed in high-pressure experiments, at 40 and 60 °C, 400 bar with 45.0±16.3 and 51.7±1.6 µg/g dry biomass respectively. Whereas, in low-pressure, 75 bar, about 5-8 µg/g dry biomass of cholesterol was extracted. Campesterol, stigmasterol and β-sitosterol were also found in brown shrimp<sup>224</sup> and shellfish at a very low level, which were compatible with our results as well.<sup>44,53,224,235,236</sup>

#### 4.5 Effect of extraction time

Using hexane Soxhlet extraction, it was possible to obtain lipid yields of 6.43% from the mixture of cephalothorax and hepatopancreas of *L. vannamei* by-product. However, the highest lipid yield afforded by scCO<sub>2</sub> extraction was 1.14%, which means, the majority of lipid compounds still remained in the raw material. As the lipids contained in *L. vannamei* are valuable, further experiments were investigated in order to determination an optimal extraction time. Identical fresh biomass with the moisture content 73% of dry weight were still used as in previous experiments and the experiments were carried out at 40°C, 400 bar (adopted as the highest

extraction yield obtained previously), the extracts were collected at 30, 60, 90, 120 and 240 minutes and the yields were obtained for each fraction (**Figure 4-26**).

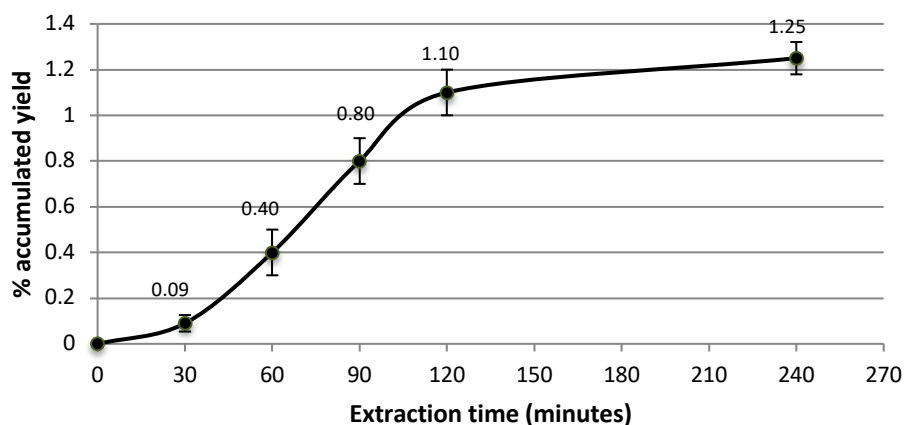


**Figure 4-26** Effect of time on percentage yield of lipid extracts at 40°C, 400 bar.

At the beginning of the extraction, 0-30 minutes, the rate of extraction was very low, unlike the previous studies that the highest extraction rate was observed in the first 40 minutes.<sup>235</sup> This s-curved shape can be explained by the presence of high moisture content in the original biomass, 73% of dry weight, the water content of the biomass influenced negatively the extraction process, the solvent capacity of carbon dioxide varied, which resulted in low extraction yield.<sup>234</sup> Similar shape of curve was observed when the moisture content was high (20%), because large volume of water acted as a barrier to the penetration by the CO<sub>2</sub> and protected the solute from the solvent, therefore, the extraction process could not easily occur.<sup>218</sup> After 30 minutes, the rate of extraction increased until it started to reach the plateau at 120 minutes. Extending the time until 240 minutes did not demonstrate a significant increase in term of lipid yield. Finally, it could be concluded that the optimal extraction time for the mixture of cephalothorax and hepatopancreas as raw material with the moisture content of 73%, was 2 hours. However, the extraction rate could be developed if the humidity of the biomass is lower.

## 4.6 Conclusion

In this study, the supercritical extraction was effectively utilised for the recovery of hydrophobic compounds from prawn residue (*Litopenaeus vannamei*) waste streams. The optimisation of lipid extraction from prawn cephalothorax (heads) by scCO<sub>2</sub> was undertaken and demonstrated yields of 1.14% at 400 bar and 40 °C for 2 hours (40 g min<sup>-1</sup>). Extraction efficiency strongly correlated density, with the highest yield being obtained at the highest density of CO<sub>2</sub>, 0.96 g/cm<sup>3</sup>. Therefore, it can be concluded that the density of the CO<sub>2</sub> is the most important factor for the scCO<sub>2</sub> extraction of the pacific white shrimp waste. While the optimal extraction time for the mixture of cephalothorax and hepatopancreas as raw material with the moisture content of 73%, was 2 hours. However, the extraction rate could be developed if the humidity of the biomass is lower. The added-value components were characterised, quantified and their potential applications were identified. It was determined that scCO<sub>2</sub> was an effective solvent for the extraction of polyunsaturated fatty acids. PUFAs have importantly been shown to reduce cardiovascular disease and improve cognitive development.

The free fatty acid (FFA) profile of the scCO<sub>2</sub> extract differed to that of the hexane Soxhlet. Firstly, a greater abundance of FFA in the hexane Soxhlet extraction over 2 hours, 20789.8 ± 257.3 µg/g of dry biomass compared to 2819.4 ± 87.8 µg/g of dry biomass by scCO<sub>2</sub> (40°C and 400 bar for 2 hours). It was suggested that these differences were likely due to several important factors, 1) high water content in the biomass adversely affects the efficiency of scCO<sub>2</sub> extraction and 2) enzymes within the biomass hydrolyse triglycerides to form FFA within the hexane system but water removal from the active site of the enzyme with scCO<sub>2</sub> may reduce the rate of this process. Further discussion on the active enzyme in the cephalothorax of *L. vannamei* and the implications on lipid yield will be presented in Chapter 5.

## **Chapter 5**

### **The influence of inherent prawn enzyme on extraction of PUFA by scCO<sub>2</sub>**

## 5 The influence of inherent prawn enzyme on extraction of PUFA by scCO<sub>2</sub>

### 5.1 Introduction

It was previously found in Chapter 4 that the very high moisture content of prawn waste could affect the efficiency and kinetics of scCO<sub>2</sub> extraction of lipids. High water content not only slowed down the extraction process but could also have a significant influence on the total lipid recovery. Moreover, it has been reported that an internal organ called hepatopancreas located in the cephalothorax of *L. vannamei* contains an active enzyme that could play an important role in this study. Therefore, the influence of moisture content will be investigated with different drying methods including oven-drying, microwave drying and freeze-drying.

### 5.2 The influence of moisture content on scCO<sub>2</sub> extraction efficiency.

The optimisation of fresh Pacific white shrimp (*L. vannamei*) by-product was previously carried out successfully using a factorial experimental design; the experimental data were discussed in Chapter 4. The optimal condition determined was 40 °C at 400 bar, giving 1.10% of crude yield. It was observed that the extraction began quite slowly, which might be due to the high moisture content of the biomass itself, as reported in a previous study.<sup>234</sup> Therefore, for further understanding, a series of experiments were undertaken; three drying methods, freeze-drying, vacuum oven and vacuum microwave-assisted drying, were used as pre-treatment processes prior to scCO<sub>2</sub> extractions at 40°C, 400 bar. The extracts were collected at 30, 60, 90, 120 and 240 minutes and the yields were calculated and presented in **Figure 5-1**.

### 5.2.1 Comparison of extraction kinetics and lipid recoveries with different drying methods.

The results of accumulated yields from oven-drying, microwave drying and freeze-drying illustrated in **Figure 5-1** confirmed that the hypothesis on the appearance of an s-curve plot during the extraction of fresh biomass was due to its high moisture content (73%wt). It was obviously seen that high moisture content in prawn waste affected solubility and mass transfer kinetics in supercritical carbon dioxide extraction.<sup>228</sup>

The dried samples followed different patterns and the s-curve trend totally disappeared, indicating a dramatic improvement in the extraction rate (See Chapter 4). This was likely due to the water chemically interacting with the structure of the biomass and acting as barrier to prevent the penetration of the lipophilic scCO<sub>2</sub> into the biomass, consequently, the target solute is protected from the solvent.<sup>64,234</sup>

The extraction rates improved significantly when the biomasses were dried by all assessed drying methods. **Figure 5-1** demonstrated the dependence of the moisture content on the total lipid recovery from prawn by-product of *L. vannamei*. Freeze-dried feedstock with the lowest moisture content (0.8%) resulted in a highest extraction yield and rate. Vacuum-microwave and vacuum-oven drying with the moisture contents of 8% and 1.7% respectively, showed moderate extraction efficiencies due to intermediate moisture contents compared with the result obtained from the fresh prawn waste. However, the moisture content is apparently not the only factor that affected the scCO<sub>2</sub> extraction efficiency, since the microwave-dried sample with higher moisture content finally yielded higher lipid extract than the oven-dried sample. As a consequence, other factors such as textual structure, density and porosity should be taken into account.<sup>237-239</sup>

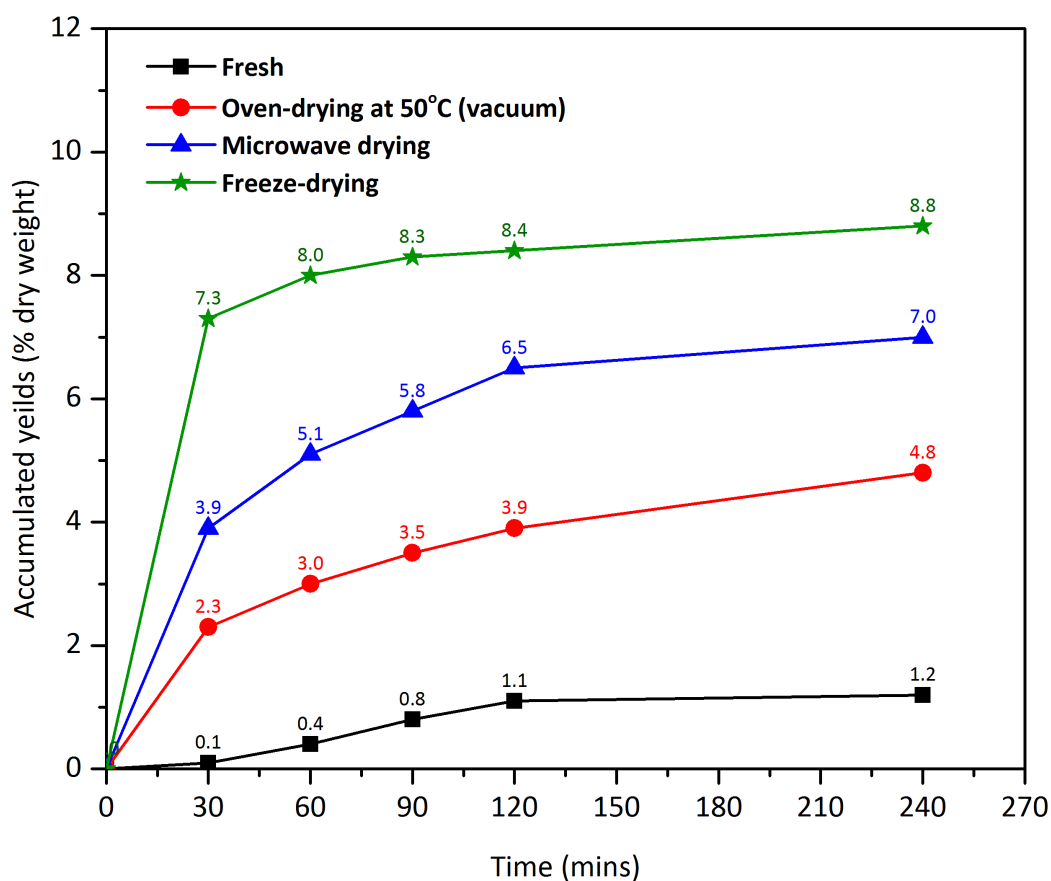


Figure 5-1 Accumulated yields of different drying methods.

It was clearly seen that the plateau could be reached quickly in the case of freeze-dried prawn waste, with 83% of total lipid (recovered in 4 hours) obtained in 30 minutes and 94% obtained within only 1.5 hours of extraction time. Therefore, shorter extraction time can be applied with advantages of energy efficiency and cost reduction. The freeze-dried sample resulted in the highest extraction efficiency with the highest crude lipid recovered. Among the dried samples, freeze dried prawn waste seems to have the lowest density with the appearance of light-weight white powder, this is due to the fact that the process leads to ice sublimation, leaving pores within the biomass structure.<sup>240–244</sup> Because of this porous structure, the  $scCO_2$  was able to be in contact with the solute more easily, as a consequence, the mass transfer was significantly enhanced.<sup>239,245–247</sup> In the case of vacuum-microwave dried sample, 56% of the total four-hour-extraction was recovered in 30 minutes and 93% was yielded after 2 hours and the plateaus appeared after 2 hours in both cases. The extraction kinetics of vacuum-oven and vacuum-



microwave dried samples were significantly slower than that of the freeze-dried prawn waste, which can also be explained by the post-drying structure and the density of the dried materials. It has been reported in a study of carrot slices that the order of bulk density from high to low was hot air drying, vacuum-microwave drying and freeze-drying respectively.<sup>239</sup> As such, vacuum-microwave drying allows rapid mass transfer within the sample.

As the microwaves heat from the inside of the biomass, there is a remarkable difference of the vapour pressure between the centre and the surface of the material. This high internal vapour pressure combined with the low chamber pressure caused by the vacuum produced expansion and puffing effects within the biomass. Because of this puffy structure within the vacuum-microwave dried sample, its density became lower than that of the oven-dried sample, which also led to better mass transfer during the drying process, than that resulting from the oven-dried sample. This is therefore the reason we assume why the extraction efficiency of microwave-dried was greater than the oven-dried prawn by-product.<sup>239,243,248,249</sup> Microwave drying resulted in a lower yield of PUFA compared to vacuum oven dried samples. This may be due to denaturing of the enzyme resulting from the formation of hot spots within the microwave treated sample, however further work would be need to confirm this postulation.

Freeze-drying proved to be the best method of water removal with highest product quality , originality of the nutrient presented in the food, compared to others methods<sup>250</sup>, however, it has been considered as a high cost preservation method.<sup>241</sup> Freeze-drying might give a reasonable result in both terms mentioned but a 72-hour-process should receive more attention for energy consumption compared to 24 hours in vacuum oven or a short time (less than 10 minutes) process for microwave-assisted drying. In this current study, microwave-assisted drying was demonstrated to be a viable alternative as it resulted in appropriate extraction efficiency (yielded 6.5%wt extract in 2 hours) and also gave a relatively high concentration of fatty acids and polyunsaturated fatty acids (PUFAs), 17211 and 7324 µg/g of dry biomass respectively. This is especially promising when considering that the microwave-assisted drying process can be achieved in less than 10 minutes. However, an important issue in microwave-assisted drying involves potential physical damage due to difficult on-line temperature control within the microwave field and uniform heating when handling larger samples.<sup>251</sup>

### 5.2.2 Quantification and comparison of lipid profiles.

It was confirmed that dried samples result in enhanced lipid recovery relative to the fresh wet sample, as the surface structure and activity of material are determined by its moisture content and internal structure.<sup>228</sup> As the aim of this study is not only to obtain the highest quantity of lipid but also to recover specific high value chemicals such as PUFAs, as these have various applications in different industrial sectors. To be able to assess the process correctly, the full quantification of each lipophilic family compounds from selected drying methods was carried on and is presented in **Table 5-1**. Although, freeze-drying proved to be the most effective drying method in terms of high product recovery, the target compounds as PUFAs were obtained in lower concentration compared to the vacuum-oven dried sample,  $9827.1 \pm 127.6$  and  $11566.1 \pm 82.7$   $\mu\text{g/g}$  of dry biomass respectively. Among the three methods, the oven-dried sample yielded the highest concentrations in ARA, EPA and DHA. **Figure 5-2** demonstrates the effect of drying methods on the concentrations of n-3 (EPA and DHA) and n-6 (ARA) PUFAs. The concentrations of PUFAs increased dramatically when the prawn waste was dried prior to the  $\text{scCO}_2$  extraction. From the fresh prawn waste, the target PUFAs were extracted with relatively low yields of  $29.7 \pm 1.5$ ,  $84.8 \pm 10.5$ ,  $195.3 \pm 14.8$   $\mu\text{g/g}$  of dry biomass for ARA, EPA and DHA respectively. The amounts of ARA increased about 5-fold, 6-fold and 10-fold higher than that obtained from  $\text{scCO}_2$  of fresh biomass with the vacuum-microwave dried, freeze dried and vacuum-oven dried samples respectively. The EPA followed a relatively similar trend as the ARA with 5-fold, 5-fold and 8-fold higher. Finally the DHA showed a 4-fold, 4-fold and 6-fold increase compared with the extract of fresh sample; using vacuum-microwave dried, freeze dried and vacuum-oven dried samples respectively. There was no significant difference on the concentration of ARA, EPA and DHA between the extracts obtained from freeze-drying and vacuum-microwave drying. Therefore, there is no need to invest in an expensive freeze-drying process in order to produce a near equal amount of PUFAs from prawn waste. However, the mild condition oven-drying at  $50^\circ\text{C}$  was highly effective at increasing the concentration of PUFAs

within the prawn waste extract. This temperature of 50°C was reported to be the optimum temperature of the protease in Brown pacific shrimp.<sup>252</sup>

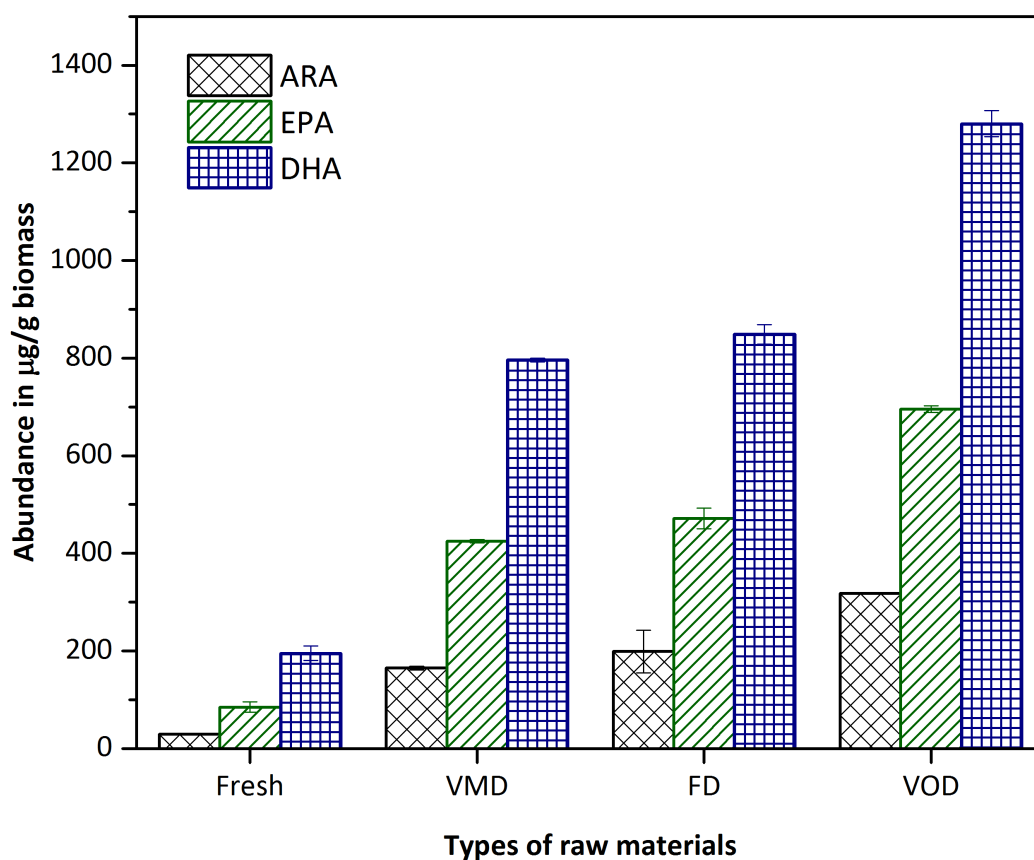


**Figure 5-2** The influence of different drying methods on the quantities of ARA, EPA and DHA from scCO<sub>2</sub> extraction at 40 °C and 400 bar in 2 hours.

(Note: Vacuum-microwave drying (VMD), Freeze-drying (FD) and Vacuum-oven drying (VOD))

Freeze-drying is well-known as a promising dehydration technique for thermo-sensitive compounds due to the absence of liquid water and most importantly a low temperature applied during the process.<sup>241,243</sup> Therefore, more of the chemicals components within the prawn waste would effectively be protected during the freeze-drying. The majority of hydrophobic components in prawn cephalothorax are in the forms of large lipid molecules such as lipoprotein, phospholipid and acylglycerols, which are not fully GC-analysable and required other analytical methods.<sup>33,72,253</sup> Vacuum-microwave drying is another alternative method to obtain the quality of dehydrated products as it operated at low temperature and the energy

transfer effectively enhanced with the combination of vacuum resulting in rapid heating and mass transfer as well as low temperature drying process. Moreover, another advantage is that the absence of air is likely to minimize oxidation and therefore, it is able to largely preserve the initial colour and nutrients of the products.<sup>239,254</sup> This could also explain why the concentrations of ARA, EPA and DHA of microwave-dried and freeze dried extracts are almost identical in this current study.

However, the effect of vacuum-oven drying is interestingly different from the other two methods described in terms of the lipid profile and quantification. The cephalothorax of prawn contains a digestive organ called hepatopancreas, where various enzymes are stored, especially protease, lipase and phospholipase. This lipolysis process involved will be discussed in detail afterward in this chapter.

By assessing the above quantification of components in the various extracts (**Table 5-1**), the concentration of fatty acid from the vacuum oven at 50 °C was far higher than other drying methods, which could be an indication that the enzymatic hydrolysis was ongoing at a significant rate. Moreover, the presence of the enzymatic process in the vacuum oven at 50 °C was reconfirmed by the abundances of mono- and diglycerides. Microwave and freeze drying showed high concentrations on both groups of compounds (monoglycerides,  $910.3 \pm 5.5$  and  $1117.8 \pm 21.3$  µg/g dry biomass and diglycerides,  $80.5 \pm 0.7$  and  $146.9 \pm 0.2$  µg/g dry biomass for microwave and freeze drying respectively), however, vacuum oven drying showed a different result, 99 and 0.4 µg/g dry biomass for mono- and diglycerides respectively. This means there was potentially another enzyme contained in the prawn waste, which could be a lipase hydrolysing TAG to release free fatty acids and glycerols during the drying process.<sup>33,72</sup>

**Table 5-1** Comparison of lipid composition (in  $\mu\text{g/g}$  dry biomass) after different drying methods prior to  $\text{scCO}_2$  at  $40^\circ\text{C}$ , 400 bar of the fractions collected in 2 hours.

Compound names	Fresh	Different drying methods		
		Oven-drying (vacuum)	Microwave	Freeze-drying
<b>Free fatty acids</b>				
C12:0	$3.6 \pm 0.2$	$1.4 \pm 0.1$	$4.9 \pm 1.2$	$20.8 \pm 0.2$
C14:0	$26.0 \pm 0.1$	$536.6 \pm 3.7$	$184.2 \pm 2.3$	$242.2 \pm 2.6$
C15:0	$13.4 \pm 1.2$	$273.7 \pm 4.1$	$66.4 \pm 0.6$	$89.7 \pm 0.2$
C16:1 (n-7)	$90.4 \pm 0.4$	$1379.0 \pm 3.2$	$763.1 \pm 2.6$	$1069.3 \pm 11.5$
C16:0	$395.7 \pm 0.8$	$8819.2 \pm 1.7$	$2075.4 \pm 23.8$	$2799.1 \pm 10.7$
C17:1 (n-7)	$16.1 \pm 1.4$	$255.7 \pm 5.8$	$107.4 \pm 1.0$	$124.0 \pm 2.0$
C17:0	$17.0 \pm 2.4$	$261.4 \pm 23.8$	$55.3 \pm 0.3$	$72.0 \pm 1.7$
C18:2(n-6)	$763.7 \pm 16.4$	$8604.1 \pm 32.9$	$5507.7 \pm 8.1$	$7713.4 \pm 14.9$
C18:1(n-9)	$800.5 \pm 25.4$	$5587.7 \pm 303.4$	$4753.8 \pm 0.7$	$6222.7 \pm 68.6$
C18:1(n-7)	$114.9 \pm 3.7$	$870.4 \pm 2.6$	$795.8 \pm 62.4$	$987.0 \pm 37.8$
C18:0	$123.6 \pm 1.8$	$1754.8 \pm 4.5$	$680.0 \pm 26.6$	$1054.7 \pm 132.7$
C20:5 (n-3) (EPA)	$84.8 \pm 10.5$	$695.5 \pm 6.7$	$424.8 \pm 3.1$	$471.5 \pm 20.9$
C20:4 (n-6) (ARA)	$29.7 \pm 1.5$	$317.8 \pm 1.2$	$165.1 \pm 3.9$	$198.8 \pm 43.4$
C20:2 (n-6)	$71.7 \pm 3.7$	$668.4 \pm 14.9$	$430.7 \pm 1.9$	$594.6 \pm 28.1$
C20:1 (n-9)	$53.1 \pm 2.0$	$490.2 \pm 3.2$	$243.8 \pm 2.6$	$302.8 \pm 10.6$
C20:0	$12.1 \pm 0.2$	$157.4 \pm 2.0$	$56.0 \pm 3.8$	$145.5 \pm 1.2$
C22:6 (n-3) (DHA)	$195.3 \pm 14.8$	$1280.4 \pm 26.9$	$796.1 \pm 4.0$	$848.7 \pm 20.2$
C24:1 (n-9)	$2.5 \pm 0.2$	$3.7 \pm 0.7$	$14.2 \pm 3.5$	$74.2 \pm 1.9$
C24:0	$5.2 \pm 1.1$	$32.5 \pm 2.6$	$86.5 \pm 0.5$	$69.2 \pm 0.4$
<i>Total SFA</i>	$596.6 \pm 7.8$	$11837.1 \pm 42.5$	$3208.7 \pm 59.1$	$4493.2 \pm 149.6$
<i>Total MUFA</i>	$1077.6 \pm 33.1$	$8586.7 \pm 318.9$	$6678.2 \pm 72.8$	$8780.1 \pm 132.3$
<i>Total PUFA</i>	$1145.2 \pm 46.9$	$11566.1 \pm 82.7$	$7324.3 \pm 21.0$	$9827.1 \pm 127.6$
<b>Total Free fatty acids</b>	<b><math>2819.4 \pm 87.8</math></b>	<b><math>31990.0 \pm 444.1</math></b>	<b><math>17211.2 \pm 152.8</math></b>	<b><math>23100.5 \pm 409.5</math></b>
<b>Free fatty alcohol</b>				

1-hexadecanol	2.5 ± 0.7	9.0 ± 1.2	5.2 ± 0.4	4.9 ± 0.1
<b>Total free fatty alcohol</b>	<b>2.5 ± 0.7</b>	<b>9.0 ± 1.2</b>	<b>5.2 ± 0.4</b>	<b>4.9 ± 0.1</b>
<b>Monoglycerides</b>				
β-glyceryl pentadecanoate	0.7 ± 0.2	4.7 ± 1.0	13.2 ± 0.2	18.8 ± 1.2
β-glyceryl palmitate	38.1 ± 6.6	39.8 ± 2.9	91.2 ± 0.6	31.3 ± 3.9
α-glyceryl palmitate	13.6 ± 1.8	24.2 ± 1.8	506.9 ± 0.7	667.9 ± 6.4
α-glyceryl heptadecanoate	2.6 ± 0.8	11.3 ± 1.5	10.9 ± 0.3	11.3 ± 0.1
α-glyceryl stearate	0.4 ± 0.2	11.7 ± 0.7	52.5 ± 2.1	56.1 ± 1.2
β-glyceryl oleate	18.3 ± 0.5	6.2 ± 0.9	219.3 ± 1.4	303.6 ± 6.3
α-glyceryl oleate	6.0 ± 3.1	1.8 ± 0.2	16.3 ± 0.1	28.9 ± 2.2
<b>Total monoglycerides</b>	<b>79.8 ± 13.2</b>	<b>99.6 ± 9.1</b>	<b>910.3 ± 5.5</b>	<b>1117.8 ± 21.3</b>
<b>Diglycerides</b>				
Glycerol 1,2-dipalmitate	2.7	0.2	21.3 ± 0.1	63.4 ± 0.1
Glycerol 1,3-dipalmitate	0.6	0.3	59.3 ± 0.6	83.5 ± 0.1
<b>Total diglycerides</b>	<b>3.3</b>	<b>0.4</b>	<b>80.5 ± 0.7</b>	<b>146.9 ± 0.2</b>
<b>Ethers of glycerol</b>				
1-O-hexadecylglycerol	2.7	23.4 ± 0.3	8.8 ± 0.6	14.5 ± 0.6
1-O-octadecylglycerol	0.6	16.8 ± 0.8	16.0 ± 0.2	18.3 ± 0.6
<b>Total ethers of glycerol</b>	<b>3.3</b>	<b>40.2 ± 1.1</b>	<b>24.8 ± 0.8</b>	<b>32.7 ± 1.2</b>
<b>Sterols</b>				
Cholesterol	45.0 ± 16.3	1305.6 ± 32.3	1956.2 ± 3.4	2210.9 ± 3.2
Campesterol	3.5 ± 1.3	25.7 ± 1.3	27.5 ± 0.2	35.0
Stigmasterol	2.4 ± 0.5	21.9 ± 1.4	13.7 ± 0.2	20.1
β-sitosterol	4.4	33.6 ± 1.0	38.2 ± 1.1	26.8 ± 26.9
<b>Total sterols</b>	<b>55.3 ± 18.1</b>	<b>1386.8 ± 36.0</b>	<b>2035.6 ± 4.9</b>	<b>2292.8 ± 30.2</b>
<b>Total identified</b>	<b>2962.3 ± 120.4</b>	<b>33526.0 ± 491.5</b>	<b>20267.7 ± 165.0</b>	<b>26695.6 ± 462.5</b>

It was evident from the quantification analysis that PUFA could be obtained in the high concentration by vacuum oven at 50 °C, however, the saturated fatty acid (SFA) were also present in significant amount. Whereas, microwave and freeze drying produced a lot less of SFA. Therefore, it can be concluded that for maximum fatty acid production, vacuum oven at 50 °C was the most suitable method, but for a selective production of MUFAs and PUFAs, microwave and freeze drying were more appropriate methods. Although freeze drying can be used to protect the biomass from heat damage and produced excellent structure retention, the process is costly.<sup>239</sup>

### **5.3 The effect of autolysis time on the enzymatic process at room temperature**

It was reported in previous studies that hepatopancreas of Pacific white shrimp is a source of serine protease consisting mainly of trypsin and chymotrypsin<sup>255</sup> and lipase including phospholipase.<sup>256,257</sup> The protease contained in hepatopancreas of Pacific white shrimp could hydrolyse lipoprotein and in doing so release more free lipids such as triglycerides, sterols etc., which could be subsequently more easily extracted. The protease reactivity from *Panaeus Orientalis* was reported to be maximal at 40 to 50 °C, however, at 60 °C the reactivity decreased to 40% and the protease was completely inactivated at 70 °C.<sup>258</sup> The autolysis of hepatopancreas from Pacific white shrimp was investigated and achieved at 60 °C. Yield of extracted lipid also increased from 7.4 to 8.8% when autolysis time increased from 0 (control) to 150 minutes. During this autolysis process, proteins associated with lipids were liberated and therefore, the extraction yields were observed to be higher when autolysis mediated by endogen proteases was performed.<sup>33</sup> Takeungwongtrakul *et al.* showed that autolysis can also occur at 0 °C and an increase in lipid content was observed.<sup>72</sup> This means the autolysis can occurring facilely in a wide range of temperatures whether there is a presence of heat or not.

In this study, three portions of fresh ground cephalothorax, previously frozen, and hepatopancreas were left at room temperature for 0 (control), 3, 6 and 24 hours prior to scCO<sub>2</sub> extraction at the optimal condition determined in Chapter 5, 40 °C, 400 bar. The moisture content was assumed to be unchanged as the samples were stored in sealed plastic bags. The

extraction yields are shown in **Figure 5-3**. The autolysis apparently occurred despite no heat being applied to the process, as lipid yield increased from 1.1 to 1.4, 2.1 and 3.3% of dry weight when autolysis time increased from 0 (control), 3, 6 and 24 hours respectively. However, the yields obtained from the aforementioned condition were not quite comparable to that of the conventional hexane soxhlet with the yield of 8.4% of dry weight. The current investigation was also in agreement with the previous studies with observation of an increase of total lipid recovery when autolysis involved.<sup>33,72</sup> However, previous studies have highlighted that scCO<sub>2</sub> can be effective at removal of water from the active sites of enzymes, thereby reducing their activity.<sup>231,259</sup> This would therefore reduce the autolysis taking place during supercritical extraction, in contrast such an effect may not be observed in hexane soxhlet extraction due to the lack of water solubility in the organic solvent. Several prior studies have demonstrated the use of hexane as a suitable solvent for lipase catalysed reactions.<sup>260–265</sup> It is therefore important to maximise the autolysis prior to extraction by scCO<sub>2</sub>. Autolysis by protease could be responsible for the increase of crude lipid yield, as some triglycerides were released from lipoproteins by this enzymatic process.<sup>230,266,267</sup>

### 5.3.1 Extraction yields

Enzymatic extraction using protease was reported to be an alternative method for lipid recovery as the process can be undergone under mild condition for short time. Mbatia *et al* used commercial protease for lipid extraction of Nile perch and salmon heads at 55 °C.<sup>268</sup> Moreover, crude protease from Pacific white shrimp hepatopancreas was used in lipid extraction striped catfish muscle. The recovery of lipid increased by adding crude protease to striped catfish mince, the increase in fatty acids and phospholipid content were observed. The hydrolysis of ester bonds in triglycerides effectively happened with increasing of hydrolysis time.<sup>230</sup> However, it was reported that hydrolysis rate was high within the first 60 minutes then followed by slower rate. The fast rate at the beginning of the process was due to the high availability of peptide and ester bonds, which were hydrolysed. The decrease in hydrolysis rate was then observed with



increasing in hydrolysis time, this was mainly due to the reduction in hydrolysis sites as well as enzyme auto digestion and/or product inhibition.<sup>33</sup>

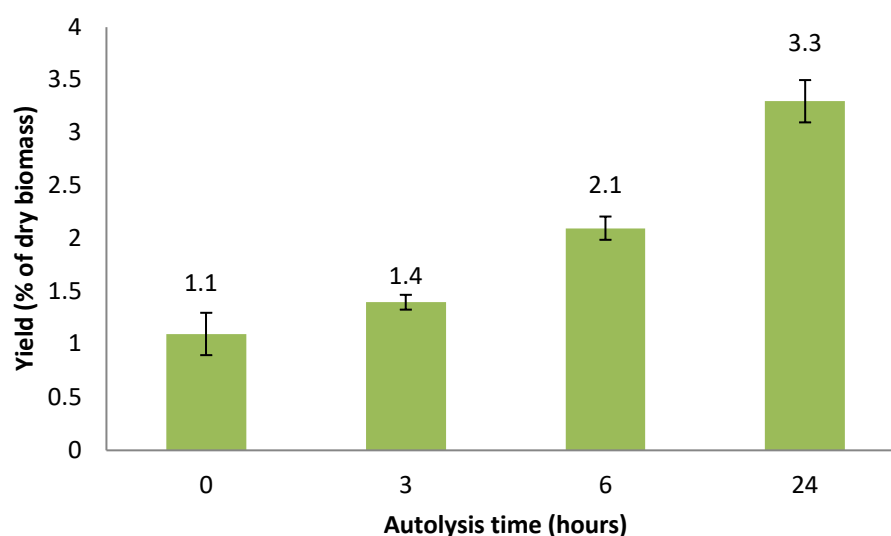


**Figure 5-3** Yield of lipid from the mixture of cephalothorax and hepatopancreas of Pacific white shrimp affected by autolysis at 0, 3, 6 and 24 hours.

Hepatopancreas is also the major source of lipase, which is able to hydrolyse the ester bond of triglycerides.<sup>269</sup> Generally, lipid hydrolysis takes place in the presence of moisture and heat, the optimal temperature for lipase from hepatopancreas of squid (*Todarodes pacificus*) was previously found to be 35 to 40 °C.<sup>270</sup> As the hepatopancreas of Pacific white shrimp also contains lipase, endogenous lipase and phospholipase might be involved in hydrolysis of triglycerides and phospholipids to produce free fatty acids. However, hydrolysis also was observed at 0 °C under ice storage. After 6 days of ice storage, lipid yield increased from 20 g/100 g to 92 g/100 g of lipid content with a sharp increase after 2 days of storage. The result confirmed that the hepatopancreas of *Litopenaeus vannamei* contained active lipase and phospholipase, which are responsible for lipid hydrolysis resulting in a reduction of triglyceride and phospholipid contents after the extending storage time.<sup>72</sup>

### 5.3.2 Quantification of lipophilic compounds after autolysis at room temperature at different duration.

Table 5-2 showed the abundance of main groups of compounds from different autolysis time before scCO<sub>2</sub> extraction. Not only was the extraction exponentially improved, but also it can be clearly seen that abundances of the total lipophilic content identified by the GC-FID increased with the autolysis time, 2962.3 ± 120.4, 8969.8 ± 81.1, 12120.4 ± 508.0 and 15374.2 ± 65.6 µg/g of dry biomass for 0 (control), 3, 6 and 24 hours of autolysis respectively. After autolysis, most of the main groups of compounds including fatty acids, mono- and diglycerides, glycerol ethers and sterols were also found in higher concentration compared to the control experiment (0 hours of autolysis).

**Table 5-2** Abundances (in µg/g dry biomass) of lipophilic components as extracted by scCO<sub>2</sub> in 2 hours of prawn by-product after autolysis of 3, 6 and 24 hours.

Compounds	Hexane <sup>a</sup>	Autolysis time prior to scCO <sub>2</sub> extraction			
		Control <sup>b</sup>	3 hours <sup>b</sup>	6 hours <sup>b</sup>	24 hours <sup>b</sup>
<b>Free fatty acids</b>					
C12:0	62.8 ± 4.0	3.6 ± 0.2	26.5 ± 0.0	6.6 ± 0.7	39.8 ± 0.7
C14:0	326.4 ± 1.1	26.0 ± 0.1	93.3 ± 0.0	105.1 ± 0.9	153.1 ± 0.9
C15:0	183.0 ± 0.5	13.4 ± 1.2	50.7 ± 0.0	54.9 ± 0.3	65.2 ± 0.3
C16:1 (n-7)	856.9 ± 8.6	90.4 ± 0.4	279.1 ± 0.4	369.2 ± 1.1	552.8 ± 1.1
C16:0	4905.8 ± 10.3	395.7 ± 0.8	1655.2 ± 0.9	1625.2 ± 0.7	2151.6 ± 0.7
C17:1 (n-7)	146.3 ± 0.3	16.1 ± 1.4	55.5 ± 0.1	89.6 ± 8.7	86.9 ± 8.7
C17:0	221.1 ± 0.8	17.0 ± 2.4	57.3 ± 0.2	65.7 ± 3.9	54.3 ± 3.9
C18:2(n-6)	3537.7 ± 18.0	763.7 ± 16.4	2256.4 ± 6.0	3239.1 ± 6.6	4222.4 ± 6.6
C18:1(n-9)	5155.2 ± 100.3	800.5 ± 25.4	1833.2 ± 3.1	3108.0 ± 6.5	3649.6 ± 6.5
C18:1(n-7)	1014.1 ± 16.6	114.9 ± 3.7	304.9 ± 2.1	444.4 ± 7.0	490.2 ± 7.0
C18:0	1805.1 ± 6.1	123.6 ± 1.8	426.9 ± 1.0	460.0 ± 0.9	662.8 ± 0.9
C20:5 (n-3) (EPA)	118.2 ± 0.8	84.8 ± 10.5	300.1 ± 1.6	376.2 ± 4.0	299.3 ± 4.0
C20:4 (n-6) (ARA)	124.3 ± 5.1	29.7 ± 1.5	134.9 ± 1.2	142.7 ± 0.6	124.6 ± 0.6
C20:2 (n-6)	996.5 ± 9.9	71.7 ± 3.7	219.0 ± 0.8	320.3	277.7
C20:1 (n-9)	420.3 ± 25.1	53.1 ± 2.0	153.3 ± 2.7	121.1 ± 1.8	185.9 ± 1.8
C20:0	364.2 38.4	12.1 ± 0.2	28.0 ± 1.8	45.8 ± 0.7	45.4 ± 0.7

C22:6 (n-3) (DHA)	489.0 ± 10.4	195.3 ± 14.8	698.4 ± 29.5	924.1 ± 13.7	574.6 ± 13.7
C24:1 (n-9)	41.5 ± 0.1	2.5 ± 0.2	15.3 ± 0.1	11.9 ± 0.4	30.8 ± 0.4
C24:0	21.3 ± 1.0	5.2 ± 1.1	3.3	11.6	33.2
<i>Total SFA</i>	<i>7889.7 ± 62.2</i>	<i>596.6 ± 7.8</i>	<i>2341.1 ± 4.0</i>	<i>2374.9 ± 45.8</i>	<i>3205.3 ± 8.1</i>
<i>Total MUFA</i>	<i>7634.4 ± 150.9</i>	<i>1077.6 ± 33.1</i>	<i>2641.4 ± 8.6</i>	<i>4144.2 ± 268.5</i>	<i>4996.1 ± 25.4</i>
<i>Total PUFA</i>	<i>5265.7 ± 44.1</i>	<i>1145.2 ± 46.9</i>	<i>3608.8 ± 39.0</i>	<i>5002.3 ± 145.6</i>	<i>5498.7 ± 24.9</i>
<b>Total Free fatty acids</b>	<b>20789.8 ± 257.3</b>	<b>2819.4 ± 87.8</b>	<b>8591.2 ± 51.5</b>	<b>11521.3 ± 459.9</b>	<b>13700.1 ± 58.4</b>
<b>Free fatty alcohol</b>					
1-hexadecanol	35.7 ± 2.0	2.5 ± 0.7	1.5	2.2 ± 0.3	3.1 ± 0.3
<b>Total free fatty alcohol</b>	<b>35.7 ± 2.0</b>	<b>2.5 ± 0.7</b>	<b>1.5</b>	<b>2.2 ± 0.3</b>	<b>3.1 ± 0.3</b>
<b>Monoglycerides</b>					
β-glyceryl pentadecanoate	27.0 ± 0.3	0.7 ± 0.2	4.5	3.7 ± 0.5	5.1 ± 0.1
β-glyceryl palmitate	34.9 ± 0.5	38.1 ± 6.6	19.5 ± 0.1	23.3 ± 1.2	57.1 ± 0.8
α-glyceryl palmitate	500.3 ± 7.9	13.6 ± 1.8	40.3	100.0 ± 9.8	214.3 ± 0.4
α-glyceryl heptadecanoate	17.8 ± 0.6	2.6 ± 0.8	10.6	8.4 ± 0.9	5.4 ± 0.0
α-glyceryl stearate	48.1 ± 4.8	0.4 ± 0.2	3.5 ± 0.0	11.7 ± 0.7	21.5 ± 0.0
β-glyceryl oleate	149.0 ± 1.5	18.3 ± 0.5	13.3 ± 0.0	38.9 ± 5.1	93.7 ± 1.5
α-glyceryl oleate	29.8 ± 0.3	6.0 ± 3.1	4.5 ± 0.0	3.1 ± 0.7	10.7 ± 0.0
<b>Total Monoglycerides</b>	<b>807.0 ± 15.9</b>	<b>79.8 ± 13.2</b>	<b>96.3 ± 0.2</b>	<b>189.2 ± 18.9</b>	<b>407.8 ± 2.9</b>
<b>Diglycerides</b>					
Glycerol 1,2-dipalmitate	27.3 ± 0.0	2.7 ± 0.0	2.3 ± 0.0	12.6 ± 1.0	13.2 ± 0.0
Glycerol 1,3-dipalmitate	52.2 ± 0.2	0.6 ± 0.0	3.7 ± 0.1	7.4 ± 0.3	22.8 ± 0.2
<b>Total diglycerides</b>	<b>79.5 ± 0.2</b>	<b>3.3 ± 0.0</b>	<b>5.9 ± 0.1</b>	<b>20.1 ± 1.2</b>	<b>36.0 ± 0.3</b>

<b>Ethers of glycerol</b>					
1- <i>O</i> -hexadecylglycerol	23.5 ± 0.4	2.7 ± 0.0	1.4 ± 0.1	3.7 ± 0.9	7.9 ± 0.0
1- <i>O</i> -octadecylglycerol	18.0 ± 0.0	0.6 ± 0.0	3.2 ± 0.0	5.1 ± 1.3	9.6 ± 0.1
<b>Total ethers of glycerol</b>	<b>41.5 ± 0.4</b>	<b>3.3 ± 0.0</b>	<b>4.6 ± 0.1</b>	<b>8.8 ± 2.2</b>	<b>17.5 ± 0.1</b>
<b>Sterols</b>					
Cholesterol	1538.0 ± 11.6	45.0 ± 16.3	239.9 ± 3.1	357.2 ± 19.1	1142.2 ± 2.6
Campesterol	75.8 ± 3.0	3.5 ± 1.3	22.3 ± 26.0	4.7 ± 0.6	20.8 ± 0.2
Stigmasterol	42.9 ± 2.1	2.4 ± 0.5	1.9 ± 0.0	9.1 ± 3.4	12.6 ± 0.4
β-sitosterol	39.5 ± 1.3	4.4 ± 0.0	6.1 ± 0.1	7.9 ± 2.3	33.9 ± 0.5
<b>Total sterols</b>	<b>1696.2 ± 18.0</b>	<b>55.3 ± 18.1</b>	<b>270.2 ± 29.2</b>	<b>378.8 ± 25.4</b>	<b>1209.6 ± 3.6</b>
<b>Total identified</b>	<b>23449.7 ± 293.8</b>	<b>2962.3 ± 120.4</b>	<b>8969.8 ± 81.1</b>	<b>12120.4 ± 508.0</b>	<b>15374.2 ± 65.6</b>

<sup>a</sup> Hexane soxhlet for 2 hours

<sup>b</sup> ScCO<sub>2</sub> at 40 °C and 400 bar for 2 hours

Overall, the quantities of the main group of compounds identified by GC-FID increased considerably with increasing autolysis duration. **Figure 5-4** illustrates the changes in concentrations of fatty alcohol, ethers of glycerol, monoglycerides, diglycerides and sterols in the extracts. Apart from free fatty acids, sterols and monoglycerides indicated considerable changes with increases in concentrations when autolysis was prolonged. As a consequence, the highest quantities of both groups were observed at 24-hour-autolysis. Even though the changes of the other groups were not seemingly remarkable in the plot, the concentration of diglycerides and ethers did rise by almost 12-fold and 6-fold higher respectively compared to the control experiment with 24-hour autolysis. Interestingly, considerable change occurred to free fatty acid content, 2819.4 ± 87.8, 8591.2 ± 51.5, 11521.3 ± 459.9 and 13700.1 ± 58.4 µg/g dry biomass for the autolysis time 0 (control), 3, 6 and 24 hours respectively. This confirmed that the free fatty acids were being enzymatically produced during autolysis study.

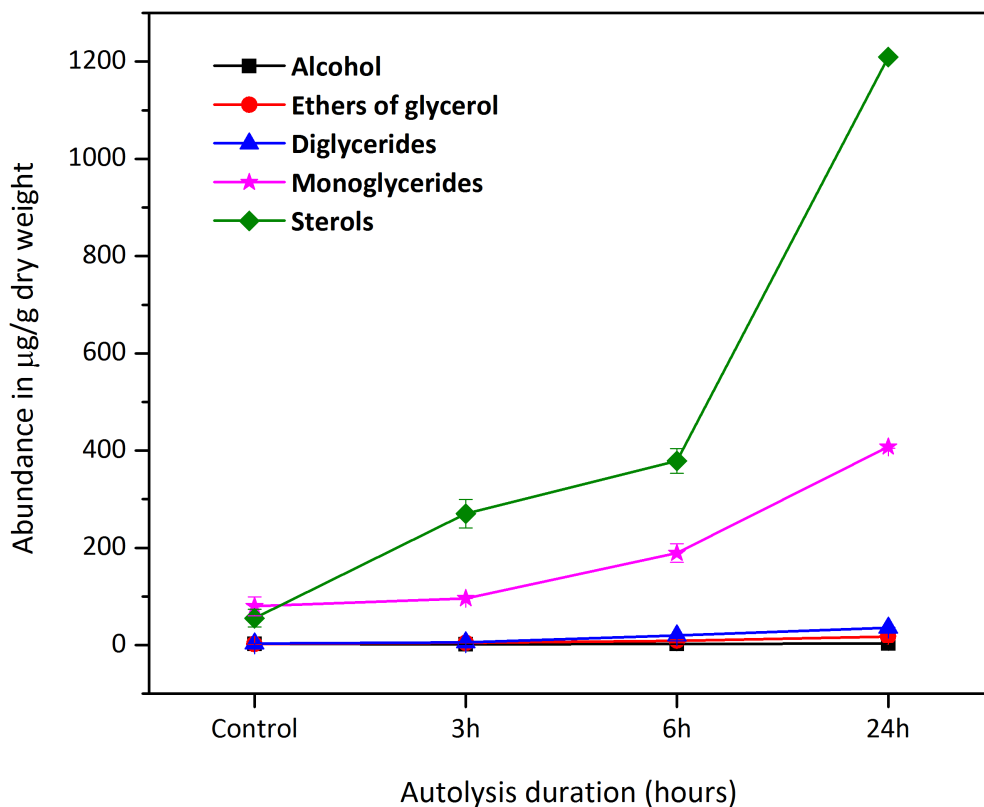


**Figure 5-4** Abundance of fatty alcohol, ethers of glycerol, monoglycerides, diglycerides and sterols after autolysis of 3, 6 and 24 hours at room temperature (scCO<sub>2</sub> extraction at 40 °C, 400 bar for 2 hours).

**Figure 5-5** indicates that the most dramatic increase actually occurred after the prawn waste was subjected to autolysis for 3 hours. Each of SFAs, MUFAs and PUFAs yields were found significantly higher compared with that of the control experiment. Additionally, the concentration of MUFAs and PUFAs continued to increase after 6-hour autolysis, whereas, the total SFAs stayed almost unchanged. That might be due to the fact that the enzymatic hydrolysis was effectively taking place and the oxidation of the double bonds did not yet take place during this stage. During 24 hours, the concentrations of MUFAs and PUFAs were continuously increased, however, the quantity of SFAs also appeared to rise, which may indicate the start of an oxidation process occurring at the same time as the enzymatic hydrolysis ongoing with the increase of hydroperoxides as observed in previous studies.<sup>33,72</sup> In order to obtain high concentration of polyunsaturated fatty acids, the six-hour-autolysis showed to be the optimal

time  $5002 \pm 145.6 \mu\text{g/g}$  of dry biomass. After which time, 6 hours, the production of PUFAs significantly slowed down and stabilised with the concentration detected of  $5498 \pm 24.9 \mu\text{g/g}$  of dry biomass. Leaving the enzymatic process for an extended time at room temperature was not recommended to obtain higher concentration of polyunsaturated fatty acids as the autoxidation might occur.<sup>271</sup> As the study focused on the production of PUFAs, especially ARA, EPA and DHA, the changing trend on their concentrations must be taken into account in priority, the optimal autolysis time will therefore be determined according to the abundance of those three PUFAs.

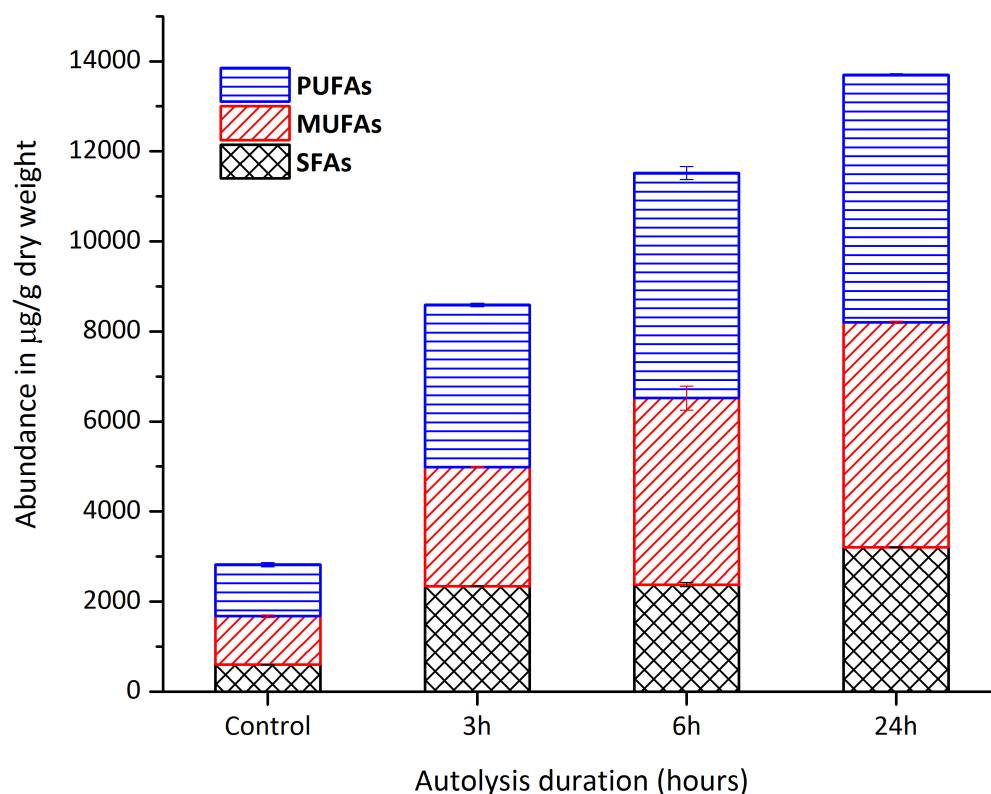


**Figure 5-5** Concentrations of saturated fatty acids (SFAs), monounsaturated fatty acids (MUFAs) and polyunsaturated fatty acids (PUFAs) after autolysis of 3, 6 and 24 hours at room temperature. (scCO<sub>2</sub> extraction at 40 °C, 400 bar for 2 hours)

**Figure 5-6** illustrates the increase trends of the three targets PUFAs which are ARA, EPA and DHA during autolysis of 3, 6 and 24 hours prior to scCO<sub>2</sub> extraction at 40 °C, 400 bar for 2 hours. In comparison with the control experiment, the sharpest increase of those PUFAs was observed with 3-hour autolysis experiment. ARA importantly increased with a 4.5-fold increase ( $134.9 \pm$

1.2 (3 hours)  $\mu\text{g/g}$  dry weight) compared to the control in 3 hours autolysis ( $29.7 \pm 1.5$  (control)). After this time the concentration of ARA only increased slightly after 6-hour autolysis to  $142.7 \pm 0.6 \mu\text{g/g}$  dry weight and finally a modest decline was recorded after being left for 24 hours of autolysis. EPA followed relatively similar pattern of the ARA, the most significant increase took place within the initial 3 hours of autolysis ( $300.1 \pm 1.6$  (3 hours)  $\mu\text{g/g}$  dry weight) compared to the control ( $84.8 \pm 10.5$ (control)). A slight increase was seen after 6 hours with the total concentration of EPA  $376.2 \pm 4.0 \mu\text{g/g}$  dry weight and at the end of 24 hours, the concentration of EPA obviously declined to  $299.3 \pm 4.0 \mu\text{g/g}$  dry weight. In the case of DHA that is the most abundant of those three target PUFAs, the dramatic increase, very sharp compared to the ARA and EPA, also occurred with a 3.5-fold to the control the extract of 3-hour autolysis ( $195.3 \pm 14.8$ (control) and  $698.4 \pm 29.5$  (3 hours)  $\mu\text{g/g}$  dry weight). DHA continued to increase efficiently, a little less, when 6-hour autolysis was carried on with the highest concentration of DHA at  $924.1 \pm 13.7 \mu\text{g/g}$  dry weight, before dropping notably to  $574.6 \pm 13.7 \mu\text{g/g}$  dry weight. The repeated declines of ARA, EPA and DHA after 24-hour autolysis provides some further evidence of the auto-oxidation or decomposition during the autolysis process; it was therefore unsuitable to leave the fresh prawn waste longer than 6 hours in order to successfully obtain the highest concentration of ARA, EPA and DHA. In order to confirm the optimum condition, comparison of ARA, EPA and DHA via  $\text{scCO}_2$  extraction with conventional hexane Soxhlet should be made and discussed

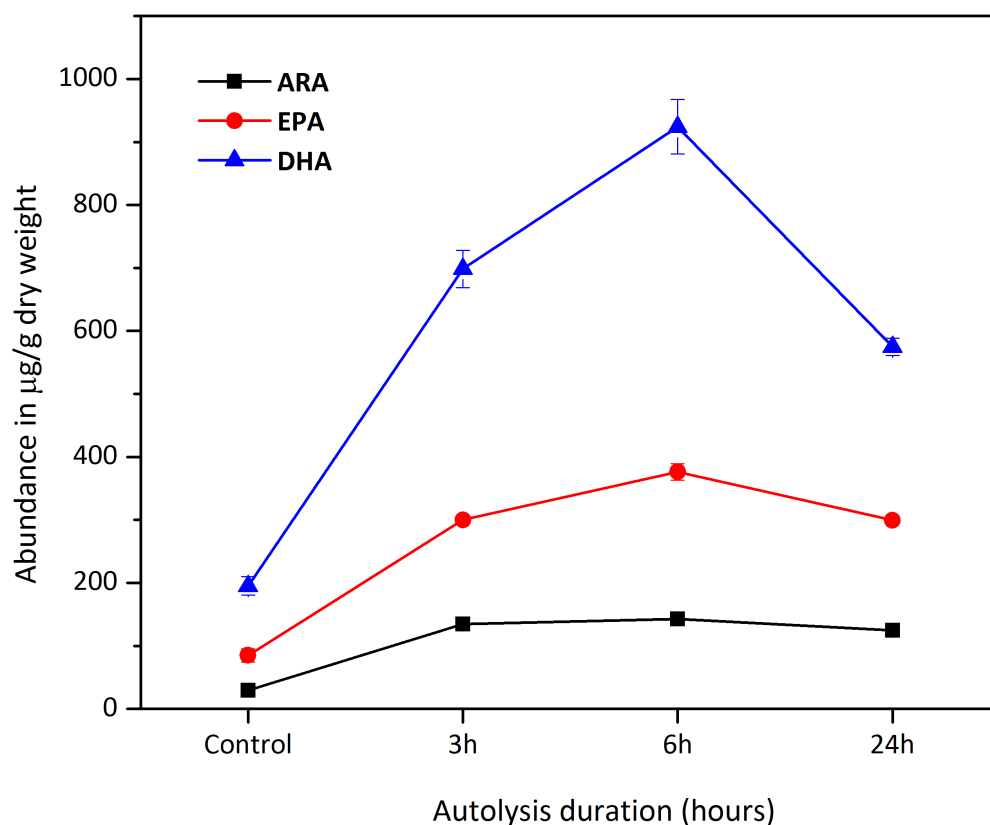


**Figure 5-6** The increase trend of ARA, EPA and DHA after autolysis of 3,6 and 24 hours via scCO<sub>2</sub> extraction at 40 °C, 400 bar for 2 hours.

As it was previously seen in the Chapter 5 that scCO<sub>2</sub> extraction of fresh prawn waste had dramatically lower yields as compared to the traditional hexane Soxhlet extraction. As the latter proved to be more effective in terms of both extraction yield and lipid composition, especially PUFAs hexane was previously indicated to be a more efficient extraction method for the high moisture content prawn by-product, with high lipid recovery, 8.3 % of dry biomass compared to scCO<sub>2</sub> extraction, 1.1% of dry biomass (see **Figure 5-3**). Regarding the total lipid recovery, hexane is still the most suitable extraction method with the highest yield of crude lipid compared with all the autolysis experiments. However, with regard to the concentrations of PUFAs, especially those three PUFAs in question: ARA, EPA and DHA, scCO<sub>2</sub> extraction combined with autolysis process appeared to be more potent for the production of ARA, EPA and DHA.

In **Figure 5-7**, autolysis outstandingly enhanced the concentration of those three PUFAs, particularly EPA and DHA compared to those of hexane extract. By leaving the prawn waste at



room temperature for 3 or 6 hours before scCO<sub>2</sub> extraction, the quantities of EPA were about 3-fold and 4-fold respectively ( $300.1 \pm 1.2 \mu\text{g/g}$  dry weight (3 hours) and  $376.2 \pm 4.0 \mu\text{g/g}$  dry weight (6 hours)) compared with that of hexane extract ( $118.2 \pm 0.8 \mu\text{g/g}$  dry weight). Similarly, the amount of DHA was doubled of the hexane extract with 6-hour autolysis,  $489.0 \pm 10.4$  and  $924.1 \pm 13.7 \mu\text{g/g}$  of dry weight for hexane and 6-hour-autolysis extracts respectively. As consequence, it is conclusive to say that 6-hour autolysis at room temperature is the optimum duration to effectively produce to ARA, EPA and DHA.

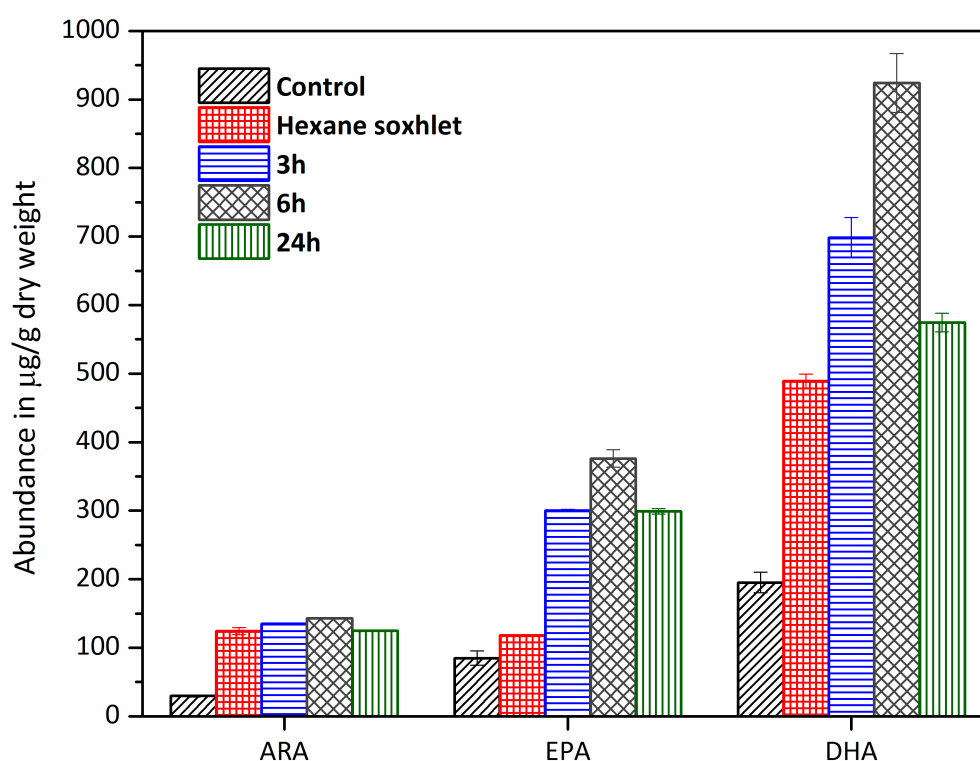


**Figure 5-7** Comparison in abundance of ARA, EPA and DHA between scCO<sub>2</sub> extraction in 2 hours at 40 °C, 400 bar, with 3, 6 and 24 hours autolysis and hexane soxhlet extraction of fresh prawn waste in 2 hours.

An increase in cholesterol was also the other main concern in the enzymatic process as it is considered as undesirable in dietary.<sup>234</sup> Crustaceans such as prawn have a lack of sterol-synthesizing ability and require sterols for growth. In crustaceans, there are two forms of cholesterol, free cholesterol and esterified cholesterol.<sup>272</sup> The latter can be hydrolysed by

cholesterol esterase for the generation of a higher yield.<sup>273</sup> It was previously reported in this study that ARA, EPA and DHA continuously increased within the initial 6 hours of autolysis, and then a significant decrease was recorded after 24 hours. In contrast, the concentration of cholesterol was proportional to the autolysis duration with a linear increase trend, illustrating in **Figure 5-8**. Importantly, there were 5-fold, an 8-fold and a 25-fold increases in cholesterol concentration detected in the scCO<sub>2</sub> extracts of 3, 6 and 24 hours of autolysis respectively compared to the control experiment. The abundance continuously rose from 45.0 ± 11.6 µg/g dry weight in the control experiment to 239.9 ± 3.1, 357.2 ± 19.1 and 1142.2 ± 2.6 µg/g dry weight in the extracts of 3, 6 and 24 hour-autolysis respectively. It was not surprised as scCO<sub>2</sub> was found to be an effective extraction method for cholesterol in goat pancetta at 47.5 °C, 300 bar)<sup>234</sup>. Despite the increasing cholesterol yields by scCO<sub>2</sub> extraction as a function of autolysis time, the yields were still lower than that of hexane soxhlet extraction for 4 hours, 1538.0 ± 11.6 µg/g dry weight in the hexane extracts (4 hour extraction) as compared to 1142.2 ± 2.6 µg/g dry weight in the extracts of 24 hour-autolysis as extracted by scCO<sub>2</sub>. This is a distinct advantage, especially when autolysis after the optimal 6 hours yields only 357.2 ± 19.1 µg/g dry weight. Importantly, scCO<sub>2</sub> leaves no solvent residues at the end of extraction, which could be considered a distinct advantage over hexane extracts for food or nutraceutical applications.

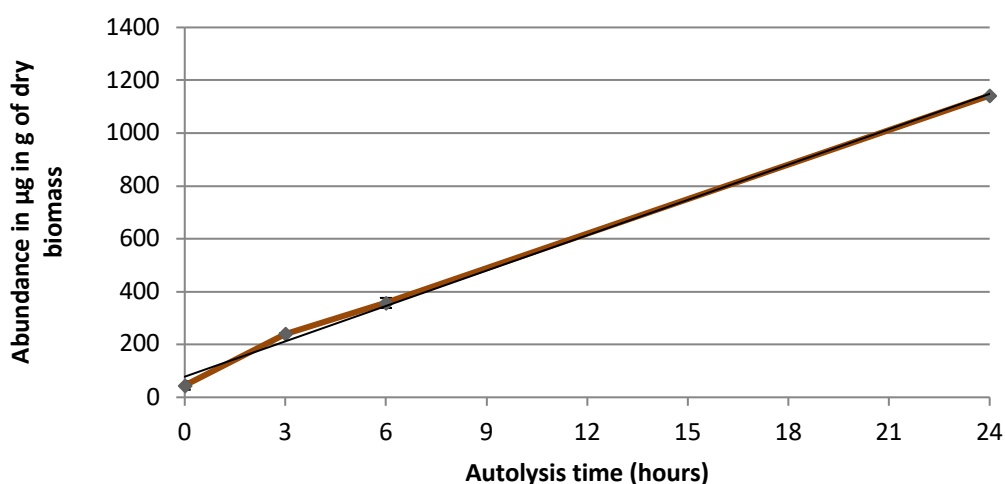


**Figure 5-8** Increasing linear trend of cholesterol after autolysis 3, 6 and 24 hours.

### 5.3.3 Proposed enzymatic process during autolysis of prawn by-product.

In all experiments of the study on the prawn waste biorefinery, only head part of *L. vannamei* was used, it includes the mixture of the cephalothorax and hepatopancreas (digestive organ). Cephalothorax and hepatopancreas of *L. vannamei* contain highly active protease, which has comparable activity to Alcalase.<sup>230,274</sup> As discussed earlier, lipoproteins were cleaved to a higher extent during the time of autolysis. Therefore, lipids were liberated from proteins and the scCO<sub>2</sub> extraction efficiency became higher when the hydrolysis by endogenous protease was ongoing. Moreover, hepatopancreas is the major source of lipase, which is able to hydrolyse the ester bond of triglycerides.<sup>269</sup> Lipases and phospholipases are crucial enzymes in lipid hydrolysis. Generally, enzymatic hydrolysis of lipid is able to perform in the presence of moisture content and heat.<sup>275</sup>

In previous research of Takeungwongtrakul *et al.*, lipid profiles of cephalothorax and hepatopancreas of *L. vannamei* were separately investigated and quantified in **Table 5-3**.<sup>203</sup> It was noted that lipid from cephalothorax had phospholipids (PL) as major lipophilic components with 82.51% of total lipid content, followed by triglycerides (TG) and diglycerides (DG) accounting for 8.88% and 5.08% of total lipid content respectively. In hepatopancreas, 43.35% TG were identified and 38.08% of PL was presented. In this study, the mixture of cephalothorax and hepatopancreas was used, PL and TG were assumed to be in high concentration. This data will be used as reference of lipid composition in this study as the origin of biomass was the same, Thailand.

**Table 5-3** Composition of lipids extracted from cephalothorax and hepatopancreas of Pacific white shrimp (*Litopenaeus vannamei*) using Bligh and Dyer method.<sup>72</sup>

Raw materials	Composition (% of total lipid content)				
	TG	FFA	DG	MG	PL
Cephalothorax	8.88 ± 0.85	2.68 ± 0.12	5.08 ± 0.64	0.84 ± 0.54	82.51 ± 1.92
Hepatopancreas	43.35 ± 3.90	8.71 ± 1.30	4.12 ± 0.63	3.79 ± 0.26	38.03 ± 5.71

Hepatopancreas was the main organ for lipid storage in crustaceans including prawn. The majority of lipid is stored in the form of lipoprotein mainly composed of triglycerides, phospholipids and cholesterol.<sup>33,207,270,276</sup> Hepatopancreas is digestive organ, which contains various enzymes such as protease, lipase and carbohydrase.<sup>257</sup> In this study, the aim is to investigate the lipid composition and the production of PUFA. Therefore, the enzymes in question are the ones involving in the hydrolysis process including protease, lipase, phospholipase and cholesterol esterase. **Figure 5-9** illustrates enzymatic hydrolysis process (starting from lipoproteins), which could possibly occur in the prawn by-product containing hepatopancreas as source of endogenous enzymes including protease, lipase, phospholipase and cholesterol esterase.<sup>33,230,256,257</sup> Plasma lipoproteins are composed of a hydrophobic core of cholesterol esters and triglycerides coated by an outer part layer consisting of amphiphilic phospholipids, non-esterified cholesterol and apolipoproteins.<sup>277</sup> Different types of enzymatic hydrolysis were simultaneously taken place during autolysis of the prawn wastes. Active protease of *L. vannamei* hepatopancreas was used previously in the lipid extraction process in order to increase the extraction yield from striped catfish muscle. At the moment of the hydrolysis occurred, molecules of proteins coexisted with lipids such as lipoprotein and protein-lipid complex were hydrolysed to liberate lipids from the proteins.<sup>230,267</sup> As a result, neutral and polar lipids, free and esterified cholesterols, phospholipids and triglycerides were released due to the breakdown of protein network. This step of hydrolysis is responsible for the increase in extraction yield. Then, these high molecular weight lipid components were hydrolysed at higher extent. Lipase has its natural substrates, which are primarily long chain fatty acid triacylglycerides and the main products produced are monoacylglycerides and free fatty acids. Phospholipases catalyse the cleavage of phospholipids, some phospholipase is able to react with other lipid substrates such as triglycerides, resulting in free fatty acids and other compounds.<sup>278</sup> Cholesterol esterase is another endogenous enzyme involved in this process, as it is normally found in pancreas and catalyses the hydrolysis of sterol esters into their corresponding component sterols and free fatty acids.<sup>273</sup> From the activities mentioned, it can be clearly seen why the concentration of the free fatty acids was significantly affected during the autolysis, since these three enzymes existing in the prawn waste coincidentally resulted in free fatty acids. Moreover, other by-products including monoglycerides, diglycerides and cholesterol are considered as indicators of hydrolysis process.

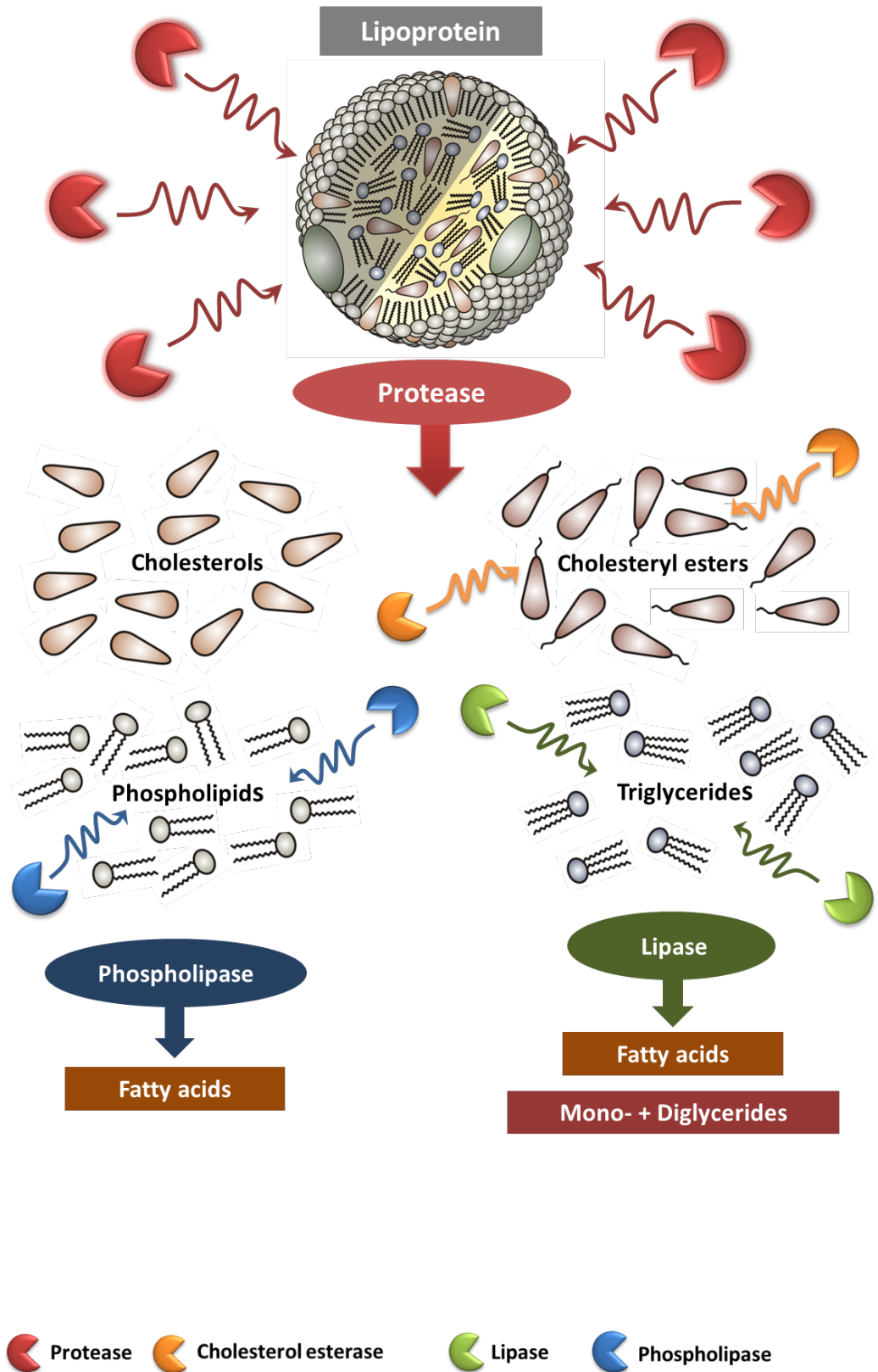


Figure 5-9 Proposed enzymatic process during autolysis of prawn-by products.

The digestive enzymes of crustaceans have been studied for a long time period for applications in physiology, biochemistry and food science.<sup>252,255,279</sup> Serine proteases trypsin and chymotrypsin are the most common digestive enzyme found in crustaceans. These digestive enzymes have their highest activities under neutral or slightly alkaline conditions, around pH 8.<sup>279</sup> The Pacific white shrimp (*L. vannamei*) had the highest activity at alkaline pH compared with *P. stylirostris* and *P. calofoniensis*. Moreover, the mid gland of *L. vannamei* had the highest proteolytic activity towards synthetic specific substrates.<sup>279</sup> Senphan and Benjakul was found that the maximum autolysis of hepatopancreas of *L. vannamei* could be observed at 60 °C with the highest rate of hydrolysis of lipoprotein.<sup>33</sup>

#### **5.4 Effect of temperature and different atmospheres on autolysis of prawn waste**

It was previously reported that the hepatic enzyme found within the hepatopancreas of Pacific white shrimp, was responsible for enzymatic hydrolysis resulting in higher lipid content in the prawn waste.<sup>33</sup> Generally, proteolytic enzymes are highly active in a wide temperature range from 40-70 °C.<sup>270,280</sup> Autolysis of muscle protein in crustacean seafood occurs rapidly after harvest and has been attributed to digestive protease. Moreover, the hepatopancreas of panaeids is known to have high proteolytic activities.<sup>255</sup> It was previously discussed that different drying methods had crucial influence on extraction efficiency of scCO<sub>2</sub> and the composition of lipid compounds within the extraction especially n-3 and n-6 PUFAs (ARA, EPA and DHA). Oven-drying at 50 °C yielded the highest quantities of ARA, EPA and DHA among all the selected methods as the autolysis effectively occurred at this temperature. Secondly, autolysis duration also had considerable influence on the production of ARA, EPA and DHA as extending time to 24 hours resulted in auto-oxidation of PUFAs and higher amount of SFAs. Therefore, further investigation on the effect of temperature as well as different atmospheres will be carried on herein. The study is based on 24-hours autolysis as the auto-oxidation in different atmospheres including air, vacuum and nitrogen will be evaluated and the add-on experiment of pre-treating the biomass at 105 °C was performed to see how the denaturation of the biomass affect the

lipid composition. After all the selected pre-treatment conditions, the resulting prawn residues were extracted using scCO<sub>2</sub> at 40 °C, 400 bar for 2 hours and analysed and quantified by GC-FID.

#### 5.4.1 Extraction yields

**Figure 5-10** presents yields obtained by scCO<sub>2</sub> following different pre-treatment conditions. The experiment at room temperature will be considered as the control in the following comparisons. The lowest yield belonged to the control experiment; result was taken from the previous study, with the total crude lipid recovery 3.3% dry biomass. Then, treating the prawn by-product at 105 °C in the oven and 50 °C in the vacuum-oven similarly yielded 3.9% of total crude extract. Next, heating the waste biomass in the presence of air using water bath at 50 °C, was able to double the total lipid recovery of the control experiment and yielded 6.7% dry weight. Finally, the highest lipid yield was obtained by treating the prawn residue under nitrogen atmosphere in a water bath with 7.5% dry weight. It was clear that different atmospheres had essential influence on the scCO<sub>2</sub> extraction efficiency as well as temperature. Heating the biomass at 105 °C did not have positive effect on the extraction even though the moisture content was completely removed and was likely to be a result of denaturing of the enzyme. Moreover, the autolysis still occurred normally and effectively under inert atmosphere and either in the presence or absence of air.

It is documented in previous studies that enzymatic lipid extraction provided by either endogenous or commercial proteases was responsible for the increases in total lipid recovery.<sup>33,230,267,268,280</sup> When hydrolysis by protease occurred, proteins associated with lipids such as lipoproteins and protein-lipid complex were broken down to a higher extent. As consequence, lipids, polar and neutral molecules, were released from the protein matrix.<sup>33</sup> Identical results were obtained in hydrolysis of cuttlefish and sardine viscera using Protamex™, Alcalase and Flavourzyme in which neural lipids and large amount of polar lipid were successfully obtained.<sup>266</sup> Nile perch and salmon heads were also enzymatically extracted using commercial proteases, bromelain and Protex 30L, in order to obtain n-3 fatty acids. Total lipid recoveries of 11.2% and 15.7% of wet weight were obtained from Nile perch and salmon heads, respectively compared to 13.8% and 17.6%, respectively yielded by solvent extraction.<sup>268</sup> However, the full quantification of each group of lipophilic compounds, especially free fatty acids is needed to be discussed thoroughly about the production of PUFA and the suitability of the process.

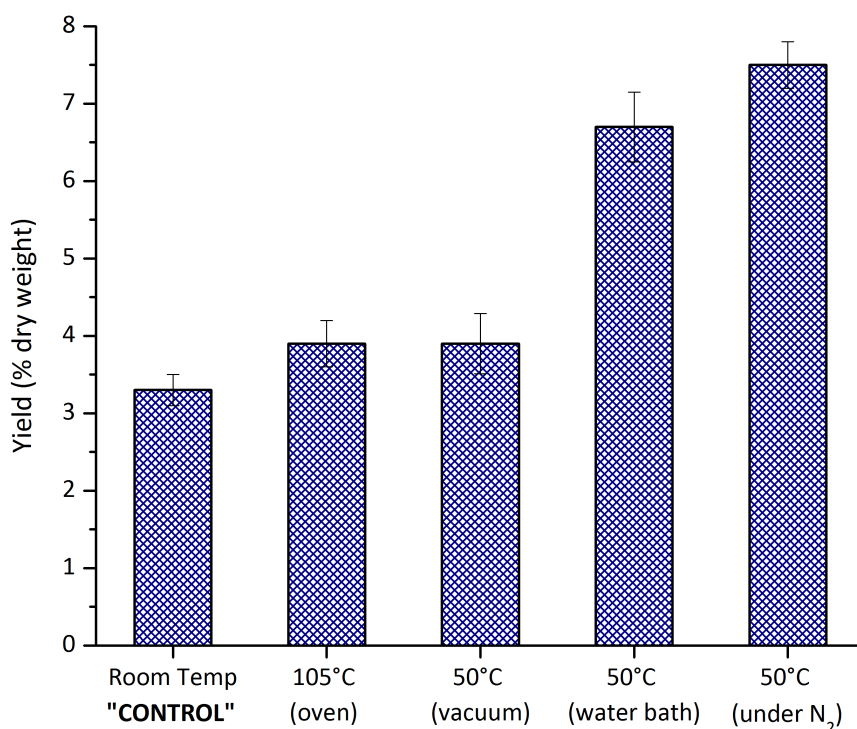


**Figure 5-10** Yields of crude lipid by scCO<sub>2</sub> in 2h after different condition of autolysis for 24h.

As previously discussed, the enzymatic hydrolysis occurred during the drying process in the vacuum oven at 50 °C, resulted in higher extraction efficiency mainly due to low moisture content of the prawn waste samples and the endogenous enzymatic process. Herein, the pre-treatment via vacuum-oven did not show to be the best option for either extraction efficiency or crude lipid recovery. The experiments at 50°C in the air and under nitrogen heated by water bath proved to be the more effective choices as the yields were significantly higher despite of relatively high moisture content (6.7% and 7.5% in the atmosphere and under nitrogen respectively). The biomasses were still wet with high moisture content (50-60%) after pre-treatment and before scCO<sub>2</sub> extraction. This therefore highlights the importance of autolysis prior to scCO<sub>2</sub> extraction, which may inhibit this process during extraction.

Prawn by-product contains large quantities of triglycerides and phospholipids.<sup>271</sup> It is logical to say that the amount of triglycerides in the prawn by-product decreased with increasing of fatty acids as the enzymatic hydrolysis underwent. In scCO<sub>2</sub>, fatty acids are soluble in higher pressure; however, triglycerides are, at pressure below 96 bar.<sup>258</sup> Also, increasing in molecular weight of a compound leads to a decrease in its solubility within scCO<sub>2</sub>.<sup>230,267,268,280</sup> Therefore, the low extraction yield was obtained in the control experiment (1.3% dry weight), assuming that no



autolysis occurred, as the majority of lipid compounds were in the form of high molecular weight as TG and PL, which were barely extractable by scCO<sub>2</sub> at 40°C, 400 bar. Since, the autolysis took place within the biomass, TG transformed into free fatty acids resulting in lower TG in the sample. These fatty acids released can be easily extracted under this scCO<sub>2</sub> condition. This is the reason why the yields were high at pre-treatment at 50°C in the atmosphere and under nitrogen (6.7% and 7.5% respectively), as there were more fatty acids available to be extracted.<sup>236</sup>

#### 5.4.2 Quantification of lipophilic compounds

To be able to discuss the influence of each factor, there is not only the extraction yield, which should be taken into account but the quantification of lipophilic compounds is crucial. The full quantification is presented in **Table 5-4**. There were three groups of compounds of which the concentrations of the extract changed dramatically as they are the main products of enzymatic hydrolysis. Fatty acids, sterols, monoglycerides and diglycerides were the most affected in terms of concentration due to different conditions of pre-treatment applied. Therefore, the detail discussion is needed further. Apart from these molecules, the concentration of fatty alcohols and ethers of glycerol varied, 1-*O*-hexadecylglycerol and 1-*O*-octadecylglycerol, even though they were insignificant. The lipid composition of prawn by-product was importantly affected by the pre-treatment methods employed. Fatty alcohol was obtained at the highest concentration after Pre-treating the prawn waste at 50 °C in the air with  $17.7 \pm 0.1$  µg/g of dry biomass, whereas, the lowest concentration was recorded in the control experiment, at room temperature,  $3.1 \pm 0.3$  µg/g of dry biomass. Unlike the ethers of glycerol, the greatest amount was recovered with the vacuum-oven pre-treated sample with the concentration of  $40.2 \pm 1.1$  µg/g of dry biomass and the lowest belonged to the experiment under nitrogen with  $16.6 \pm 1.1$  µg/g of dry biomass.

**Table 5-4** Abundances (in µg/g dry biomass) of lipid as extracted by supercritical carbon dioxide in 2 hours of prawn by-product after autolysis in different conditions in 24 hours

Compounds	Autolysis conditions				
	Room Temp.	105°C (oven)	50°C (vacuum)	50°C (water bath)	50°C (under N <sub>2</sub> )
<b>Free fatty acids</b>					
C12:0	39.8 ± 0.7	5.6 ± 0.3	1.4 ± 0.1	93.0 ± 1.0	108.6 ± 0.8
C14:0	153.1 ± 0.9	121.9 ± 1.9	536.6 ± 3.7	548.9 ± 4.3	469.9 ± 5.1
C15:0	65.2 ± 0.3	38.2 ± 1.1	273.7 ± 4.1	281.4 ± 0.3	266.1 ± 2.1
C16:1 (n-7)	552.8 ± 1.1	352.5 ± 1.6	1379.0 ± 3.2	1427.1 ± 17.7	1423.6 ± 2.7
C16:0	2151.6 ± 0.7	1161.9 ± 13.1	8819.2 ± 1.7	9366.8 ± 46.4	8893.2 ± 54.2
C17:1 (n-7)	86.9 ± 8.7	42.1 ± 3.6	255.7 ± 5.8	286.9 ± 2.0	284.0 ± 0.3
C17:0	54.3 ± 3.9	30.2 ± 0.5	261.4 ± 23.8	365.2 ± 38.1	310.3 ± 1.2
C18:2(n-6)					12201.2 ±
	4222.4 ± 6.6	2199.8 ± 44.6	8604.1 ± 32.9	11821.8 ± 6.3	327.7
C18:1(n-9)			5587.7 ±		8276.9 ±
	3649.6 ± 6.5	1836.3 ± 38.5	303.4	8052.8 ± 33.9	283.4
C18:1(n-7)	490.2 ± 7.0	392.0 ± 7.9	870.4 ± 2.6	1474.0 ± 7.8	1440.4 ± 12.5
C18:0	662.8 ± 0.9	358.4 ± 6.5	1754.8 ± 4.5	2285.9 ± 8.9	2150.9 ± 10.6
C20:5 (n-3) (EPA)	299.3 ± 4.0	197.7 ± 2.7	695.5 ± 6.7	782.1 ± 1.7	1560.5 ± 6.2
C20:4 (n-6) (ARA)	124.6 ± 0.6	80.1 ± 0.8	317.8 ± 1.2	459.9 ± 1.5	734.2 ± 15.7
C20:2 (n-6)	277.7 ± 0.0	209.9 ± 6.4	668.4 ± 14.9	1024.2 ± 17.8	1075.6 ± 25.1
C20:1 (n-9)	185.9 ± 1.8	99.0 ± 2.2	490.2 ± 3.2	724.9 ± 10.3	745.6 ± 0.8
C20:0	45.4 ± 0.7	22.4 ± 2.0	157.4 ± 2.0	169.5 ± 6.7	147.1 ± 17.1
C22:6 (n-3) (DHA)	574.6 ± 13.7	316.6 ± 3.3	1280.4 ± 26.9	2276.7 ± 9.5	3583.4 ± 26.5
C24:1 (n-9)	30.8 ± 0.4	36.0 ± 0.3	3.7 ± 0.7	88.2 ± 5.5	84.1 ± 2.3
C24:0	33.2 ± 0.0	40.7 ± 0.5	32.5 ± 2.6	20.3 ± 1.1	19.3 ± 0.6
<i>Total SFA</i>			11837.1 ±	13131.1 ±	12365.6 ±
	3205.3 ± 8.1	1779.2 ± 25.8	42.5	106.9	91.7
<i>Total MUFA</i>	4996.1 ±		8586.7 ±	12053.9 ±	12254.6 ±
	25.4	2757.9 ± 54.2	318.9	77.1	302.1
<i>Total PUFA</i>	5498.7 ±		11566.1 ±	16364.8 ±	19154.9 ±
	24.9	3004.1 ± 57.8	82.7	36.8	401.2
<b>Total fatty acids</b>	<b>13700.1 ±</b>	<b>7541.2 ±</b>	<b>31990.0 ±</b>	<b>41549.7 ±</b>	<b>43775.1 ±</b>
	<b>58.4</b>	<b>137.8</b>	<b>444.1</b>	<b>220.7</b>	<b>795.0</b>

<b>Fatty alcohol</b>					
1-hexadecanol	3.1 ± 0.3	7.4 ± 0.2	9.0 ± 1.2	17.7 ± 0.1	4.1 ± 0.3
<b>Total fatty alcohol</b>	<b>3.1 ± 0.3</b>	<b>7.4 ± 0.2</b>	<b>9.0 ± 1.2</b>	<b>17.7 ± 0.1</b>	<b>4.1 ± 0.3</b>
<b>Monoglycerides</b>					
β-glyceryl pentadecanoate	5.1 ± 0.1	7.1 ± 0.1	4.7 ± 1.0	7.9 ± 0.8	16.4 ± 0.6
β-glyceryl palmitate	57.1 ± 0.8	69.2 ± 4.2	39.8 ± 2.9	50.7 ± 5.2	94.2 ± 0.3
α-glyceryl palmitate	214.3 ± 0.4	267.1 ± 0.5	24.2 ± 1.8	63.8 ± 4.6	79.6 ± 5.0
α-glyceryl heptadecanoate	5.4	6.8 ± 0.3	11.3 ± 1.5	38.8 ± 0.0	25.6 ± 3.0
α-glyceryl stearate	21.5	16.2 ± 0.2	11.7 ± 0.7	73.6 ± 1.2	15.4 ± 1.0
β-glyceryl oleate	93.7 ± 1.5	119.2 ± 0.1	6.2 ± 0.9	34.8 ± 1.4	39.5 ± 0.6
α-glyceryl oleate	10.7	10.3 ± 0.1	1.8 ± 0.2	8.1 ± 0.1	17.3 ± 0.3
<b>Total monoglycerides</b>	<b>407.8 ± 2.9</b>	<b>496.0 ± 5.5</b>	<b>99.6 ± 9.1</b>	<b>277.8 ± 13.3</b>	<b>288.0 ± 10.9</b>
<b>Diglycerides</b>					
Glycerol 1,2-dipalmitate	13.2	31.3	0.2	9.4 ± 3.2	6.1
Glycerol 1,3-dipalmitate	22.8 ± 0.2	42.6 ± 0.5	0.3	3.5 ± 0.1	12.3 ± 0.1
<b>Total diglycerides</b>	<b>36.0 ± 0.3</b>	<b>74.0 ± 0.5</b>	<b>0.5</b>	<b>12.9 ± 3.3</b>	<b>18.4 ± 0.1</b>
<b>Ethers of glycerol</b>					
1-O-hexadecylglycerol	7.9	9.1	23.4 ± 0.3	8.8	8.1 ± 0.6
1-O-octadecylglycerol	9.6 ± 0.1	19.7 ± 1.3	16.8 ± 0.8	19.5 ± 0.4	8.5 ± 0.5
<b>Total ethers of glycerol</b>	<b>17.5 ± 0.1</b>	<b>28.8 ± 1.3</b>	<b>40.2 ± 1.1</b>	<b>28.3 ± 0.5</b>	<b>16.6 ± 1.1</b>
<b>Sterols</b>					
Cholesterol	1142.2 ± 2.6	1145.5 ± 10.8	1305.6 ± 32.3	920.3 ± 33.9	1160.8 ± 10.7
Campesterol	20.8 ± 0.2	18.9	25.7 ± 1.3	21.8 ± 1.5	19.4
Stigmasterol	12.6 ± 0.4	10.1 ± 0.4	21.9 ± 1.4	9.5 ± 0.5	3.6
β-sitosterol	33.9 ± 0.5	22.4 ± 0.1	33.6 ± 1.0	22.7 ± 0.7	27.4 ± 0.3
<b>Total sterols</b>	<b>1209.6 ± 3.6</b>	<b>1196.9 ± 11.2</b>	<b>1386.8 ± 36.0</b>	<b>974.3 ± 36.6</b>	<b>1211.2 ± 11.0</b>
<b>Total identified</b>	<b>15374.2 ± 65.6</b>	<b>9344.3 ± 156.5</b>	<b>33526.0 ± 491.5</b>	<b>42860.7 ± 274.5</b>	<b>45313.5 ± 818.4</b>

**Figure 5-11** shows the groups of lipid constituents, which were affected by enzymatic hydrolysis during the autolysis experiments, these include free fatty acids, monoglycerides, diglycerides and sterols. Firstly, the changes in free fatty acids are the most remarkable among all. The concentration of free fatty acids was the lowest with  $496.0 \pm 5.5 \mu\text{g/g}$  of dry biomass in the pre-treatment condition with  $105^\circ\text{C}$  in the oven. At this temperature, the enzymes must be inactivated and denatured completely.<sup>281</sup> The prawn protease is found with high activity at temperature ranged from  $40\text{-}60^\circ\text{C}$ ,<sup>152</sup> and the optimal temperature for lipase from hepatopancreas of *L. vannamei* was reported with the range of  $30\text{-}50^\circ\text{C}$ .<sup>276</sup> Therefore, thermal damage and breakout of the enzyme must occur.<sup>239</sup> As a result, high concentration of sterols, MG and DG might be due to the thermal degradation of the lipoproteins as lipids in marine animals are usually stored in this form.<sup>267,268,270,282</sup> In general, hydrolysis of lipid is able to occur in the presence of moisture content and heat.<sup>275</sup> In the case of treating the prawn sample at  $105^\circ\text{C}$ , the evaporation of water rapidly decreased the moisture content available in the biomass. Therefore, reducing and stopping the enzymatic hydrolysis. Besides, it was reported that marine lipids are known to contain high content of PUFA which are likely prone to oxidation.<sup>283</sup> Autoxidation of lipid extracted from *L. vannamei* increased sharply when temperature of  $60^\circ\text{C}$  was applied. Even though this temperature was previously proved to be the optimum temperature for endogenous enzymatic hydrolysis of prawn waste,<sup>33,230</sup> the temperature of  $50^\circ\text{C}$  was selected in order to investigate the different atmospheres to avoid some degree of autoxidation.

The experiment under vacuum with the heating at  $50^\circ\text{C}$  demonstrated important increase in free fatty acids compared to the control experiment at room temperature ( $31990 \pm 444.1$  (vacuum) and  $13700.1 \pm 58.4$  (control)  $\mu\text{g/g}$  dry biomass), which indicated that higher temperature accelerated hydrolysis rate and increased lipolytic capability of the enzymes within the waste biomass. However, the free fatty acid concentration from this experiment was less significant compared with those of experiments under air and nitrogen,  $41549.7 \pm 220.2$  (air) and  $43775.1 \pm 795$  ( $\text{N}_2$ )  $\mu\text{g/g}$  dry biomass. This might be due to the fact that the prawn waste lost its moisture content relatively quickly and was completely dried after 24 hours. However, moisture content is one of the essential factors required in enzymatic hydrolysis. Consequently, the lipolytic properties of the enzyme decreased and were not able to carry on hydrolysis of the lipid matrix. Therefore, the concentrations of free fatty acids, monoglycerides and diglycerides

were less important compared to the other two experiments. However, high quantity of cholesterol was detected, which indicated that the cholesterol esters were successfully hydrolysed in this case and the free fatty acids identified were mainly the products from the hydrolysed cholesterols. The moisture content of the sample treated under air and nitrogen were still relatively high and the heat was present, the enzymatic hydrolysis carried on successfully with all the essential factors. The concentration of free fatty acids, cholesterols, mono- and diglycerides were found higher, which indicated the higher degree of hydrolysis of TG and possibly phospholipids. The experiments under air and nitrogen, not only enhanced dramatically the extraction efficiency showing in **Figure 5-10**, but also effectively increased the concentrations of free fatty acids with higher concentration than that of hexane extract. Moreover, the experiment under N<sub>2</sub> showed the highest yield and also the highest concentration of PUFA, which confirmed the dependence on temperature of the enzyme.

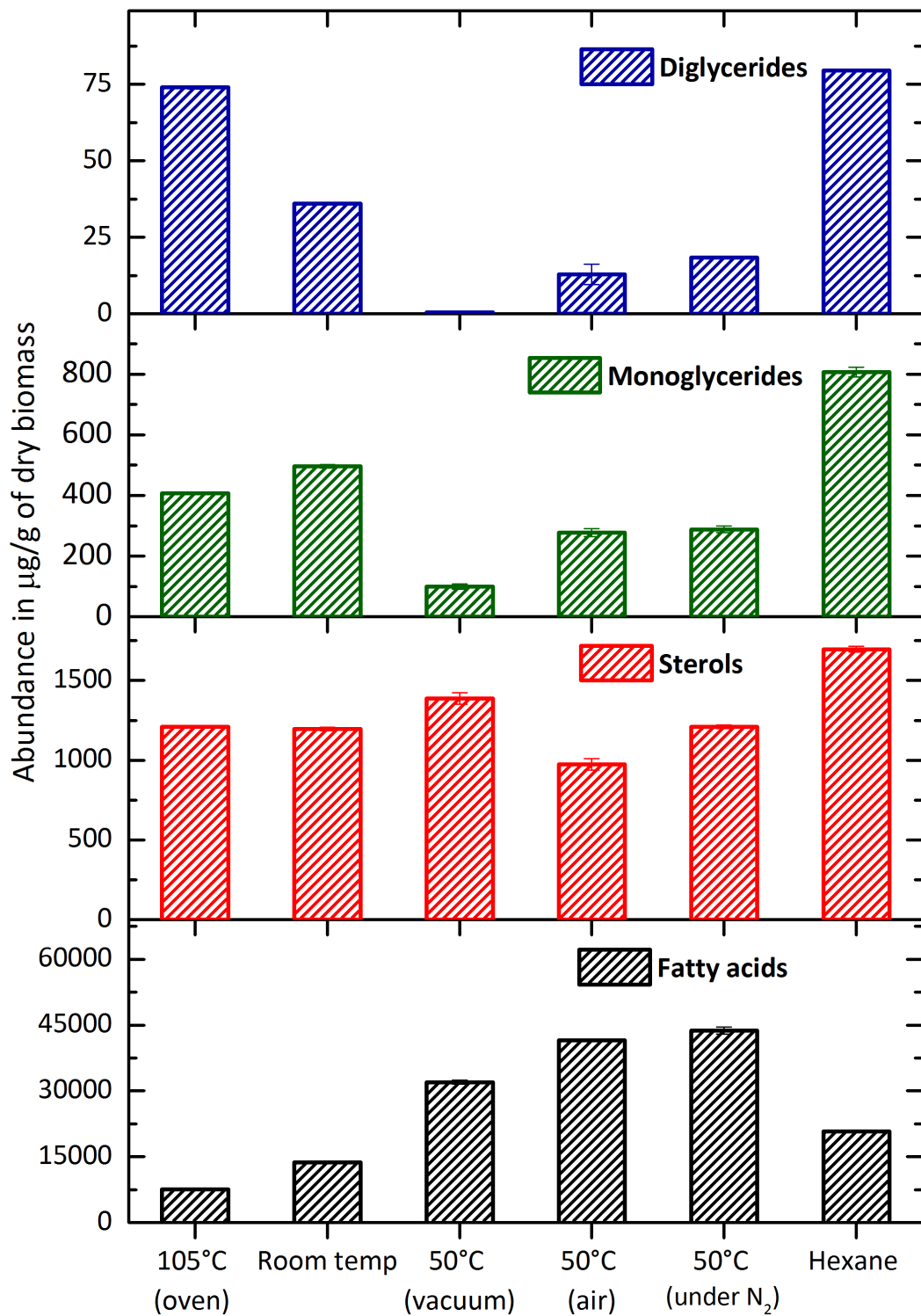


**Figure 5-11** Concentrations of A) Diglycerides B) Monoglycerides C) Sterols and D) Fatty acids with different pre-treatment conditions prior to scCO<sub>2</sub> extraction at 40 °C, 400 bar for 2 hours.

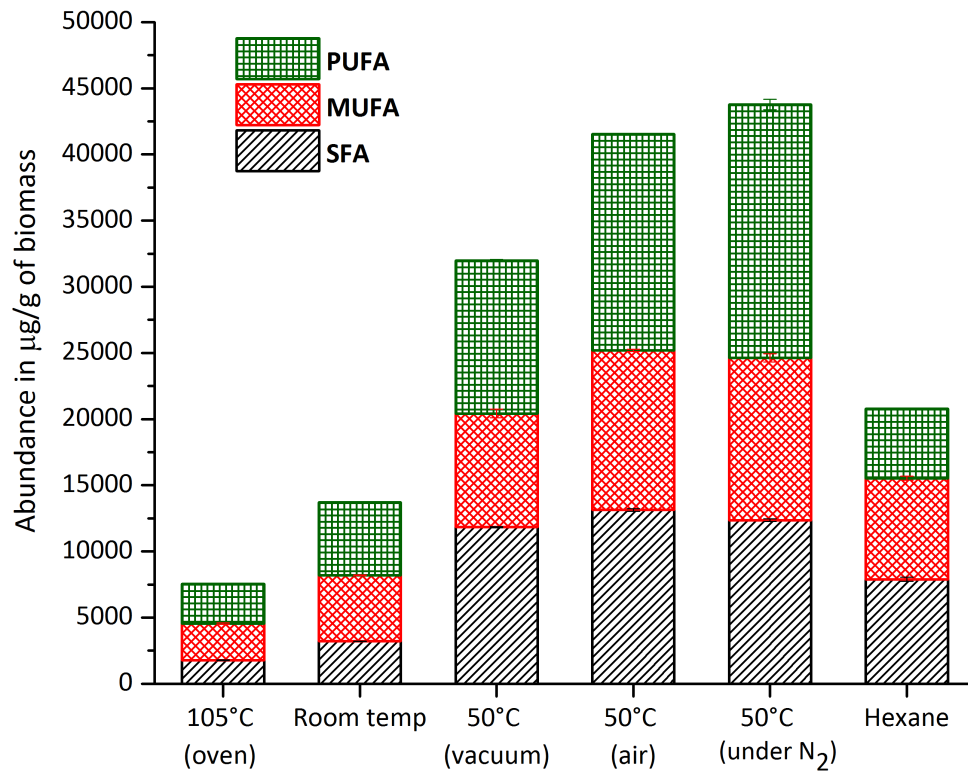


**Figure 5-12** Comparison of SFA, MUFA and PUFA from different conditions prior to scCO<sub>2</sub> extraction at 40 °C, 400 bar for 2 hours.

The increases in SFA, MUFA and PUFA were significant when the samples were pre-treated at suitable temperature (see **Figure 5-12**). The temperature of 105 °C was too high to allow enzymatic hydrolysis to occur resulting in the lowest concentrations of the three groups of free fatty acids. By applying heat at 50 °C, the amount of SFA, MUFA and PUFA increased efficiently. The abundance SFA from the extracts under vacuum, air and nitrogen were insignificantly different,  $11837.1 \pm 42.5$  (under vacuum),  $13131.1 \pm 106.9$  (air) and  $12365.6 \pm 91.7$  (nitrogen) µg/g of dry biomass. However, these increases were exceptional compared to that of the control ( $1779.2 \pm 25.8$  µg/g of dry biomass). The concentrations of MUFA were marked as considerable change in the extracts under air and nitrogen and less dramatic under vacuum compared to the control,  $2757.9 \pm 54.2$  (control),  $8586.7 \pm 318.9$  (under vacuum),  $12053.9 \pm 77.1$  (air) and  $12254.6 \pm 302.1$  (nitrogen) µg/g of dry biomass. The PUFA were produced at greatest concentration under nitrogen followed by under air and vacuum compared with the control, with the concentration of  $3004.1 \pm 57.8$  (control),  $11566.1 \pm 82.7$  (under vacuum),  $16364.8 \pm 36.8$  (air)

and  $19154.9 \pm 401.2$  (nitrogen)  $\mu\text{g/g}$  of dry biomass in the control, under vacuum, air and nitrogen extracts, respectively. The hexane extract was used to compare the efficiency of the process, all SFA, MUFA and PUFA detected in hexane were significantly lower than the extracts obtained under air, vacuum-oven and under nitrogen. This autolysis process with mild heating showed to be more effective than the conventional solvent extraction.

**Figure 5-13** demonstrates the breakdown concentrations of ARA, EPA and DHA in the  $\text{scCO}_2$ -extracts of prawn wastes pre-treated at  $50^\circ\text{C}$  under vacuum, air, nitrogen and  $105^\circ\text{C}$  in the oven and compared with hexane extract. Among all the three targets PUFA, ARA was present in the lowest concentration in prawn by-products followed by EPA and DHA was identified as the greatest amount in all of the  $\text{scCO}_2$ -extracts. The pre-treatment at  $105^\circ\text{C}$  reconfirmed to the least effective method for the production of the target PUFA, the concentrations of ARA, EPA and DHA obtained were lower than those of the control experiments. The experiments under vacuum, air and nitrogen proved to be more reliable towards the production of ARA, EPA and DHA. The best condition of pre-treatment was the autolysis under nitrogen followed by under air and vacuum compared to the control experiment,  $734.2 \pm 15.7$  (nitrogen),  $459.9 \pm 1.5$  (air),  $317.8 \pm 1.2$  (under vacuum) and  $80.1 \pm 0.8$  (control)  $\mu\text{g/g}$  of dry biomass from  $\text{scCO}_2$ -extracts. Similarly, EPA was successfully produced at the highest concentration under nitrogen atmosphere, followed by under air and vacuum, the EPA quantities recorded from the extracts under air and vacuum were comparable with the abundance order as follow  $1560.5 \pm 6.2$  (nitrogen),  $782.1 \pm 1.7$  (air),  $695.5 \pm 6.7$  (under vacuum) and  $197.7 \pm 2.7$  (control)  $\mu\text{g/g}$  of dry biomass. Identical trend was observed in DHA, the concentration of DHA pre-treated under nitrogen outstandingly yielded the highest amount of DHA compared with the control, a 6-fold higher,  $3004.1 \pm 57.8$  (control) and  $19154.9 \pm 401.2$  (nitrogen)  $\mu\text{g/g}$  of dry biomass. The experiments under vacuum and air also resulted in high amounts of DHA with  $11566.1 \pm 82.7$  (air) and  $16364.8 \pm 36.8$  2 (nitrogen)  $\mu\text{g/g}$  of dry biomass. Interestingly, the concentration of ARA, EPA and DHA obtained by hexane were dramatically lower compared to those obtained by  $\text{scCO}_2$  with pre-treatment at  $50^\circ\text{C}$  under air, vacuum and nitrogen. These results totally highlighted that the  $\text{scCO}_2$  combined with autolysis process is an alternative method to produce and obtain n-3 and n-6 PUFA especially ARA, EPA and DHA in high concentration.



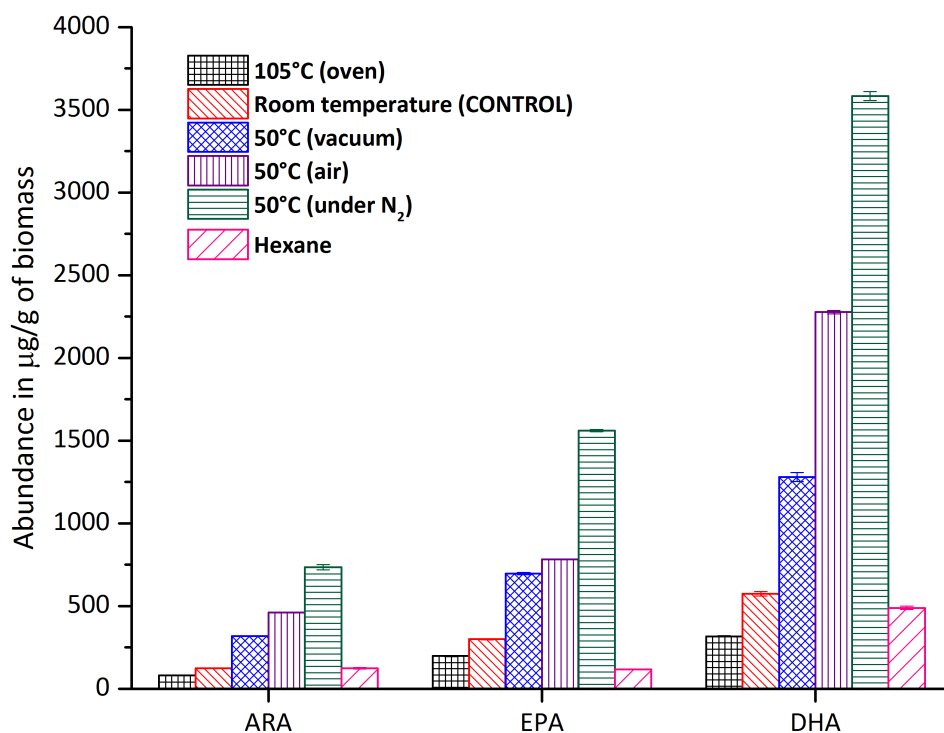


**Figure 5-13** Comparison of abundance in ARA, EPA and DHA from different conditions prior to scCO<sub>2</sub> extraction at 40°C, 400 bar for 2 hours.

A comparative study of lipase activity in hepatopancreas extracts from *L. vannamei* was carried on previously and was noted that this endogenous lipase has a tendency of hydrolysis towards long chain triglycerides such as triolein, tripalmitin and tristearin.<sup>257,276</sup> Furthermore, remarkable degree of hydrolysis was reported with  $\omega$ -3 series oil as shark oil and  $\omega$ -6 series oil as sunflower oil, sesame oil were utilized.<sup>257</sup> This is in accordance with the results obtained in this study as palmitic acid (C<sub>16:0</sub>) and oleic acid (C<sub>18:1(n-9)</sub>) were detected in very high concentration in extracts of *L. vannamei* wastes. Moreover,  $\omega$ -6 PUFA such as ARA and linoleic acid (C<sub>18:2(n-6)</sub>) were identified in high concentration especially linoleic acid, which was the most abundant free fatty acid in this prawn waste (See **Table 5-4** for full quantification). Furthermore, it was previously seen that the majority of lipid of pacific white shrimp by-products were in the form of phospholipids as in body tissue of fish (See **Table 5-3**).<sup>72,267</sup> Phospholipids are major lipid components of cell membranes and classed as lipid category of great interest due to their ability as carriers of long chain PUFA.<sup>284</sup> As a result, long chain PUFA were found to be particularly high

in phospholipid molecules and were considered to be readily prone to oxidative deterioration due to their high unsaturation degree of fatty acid composition.<sup>285</sup> In addition, autoxidation of lipid is generally accelerated by the presence of free fatty acids, mono- and diglycerides as well as the presence of heat with extended of processing time.<sup>33,271</sup> During the enzymatic process, lipids with more unsaturated are oxidized more quickly than less in unsaturated ones. Moreover, heat, metal catalysts, and ultraviolet and visible light can favour free radical formation of fatty acids or acylglycerols. Also, free fatty acids are more susceptible to autoxidation than esterified fatty acids.<sup>230</sup> From these reasons, it can be explained why the concentrations of PUFA including ARA, EPA and DHA were lower when the waste biomass was exposed to air compared with the experiment carried on under nitrogen atmosphere.

An attempt to use the prawn by-product as catalyst in the transesterification reaction of sunflower oil was carried on. Fatty acid methyl esters (FAME) were detected by GC-MS (see **Figure 5-14**). Endogenous lipase of *L. vannamei* was able to successfully convert TG into FAME. However, the conversion and yield were assumed to be low as the fresh biomass was used without prior purification. The prawn enzyme can potentially be used as catalyst in the production of biodiesel. However, further work would be needed for purification of the enzyme to increase the proportion of lipase and thus activity. An experimental design for optimal condition would also be an interesting addition to the future work. This prawn enzyme might be a new door to various chemical reactions for use in many industries.

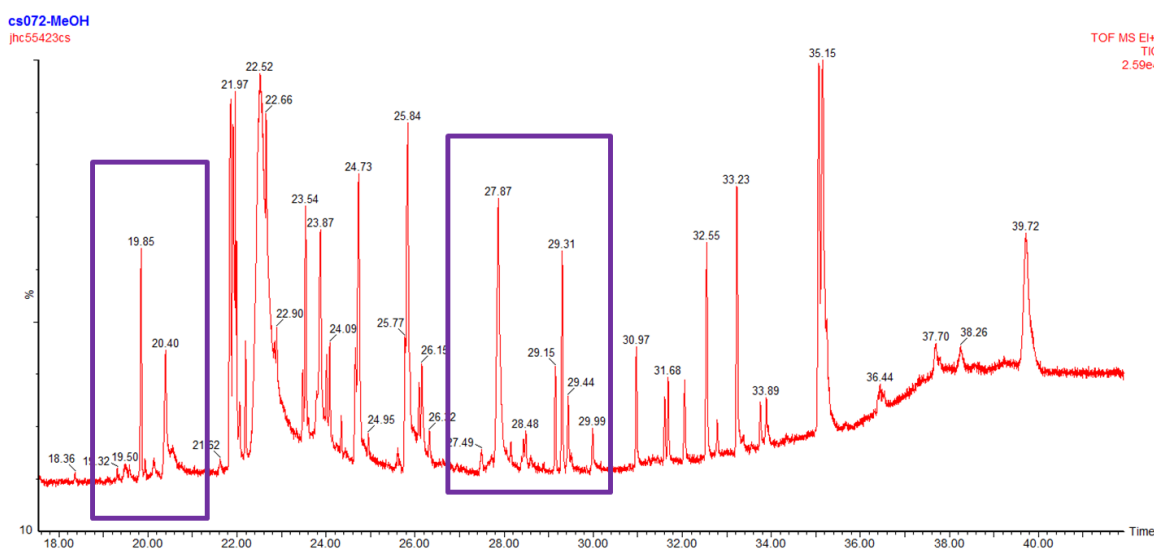


**Figure 5-14** Chromatogram of transesterified sample catalysed by *L.vannamei* by-product.

## 5.5 Conclusion and Future work

The main focus of this chapter is to use the bio-waste of Pacific white shrimp or *Litopenaeus vannamei* as new and reliable source of the production of PUFA targeted to ARA, EPA and DHA as the value and demand in the market are high due to the health benefits. The study on the effect of moisture content on the extraction efficiency of scCO<sub>2</sub> extraction of Pacific white shrimp or *Litopenaeus vannamei* was successfully performed. Three drying methods, vacuum-oven drying, vacuum-microwave drying and freeze-drying, were selected as they are currently and widely used in food industry. All of the drying methods effectively improved extraction efficiency and kinetic, as a result, the s-curve, low extraction efficiency at the beginning of the extraction process completely disappeared. Freeze-dried sample yielded the highest lipid recovery with greatest rate of extraction, followed by vacuum-microwave dried and vacuum-oven dried samples. However, the concentration of PUFA especially ARA, EPA and DHA, which are the target compounds in this study, was significantly obtained from vacuum-oven drying at 50 °C for 24 hours due to autolysis via enzymatic hydrolysis catalysed by endogenous protease and lipases. Moreover, the concentration of ARA, EPA and DHA were dramatically higher obtained by scCO<sub>2</sub> with pre-treatment at 50 °C under air, vacuum and nitrogen than that of hexane extract. This results excellently emphasised that the scCO<sub>2</sub> combined with autolysis process is a new suitable method for the production of n-3 and n-6 PUFA especially ARA, EPA and DHA.

The investigation of autolysis within prawn by-product at room temperature was then carried out at 3-, 6- and 24-hours prior to scCO<sub>2</sub> extraction. The total lipid highly increased with extended autolysis time. However, ARA, EPA and DHA were obtained in higher concentration when the prawn waste was allowed to autolyse for 6 hours, however, after 24 hours of autolysis, the concentrations of those targets PUFA obviously decreased. This was due to the fact that autoxidation and enzymatic hydrolysis of lipid occurred simultaneously. Therefore, the 6-hour autolysis was suitable for the production of ARA, EPA and DHA at room temperature.

Next, a study on the effect of temperature and different atmosphere on the enzymatic hydrolysis was undertaken. The temperatures used in this study were 50 °C and 105 °C. The pre-treatment at 50 °C was found to enhance the hydrolysis process with higher lipid yields obtained, whereas, pre-treating the biomass at 105 °C negatively affected the enzymatic process and

resulted in lower total lipid recovery. Since the endogenous enzymes were deactivated and denatured at the high temperature, while the pre-treatment at 50 °C was suitable a suitable temperature for the catalysis to occur. Different atmospheres, under vacuum, air and nitrogen, were used at 50 °C with 24 hours of autolysis prior to extraction with scCO<sub>2</sub>. The nitrogen treated extract gave the highest yield as well as the greatest concentration in ARA, EPA and DHA. In contrast, vacuum-oven treated sample yielded the lowest total lipid recovery and ARA, EPA and DHA in the extract. PUFA obtained from this prawn waste were prone to oxidation due to the high degree of unsaturation, therefore, exposing the biomass to inert atmosphere helped reducing autoxidation of lipids.

In conclusion, the by-products of *L. vannamei* can potentially serve as new source of  $\omega$ -3 and  $\omega$ -6 PUFA. The ARA, EPA and DHA can be obtained in high concentration via autolysis using endogenous protease and lipases of the digestive organ called hepatopancreas as catalyst to hydrolyse lipoproteins, triglycerides and phospholipids in order to liberate free fatty acids. The best condition was the pre-treatment of 6-hour autolysis at 50 °C under nitrogen prior to scCO<sub>2</sub> extraction.

## **Chapter 6**

### **Materials and Methods**

## 6 Materials and method

### 6.1 Chemicals

#### 6.1.1 Solvents

Organic solvents *n*-hexane was purchased from Fisher Scientific UK Limited. Dichloromethane (DCM) and ethanol were obtained from VWR (International) chemicals.

#### 6.1.2 Gases

Carbon dioxide (supercritical grade – 99.99%), helium, hydrogen and nitrogen were sourced from BOC Ltd. and all were used without any further purification.

#### 6.1.3 Standards

Linoleic acid (99%), 1-octacosanol (90+%) and stigmasterol (95%) were obtained from Acros Organics. Azelaic acid (98%), dodecanal ( $\geq 95\%$ ), *N*,*O*-bis(trimethylsilyl)trifluoroacetamide (BSTFA,  $\geq 99\%$ ), tetradecane ( $\geq 99\%$ ) and Vitamin K1 ( $\geq 99\%$ ) were purchased from Aldrich. Stearic acid (98%) was obtained from Alfa Aesar. Hentriacontane ( $\geq 98\%$ ) was purchased from Fluka.  $\beta$ -sitosterol ( $\geq 70\%$ ) and stearyl palmitate ( $\geq 99\%$ ) were purchased from Sigma. ASTM<sup>®</sup> D5442 C16 – C44 Qualitative Retention Time Mix (containing docosane, dotriacontane, eicosane, hexacosane, hexadecane, hexatriacontane, octacosane, octadecane, tetracontane, tetracosane, tetratetracontane and triacontane; 8.3% (*w/w*) each component) was sourced from Supelco. Arachidonic acid (C20:4n-6), Eicosapentaenoic acid (C20:5n-3), Docosahexaenoic acid (C22:6n-3), Tetracosanic acid (C24:0), cholesterol,  $\beta$ -sitosterol, Batyl alcohol 99%, DL- $\alpha$ -Palmitin,  $\geq 99\%$  and 1,2-Dipalmitoyl-*rac*-glycerol were also purchased from Sigma.

Candelilla wax was obtained from Aldrich. Beeswax was purchased from Fisher Scientific Limited. The cellulose thimbles for the soxhlet extractions were obtained from Fisher Scientific Limited.

## **6.2 Waste biomass**

### **6.2.1 Rice straw**

The rice straw (*Oryza sativa* L.), naturally sun-dried, harvested in July 2013 was obtained from Faculty of Agricultural, University of Khon Khan, Thailand. The biomass was milled shredded to the small pieces less than 0.5 mm by a hammer mill and was kept until use at room temperature. The lignocellulosic contents (i.e., cellulose, hemicellulose and lignin) were using Thermogravimetric analysis (TGA) and the gross calorific value was determined by a PARR 6200 calorimeter.

### **6.2.2 Prawn by-product**

Farmed Pacific white shrimps from Thailand were purchased from Sainsbury's. The biomass came as frozen and shelled on. The prawn were peeled, shells and heads (cephalothorax and hepatopancreas) were separated and ground by a coffee blender. The ground biomass was kept in the freezer until the experiments.

### **6.2.3 Moisture content of biomasses**

Biomass was dried, with 3 replicates, in an oven at  $105\text{ }^{\circ}\text{C} \pm 5\text{ }^{\circ}\text{C}$  for 24 hours, then cooled and weighed. These procedures were repeated 3 times in order to obtain accurate moisture content.

$$\% \text{ Moisture content} = [(\text{Initial mass} - \text{Mass after drying}) / \text{Initial mass}] \times 100$$

### 6.3 Typical Soxhlet extraction

10g of milled biomass (rice straw and prawn waste) was placed in a Soxhlet thimble which was inserted into the Soxhlet apparatus. This was fitted to a 250 ml round bottom flask containing hexane (200 ml). A Radleys Discovery Technologies 2006T thermocouple was used to monitor the temperature during the extraction. The solution was allowed to reflux for 4 hours and 2 hours for rice straw and prawn waste respectively. The resulting solution was filtered (to remove any biomass present in the product) and the solvent was removed *in vacuo*. The samples were further dried at room temperature for 24 hours before weighing to ensure the removal of traces of residual solvent. The crude lipid product was weighed and the % yield calculated. For each biomass three extractions were carried out and an average % yield calculated.<sup>28,65,153,286–288</sup>

### 6.4 Lab-scale supercritical fluid extraction of rice straw and prawn by-product.

The scCO<sub>2</sub> extractions were carried out using a SFE-500 provided by Thar technologies. Supercritical fluid grade carbon dioxide (99.99%) was used to conduct the extractions. ≈90 g of milled rice straw or 10 g of prawn waste biomass was placed into the 500 cm<sup>3</sup> extraction vessel and connected to the extraction system. Liquid CO<sub>2</sub> was passed through a pre-heater set at the required temperature. The extractor was heated to the required temperature (range of extractions from 35 °C – 65 °C for rice straw and 40 °C - 60 °C for prawn waste) and 5 minutes were allowed for it to equilibrate. An internal pump was used in order to obtain the required pressure (range of extractions from 75 bar – 400 bar). An automated back pressure regulator (ABPR) maintained the pressure throughout the system. The system was run in dynamic mode, in which the carbon dioxide which contained the epicuticular lipids, was allowed to flow into the collection vessel. A flow rate of 40 g min<sup>-1</sup> of liquid CO<sub>2</sub> was applied for rice straw, while 30 g min<sup>-1</sup> was applied for prawn waste. The extraction was carried out for 4 and 2 hours for rice straw and prawn biomass respectively. When the extraction was terminated, depressurisation of the system was carried out over a period of 15-75 mins (depending on the pressure applied). The wax was collected by rinsing the collection vessel twice with approximately 100 ml of DCM.



Anhydrous magnesium sulphate was added to any product samples that contained water (small amounts of water could be extracted by scCO<sub>2</sub> during the extraction process). The solution was subsequently filtered and DCM was passed through the filter paper to re-dissolve any wax found on the filter paper. The solvent was removed *in vacuo*. The crude wax product was weighed and the % yield was calculated. The plant material was removed and a brush was used to clean the extraction vessel. The system was washed in dynamic mode using a combination of scCO<sub>2</sub> and ethanol (10%) for 45 minutes at the extraction pressure. The pump supplying the modifier was then turned off and carbon dioxide was allowed to pass through the system for an additional 20 minutes.<sup>70,104</sup>

## **6.5 Lab-scale supercritical extraction of rice straw and prawn by-product (kinetics).**

The supercritical carbon dioxide extractions were carried out using a SFE-500 provided by Thar technologies. Supercritical fluid grade carbon dioxide (99.99%) was used to conduct the extractions. ≈90 g of milled rice straw was placed into the 500 ml extraction vessel and connected to the extraction system. The required temperature and pressure were applied. The reaction vessel was heated to the required temperature (60 °C for rice straw and 40 °C for prawn waste) and 5 minutes were allowed for it to equilibrate. An internal pump was used in order to obtain the required pressure, 400 bar. The pressure of the system was maintained by means of an ABPR. The system was run in dynamic mode, in which the carbon dioxide which contained the epicuticular lipids, was allowed to flow into the collection vessel. A flow rate of 40 g/min of liquid CO<sub>2</sub> was applied for rice straw, while 30 g min<sup>-1</sup> was applied for prawn waste and the extraction was carried out for 6 hours and 4 hours for rice straw and prawn waste respectively. The system was stopped at specific time intervals; whereby prawn extract samples were collected after 30, 60, 90, 120 and 240 mins and rice straw wax were 30, 60, 120, 180, 300 and 360 minutes. The % yield of crude extracted was recorded for each sample collected. When the extraction was terminated, depressurisation of the system was carried out over a period of 75 mins for the two biomass.<sup>159</sup>

## 6.6 Drying process of prawn-by-products

### 6.6.1 Vacuum-microwave drying

A ROTO SYNTH Rotative Solid Phase Microwave Reactor (Milestone) was used for the drying process. This is a multimode microwave reactor and the apparatus set up is shown in **Figure 6-1**. Fresh prawn waste (60g) was put into the sample vessel for the drying process. Three drying conditions were applied, including atmospheric pressure drying, vacuum (500 mbar) with the microwave power 1200W. The drying process took less 10 minutes to reduce the moisture content from 78% to 8% of dry weight.<sup>289</sup> Then the dried sample was extracted using scCO<sub>2</sub> method as explained in section 6.4.

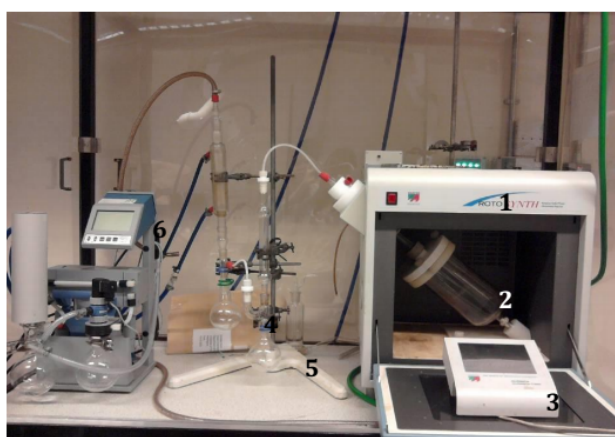


**Figure 6-1** Set-up for drying process. (1) Microwave reactor, (2) sample vessel, (3) system control and monitoring console, (4) and (5) round bottom flasks for collection water, (6) vacuum pump.

### 6.6.2 Freeze-drying

The fresh frozen prawn wastes (10g) were placed in a round bottom flask of 250 ml. 100 ml of water was added and the mixture was pre-frozen in liquid nitrogen before freeze drying for 72 hours in SP Scientific Sentry 2.0 freeze drier. Then the dried sample was extracted using scCO<sub>2</sub> method as previously seen in section 6.4

### 6.6.3 Vacuum-oven drying

The fresh frozen prawn wastes (10g) were placed in a Petri dish recovered with aluminium foil, then oven-dried at 50 °C under vacuum for 24 hours. The moisture content was reduced from 78% to 1.75% of dry weight. Then the dried sample was extracted using scCO<sub>2</sub> method as described in section 6.4

## 6.7 Analysis of the extracts

### 6.7.1 Derivatisation of prior to gas chromatography analysis

200 µL *N,O*-bis(trimethylsilyl)trifluoroacetamide and 1 mL of toluene was add to a vial containing crude lipid extract (~20 mg). The closed vial was then heated on a stirrer hot plate at 75 °C for 30 minutes. The solution was allowed to cool and analysed by high temperature-gas chromatography (HT-GC).<sup>70,104</sup>

### 6.7.2 High temperature- gas chromatography (HT-GC) method for analysis of rice straw wax and prawn waste lipid extract.

HT-GC analysis was performed on an Agilent Technologies 6890N Network GC System. A ZB-5HT capillary column (30m x 250 µm x 0.25 µm nominal) was fitted at constant pressure of 22.35 psi. The carrier gas used was helium. The injector temperature and the flame ionisation detector temperature were maintained at 300 °C. The samples were injected by automated injection (1 µl injection volume) with a split 281 ratio of 5:1. An initial oven temperature of 60 °C was maintained for 1 minute. The temperature was increased at a ramp rate of 8 °C min<sup>-1</sup> until 360 °C and held at this temperature for 30 minutes. Quantification of the lipid components was carried out by means of internal standard calibration and response factors (Rf). Five point linear calibration graphs were produced using external standards for the quantification of hydrophobic compounds (fatty acids, alcohols, aldehydes, alkanes, wax esters, sterols, monoglycerides, diglycerides, 1-*O*-alkylglycerol, fatty aldehydes and wax esters.<sup>53,70,104,159</sup> Three sequential injections were applied in order to calculated the standard deviations.

$$\text{Mass}_{(\text{Product})} / \text{Mass}_{(\text{Standard})} = R_f \times \text{Area}_{(\text{Product})} / \text{Area}_{(\text{Standard})}$$

Silylated calibration curves were also produced for the groups of compounds that were silylated. Octadecanoic acid, octadecanol, cholesterol, monopalmitin, dipalmitin, 1-O-Octadecylglycerol were used to produce five point linear calibration graphs for the quantification of fatty acids, fatty alcohols, sterols, monoglycerides, diglycerides and 1-O-alkylglycerol respectively.

An example of this calibration for cholesterol is shown in **Figure 6-2**. Multiple samples were prepared accurately containing known ratios of cholesterol and tetradecane (standard). The area ratio of the two gas chromatography peaks was plotted against the mass ratio and the  $R_f$  was calculated from the gradient. In the case of cholesterol this was 0.732.

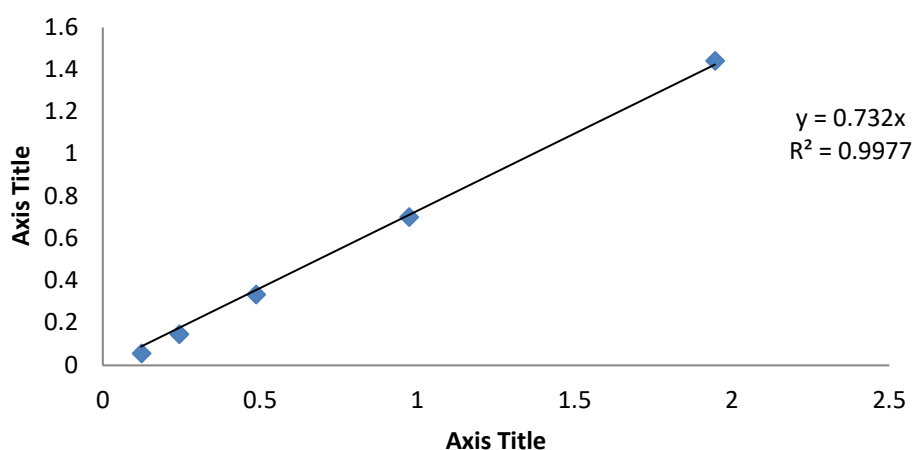


**Figure 6-2** Calculation of response factor for silylated cholesterol.

### **6.7.3 HT-GC-MS (High temperature-gas chromatography mass spectrometry) procedure for analysis of extracts from rice straw and prawn by-product.**

HT-GC-MS was performed on a Perkin Elmer Clarus 500 GC coupled with a Clarus 500 quadrupole mass spectrometer. This was fitted with a DB5HT capillary column (30 m x 250  $\mu\text{m}$  x 0.25  $\mu\text{m}$  nominal) at constant pressure of 22.35 psi. The carrier gas used was helium. The temperature

of the injector was 300 °C and the flow rate was set to 1.2 ml/min. The initial oven temperature was maintained at 60 °C for 1 minute. The temperature was then ramped at a rate of 8 °C min<sup>-1</sup> until 360 °C and held for 10 minutes. The Clarus 500 quadrupole mass spectra was operated in the electron ionisation mode (EI) at 70 eV, a source temperature of 300 °C, quadrupole at in the scan range of 30 - 1200 amu per second.<sup>69</sup>

#### **6.7.4 Differential scanning calorimetry (DSC) analysis**

The thermal characteristics of the rice straw wax samples were measured on a MDSC Q2000 modulated differential scanning calorimeter. The wax extract (5 mg) was weighed into an open aluminium DSC pan and analysed under nitrogen gas using a three-stage heating profile in order to remove any prior thermal character. The DSC measurements were recorded against an empty aluminium reference pan in the final heating cycle of analysis. In determining the melting point, the cell was purged with a flow of nitrogen gas (150 mL/min) and was cooled by nitrogen (150 mL/min) in a refrigerated cooling system. The sample was heated from 20 to 105 °C at a rate of 10 °C /min. It was held at 105 °C for 1 minute and cooled to -10 °C at 10 °C /min. The sample was held at -10 °C for 1 min and then heated from -10 to 105 °C at 10 °C/min and held for 1 min at 105 °C. The melting point range was determined using the differential scanning calorimetry (DSC) curves of the last heating cycle. Thermal characteristics of commercially available waxes (candelilla wax and beeswax) were also measured to compare with the waxes obtained in this study.<sup>159</sup>

### **6.8 Microwave-assisted pyrolysis of rice straw**

#### **6.8.1 Biomass preparation**

Previously milled rice straw was sieved using laboratory sieves to obtain six different particle sizes, >2000 µm, 500-2000 µm, 300-500 µm, 180-300 µm, 125-180 µm and <125 µm. **Figure 6-3** shows the distribution of untreated rice straw and scCO<sub>2</sub> treated rice straw.

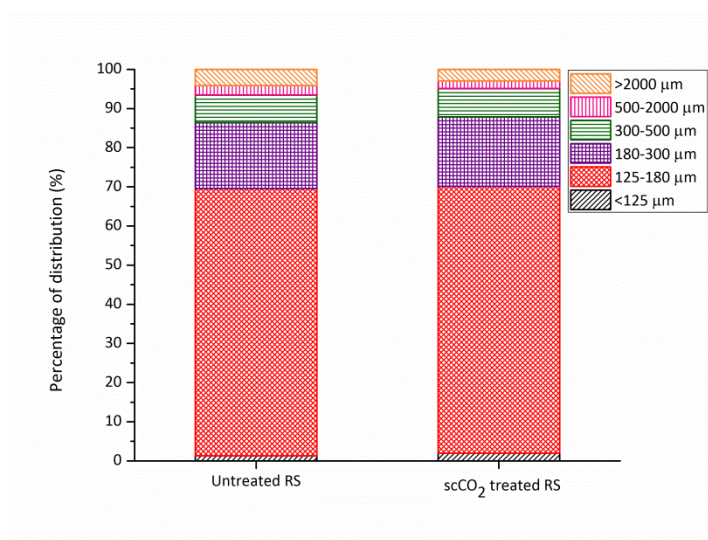


**Figure 6-3** Particle size distribution of untreated and scCO<sub>2</sub> treated rice straw after sieving.

### 6.8.2 Pre-treatment of rice straw with water

To investigate the effect of inorganic components in rice straw on the behaviour of the biomass when it was activated with microwave irradiation, the small pieces of rice straw were accurately weighed (about 20 g) and soaked in 500 mL of deionized water (sample mass : water, 1 : 25). It was heated at 100 °C for 20 min to extract or remove the inorganic compounds from rice straw. Then the treated rice was filtered using Buchner funnel and gently oven-dried the biomass at 50 °C for 72 hours. The aqueous fraction was directly boiled in order to remove maximum of water, the 2 volume of ethanol were added to the remaining aqueous solution. Finally, the mixture ethanol-water was evaporated under vacuum. The solid obtained after water removal was then dried at 105 °C in the oven for 24 hours.

### 6.8.3 Potassium salt impregnation

These six potassium salts were used including potassium chloride (KCl), potassium carbonate (K<sub>2</sub>CO<sub>3</sub>), potassium acetate (CH<sub>3</sub>COOK), potassium hydroxide (KOH), potassium phosphate (K<sub>3</sub>PO<sub>4</sub>), potassium formate (HCOOK) and potassium sulphate (K<sub>2</sub>SO<sub>4</sub>). Each salt was weighed accordingly to meet the concentration of potassium (K<sup>+</sup>) in the untreated rice straw (20 mg/g

and 2 mg/g of biomass, the concentration of K was kept constant). The pre-weighed salts were dissolved in 5 mL of deionised water and 1g of water treated rice straw was used for each sample. The samples were left rotating for 72 hours then oven-dried for 72 hours at 50 °C.

#### **6.8.4 Small scale single microwave-assisted pyrolysis of rice straw.**

Prior to the microwave pyrolysis, the untreated and scCO<sub>2</sub> treated rice straw were sieved to obtain six different particle sizes, <125 µm, 125-180 µm, 180-300 µm, 300-500 µm, 500-2000 µm and >2000 µm. Only rice straw having particle size 500-2000 µm, were used in Chapter 3. Microwave pyrolysis was subsequently conducted in a CEM-Discover microwave reactor model. The experiments were carried out under fixed power mode with a maximum power of 300 W and in a microwave pressure vial (10mL CEM Discover SP, CEM Corp., USA). The temperature was measured by an IR detector. However, the microwave pyrolysis of the sample was stopped on reaching the target pressure (280 psi). 300 mg of milled rice straw and rice straw residue after scCO<sub>2</sub> extraction were used without further pretreatment. Pyrolysed biomass was extracted with ethanol; the char (insoluble) and bio oil (ethanol soluble) were then collected by filtration. The solvent was removed and the solid was dried in an oven until constant weight was obtained.

### **6.9 Analysis of products from microwave-assisted pyrolysis of rice straw.**

#### **6.9.1 Inductively Coupled Plasma (ICP)**

Inductively Coupled Plasma Atomic Emissions Spectroscopy (ICP-AES) was carried out by Yara Analytical Services, York and was analysed for 39 inorganic elements.

#### **6.9.2 Scanning electron microscopy (SEM) and Scanning electron microscope coupled with Energy-dispersive X-ray spectroscopy (SEM/EDX)**

Scanning electron micrographs and energy dispersive spectroscopic mapping images were carried out by Carl zeiss EVO HD scanning electron microscope equipped with Oxford Instruments X-max20 silicon drift detector (SDD) with collaboration with College of Nanotechnology, King Monkut's institute of Technology, Thailand (data used in Chapter 3).

### 6.9.3 SEM analysis

The appearance of pectin aerogels was investigated and the micrographs were recorded with JEOL JSM-6490LV scanning electron microscope. The samples, mounted on an aluminium plate, were coated with Au-Pd prior to analysis. The acceleration voltage beam energy was 5 kV. The analysis was performed by Meg Stark (Biology Department, University of York) (Data used in Chapter 2).

### 6.9.4 Elemental analysis

Elemental analysis based on carbon, hydrogen and nitrogen content was carried out using an Exeter Analytical (Warwick, UK) CE440 Elemental Analyser, calibrated against acetanilide with an S-benzyl-thiuronium chloride as internal standard.

### 6.9.5 Characterisation of gas fraction

The apparatus for thermal decomposition of rice straw consisted of a microwave connected to IR gas cell for monitoring of gases, with the IR cell and transfer pipe heated at 200 °C. 0.9 g of rice straw were placed inside the microwave reactor and 300W of microwave and the similar method described in section 6.7.3 was applied. Fourier transform infrared spectroscopy (FT-IR), a Bruker VERTEX 70 infrared spectroscopy and ATR probe with Golden gate attachment were used to perform this analysis. Samples spectra were collected between 500 and 4000  $\text{cm}^{-1}$  at a resolution of 4  $\text{cm}^{-1}$  and a scan number of 64, scanning over a wavelength range of 4000 – 500  $\text{cm}^{-1}$  at a resolution of 4  $\text{cm}^{-1}$ . The spectra were subsequently analysed to determine possible bond types and functional group of the gas. The spectra were collected using a rapid scan software running under OPUS 5.5 and the spectrum of each sample was calculated from an average of 16 scans.<sup>103</sup>

### 6.9.6 Characterisation of liquid fraction

GC/MS was used to examine the oils produced from pyrolysis experiments to tentatively determine their composition. Samples were prepared at a concentration of 20mg/mL of pyrolysis oil in ethanol. A sample of 0.5 $\mu\text{L}$  was injected on to a Perkin ElmerClarus 500 Gas chromatography and Clarus 560S Mass spectrometer at an injector temperature of 350 °C and a column flow rate of 1.0ml/min with a 1:10 split ratio applied. The oils were passed onto a DB5-



HT column (30m × 0.25m × 0.25µm) at a temperature of 60 °C. The column was held for 1 minute at this temperature and then ramped to 360 °C at 8 °C/min. It was then held for further 10 minutes. During the GC run the mass spectrometer with  $Ei^+$  source of 70eV was scanning between 40 to 1200 Da at a scan duration of 0.39s and cycle time of 0.400s, with an inter scan delay of 0.050s. The subsequent m/z spectra recorded were compared against the NIST 2005 spectral database and possible chemical matches identified.<sup>290</sup>

### **6.9.7 Simultaneous thermal analysis**

Thermogravimetric analysis (TGA) analysis were carried out simultaneously on a PL Thermal Sciences STA 625. Milled rice straw or biochar (10 mg) was accurately weighed into an aluminium cup and analysed against an empty aluminium reference pan from 20 °C to 625 °C at a heating rate of 10 Kmin<sup>-1</sup> under a 60ml min<sup>-1</sup> flow of nitrogen. All biochars were washed and dried prior to analysis. Analyses were carried out in duplicate.<sup>103,291</sup>

## **6.10 Autolysis of prawn by-product**

### **6.10.1 Autolysis at room temperature**

Each sample the *L.vannamei* by-products, 10g were placed in a petri dish under a fume hood at room temperature for 3, 6 and 24 hours, prior to scCO<sub>2</sub> extraction, using the same method of scCO<sub>2</sub> extraction described in section 6.4.

### **6.10.2 Autolysis at different atmospheres and denaturation of the prawn enzyme.**

Four samples of ground *L.vannamei* by-product were used in this experiment. A sample (10g) was dried in the convective oven at 105 °C for 24 hours in order to investigate the effect of the pre-treatment at high temperature on the activity of the prawn enzyme. The other three samples were treated at three different atmospheres at the same temperature, 50 °C. The first sample was placed in a 100ml beaker and the sample was kept at 50 °C by water bath in the air for 24 hours. The second sample was placed in a round bottom flask of 250ml connected with a balloon filled with nitrogen gas and kept at 50 °C in water bath for 24 hours. The third sample

was treated the same way as described in 6.6.3 Vacuum-oven drying. Finally, the treated samples were extracted using scCO<sub>2</sub> extraction with the procedure described in section 6.4.

## **Chapter 7**

### **Conclusion and Future work**

## 7 Conclusion and Future work

### 7.1 Chapter 2 ScCO<sub>2</sub> extraction as a first step in a holistic rice straw biorefinery

Supercritical carbon dioxide (scCO<sub>2</sub>) extraction of rice straw was successfully carried on as well as the optimal condition was determined with the highest wax yield obtained, 0.70% of dry weight, which comparable to that of the extract obtained from hexane, 1.05% dry weight. The chemical composition of the extracts using these two extraction methods was completely identical. The wax components identified in the rice straw included fatty acids, fatty alcohol, fatty aldehydes, steroid ketones, phytosterols, *n*-alkanes and wax esters. The most abundant group of compounds belonged to fatty acids, with  $681.5 \pm 10.3 \mu\text{g/g}$  of biomass using scCO<sub>2</sub> extraction at 65 °C, 400 bar compared to  $1004.5 \pm 15.7 \mu\text{g/g}$  of dry straw

This extraction method also suitable as a pre-treatment step to provide enhanced interactions between microwaves and the resulting extracted biomass. Microwave pyrolysis of rice straw was carried on with untreated rice straw and scCO<sub>2</sub>-treated rice straw with six different particle sizes, <125 μm, 125-180 μm, 180-300 μm, 300-500 μm, 500-2000 μm and >2000 μm. it was observed that the decomposition of rice straw occurred very early around 120 °C with the particle size larger than 500μm during the microwave irradiation. The gas product was predominant in the pyrolysis of both straw with particle size larger than 500μm; however, there was no production of gas for smaller particle size. Therefore, particle size has a great influence on microwave pyrolysis of rice straw.

In addition, high heating rate and pressure change rate are high in both raw materials, greater heating rates were recorded in experiments in the case of scCO<sub>2</sub> treated rice straw and the heating. These results indicate that the wax removal by scCO<sub>2</sub> has an influence on the dielectric property of the rice straw, as the scCO<sub>2</sub> treated rice straw became a better microwave absorber with a constant high heating rate and higher final temperature. This therefore shows that scCO<sub>2</sub> extraction has a positive effect on the microwave pyrolysis process, further illustrating the

benefits of introducing this technology within a holistic biorefinery. However, further investigation is needed for a better understanding of this from a mechanistic point of view.

Future work on product analysis need to be carried on in order to understand the overall process and the potential application of each product should be proposed. Moreover, the economic study of the combined scCO<sub>2</sub> extraction and microwave technology should be also considered.

## **7.2 Chapter 3 The influence of K<sup>+</sup> in microwave-assisted pyrolysis of rice straw**

This chapter study focused on the essential factor that played important role and enhanced on self-gasification during the microwave-assisted pyrolysis of rice straw. Three hypotheses on potential microwave energy absorbers present in the biomass were proposed for further investigation from Chapter 2. Firstly, water was the first microwave absorber in question due to its high availability in plant and its dielectric and polar properties. Surprisingly, not only the absence of moisture content did not have any adverse effect, but it also positively enhanced the process as the decomposition of cellulose occurred significantly at lower temperature (95 °C) compared with the untreated rice straw (120 °C). Secondly, another microwave absorber was silicate compounds due to its high silicon-content. As such, rice straw was treated (washed) in hot water to remove soluble silicates prior to the microwave pyrolysis. The water-washed rice straw behaved totally different during the microwave irradiation with no incondensable gas produced during the process unlike in the case of the untreated biomass. Therefore, key component was washed out with water and the water-soluble components were likely to be mineral inorganic salts, potentially potassium containing, but impossible to be the silicate as the concentration in the biomass was unchanged after washing (as determined by ICP-MS). The third microwave absorber is K-containing compound. In plants, potassium usually stays in the form of salts after the biomass is dried. Consequently, potassium salt impregnation was carried out to see if enhanced microwave pyrolysis could be returned to the previously water washed material. K-impregnated rice straw with K<sub>2</sub>CO<sub>3</sub>, CH<sub>3</sub>COOK, KOH, K<sub>3</sub>PO<sub>4</sub> and HCOOK demonstrated the catalytic effect of gasification during the pyrolysis, which have similar behaviour to the untreated rice straw. In contrast, KCl and K<sub>2</sub>S<sub>2</sub>O<sub>8</sub> impregnation sample did not result any gas

production. This observation can be explained by the relationship between  $pK_a$  and  $pK_b$ . To be able to catalyse the gasification, the  $pK_b$  of the conjugate bases needed to be ranged between -1.7-11.9 in order to protonate the hydroxyl group within the cellulose. Moreover, the concentration of K should be at least 5100  $\mu\text{g/g}$  of straw in order to catalyse self-gasification. Therefore, the deprotonated cellulose became microwave active after K-impregnation. Among all the alkali catalysts, potassium phosphate impregnated straw had a much closer behaviour to the untreated rice straw in term of initial temperature of pyrolysis and the pressure change rate even though the other salts were also effective catalysts. Our conclusion is drawn to potassium phosphate being the main salt responsible due to the strong correlation with the earlier obtained ICP-MS data that showed high levels of K and P in the active untreated rice straw, and reduced levels of both in the inactive washed material.

For future work, within the concept of biorefinery it would be sustainably beneficial to investigate the product distribution and composition of the pyrolysis oil, gas and char to give a better understanding about using potassium salts in the catalytic pyrolysis process. The optimisation of the concentration of alkali metal catalyst could also be of interest in terms of energy efficiency. Product selection with the gas and oil could potentially be possible as different salts results in different behaviour in microwave. Moreover, potassium salts are cheap and widely available, which has a positive practical economic point of view, though concerns around the availability of phosphorous should be considered carefully. Crucially, this study provides important information for Thailand and how rice straw can be microwave treated to yield a significant quantity of gas, which maybe potentially used as synthesis gas for the production of fuels and chemicals.

### **7.3 Chapter 4 Prawn waste residues as a source of valuable lipophilic compounds**

In this chapter, the  $\text{scCO}_2$  extraction was successfully performed for the recovery of lipid compounds from prawn residue (*Litopenaeus vannamei*) waste streams. The optimisation of lipid extraction from prawn cephalothorax (heads) by  $\text{scCO}_2$  was undertaken and demonstrated yields of 1.14% at 400 bar and 40 °C for 2 hours ( $40 \text{ g min}^{-1}$ ) using fresh biomass with high

moisture content of 78% dry weight. Extraction efficiency strongly correlated density, with the highest yield being obtained at the highest density of CO<sub>2</sub>, 0.96 g/cm<sup>3</sup>. Therefore, it can be concluded that the density of the CO<sub>2</sub> is the most important factor for the scCO<sub>2</sub> extraction of the Pacific white shrimp waste. The optimal extraction time for prawn waste was 2 hours. However, the extraction rate could be developed if the humidity of the biomass is lower. The added-value components were characterised, quantified and their potential applications were identified. It was determined that scCO<sub>2</sub> was an effective solvent for the extraction of polyunsaturated fatty acids. PUFAs have importantly been shown to reduce cardiovascular disease and improve cognitive development.

The free fatty acid (FFA) profile of the scCO<sub>2</sub> extract differed to that of the hexane Soxhlet. Firstly, a greater abundance of FFA in the hexane Soxhlet extraction over 2 hours, 20789.8 ± 257.3 µg/g of dry biomass compared to 2819.4 ± 87.8 µg/g of dry biomass by scCO<sub>2</sub> (40°C and 400 bar for 2 hours). It was suggested that these differences were likely due to several important factors, 1) high water content in the biomass adversely affects the efficiency of scCO<sub>2</sub> extraction and 2) enzymes within the biomass hydrolyze triglycerides to form FFA within the hexane system but water removal from the active site of the enzyme with scCO<sub>2</sub> may reduce the rate of this process. Further discussion on the active enzyme in the cephalothorax of *L. vannamei* and the implications on lipid yield will be presented in Chapter 5.

#### **7.4 Chapter 5 The influence of moisture content on scCO<sub>2</sub> extraction efficiency.**

The aim of this chapter is to use the bio-waste of Pacific white shrimp or *Litopenaeus vannamei* as a new and reliable source of the production of PUFA targeted to ARA, EPA and DHA as the value and demand in the market are high due to the health benefits with low energy consumption possible. The study on the effect of moisture content on the extraction efficiency of scCO<sub>2</sub> extraction of Pacific white shrimp or *Litopenaeus vannamei* was successfully performed. Three

drying methods based on industrial applications were selected vacuum-oven drying, vacuum-microwave drying and freeze-drying, were. All of the drying methods effectively improved extraction efficiency and kinetic, as a result, the s-curve, low extraction efficiency at the beginning of the extraction process completely disappeared. Freeze-dried sample yielded the highest lipid recovery with greatest rate of extraction, followed by vacuum-microwave dried and vacuum-oven dried samples. However, the concentration of PUFA especially ARA, EPA and DHA, which are the target compounds in this study, was significantly obtained from vacuum-oven drying at 50 °C for 24 hours due to autolysis via enzymatic hydrolysis catalysed by endogenous protease and lipases. Moreover, the concentration of ARA, EPA and DHA were dramatically higher obtained by scCO<sub>2</sub> with pre-treatment at 50 °C under air, vacuum and nitrogen that that of hexane extract. This results excellently emphasised that the scCO<sub>2</sub> combined with autolysis process is a new suitable method for the production of n-3 and n-6 PUFA especially ARA, EPA and DHA.

The investigation of autolysis within prawn by-product at room temperature was then carried out at 3-, 6- and 24-hours prior to scCO<sub>2</sub> extraction. The total lipid highly increased with extended autolysis time. However, ARA, EPA and DHA were obtained in higher concentration when the prawn waste was allowed to autolyse for 6 hours, however, after 24 hours of autolysis, the concentrations of those targets PUFA obviously decreased. This was due to the fact that autoxidation and enzymatic hydrolysis of lipid occurred simultaneously. Therefore, the 6-hour autolysis was suitable for the production of ARA, EPA and DHA at room temperature.

Next, a study on the effect of temperature and different atmosphere on the enzymatic hydrolysis was undertaken. The temperatures used in this study were 50 °C and 105 °C. The pre-treatment at 50 °C was found to enhance the hydrolysis process with higher lipid yields obtained, whereas, pre-treating the biomass at 105 °C negatively affected the enzymatic process and resulted in lower total lipid recovery. Since the endogenous enzymes were deactivated and denatured at the high temperature, while the pre-treatment at 50 °C was suitable a suitable temperature for the catalysis to occur. Different atmospheres, under vacuum, air and nitrogen, were used at 50 °C with 24 hours of autolysis prior to extraction with scCO<sub>2</sub>. The nitrogen treated extract gave the highest yield as well as the greatest concentration in ARA, EPA and DHA. In contrast, vacuum-oven treated sample yielded the lowest total lipid recovery and ARA, EPA and



DHA in the extract. PUFA obtained from this prawn waste were prone to oxidation due to the high degree of unsaturation, therefore, exposing the biomass to inert atmosphere helped reducing autoxidation of lipids.

In conclusion, the by-products of *L.vannamei* can potentially serve as new source of  $\omega$ -3 and  $\omega$ -6 PUFA. The ARA, EPA and DHA can be obtained in high concentration via autolysis using endogenous protease and lipases of the digestive organ called hepatopancreas as catalyst to hydrolyse lipoproteins, triglycerides and phospholipids in order to liberate free fatty acids. The best condition was the pre-treatment of 6-hour autolysis at 50 °C under nitrogen prior to scCO<sub>2</sub> extraction.

An attempt to use the prawn by-product as catalyst in the transesterification reaction of sunflower oil was carried on. Fatty acid methyl esters (FAME) were detected by GC-MS. Endogenous lipase of *L. vannamei* was able to successfully convert TG into FAME. However, the conversion and yield were assumed to be low as the fresh biomass was used without prior purification. The prawn enzyme can potentially be used as catalyst in the production of biodiesel. However, further work would be needed for purification of the enzyme to increase the proportion of lipase and thus activity. An experimental design for optimal condition would also be an interesting addition to the future work. This prawn enzyme might be a new door to various chemical reactions for use in many industries.

## Abbreviation

ScCO <sub>2</sub>	-	Supercritical carbon dioxide
MW	-	Microwave
MAP	-	Microwave-assisted pyrolysis
FFA	-	Free fatty acid
SFA	-	Saturated fatty acid
MUFA	-	Monosaturated fatty acid
PUFA	-	Polyunsaturated fatty acid
TG	-	Triglycerides
DG	-	Diglycerides
MG	-	Monoglycerides
EPA	-	Eicosapentaenoic acid
ARA	-	Arachidonic acid
DHA	-	Docosahexaenoic acid
FD	-	Freeze drying
VMD	-	Vacuum microwave drying
VOD	-	Vacuum oven drying
RS	-	Rice straw

## References

- 1 B. Hopwood, M. Mellor and G. O. Brien, *Sustain. Dev.*, 2005, **52**, 38–52.
- 2 P. Glavič and R. Lukman, *J. Clean. Prod.*, 2007, **15**, 1875–1885.
- 3 E. Holden, K. Linnerud and D. Banister, *Glob. Environ. Chang.*, 2014, **26**, 130–139.
- 4 A. Azapagic, S. Podan and R. Clift, *Sustainable Development in Practice*, Wiley, London, 2004.
- 5 J. H. Clark and F. E. I. Deswarte, *The introduction to Chemicals from Biomass*, John Wiley & Sons, Chichester, second edi., 2015.
- 6 J. H. Clark, *Green Chem.*, 2006, **8**, 17–21.
- 7 A. R. Morais and R. Bogel-Lukasik, *Sustain. Chem. Process.*, 2013, **1**, 18.
- 8 R. . Langkey and P. . Anastas, *Advancing Sustainability through Green Chemistry and Engineering*, American Chemical Society, Washington, ASC Syme., 2002.
- 9 R. Mullin, *Chem. Eng. News*, 2004, **82**, 29–37.
- 10 M. Lancaster, *Green Chemistry: An Introductory Text*, The Royal Society of Chemistry, Cambridge, UK, 2002.
- 11 P. T. Anastas and T. C. Williamson, *Green Chemistry: Designing Chemistry for the Environment*, American Chemical Society, Washington, DC, 1996.
- 12 P. . Anastas and J. . Warner, *Green Chemistry Theory and Practice*, University Press, Oxford, Oxford, 1998.
- 13 K. Alfonsi, J. Colberg, P. J. Dunn, T. Fevig, S. Jennings, T. a. Johnson, H. P. Kleine, C. Knight, M. a. Nagy, D. a. Perry and M. Stefaniak, *Green Chem.*, 2008, **10**, 31.
- 14 F. Cherubini, *Energy Convers. Manag.*, 2010, **51**, 1412–1421.
- 15 P. J. Van Soest, *Anim. Feed Sci. Technol.*, 2006, **130**, 137–171.
- 16 S. Muthayya, J. D. Sugimoto, S. Montgomery and G. F. Maberly, *Ann. N. Y. Acad. Sci.*, 2014, **1324**, 7–14.
- 17 B. Gadde, C. Menke and R. Wassmann, *Biomass and Bioenergy*, 2009, **33**, 1532–1546.
- 18 T. Silalertruksa and S. H. Gheewala, *Bioresour. Technol.*, 2013, **150**, 412–419.
- 19 M. K. Delivand, M. Barz and S. H. Gheewala, *Energy*, 2011, **36**, 1435–1441.
- 20 B. Gadde, S. Bonnet, C. Menke and S. Garivait, *Environ. Pollut.*, 2009, **157**, 1554–8.
- 21 N. T. Kim Oanh, B. T. Ly, D. Tipayarom, B. R. Manandhar, P. Prapat, C. D. Simpson and L. J. Sally Liu, *Atmos. Environ.*, 2011, **45**, 493–502.
- 22 Y. Miura and T. Kanno, *Soil Sci. plant Nutr.*, 1997, **43**, 849–854.
- 23 D. G. Streets, K. F. Yarber, J.-H. Woo and G. R. Carmichael, *Global Biogeochem. Cycles*, 2003, **17**, 1099.

- 24 Y. F. Huang, W. H. Kuan, S. L. Lo and C. F. Lin, *Bioresour. Technol.*, 2008, **99**, 8252–8258.
- 25 J. Ma and E. Takahashi, *Soil Sci. Plant Nutr.*, 1989, **35**, 663–667.
- 26 P. Binod, R. Sindhu, R. R. Singhanian, S. Vikram, L. Devi, S. Nagalakshmi, N. Kurien, R. K. Sukumaran and A. Pandey, *Bioresour. Technol.*, 2010, **101**, 4767–4774.
- 27 B. M. Jenkins, R. R. Bakker and J. B. Wei, *Biomass and Bioenergy*, 1996, **10**, 177–200.
- 28 X. F. Sun and R. Sun, *J. Wood Chem. Technol.*, 2001, **21**, 397–411.
- 29 S. A. Sadeek, N. A. Negm, H. H. H. Hefni and M. M. Abdel Wahab, *Int. J. Biol. Macromol.*, 2015, **81**, 400–409.
- 30 A. E. Pütün, E. Apaydm and E. Pütün, *Energy*, 2004, **29**, 2171–2180.
- 31 Food and Agriculture Organisation of the United Nations (FAO), *The State of World Fisheries and Aquaculture 2012*, 2012.
- 32 L. Lebel, R. Mungkung, S. H. Gheewala and P. Lebel, *Environ. Sci. Policy*, 2010, **13**, 291–302.
- 33 T. Senphan and S. Benjakul, *Food Chem.*, 2012, **134**, 829–835.
- 34 S. Takeungwongtrakul, S. Benjakul, J. Santoso, W. Trilaksani and M. Nurilmala, *J. Food Process. Preserv.*, 2015, **39**, 10–18.
- 35 M. N. . Ravi Kumar, *React. Funct. Polym.*, 2000, **46**, 1–27.
- 36 G. G. D’Ayala, M. Malinconico and P. Laurienzo, *Molecules*, 2008, **13**, 2069–2106.
- 37 B. Krajewska, *Enzyme Microb. Technol.*, 2004, **35**, 126–139.
- 38 M. Rinaudo, *Prog. Polym. Sci.*, 2006, **31**, 603–632.
- 39 S. Hajji, I. Younes, O. Ghorbel-Bellaaj, R. Hajji, M. Rinaudo, M. Nasri and K. Jellouli, *Int. J. Biol. Macromol.*, 2014, **65**, 298–306.
- 40 A. P. Sánchez-Camargo, M. Â. a Meireles, A. L. K. Ferreira, E. Saito and F. a. Cabral, *J. Supercrit. Fluids*, 2012, **61**, 71–77.
- 41 M. E. Franco-Zavaleta, R. Jiménez-Pichardo, a. Tomasini-Campocosio and I. Guerrero-Legarreta, *J. Food Sci.*, 2010, **75**, 394–399.
- 42 J. Pu, P. J. Bechtel and S. Sathivel, *Biosyst. Eng.*, 2010, **107**, 364–371.
- 43 N. C. F. Corrêa, C. D. S. MacEdo, J. D. F. C. Moraes, N. T. MacHado and L. F. De França, *J. Supercrit. Fluids*, 2012, **66**, 176–180.
- 44 V. Treyvaud Amiguet, K. L. Kramp, J. Mao, C. McRae, A. Goulah, L. E. Kimpe, J. M. Blais and J. T. Arnason, *Food Chem.*, 2012, **130**, 853–858.
- 45 T. C. Adarme-Vega, S. R. Thomas-Hall and P. M. Schenk, *Curr. Opin. Biotechnol.*, 2014, **26**, 14–18.
- 46 L. Fay and U. Richli, *J. Chromatogr.*, 1991, **541**, 89–98.
- 47 J. H. Clark, V. Budarin, F. E. I. Deswarte, J. J. E. Hardy, F. M. Kerton, A. J. Hunt, R. Luque,

- D. J. Macquarrie, K. Milkowski, A. Rodriguez, O. Samuel, S. J. Tavener, R. J. White and A. J. Wilson, *Green Chem.*, 2006, **8**, 853–860.
- 48 M. Wellisch, G. Jungmeier, A. Karbowski, M. K. Patel and M. Rogulska, *Biofuels, Bioprod. Biorefining*, 2010, **4**, 276–286.
- 49 J. J. Bozell and G. R. Petersen, *Green Chem.*, 2010, **12**, 539–554.
- 50 Star-COLIBRI, Joint European Biorefinery Vision for 2030, <http://www.star-colibri.eu/publications/>.
- 51 H. Hellsmark and P. Söderholm, *Biofuels, Bioprod. Biorefining*, 2016, **8**, 000–000.
- 52 V. Budarin, M. Gronnow, P. Shuttleworth and J. Clark, in *An introduction to Green chemistry methods*, Future Medicine, London, 2013, pp. 98–114.
- 53 E. H. K. Sin, R. Marriott, A. J. Hunt and J. H. Clark, *Comptes Rendus Chim.*, 2014, **17**, 293–300.
- 54 M. D. Luque de Castro and L. E. García-Ayuso, *Anal. Chim. Acta*, 1998, **369**, 1–10.
- 55 W. Guan, S. Li, R. Yan, S. Tang and C. Quan, *Food Chem.*, 2007, **101**, 1558–1564.
- 56 T. W. Randolph, *Trends Biotechnol.*, 1990, **8**, 78–82.
- 57 C. A. Eckert, B. L. Knutson and P. G. Debenedetti, *Nature*, 1996, **383**, 313–318.
- 58 R. Noyori, *Chem. Rev.*, 1999, **99**, 353–354.
- 59 T. M. Attard and A. J. Hunt, in *Supercritical and Other High-pressure Solvent Systems: For Extraction, Reaction and Material Processing*, The Royal Society of Chemistry, 2018, pp. 1–13.
- 60 R. S. Oakes, A. A. Clifford and C. M. Rayner, *J. Chem. Soc. Perkin Trans. 1*, 2001, 917–941.
- 61 A. J. Hunt, E. H. K. Sin, R. Marriott and J. H. Clark, *ChemSusChem*, 2010, **3**, 306–322.
- 62 B. Subramaniam, R. A. Rajewski and K. Snavely, *J. Pharm. Sci.*, 1997, **86**, 885–890.
- 63 M. M. R. De Melo, A. J. D. Silvestre and C. M. Silva, *J. Supercrit. Fluids*, 2014, **92**, 115–176.
- 64 a Molero Gomez, C. Pereyra Lopez and E. Martinez de la Ossa, *Chem. Eng. J.*, 1996, **61**, 227–231.
- 65 Y. Athukorala and G. Mazza, *Ind. Crops Prod.*, 2010, **31**, 550–556.
- 66 P. F. F. Rui, T. A. P. Rocha-santos and A. C. Duarte, 2016, **76**, 40–51.
- 67 T. M. Attard, N. Bukhanko, D. Eriksson, M. Arshadi, P. Geladi, U. Bergsten, V. L. Budarin, J. H. Clark and A. J. Hunt, *J. Clean. Prod.*, 2018, **177**, 684–698.
- 68 W. H. Morrison, R. Holser and D. E. Akin, *Ind. Crops Prod.*, 2006, **24**, 119–122.
- 69 F. E. I. Deswarte, J. H. Clark, J. J. E. Hardy and P. M. Rose, 2006, **44**, 39–42.
- 70 T. M. Attard, C. R. McElroy, C. a. Rezende, I. Polikarpov, J. H. Clark and A. J. Hunt, *Ind. Crops Prod.*, 2015, **76**, 95–103.
- 71 T. M. Attard, C. R. McElroy, R. J. Gammons, J. M. Slattery, N. Supanchaiyamat, C. L. A.

- Kamei, O. Dolstra, L. M. Trindade, N. C. Bruce, S. J. McQueen-Mason, S. Shimizu and A. J. Hunt, *ACS Sustain. Chem. Eng.*, DOI:10.1021/acssuschemeng.6b01220.
- 72 S. Takeungwongtrakul, S. Benjakul and A. H-Kittikun, *Food Chem.*, 2012, **134**, 2066–2074.
- 73 M. M. Küçük and A. H. Demirbağ, *Energy Convers. Manag.*, 1997, **38**, 151–165.
- 74 C. N. Hamelinck, G. Van Hooijdonk and A. P. Faaij, *Biomass and Bioenergy*, 2005, **28**, 384–410.
- 75 H. Zabed, J. N. Sahu, A. N. Boyce and G. Faruq, *Renew. Sustain. Energy Rev.*, 2016, **66**, 751–774.
- 76 R. T. Romano and R. Zhang, *Bioresour. Technol.*, 2008, **99**, 631–637.
- 77 R. T. Romano and R. Zhang, *Biomass and Bioenergy*, 2011, **35**, 4174–4179.
- 78 S. Pekka, R. Hanne, K. Alexander, B. Ar, R. Matti, K. Outi and N. Marita, *Fuel*, 2011, **90**, 1076–1089.
- 79 N. L. Panwar, R. Kothari and V. V Tyagi, *Renew. Sustain. Energy Rev.*, 2012, **16**, 1801–1816.
- 80 A. Perna, M. Minutillo, S. P. Cicconardi, E. Jannelli and S. Scarfogliero, *Energy Prodedia*, 2015, **82**, 687–694.
- 81 E. B. Machin, D. T. Pedroso, J. J. Roberts, J. S. Antunes and J. L. Silveira, *Appl. Therm. Eng.*, 2015, **90**, 1–12.
- 82 T. Damartzis and A. Zabaniotou, *Renew. Sustain. Energy Rev.*, 2011, **15**, 366–378.
- 83 H. B. Goyal, D. Seal and R. C. ã. Saxena, *Renew. Sustain. Energy Rev.*, 2008, **12**, 504–517.
- 84 Y. F. Huang, W. R. Chen, P. T. Chiueh, W. H. Kuan and S. L. Lo, *Bioresour. Technol.*, 2012, **123**, 1–7.
- 85 W. Chen, J. Peng and X. T. Bi, *Renew. Sustain. Energy Rev.*, 2015, **44**, 847–866.
- 86 P. T. Williams and S. Besler, *Renew. Energy*, 1996, **7**, 233–250.
- 87 A. V. Bridgwater and G. V. C. Peacocke, *Renew. Sustain. energy Rev.*, 2000, **4**, 1–73.
- 88 S. S. Lam and H. A. Chase, *Energies*, 2012, **5**, 4209–4232.
- 89 C. O. Kappe, *Angew. Chemie Int. Ed.*, 2004, **43**, 6250–6284.
- 90 R. Gedye, F. Smith, K. Westaway, H. Ali, L. Baldisera, L. Laberge and J. Rousell, *Tetrahedron Lett.*, 1986, **27**, 279–282.
- 91 X. Zhao, M. Wang, H. Liu, L. Li, C. Ma and Z. Song, *Bioresour. Technol.*, 2012, **104**, 673–678.
- 92 D. J. Macquarrie, J. H. Clark and E. Fitzpatrick, *Biofuels, Bioprod. Biorefining*, 2012, **6**, 549–560.
- 93 E. Yagmur, M. Ozmak and Z. Aktas, *Fuel*, 2008, **87**, 3278–3285.
- 94 A. Domínguez, J. A. Menéndez, Y. Fernández, J. J. Pis, J. M. V. Nabais, P. J. M. Carrott and

- M. M. L. R. Carrott, *J. Anal. Appl. Pyrolysis*, 2007, **79**, 128–135.
- 95 B. A. Lanigan, University of York, 2010.
- 96 V. L. Budarin, J. H. Clark, B. A. Lanigan, P. Shuttleworth, S. W. Breeden, A. J. Wilson, D. J. Macquarrie, K. Milkowski, J. Jones, T. Bridgeman and A. Ross, *Bioresour. Technol.*, 2009, **100**, 6064–6068.
- 97 Y. F. Huang, W. H. Kuan, S. L. Lo and C. F. Lin, *Bioresour. Technol.*, 2010, **101**, 1968–1973.
- 98 A. A. Salema and F. N. Ani, *Bioresour. Technol.*, 2011, **102**, 3388–3395.
- 99 M. qiang Chen, J. Wang, M. xu Zhang, M. gong Chen, X. feng Zhu, F. fei Min and Z. cheng Tan, *J. Anal. Appl. Pyrolysis*, 2008, **82**, 145–150.
- 100 J. A. Menéndez, \* A. Domínguez, and Y. Fernández and J. J. Pis, 2006, 373–378.
- 101 C. A. Mullen, A. A. Boateng, N. M. Goldberg, I. M. Lima, D. A. Laird and K. B. Hicks, *Biomass and Bioenergy*, 2010, **34**, 67–74.
- 102 D. Mohan, C. U. Pittman and P. H. Steele, *Energy and Fuels*, 2006, **20**, 848–889.
- 103 V. L. Budarin, P. S. Shuttleworth, J. R. Dodson, A. J. Hunt, B. Lanigan, R. Marriott, K. J. Milkowski, A. J. Wilson, S. W. Breeden, J. Fan, E. H. K. Sin and J. H. Clark, *Energy Environ. Sci.*, 2011, **4**, 471–479.
- 104 T. M. Attard, E. Theeuwes, L. D. Gomez, E. Johansson, I. Dimitriou, P. C. Wright, J. H. Clark, S. J. McQueen-Mason and A. J. Hunt, *RSC Adv.*, 2015, **5**, 43831–43838.
- 105 B. Ritter, J. Schulte, E. Schulte and H. P. Thier, *Eur. Food Res. Technol.*, 2001, **212**, 603–607.
- 106 J. L. Hargrove, P. Greenspan and D. K. Hartle, *Exp. Biol. Med.*, 2004, **229**, 215–226.
- 107 H. Wei, 2012, **1**, 266–268.
- 108 R. Sun, X. F. Sun and B. Xiao, *J. Wood Chem. Technol.*, 2002, **22**, 1–9.
- 109 J. M. DeSimone, *Science*, 2002, **297**, 799–803.
- 110 P. S. Spencer and H. H. Schaumburg, *Proceeding R. Soc. Med.*, 1977, **70**, 37–39.
- 111 M. Arshadi, A. J. Hunt and J. H. Clark, *RSC Adv.*, 2012, **2**, 1806.
- 112 T. M. Attard, M. Arshadi, C. Nilsson, V. L. Budarin, E. Valencia-Reyes, J. H. Clark and A. J. Hunt, *Green Chem.*, 2016, 2682–2690.
- 113 M. Herrero, J. A. Mendiola, A. Cifuentes and E. Ibanez, *J. Chromatogr. A*, 2010, **1217**, 2495–2511.
- 114 Z. Moldovan, E. Jover and J. M. Bayona, *Anal. Chim. Acta*, 2002, **465**, 359–378.
- 115 R. C. Murphy, *Mass spectrometry of lipids*, Plenum Press, London, 1993.
- 116 A. P. Tulloch and L. R. Hogge, *J. Chromatogr. A*, 1978, **157**, 291–296.
- 117 K. H. I. Molnár-Perl, A. Vasánits, *Chromatographia*, 1998, **48**, 111–119.
- 118 R. C. Murphy, J. Fiedler and J. Hevko, *Chem. Rev.*, 2001, **101**, 479–526.

- 119 A. Kuksis, J. J. Myher, L. Marai and K. Geher, *Anal. Biochem.*, 1976, **70**, 302–312.
- 120 J. F. Rontani and C. Aubert, *Rapid Commun. Mass Spectrom.*, 2004, **18**, 1889–1895.
- 121 D. Cheng, P. S. Shuttleworth, M. Sarah, J. H. Clark and A. S. Matharu, *Green Chem.*, 2015, **17**, 4000–4008.
- 122 K. Hill, *Pure Appl. Chem.*, 2000, **72**, 1255–1264.
- 123 N. A. Ruston, *J. Am. Oil Chem. Soc.*, 1952, **29**, 495–498.
- 124 R. Ryhage and E. Stenhagen, *J. Lipid Res.*, 1960, **1**, 361–390.
- 125 K. A. Varady, Y. Wang and P. J. H. Jones, *Nutr. Rev.*, 2003, **61**, 376–83.
- 126 C. P. F. Marinangeli, P. J. H. Jones, A. N. Kassis and M. N. a Eskin, *Crit. Rev. Food Sci. Nutr.*, 2010, **50**, 259–267.
- 127 F. P. Schiestl, M. Ayasse, R. P. Taylor and A. P. Micolich, 1999, 421–422.
- 128 H. Kasinger and B. Bauer, *Commun. SIWN*, 2008, **4**, 133–139.
- 129 F. E. I. Deswarte, J. H. Clark, A. J. Wilson, J. J. E. Hardy, R. Marriott, S. P. Chahal, C. Jackson, G. Heslop, M. Birkett, T. J. Bruce and G. Whiteley, *Biofuels, Bioprod. Biorefining*, 2007, **1**, 245–254.
- 130 A. P. G. Phillipou, *Chem. Phys. Lipids*, 1978, **22**, 51–54.
- 131 M. C. Pérez-Camino, W. Moreda, R. Mateos and A. Cert, *J. Chromatogr. A*, 2003, **983**, 283–288.
- 132 C. Isoa, *Pat. Appl. Publ.*, 2006, US 2006/0127450 A1.
- 133 R. Bruni, A. Medici, A. Guerrini, S. Scalia, F. Poli, C. Romagnoli, M. Muzzoli and G. Sacchetti, *Food Chem.*, 2002, **77**, 337–341.
- 134 R. P. Evershed, M. C. Prescott, N. Spooner and J. L. Goad, *Steroids*, 1989, **53**, 285–309.
- 135 C. J. W. Brooks, E. C. Horning and J. S. Young, *Lipids*, 1968, **3**, 391–402.
- 136 James A. McCloskey, *Methods Enzymol.*, 1969, **14**, 382–450.
- 137 Y. xun ZHANG, M. SHAO, Y. hang ZHANG, L. min ZENG, L. yan HE, B. ZHU, Y. jie WEI and X. lei ZHU, *J. Environ. Sci.*, 2007, **19**, 167–175.
- 138 S. G. Wyllie, B. a Amos and L. Tökés, *J. Org. Chem.*, 1977, **42**, 725–732.
- 139 P. Eneroth, K. Hellstroem and R. Ryhage, *J. Lipid Res.*, 1964, **5**, 245–262.
- 140 S. N. Blair, D. M. Capuzzi, S. O. Gottlieb, T. Nguyen, J. M. Morgan and N. B. Cater, *Am. J. Cardiol.*, 2000, **86**, 46–52.
- 141 T. Heinemann, G. A. Kullak-Ublick, B. Pietruck and K. von Bergmann, *Eur. J. Clin. Pharmacol.*, 1991, **40**, 59–63.
- 142 M. H. Moghadasian, *Life Sci.*, 2000, **67**, 605–615.
- 143 F. J. Brown and C. Djerassi, *J. Am. Chem. Soc.*, 1980, **102**, 807–817.
- 144 R. H. Shapiro and C. Djerassi, *J. Am. Chem. Soc.*, 1964, **86**, 2825–2832.



- 145 R. L. Alexander-Lindo, E. Y. S. a Morrison and M. G. Nair, *Phytother. Res.*, 2004, **18**, 403–7.
- 146 P. Georges, M. Sylvestre, H. Ruegger and P. Bourgeois, *Steroids*, 2006, **71**, 647–52.
- 147 M. Kane, J. R. Dean, S. M. Hitchen, C. J. Dowle and R. L. Tranter, *Anal. Chim. Acta*, 1993, **271**, 83–90.
- 148 a. G. González, *Anal. Chim. Acta*, 1998, **360**, 227–241.
- 149 K. Urbanová, V. Vrkošlav, I. Valterová, M. Háková and J. Cvačka, *J. Lipid Res.*, 2012, **53**, 204–213.
- 150 A. J. Aasen, H. H. Hofstetter, B. T. R. Iyengar and R. T. Holman, *Lipids*, 1971, **6**, 502–507.
- 151 H. Taher, S. Al-Zuhair, A. H. Al-Marzouqi, Y. Haik, M. Farid and S. Tariq, *J. Supercrit. Fluids*, 2014, **86**, 57–66.
- 152 O. Guclu-Ustundag and F. Temelli, *Ind. Eng. Chem. Res.*, 2000, **39**, 4756–4766.
- 153 L. Wang, C. L. Weller, V. L. Schlegel, T. P. Carr and S. L. Cuppett, *Eur. J. Lipid Sci. Technol.*, 2007, **109**, 567–574.
- 154 L. Kunst and A. L. Samuels, *Prog. Lipid Res.*, 2003, **42**, 51–80.
- 155 J. J. Langenfeld, S. B. Hawthorne, D. J. Miller and J. Pawliszyn, *Anal. Chem.*, 1993, **65**, 338–344.
- 156 K. T. Hwang, C. L. Weller, S. L. Cuppett and M. A. Hanna, *Ind. Crops Prod.*, 2004, **19**, 125–132.
- 157 A. de Lucas, A. García, A. Alvarez and I. Gracia, *J. Supercrit. Fluids*, 2007, **41**, 267–271.
- 158 Y. Athukorala and G. Mazza, *Sep. Sci. Technol.*, 2010, **46**, 247–253.
- 159 T. Attard, 2015.
- 160 M. Gao, F. Xu, S. Li, X. Ji, S. Chen and D. Zhang, *Biosyst. Eng.*, 2010, **106**, 470–475.
- 161 G. Qi, F. Peng, L. Xiong, X. Lin, C. Huang, H. Li, X. Chen and X. Chen, *Prep. Biochem. Biotechnol.*, 2017, **47**, 276–281.
- 162 Y. F. Huang, P. Te Chiueh, W. H. Kuan and S. L. Lo, *Bioresour. Technol.*, 2013, **142**, 620–624.
- 163 M. J. Wang, Y. F. Huang, P. T. Chiueh, W. H. Kuan and S. L. Lo, *Energy*, 2012, **37**, 177–184.
- 164 S. Munir, S. S. Daood, W. Nimmo, A. M. Cunliffe and B. M. Gibbs, *Bioresour. Technol.*, 2009, **100**, 1413–1418.
- 165 S. S. Idris, N. A. Rahman, K. Ismail, A. B. Alias, Z. A. Rashid and M. J. Aris, *Bioresour. Technol.*, 2010, **101**, 4584–4592.
- 166 H. Yang, R. Yan, H. Chen, D. H. Lee and C. Zheng, *Fuel*, 2007, **86**, 1781–1788.
- 167 C. Song, A. Pawłowski, A. Ji, S. Shan and Y. Cao, *Environ. Prot. Eng.*, 2014, **40**, 35–43.
- 168 S. H. Jung, B. S. Kang and J. S. Kim, *J. Anal. Appl. Pyrolysis*, 2008, **82**, 240–247.

- 169 S. Zhang, Q. Dong, L. Zhang and Y. Xiong, *Bioresour. Technol.*, 2015, **191**, 17–23.
- 170 C. Wu, V. L. Budarin, M. J. Gronnow, M. De Bruyn, J. A. Onwudili, J. H. Clark and P. T. Williams, *J. Anal. Appl. Pyrolysis*, 2014, **107**, 276–283.
- 171 P. Shuttleworth, V. Budarin, M. Gronnow, J. H. Clark and R. Luque, *J. Nat. Gas Chem.*, 2012, **21**, 270–274.
- 172 H. Zhang and A. K. Datta, *Food Bioprod. Process.*, 2003, **81**, 257–265.
- 173 X. Zhao, Z. Song, H. Liu, Z. Li, L. Li and C. Ma, *J. Anal. Appl. Pyrolysis*, 2010, **89**, 87–94.
- 174 R. Luque, J. A. Menéndez, A. Arenillas and J. Cot, *Energy Environ. Sci.*, 2012, **5**, 5481–5488.
- 175 J. Fan, M. De bruyn, V. L. Budarin, M. J. Gronnow, P. S. Shuttleworth, S. Breeden, D. J. Macquarrie and J. H. Clark, *J. Am. Chem. Soc.*, 2013, **135**, 11728–11731.
- 176 J. Fan, P. S. Shuttleworth, M. Gronnow, S. W. Breeden, J. H. Clark, D. J. Macquarrie and V. L. Budarin, *ACS Sustain. Chem. Eng.*, 2018, **6**, 8–12.
- 177 C. Yin, *Bioresour. Technol.*, 2012, **120**, 273–284.
- 178 S. Horikoshi, A. Osawa, S. Sakamoto and N. Serpone, *Appl. Catal. A Gen.*, 2013, **460–461**, 52–60.
- 179 M. Ollivon, S. Quinquenet, M. Seras, M. Delmotte and C. More, *Thermochim. Acta*, 1988, **125**, 141–153.
- 180 V. I. Kovalenko, *Russ. Chem. Rev.*, 2010, **79**, 231–241.
- 181 C. Atik and S. Ates, *BioResources*, 2012, **7**, 3274–3282.
- 182 F. Khan and N. Pilpel, *Powder Technol.*, 1987, **50**, 237–241.
- 183 W. N. Stoops, *J. Am. Chem. Soc.*, 1934, **56**, 1480–1483.
- 184 A. G. Graham, B. B. Krieger and D. W. Work, *J. Appl. Polym. Sci.*, 1980, **25**, 1839–1859.
- 185 M. J. Antal, *Ind. Eng. Chem. Res.*, 1995, **34**, 703–717.
- 186 H. Teng and Y. Wei, *Ind. Eng. Chem. Res.*, 1998, **5885**, 3806–3811.
- 187 H. Lei, S. Ren and J. Julson, *Energy and Fuels*, 2009, **23**, 3254–3261.
- 188 J. F. Matthews, M. Bergenstråhle, G. T. Beckham, M. E. Himmel, M. R. Nimlos, J. W. Brady and M. F. Crowley, *J. Phys. Chem. B*, 2011, **115**, 2155–2166.
- 189 A. Nordin, 2000, 618–624.
- 190 T. Ema, T. Komiyama, S. Sunami and T. Sakai, *RSC Adv.*, 2014, **4**, 2523–2525.
- 191 K. Raveendran, A. Ganesh and K. C. Khilar, *Fuel*, 1995, **74**, 1812–1822.
- 192 J. G. Olsson, U. Ja and J. B. C. Pettersson, 1997, **0624**, 779–784.
- 193 J. M. Jones, L. I. Darvell, T. G. Bridgeman, M. Pourkashanian and A. Williams, 2007, **31**, 1955–1963.
- 194 R. Fahmi, 2007, **86**, 1560–1569.

- 195 A. Jensen, K. Dam-johansen, M. A. Wo and M. A. Serio, 1998, **0624**, 929–938.
- 196 M. J. Antal, *Ind. Eng. Chem. Res.*, 2003, **42**, 1619–1640.
- 197 R. J. Evans and T. A. Milne, *Energy & Fuels*, 1987, **1**, 123–137.
- 198 D. Sutton, B. Kelleher and J. R. H. Ross, *Fuel Process. Technol.*, 2001, **73**, 155–173.
- 199 Q. Lu, Z. B. Zhang, X. C. Yang, C. Q. Dong and X. F. Zhu, *J. Anal. Appl. Pyrolysis*, 2013, **104**, 139–145.
- 200 C. Wu, V. L. Budarin, M. J. Gronnow, M. De Bruyn, J. A. Onwudili, J. H. Clark and P. T. Williams, *J. Anal. Appl. Pyrolysis*, 2014, **107**, 276–283.
- 201 C. R. Harper and T. A. Jacobson, *Arch. Intern. Med.*, 2001, **161**, 2185–2192.
- 202 P. Facts, *Global Market for EPA / DHA Omega-3 Products*, 2012.
- 203 S. Takeungwongtrakul, S. Benjakul and A. H-kittikun, *Food Chem.*, 2012, **134**, 2066–74.
- 204 P. Beaney, J. Lizardi-Mendoza and M. Healy, *J. Chem. Technol. Biotechnol.*, 2005, **80**, 145–150.
- 205 L. A. Cira, S. Huerta, G. M. Hall and K. Shirai, *Process Biochem.*, 2002, **37**, 1359–1366.
- 206 F. Shahidi and J. Synowiecki, *J. Agric. Food Chem.*, 1991, **39**, 1527–1532.
- 207 C. D. O’Leary and A. D. Matthews, *Aquaculture*, 1990, **89**, 65–81.
- 208 A. Mika, M. Gołębiowski, E. F. Skorkowski and P. Stepnowski, *Oceanol. Hydrobiol. Stud.*, 2012, **41**, 57–64.
- 209 a J. Fellenburg, D. W. Johnson, a Poulos and P. Sharp, *Biomed. Environ. Mass Spectrom.*, 1987, **14**, 127–129.
- 210 A. B. and H. Budzikiewicz, *Org. mass Spectrom.*, 1982, **17**, 161–164.
- 211 R. T. Holman and J. J. Rahm, *Prog. Chem. Fats Other Lipids*, 1971, **9**, 13–90.
- 212 M. S. Heu, J. S. Kim and F. Shahidi, *Food Chem.*, 2003, **82**, 235–242.
- 213 M. Jalali-Heravi and M. Vosough, *J. Chromatogr. A*, 2004, **1024**, 165–176.
- 214 K. K. Sun and R. T. Holman, *J. Am. Oil Chem. Soc.*, 1968, **45**, 810–817.
- 215 S. Smith, A. Witkowski and A. K. Joshi, *Prog. Lipid Res.*, 2003, **42**, 289–317.
- 216 T. Řezanka and K. Sigler, *Prog. Lipid Res.*, 2009, **48**, 206–238.
- 217 V. a. Isidorov, M. Rusak, L. Szczepaniak and S. Witkowski, *J. Chromatogr. A*, 2007, **1166**, 207–211.
- 218 W. Binsan, S. Benjakul, W. Visessanguan, S. Roytrakul, N. Faithong, M. Tanaka and H. Kishimura, *J. Food Lipids*, 2008, **15**, 97–118.
- 219 R. C. H. S., R. S. C., S. M. J. A. and M. K. J., *J. Hum. Nutr. Diet.*, 2004, **17**, 449–459.
- 220 B. E. E, G. Sharon, H. D. R, U. Ricardo and B. D. G, *Dev. Med. Child Neurol.*, 2007, **42**, 174–181.
- 221 C. B. Johnson and R. T. Holman, *Mass Spectrom. Lipids II*, 1966, **1**, 371–380.

- 222 W. A. Barber, M., Chapman, J.R., Wolstenholm, *J. mass Spectrom. Ion Phys.*, 1968, 98–101.
- 223 T. Curstedt, *Biochim. Biophys. Acta*, 1974, **360**, 12–23.
- 224 K. M. Phillips, D. M. Ruggio, J. Exler and K. Y. Patterson, *Food Nutr. Res.*, , DOI:10.3402/fnr.v56i0.18931.
- 225 J. Lipid, .
- 226 P. Eneroth, K. Hellstroem and R. Ryhage, *Steroids*, 1965, 707–720.
- 227 G. Cherchi, D. Deidda, B. De Gioannis, B. Marongiu, R. Pompei and S. Porcedda, *Flavour Fragr. J.*, 2001, **16**, 35–43.
- 228 N. T. Dunford and F. Temelli, *J. Food Sci.*, 1997, **62**, 155–159.
- 229 Y.-R. Lin, S.-L. Huang and C.-H. Huang, *Comp. Biochem. Physiol. Part B Biochem. Mol. Biol.*, 2003, **135**, 683–687.
- 230 T. Senphan and S. Benjakul, *Food Chem.*, 2015, **166**, 498–506.
- 231 A. J. Mesiano, E. J. Beckman and A. J. Russell, *Chem. Rev.*, 1999, **99**, 623–634.
- 232 P. Maheshwari, Z. L. Nikolov, T. M. White and R. Hartel, *J. Am. Oil Chem. Soc.*, 1992, **69**, 1069–1076.
- 233 Y. Iwai, Y. Koga, H. Maruyama and Y. Arai, *J. Chem. Eng. Data*, 1993, **38**, 506–508.
- 234 G. Liu, Y. Zheng, X. Xu, X. Liu, F. Yuan and Y. Gao, *J. Food Process Eng.*, 2011, **34**, 657–670.
- 235 A. Molero Gómez and E. Martínez de la Ossa, *Chem. Eng. J.*, 2002, **88**, 103–109.
- 236 S. Machmudah, Y. Kawahito, M. Sasaki and M. Goto, *J. Supercrit. Fluids*, 2007, **41**, 421–428.
- 237 L. G. Marques, M. C. Ferreira and J. T. Freire, *Chem. Eng. Process. Process Intensif.*, 2007, **46**, 451–457.
- 238 M. Maskan, *J. Food Eng.*, 2001, **48**, 177–182.
- 239 T. M. Lin, T. D. Durance and C. H. Scaman, *Food Res. Int.*, 1998, **31**, 111–117.
- 240 V. P. Oikonomopoulou, M. K. Krokida and V. T. Karathanos, *Procedia Food Sci.*, 2011, **1**, 647–654.
- 241 C. Ratti, *J. Food Eng.*, 2001, **49**, 311–319.
- 242 M. K. Krokida, V. T. Karathanos and Z. B. Maroulis, *J. Food Eng.*, 1998, **35**, 369–380.
- 243 S. Sarangam and P. Chakraborty, 2015, 620–624.
- 244 N. Wang and J. G. Brennan, *J. Food Eng.*, 1995, **24**, 61–76.
- 245 B. C. Roy, M. Goto and T. Hirose, *Ind. Eng. Chem. Res.*, 1996, **35**, 607–612.
- 246 M. Sun and F. Temelli, *J. Supercrit. Fluids*, 2006, **37**, 397–408.
- 247 C. Crampon, A. Mouahid, S. A. A. Toudji, O. Lépine and E. Badens, *J. Supercrit. Fluids*, 2013, **79**, 337–344.

- 248 M. Popp, W. Lied, A. J. Meyer, A. Richter, P. Schiller and H. Schwitte, *J. Exp. Bot.*, 1996, **47**, 1469–1473.
- 249 C. C. Huxsoll and J. A. . Morgan, *J. Food Sci.*, 1968, **22**, 47–52.
- 250 N. Genin and F. René, *J. Food Eng.*, 1995, **26**, 391–408.
- 251 Y. Wang, M. Zhang and A. S. Mujumdar, *Dry. Technol.*, 2011, **29**, 382–394.
- 252 F. L. García-Carreño, *Comp. Biochem. Physiol. Part B Comp. Biochem.*, 1992, **103**, 575–578.
- 253 N. C. Shantha and E. Napolitano, *J. Chromatogr.*, 1992, **624**, 37–51.
- 254 N. Jovanović, A. Bouchard, G. W. Hofland, G. J. Witkamp, D. J. A. Crommelin and W. Jiskoot, *Eur. J. Pharm. Sci.*, 2006, **27**, 336–345.
- 255 M. Ezouerra and F. Garcia-carrenno, *J. Food Biochem.*
- 256 S. M. Moss, S. Divakaran and B. G. Kim, *Aquac. Res.*, 2001, **32**, 125–131.
- 257 S. G.-G. and F. S. Olimpia Carrillo-Farnés , Alina Forrellat-Barrios, *Crustaceana*, 2007, **80**, 257–275.
- 258 E. Oh, D. Kim, J. Kim and H. Kim, *J. Food Biochem.*, 2000, **24**, 251–264.
- 259 Z. Wimmer and M. Zarevúcka, *Int. J. Mol. Sci.*, 2010, **11**, 233–253.
- 260 W. Du, Y. Xu and D. Liu, *Biotechnol. Appl. Biochem.*, 2003, **38**, 103–106.
- 261 H. Fukuda, A. Kondo and H. Noda, *J. Biosci. Bioeng.*, 2001, **92**, 405–416.
- 262 L. Fjerbaek, K. V. Christensen and B. Norddahl, *Biotechnol. Bioeng.*, 2009, **102**, 1298–1315.
- 263 A. Iemhoff, J. Sherwood, C. R. McElroy and A. J. Hunt, *Green Chem.*, 2018, **20**, 136–140.
- 264 A. G. Lanctôt, T. M. Attard, J. Sherwood, C. R. McElroy and A. J. Hunt, *RSC Adv.*, 2016, **6**, 48753–48756.
- 265 G. Paggiola, A. J. Hunt, C. R. McElroy, J. Sherwood and J. H. Clark, *Green Chem.*, 2014, **16**, 2107–2110.
- 266 E. S. Kechaou, J. Dumay, C. Donnay-Moreno, P. Jaouen, J. P. Gouygou, J. P. Bergé and R. Ben Amar, *J. Biosci. Bioeng.*, 2009, **107**, 158–164.
- 267 G. a. Gbogouri, M. Linder, J. Fanni and M. Parmentier, *Eur. J. Lipid Sci. Technol.*, 2006, **108**, 766–775.
- 268 B. Mbatia, D. Adlercreutz, P. Adlercreutz, A. Mahadhy, F. Mulaa and B. Mattiasson, *Process Biochem.*, 2010, **45**, 815–819.
- 269 F. C. Phillips, W. L. Erdahl, J. a Schmit and O. S. Privett, *Lipids*, 1984, **19**, 880–887.
- 270 J. Park, S.-Y. Cho and S.-J. Choi, *BMB Rep.*, 2008, **41**, 254–258.
- 271 E. Choe and D. B. Min, *Compr. Rev. Food Sci. Food Saf.*, 2006, **5**, 169–186.
- 272 Y. K. Shin-ichi Teshima, Akio Kanazawa, *Bull. Japanese Soc. Sci. Fish.*, 1986, **52**, 719–723.

- 273 C. C. Allain, L. S. Poon, C. S. G. Chan, W. Richmond and P. C. Fu, *Clin. Chem.*, 1974, **20**, 470–475.
- 274 T. Senphan and S. Benjakul, *J. Funct. Foods*, 2014, **6**, 147–156.
- 275 S. Chantachum, S. Benjakul and N. Sriwirat, *Food Chem.*, 2000, **69**, 289–294.
- 276 C. Rivera-Pérez, F. L. García-Carreño and R. Saborowski, *Mar. Biotechnol.*, 2011, **13**, 284–295.
- 277 R. W. Mahley, T. L. Innerarity, S. C. Rall and K. H. Weisgraber, 1984, **25**, 1277–1294.
- 278 M. Bamji-Mirza and Z. Yao, Phospholipases, <http://lipidlibrary.aocs.org/Biochemistry/content.cfm?ItemNumber=39190>, (accessed 27 March 2018).
- 279 M. de los A. Navarrete del Toro, F. L. García-Carreño and J. H. Córdova-Murueta, *Aquaculture*, 2011, **317**, 99–106.
- 280 C. Sriket, S. Benjakul and W. Visessanguan, *J. Sci. Food Agric.*, 2011, **91**, 52–59.
- 281 T. Bamberge, J. Erickson and C. Cooney, *J. Chem. Eng. Data*, 1988, **33**, 327–333.
- 282 C. Sriket, S. Benjakul, W. Visessanguan, K. Hara, A. Yoshida and X. Liang, *Food Chem.*, 2012, **134**, 351–358.
- 283 D. R. Tocher and D. G. Harvie, *Fish Physiol. Biochem.*, 1988, **5**, 229–239.
- 284 F. S. Henna Lu, N. S. Nielsen, M. Timm-Heinrich and C. Jacobsen, *Lipids*, 2011, **46**, 3–23.
- 285 Y. Thiansilakul, S. Benjakul and M. P. Richards, *Food Chem.*, 2010, **121**, 1109–1119.
- 286 E. J. Conkerton, P. J. Wan and O. a Richard, *J. Am. Oil Chem. Soc.*, 1995, **72**, 963–965 ST–Hexane and heptane as extraction sol.
- 287 J. Azmir, I. S. M. Zaidul, M. M. Rahman, K. M. Sharif, F. Sahena, M. H. a Jahurul and a. Mohamed, *Ind. Crops Prod.*, 2014, **52**, 405–412.
- 288 M. K. Inglesby, G. M. Gray, D. F. Wood, K. S. Gregorski, R. G. Robertson and G. P. Sabellano, *Colloids Surfaces B Biointerfaces*, 2005, **43**, 83–94.
- 289 Y. Yuan, 2015.
- 290 J. Fan, 2013.
- 291 V. L. Budarin, Y. Zhao, M. J. Gronnow, P. S. Shuttleworth, S. W. Breeden, D. J. Macquarrie and J. H. Clark, *Green Chem.*, 2011, **13**, 2330.







